UNIVERSITÀ DEGLI STUDI
DI GENOVA

Pelagic-benthic coupling in organic matter utilization: the contribution of bacterial communities and benthic suspension feeders to carbon cycling in the Puyuhuapi Fjord ecosystem (Chilean Patagonia).

Paulina Montero Reyes

PhD program in Sciences and Technologies for the Environment and the Landscape (STAT)

XXXII cycle in Marine Science

February 2020

TABLE OF CONTENTS

I. General Introduction 5

1. Main oceanographic characteristics of Patagonian fjords 5

2. Factors that modulate primary production in Chilean Patagonia 6

3. Primary production cycle in Chilean Patagonia 7

4. Bacterial community and dissolved organic matter utilization 8

5. Benthic suspension feeders 10

6. Pelagic-benthic coupling 12

7. References 14

II. Objective and Scientific question of the thesis 27

III. List of publications and manuscripts in preparation included in this thesis 29

IV. List of the other publications 30

Chapter 1- Paper I 31

Diatom blooms and primary production in a channel ecosystem of central Patagonia

Introduction 32

Materials and Methods 33

Results 36

Discussion 43

References 47

Chapter 1- Paper II 50

A winter dinoflagellate bloom drives high rates of primary production in a Patagonian fjord ecosystem

Introduction 51

Data and methodology 52

Results 54

Discussion 56
Conclusion 61
References 61

Chapter 1- Paper III 63
Atmospheric-ocean forcing on phytoplankton productivity and carbon flow through the microbial food web in a Patagonia fjord system (44°S)
Introduction 64
Materials and Methods 68
Results 78
Suplemental Materials 98
Preliminary Discussion 100
References 104

Chapter 2- Paper IV 112
Influence of dissolved organic matter on bacterial production and community composition in fjords of Chilean Patagonia
Introduction 113
Materials and Methods 116
Results 124
Preliminary Conclusions 147
Suplemental Figures 148
References 151

Chapter 3- Paper V 161
Ingestion rates of benthic suspension feeder *Aulacomya atra* under different sources of organic matter (autochthonous and allochthonous)
Introduction 162
Materials and Methods 164
Results 170
Preliminary Conclusions 179

References 180

Chapter 4- Synthesis 186

What is the role of the bacterial community and benthic suspension feeders in carbon cycling within the Puyuhuapi fjord?

I. GENERAL INTRODUCTION

1. Main oceanographic characteristics of Patagonian fjords

The Chilean Patagonia (41°-56°S) encompasses one of the most extensive fjord regions in the world (240000 km^2) with oceanographic conditions that can sustain unique ecosystems. The region is made up mainly of fjords and channels, characterized by intertangled geomorphologies where water inputs from terrestrial and marine ecosystems overlap and mix (González et al., 2013). Patagonian fjords are characterized by highly complex geomorphology and hydrographic conditions, besides strong seasonal and latitudinal patterns in precipitation, freshwater discharge, glacier coverage, and light regime (Aracena et al., 2011). These systems receive Sub-Antarctic Water (SAAW) with high loads of nitrate and phosphate from the ocean, and freshwater with high loads of silicic acid from land (Silva, 2008). The surface freshwater layer that is formed by river discharges, high precipitation and glacier melting, gradually mixes with the deeper and salty SAAW layer through estuarine circulation (Chaigneau and Pizarro, 2005; Silva et al., 2009; Schneider et al., 2014). The interplay between oceanic waters and freshwater produces a vertical and horizontal gradient in salinity, nutrients and structure of microplanktonic community, making these fjords highly heterogeneous ecosystems. In addition, this interaction allows the transport and exchange of large amounts of organic matter between terrestrial and open-ocean environments (Sievers and Silva, 2009; González et al., 2011).

Patagonian fjords play an important role in biological productivity and in coastal carbon cycling (González et al., 2013; Iriarte et al., 2014). These highly productive ecosystems have a great potential in terms of transfer of food to higher trophic levels, and vertical carbon export (González et al., 2010, 2011; Montero et al., 2011, 2017a,b). Previous studies within this region have highlighted the role of light (Jacob et al., 2014), winds, low-pressure systems, and freshwater discharge in driving cycles of biological productivity and composition of the phytoplankton community at seasonal and shorter time scales (Montero et al., 2011, 2017a,b).

2. Factors that modulate primary production in Chilean Patagonia

The hydrodynamic mechanism that usually controls total phytoplankton production is the alternation, in time and/or space, between the destabilization and re-stratification of the water column (Legendre and Razzoulzadegan, 1996). In fjords, fresh water inputs tends to stabilise stratification while wind stress can oppose the stabilising effects of freshwater and is likely to be an important mechanism for mixing the upper water column (Goebel et al., 2005). In general, it is accepted that the interplay between wind-forced vertical mixing, solar radiation, and nutrient availability determines the occurrence of phytoplankton blooms (Sverdrup, 1953). Iriarte and González (2008) have suggested that an improvement in the light regime towards the end of winter is the main factor triggering phytoplankton production in the southern Pacific coastal area. However, this seasonal improvement in light alone may not be enough to cause phytoplankton blooms. Montero et al. (2011) suggests that the annual solar radiation cycle interact with mesoscale patterns of wind variability to modulate primary productivity in fjords. These authors reported that the onset of the productive season in Reloncaví Fjord (41°S; 72°W) coincided with seasonal changes in the direction and intensity of meridional winds. Low-pressure synoptic (LPS) events have also been shown to be important drivers of phytoplankton productivity during winter in Puyuhuapi fjord (44°S; 72°W) (Montero et al., 2017b). In that study, the area was under low surface irradiance levels and was subjected to the passage of several LPS separated by intervals of 2 to 4 days. During these events, strong northern winds (10-20 m s^{-1}) contributed to the mixing of the water column, resulting (subsequent to water column re-stratification) in enhanced phytoplankton productivity at very low irradiance (1-10 μE m^{-2} s^{-1}) (Montero et al., 2017b). These results are novel and challenge the so far established paradigm of low levels of irradiance as a key factor limiting phytoplankton blooms in fjords ecosystems. This research has also highlighted the importance of LPS events to ecosystem productivity. During these events, periods of intensive freshwater inputs also appear to modulate pulses of primary production (including the onset of productive season) in the Puyuhuapi fjord (44°S; 72°W) (Montero et al., 2017a). Freshwater input stabilizes the water column and increase the concentration of silicic acid in the upper layers, favouring the occurrence of diatom dominated phytoplankton blooms (Montero et al., 2017a).

3. Primary production cycle in Chilean Patagonia

The productivity cycle within a number of Patagonian fjords (41-51ºS) has been typically described as a two-phase system consisting of a short non-productive winter phase (May to July) and a productive phase extending from late winter (August) to autumn (April) (Iriarte et al., 2007; Montero et al., 2011, 2017a). Nevertheless, more recently, the occurrence of highly productive winter blooms of phytoplankton challenges our earlier perception of winter as a low production season in these fjords (Montero et al., 2017b).

The productive season has been characterized by the occurrence of diatom blooms associated with high primary production rates (1-3 g C m^{-2} d^{-1}), while winter phytoplankton productivity, characterized by the dominance of small phytoplankton cells, has been reported to be a small fraction (<0.5 g C m^{-2} d^{-1}) of the total annual productivity (Iriarte et al., 2007; Iriarte and González 2008; Czypionka et al. 2011; Montero et al., 2011; Paredes and Montecinos, 2011). Diatoms of the genera *Pseudonitzchia*, *Skeletonema* and *Chaetoceros* usually dominate the phytoplankton community during the productive season, when warmer waters have been associated with high concentrations of *Pseudo-nitzschia* spp., and silicate-rich waters with *Skeletonema* spp. and *Chaetoceros* spp. blooms (Montero et al., 2017a). Diatoms are known to represent a significant component of the overall phytoplankton biomass in Patagonian waters (Iriarte et al. 2001; Cassis et al., 2002; Alves-de-Souza et al., 2008; Iriarte and González, 2008). They are key species that transfer energy efficiently to higher trophic levels and also significantly contribute to the downward transfer of organic carbon (Iriarte et al., 2007; González et al., 2010; Montero et al., 2011; Iriarte et al. 2013).

Low rates of primary production and low carbon sedimentation observed in the water column, mainly during winter months, suggests that most of the locally produced organic carbon is recycled within the microbial loop (Montero et al., 2011). Low temperature, and/or unfavourable light conditions, added to the dominance of small flagellates (size range: 2-20 μm) during the non-productive season, have been reported as the key factors depressing phytoplankton activity during the winter in the Patagonian fjord region (Pizarro et al., 2005; Iriarte et al., 2007; Montero et al., 2011; Montero et al., 2017a). Despite these earlier described winter characteristics, a dense bloom of the dinoflagellate

Heterocapsa triquetra (32-7900 cells mL^{-1}) was recorded during winter 2015 in the Puyuhuapi Fjord (44°S; 72°W), and was responsible for unusually high levels of winter primary production (1.6 g C m^{-2} d^{-1}) (Montero et al., 2017b). More recently, we have again recorded winter blooms in the Puyuhuapi Fjord during May/July 2018 and July 2019, this time with a high abundance of diatoms such as *Pseudo-nitzschia* spp. and *Skeletonema* spp., associated with high primary production rates (2.3-2.7 g C m^{-2} d^{-1}) (data unpublished). Thus, our preliminary data appear to suggest that the marked seasonal pattern of the productivity cycle in the Puyuhuapi fjord is changing, and showing every time a less predictable phytoplankton succession model. These findings introduce a novel variability for biological productivity that requires more focused research attention.

4. Bacterial community and dissolved organic matter utilization

Dissolved organic matter (DOM) is an important component of the total carbon pool in aquatic ecosystem (Kirchman, 2008) and heterotrophic bacterial community is the main group within the food web involved in the degradation and mineralization of this organic material.

Heterotrophic bacterial communities are able to process an important fraction of dissolved organic matter (DOM), offering a permanent and fundamental path for the transfer of matter and energy within the carbon flux (Montero et al., 2011). In the Puyuhuapi Fjord (44°S; 72°W), Reloncaví Fjord (41°S; 72°W) and in some sampling stations next to the fjord area of Southern Ice Field (49°-51°S), we have found significant correlations between primary production and bacterial secondary production rates (Daneri et al., submitted; Montero et al., 2011), reflecting a significant degree of coupling between the primary formation of organic matter and its utilization by the microbial heterotrophic community (Montero et al., 2011). Weak coupling between phytoplankton and bacterial production rates in fjord areas has been reported mainly when bacterial community uses allochthonous organic substrates as a basis for secondary production (Bukaveckas et al., 2002).

DOM consists of a heterogeneous mixture of different carbon compounds that vary in chemical quality (Benner, 2002) and include both autochthonous and allochthonous

sources. The majority of autochthonous DOM in aquatic ecosystem is produced by phytoplankton (primary production) (Cole et al., 1988; Bianchi, 2007; Nagata, 2008), while allochthonous organic matter is primarily derived from terrestrial vegetation and soils (Bianchi, 2007) that enters the water column mainly through river discharges. In addition of these natural sources of organic matter, coastal environments receive the supply of allochthonous organic substrates derived from anthropogenic activities. In the case of Chilean fjords, the installation of an extensive salmon farming industry in the region can be a significant source of allochthonous inorganic and organic material (Quiñones et al., 2019). While some studies have shown the potential effect of nutrient enrichment associated with salmon industry in Chilean fjords (e.g. Soto and Norambuena 2004; Iriarte et al., 2013), the effect of organic matter releasing remains a main challenge to be unravelled (Quiñones et al., 2019).

Different DOM sources provides a series of ecological niches that support the growth of highly diverse bacterial communities (Buchan et al., 2014; Blanchet et al., 2016; Hoikkala et al., 2016). Bacterial community composition and bacterial production rates may vary according to the DOM source (Lucas et al., 2016). Indeed, phytoplankton blooms drive the dynamic of bacterial taxa specialized in processing efficiently photolytically produced organic matter (Buchan et al., 2014). In the case of the DOM derived from salmon farming, it has been indicated that this pool could also be an important source of organic substrates for heterotrophic bacterial community (Yoshikawa et al., 2012; Yoshikawa and Eguchi, 2013; Nimptsch et al., 2015), mainly because their high level of degradability (Nimptsch et al., 2015) and rich content in proteins (Yoshikawa et al., 2017).

The responses of bacterial groups to specific DOM compounds may also vary spatially and seasonally (Bunse and Pinhassi, 2017), due to the natural variability in the composition of microbial communities associated with environmental factors (Pinhassi and Hagström, 2000). In Patagonian fjords, temperature, salinity and oxygen (Gutiérrez et al., 2018) and hydrological changes associated with meltwater discharge (Gutiérrez et al., 2015) can modify the diversity of bacterial community in the water column. In the Puyuhuapi fjord (44°S; 72°W) Gutiérrez et al. (2018), reported that the composition of the bacterial community showed a pattern of vertical zonation, where different groups Operational Taxonomic Units (OTUs) were associated to predominant water masses.

Bacterial communities represented mainly by *Actinomycetales*, *Rhodobacteraceae*, *Cryomorphaceae*, and *Flavobacteriaceae* were associated with Estuarine Fresh Waters, whereas *Cenarchaeaceae* and *Oceanospirillales* were representative of Modified Sub Antarctic Waters. Salinity and dissolved oxygen concentration were the main factors that explained bacterial segregation in these contrasting water masses (Gutiérrez et al., 2018). In addition, a dramatic reduction of richness and individual abundances within *Flavobacteriaceae*, *Rhodobacteraceae* and *Cenarchaeaceae* families was principally associated by seasonal increase of surface water temperature (Gutiérrez et al., 2018).

The composition of phytoplankton can also influence the composition of bacteria in the fjord region of Patagonia (Gutiérrez et al., 2018). Positive correlations of members of *Flavobacteriaceae, Alteromonadales, and Verrucomicrobiales* with diatoms in subsurface waters and of *Flavobacteriales* (*Cryomorphaceae*and and *Flavobacteriaceae*), *Rhodobacteraceae*, and *Pelagibacteraceae* with dinoflagellates in surface waters suggest that phytoplankton composition could define specific niches for microorganisms in Puyuhuapi fjord waters (Gutiérrez et al., 2018). These observations support previous findings in coastal environments where certain bacterial assemblages have been associated with spring diatom blooms and others with autumn blooms dominated by dinoflagellates (El-Swais et al., 2015). Since diatoms and dinoflagellates are the major primary producers in the Puyuhuapi Fjord (Montero et al., 2017a, b), the study of specific interactions between bacteria and phytoplankton and their role in carbon fluxes certainly merits further analysis.

5. Benthic suspension feeders

In aquatic ecosystems, animals that feed on suspended particles in the water are collectively known as filter feeders (Jørgensen, 1990). Benthic communities are generally dominated by suspension feeders animals (Dame et al., 2001), including those actively pumping water, passively encountering particles, or some combination of the two (Petersen, 2004; Sebens et al., 2016). Active suspension feeders produce their own internal currents and pump water through a filtering structure that separates food particles from the water (Riisgård and Larsen, 2000). Contrarily, passive suspension feeders completely rely on the current for food supply (Best, 1988). By filtering water to satisfy their nutritional demands,

these animals remove vast quantities of microscopic particles such as bacteria, phytoplankton, detritus, and suspended sediments, which collectively comprise the seston (Wright et al., 1982; Langdon & Newell 1996, Kreeger & Newell 2000, Cranford et al. 2011). Bivalve molluscs such as mussels are active suspension feeders and spatially dominant in benthic communities. Filter feeding behaviour in bivalves is known to be highly responsible to fluctuations in both the abundance and composition of suspended seston (Bayne, 1998; Prins et al., 1998), mainly due they can filter large volumes of water and retain a wide size range of particles (ca. 4-35 μm diameter) (Voudanta et al., 2016). The amount of food consumed by bivalves is determined by the filtration rate and efficiency of particle retention by the gill which has evolved to act as both a water-transporting and a particle-retaining organ (Riisgård, 1988).

The filtration rate of a bivalve is a parameter of great ecological importance in aquatic ecosystems, which is critical to understanding the impact of these species on particles fluxes in coastal environments. Having determined the filtration rate and knowing the concentration of suspended particles in the water, it is possible to calculate the amount of food retained by the gills and ingested by the animal, as long as no pseudofaeces are produced (Winter, 1978). Several studies have reported differences in the bivalve filtration rates depending on the composition and quality of suspended particles in the water column (Rosa et al., 2018 and references therein). In addition, seasonal variation of the available food sources has also been demonstrated as a crucial factor in selection of prey and the filtration rate of bivalves (Cranford et al., 2011; Cresson et al., 2016).

Bivalves exhibit little or no movement and are dependent upon food sources available in the water column. Vertical flux of organic matter (autochthonous) mainly from phytoplankton has been considered as a main food source for bivalves (Dame, 1996; Arapov et al., 2010; Greene et al., 2011). Several studies have indicated that phytoplankton abundance can be strongly controlled by bivalve grazing in shallow areas (Cloern, 1982; Prins et al., 1998; Lonsdale et al., 2009; Lucas et al., 2016), where even this "cleaning" potential could represent a mechanism to control eutrophication in coastal areas impacted by aquaculture (Officer et al., 1982; Rice, 1999; Rice et al., 2000). Bacteria and detritus have also been described as an important contribution to the diet of bivalve populations, especially in ribbed mussels, whose morphology of gill makes these species a very effective

bacterial grazer in comparison to other bivalves (Wright et al., 1982; Stuart and Klumpp, 1984; Langdon and Newell, 1990; Kreeger and Newell, 1996; Gili and Coma, 1998).

Blue mussels inhabiting in close vicinity to the fish farms have been described for their capacity to use as a potential food those waste organic material from salmon cages such as uneaten food pellets and fecal particles (Reid et al., 2010; MacDonald et al., 2012; Handa et al., 2012 a, b). Several studies have indicated that bivalves grown adjacent to salmon farming areas remove the organic matter from cages, increase their growth rates (Lander et al., 2004; Peharda et al., 2007; Sarà et al., 2009) and help reduce the ecological impacts of the salmon industry in the water column (Lefebvre et al., 2000; MacDonald et al., 2012).

In Chilean Patagonia fjords, salmon farming is the main aquaculture activity that takes place (Buschman et al., 2006), mainly due to favourable physical/chemical water conditions for fish (Katz, 2006). This industry releases a large quantity of organic wastes that modify the load of particulate and dissolved material in the water column (Quiñones et al., 2019), and represent a permanent source of allochthonous organic matter input to the system (Iriarte et al., 2014). These allochthonous materials together with the high amount of autochthonous organic matter produced by phytoplankton in fjords (Montero et al., 2011; Montero et al., 2017a, b) provide a heterogeneous pool of food available to benthic consumers. In this region very little is known about feeding behaviour in bivalves and what are the main components of the diet of these animals, mainly of those dominant species such as ribbed mussel *Aulacomya atra* present along the protected and semi-protected rocky shores in the Chilean Patagonian fjord (Försterra, 2009). Considering the importance of filter feeding bivalves to the pelagic-benthic coupling is fundamental to know if these organisms are processing both autochthonous and allochthonous organic matter. Knowing the bivalve feeding dynamic will allow a better understanding of carbon fluxes in Chilean fjords.

6. Pelagic-benthic coupling

The capture and ingestion of particulate organic matter by benthic suspension feeders is one pathway through which carbon and nutrients are transferred from the water

column to the benthos, resulting in their retention, utilization and cycling (Monaghan et al., 2011). Bivalves filter considerable amounts of particles. The amount of material filtered is determined by their biomass, activity and the supply of organic matter to the benthos.

In Chilean Patagonian fjords, high rates of primary production (Montero et al., 2017a, b) result in the efficient export of organic carbon to sediments (González et al., 2013). In addition, particulate organic matter from terrestrial origin (Quiroga et al., 2016) together with those derived from salmon cages augments the vertical flux of particles reaching the benthos.

The influence of terrestrial and aquaculture derived carbon sources on hard-bottom benthic communities from Chilean fjords has, to date, been poorly studied. Some authors have indicated that allochthonous material from terrestrial origin plays a minor role as a food for suspension feeders (Mayr et al., 2011; Zapata-Hernández et al., 2014). In contrast, autochthonous organic matter from phytoplankton production has been highlighted as one of the main food sources in benthic suspension feeders (bivalves and ascidians) from sub-Antarctic Magellan Strait (Andrade et al., 2016).

From our recent studies in Patagonian fjords, we are beginning to better understand carbon fluxes in fjords environments, where bacterioplankton communities are able to process an important fraction of the organic carbon produced by phytoplankton, and classic and microbial food web are coupled playing a significant role in carbon export from surface to the benthos (Montero et al., 2011). However, little is known about the cycling of allochthonous organic matter, mainly those coming from salmon aquaculture and, what is the importance of this allocthonous material in sustaining the bacterial communities (both composition and activity) and benthic suspension feeder.

This research describes the main pathways of production and utilization of autochthonous and allochthonous carbon by bacterial communities and their relative importance in sustaining benthic filter feeder bivalves.

7. References

Andrade, C., Ríos, C., Gerdes, D., Brey, T., 2016. Trophis structure of shallow-water benthic communities in the sub-Antartic Strait of Magellan. Polar Biology DOI 10.1007/s00300-016-1895-0

Alves-de-Souza, C., González, M.T., Iriarte, J.L., 2008. Functional groups in marine phytoplankton assemblages dominated by diatoms in fjords of southern Chile. Journal Plankton Research. 30, 1233-1243.

Aracena, C., Lange, C.B., Iriarte, J.L., Rebolledo, L., Pantoja, S., 2011. Latitudinal patterns of export production recorded in surface sediments of the Chilean Patagonian fjords (41–55°S) as a response to water column productivity. Continental Shelf Research 31, 340-355.

Arapov, J., Ezgeta-Balic, D., Peharda, M., Gladan, Z. N., 2010. Bivalve feeding – How and what they eat?. Ribarstvo 68 (3) 105-116.

Bayne, B. L., 1998. The physiology of suspension feeding by bivalve molluscs: an introduction to the Plymouth "TROPHEE" workshop, Journal of Experimental Marine Biology and Ecology 219 (1-2), 1-19.

Benner, R., 2002. Chemical composition and reactivity. Biochemestry of marine dissolved organic matter. In D. A. Hansell, and C. A. Carlson (eds). pp 59-90.

Bianchi, T.S., 2007. Biogeochemistry of Estuaries. Oxford University Press. 706 pp

Blanchet, M., Pringault, O., Panagiotopoulos, C., Lefêvre, D., Charrière, B., Ghiglione, J.F. Fernandez, C., Aparicio, F.L., Marrasé, C., Catala, P., Oriol, P., Caparros, J., Joux, F., 2016. When riverine dissolved organic matter (DOM) meets labile DOM in

coastal waters: changes in bacterial community activity and composition. Aquatic Science doi10.1007/s00027-016-0477-0

Buchan, A., LeCleir, G.R., Gulvik, C.A., González, J.M., 2014. Master recyclers: features and functions of bacteria associated with phytoplankton blooms. Nature Reviews Microbiology. 12, 686-698. doi: 10.1038/nrmicro3326

Buschman, A. H., Riquelme, V., Hernández-González, M. C., Varela, D., Jiménez, J. E., Henríquez, L. A., Vergara, P. A., Guíñez, R., Filún, L., 2006. A review of the impacts of salmonid farming on marine coastal ecosystems in the southeast Pacific. ICES Journal of Marine Science 63, 1338-1345. doi:10.1016/j.icesjms.2006.04.021

Bukaveckas P.A, J.J Williams and S.P Hendricks (2002). Factors regulating autotrophy and heterotrophy in the main channel and an embayment of a large river impoundment. Aquatic Ecology 36: 355 -369.

Bunse, C., and Pinhassi, J. (2017). Marine bacterioplankton seasonal succession dynamics. Trends in Microbiology. 25, 494-505. doi: 10.1016/j.tim.2016.12.013

Cassis, D., Muñoz, P., Avaria, S., 2002. Variación temporal del fitoplancton entre 1993 y 1998 en una estación fija del seno Aysén, Chile (45º26'S-73º00'W). Revista de Biologia Marina y Oceanografía. 37 (1), 43-65.

Chaigneau, A., Pizarro, O., 2005. Mean surface circulation and mesoscale turbulent flow characteristics in the eastern South Pacific from satellite tracked drifters. Journal Geophysical Research, Oceans, 110, C05014, doi:10.1029/2004JC002628.

Cloern, J. E., 1982. Does the Benthos Control Phytoplankton Biomass in South San Franscisco Bay? Marine Ecology Progress Series 9, 191-202.

Cole, J.J., Findlay, S., Pace, M.L., 1988. Bacterial production in fresh and saltwater ecosystems: a cross-system overview. Marine Ecology Progress Series 43: 1-10.

Cranford, P. J., Ward, J. E., Shumway, S. E., 2011. Bivalve filter feeding: variability and limits of the aquaculture biofilter. Chapter 4 Shellfish Aquaculture and the environment, First edition. Edited by Sandra E. Shumway 81-124

Cresson, P., Ruitton, S., Harmelein-Vivien, M., 2016. Feedinf strategies of co-occurring suspension feeders in an oligotrophic environment. Food Webs 6, 19-28. http://dx.doi.org/10.1016/j.fooweb.2015.12.002

Czypionka, T., Vargas, C.A., Silva, N., Daneri, G., González, H.E, Iriarte, J.L., 2011. Importance of mixotrophic nanoplankton in Aysén Fjord Southern Chile) during austral winter. Continental Shelf Research 31 (3-4), 216-224.

Dame, R.F., 1996. Ecology of marine bivalves: an ecosystem approach. CRC Press, Boca Raton, 254 pp.

El-Swais, H., Dunn, K.A., Bielawski, J.P., Li, W.K., Walsh, D.A., 2015. Seasonal assemblages and short-lived blooms in coastal northwest Atlantic Ocean bacterioplankton. Environmental Microbiology 17, 3642-3661. doi: 10.1111/1462-2920.12629

Elizondo-Patrone, C., Hernández, K., Yannicelli, B., Olsen L.M., Molina, V., 2015. The response of nitrifying microbial assemblages to ammonium (NH_4^+) enrichment from salmon farm activities in a northern Chilean Fjord. Estuarine, Coastal and Shelf Science 166, 131-142. doi.org/10.1016/j.ecss.2015.03.02.

Gili, J.-M., Coma, R., 1998. Benthic suspension feeders: their paramount role in littoral marine food webs. Trends in Ecology & Evolution 13, 316-321.

Goebel, N.L., Wing, S.R., Boyd, P.W., 2005. A mechanism for onset of diatom blooms in a fjord with persistent salinity stratification. Estuarine, Coastal and Shelf Science. 64, 546-560.

González, H.E., Calderon, M.J., Castro, L., Clement, A., Cuevas, L.A., Daneri, G., Iriarte, J.L., Lizárraga, L., Martínez, R., Menschel, E., Silva, N., Carrasco, C., Valenzuela, C., Vargas, C.A., Molinet, C., 2010. Primary Production and plankton dynamics in the Reloncaví Fjord and the Interior Sea of Chiloé, Northern Patagonia, Chile. Marine Ecology Progress Series 402, 13-30.

González, H.E., Castro, L., Daneri, G., Iriarte, J.L., Silva, N., Vargas, C.A., Giesecke, R., Sánchez, N., 2011. Seasonal plankton variability in Chilean Patagonia fjords: carbon flow through the pelagic food web of Aysén Fjord and plankton dynamics in the Moraleda Channel basin. Continental Shelf Research 31, 225-243.

González, H.E., Castro, L.R., Daneri, G., Iriarte, J.L., Silva, N., Tapia, F., Teca, E., Vargas, C.A., 2013. Land-ocean gradient in haline stratification and its effects on plankton dynamics and trophic carbon fluxes in Chilean Patagonian fjords (47-50ºS). Progress in Oceanography 119, 32-47.

Gutiérrez, M.H., Galand, P.E., Moffat, C., Pantoja, S., 2015. Melting glacier impacts community structure of Bacteria, Archaea and Fungi in a Chilean Patagonia fjord. Environmental Microbiology 17, 3882-3897.doi: 10.1111/1462-2920.12872

Gutiérrez, M.H., Narváez, D., Daneri, G., Montero, P., Pérez-Santos, I., Pantoja, S., 2018. Linking seasonal reduction of microbial diversity to increase in winter temperature of waters of a Chilean Patagonia fjord. Frontiers in Marine Science 5:277. doi: 10.3389/fmars.2018.00277

Greene, V. E., Sullivan, L. J., Thompson, J. K., Kimmerer, W. J., 2011. Grazing impact of the invasive clam *Corbula amurensis* on the microplankton assemblage of the

northern San Francisco Estuary. Marine Ecology Progress Series 431, 183-193. doi: 10.3354/meps09099

Handa, A., Ranheim, A., Olsen, A.J., Altin, D., Reitan, K. I., Olsen, Y., Reinertsen, H., 2012. Incorporation of salmon fish feed and feces components in mussel (*Mytilus edulis*): Implications for integrated multi-trophic aquaculture in cool-temperate North Atlantic waters. Aquaculture 370/371, 40-53. dx.doi.org/10.1016/j.aquaculture.2012.09.030

Hoikkala, L., Tammert, H., Lignell, R., Eronen-Rasimus, E., Spilling, K., Kisand, V., 2016. Autochthonous dissolved organic matter drives bacterial community composition during a bloom of Filamentous Cyanobacteria. Frontiers in Marine Science. 3:111. doi: 10.3389/fmars.2016.00111

Iriarte, J.L., Kusch, A., Osses, J., Ruiz, M., 2001. Phytoplankton biomass in the sub-Antarctic area of the Straits of Magellan (53ºS), Chile during spring–summer 1997/1998. Polar Biology 24, 154-162.

Iriarte, J.L., González, H.E., Liu, K.K., Rivas, C., Valenzuela, C., 2007. Spatial and temporal variability of chlorophyll and primary productivity in surface waters of southern Chile (41.5-43ºS). Estuarine, Coastal and Shelf Science 74, 471-480. doi:10.1016/j.ecss.2007.05.015

Iriarte, J.L., Gonzalez, H.E., 2008. Phytoplankton bloom ecology of the inner Sea of Chiloé, Southern Chile. Nova Hedwigia, Beiheft 133, 67-79.

Iriarte, J.L., Pantoja, S., González, H.E., Silva, G., Paves, H., Labbé, P., Rebolledo, L., Van Ardelan, M., Häussermann, V., 2013. Assessing the micro-phytoplankton response to nitrate in Comau Fjord (42ºS) in Patagonia (Chile), using a microcosms approach. Environmental Monitoring and Assessment 185, 5055-5070. doi 10.1007/s10661-012-2925-1

Iriarte, J.L., Pantoja, S., Daneri, G., 2014. Oceanographic processes in Chilean fjords of Patagonia: from small to large-scale studies. Progress in Oceanography 129, 1-7.

Jacob, B.G., Tapia, F., Daneri, G., Iriarte, J.L., Montero, P., Sobarzo, M., Quiñones, R.A., 2014. Springtime size-fractionated primary production across hydrographic and PAR-light gradients in Chilean Patagonia (41-50ºS). Progress in Oceanography 129, 75-84. doi:10.1016/j.pocean.2014.08.003

Jørgensen, C.B., 1990. Bivalve filter feeding: hydrodynamics, bioenergetics, physiology and ecology. Olsen & Olsen. Fredensborg, Denemar.

Kamjunke, N., Nimptsch, J., Harir, M., Herzsprung, P., Schmitt-Kopplin, P., Neu, T.R., Graeber, D., Osorio, S., Valenzuela, J., Reyes, J.C., Woelfl, S., Hertkorn, N., 2017. Land-based salmon aquacultures change the quality and bacterial degradation of riverine dissolved organic matter. Scientific Reports **7**, 43739. doi: 10.1038/srep43739

Katz, J., 2006. Salmon farming in Chile. In: Chandra, V. (Ed.), Technology, Adaptation, and Exports: How Some Developing Countries Got it Right. World Bank Publications, Washington DC, pp. 193e344.

Kirchman, D.L., 2008. Introduction and overview. In book: Microbial Ecology of the Oceans, second edition. Edited by David L. Kirchman. pp 1-26

Kreeger, D. A., Newell, R. I. E., 1996. Ingestion and assimilation of carbon from cellulotyc bacteria and heterotrophic flagellates by the mussels *Geukensia demisa* and *Mytilus edulis* (Bivalvia, Mollusca). Aquatic Microbial Ecology 11, 205-214

Lander, T., Barrington, K., Robinson, S., MacDonald, B., Martin, J., 2004. Dynamics of the blue mussel as an extractive organism in an integrated multi-trophic aquaculture system. Bulletin of the Aquaculture Association of Canada 104, 19-28.

Langdon, C. J., Newell, R. I., 1990. Utilization of detritus and bacteria as food sources by two bivalve suspension-feeders, the oyster *Crassotrea virginica* and the mussel *Geukensia demisa*. Marine Ecology Progress Series 58, 299-310

Lefebvre, S., Barillé, L., Clerc, M., 2000. Pacific oyster (Crassostrea gigas) feeding responses to a fish-farm effluent. Aquaculture 185-198.

Legendre, L., Rassoulzadegan, F. 1996. Food-web mediated export of biogenic carbon in oceans: hydrodynamic control. Marine Ecology Progress Series 145: 179-193.

Lonsdale, D. J., Cerrato, R. M., Holland, R., Mass, A., Holt, L., Schaffner, R. A., Pan, J., Caron, D. A., 2009. Influnce of suspension-feeding bivalves on the pelagic food webs of shallow, coastal embayments. Aquatic Biology 6, 263-279. doi: 10.3354/ab00130

Lucas, J., Koester, I., Wichels, A., Niggemann, J., Dittmar, T., Callies, U., Wiltshire, K.H., Gerdts, G., 2016. Short-term dynamics of North Sea bacterioplankton-dissolved organic matter coherence on molecular level. Frontiers in Microbiology 7:321. doi: 10.3389/fmicb.2016.00321

MacDonald, B. A., Robinson, S. M. C., Barrington, K. A., 2011. Feeding activity of mussels (Mytilus edulis) held in the field at an integrated multi-trophic aquaculture (IMTA) site (Salmo salar) and exposed to fish food in the laboratory. Aquaculture 314, 244-251. doi:10.1016/j.aquaculture.2011.01.045

Mayr, C., Försterra, G., Häussermann, V., Wunderlich, A., Grau, J., Zieringer, M., Altenbach, A., 2011. Stable isotope variability in a Chilean fjord food web: implications for N- and C-cycles. Marine Ecology Progress Series 428, 89-104. doi: 10.3354/meps09015

Monaghan, M. T., Thomas, S. A., Minshall, W., 2001. The influence of filter-feeding benthic macroinvertebrates on the transport and deposition of particulate organic matter and diatoms in two streams. Limnology and Oceanography 46 (5), 1091-1099.

Montero, P., Daneri, G., González, H.E., Iriarte, J.L., F.J., Tapia, F.J. Lizárraga, L., Sanchez, N., Pizarro, O., 2011. Seasonal variability of primary production in a fjord ecosystem of the Chilean Patagonia: implications for the transfer of carbon within pelagic food webs. Continental Shelf Research 31, 202-215. doi:10.1016/j.csr.2010.09.003

Montero, P., Daneri, G., Tapia, F., Iriarte, J. L., Crawford, D., 2017a. Diatom blooms and primary production in a channel ecosystem of central Patagonia. Latin American Journal of Aquatic Research. 45, 999-1016. doi: 10.3856/vol45-issue5-fulltext-16

Montero, P., Pérez-Santos, I., Daneri, G., Gutiérrez, M.H., Igor, G., Seguel, R., Purdie, D., Crawford, D.W., 2017b. A winter dinoflagellate bloom drives high rates of primary production in a Patagonian fjord ecosystem. Estuarine, Coastal and Shelf Science 199,105-116. doi: 10.1016/j.ecss.2017.09.027

Nagata, T., 2008. Organic matter-bacteria interactions in seawater. In book: Microbial Ecology of the Oceans, second edition. Edited by David L. Kirchman. pp 207-241.

Nimptsch, J., Woelfl, S., Osorio, S., Valenzuela, J., Ebersbach, P., von Tuempling, W., Palma, R., Encina, F., Figueroa, D., Kamjunke, N., Graeber, D., 2015. Tracing dissolved organic matter (DOM) from land-based aquaculture systems in North Patagonia streams. Science of the Total Environment 537, 129-138. doi.org/10.1016/j.scitotenv.2015.07.160.

Officer, C.B., Smayda, T. J., Mann, R. (1982): Benthic Filter Feeding: A Natural Eutrophication Control. Marine Ecology Progress Series 9, 203-210.

Paredes, M.A., Montecino, V., 2011. Size diversity as an expression of phytoplankton community structure and the identification of its patterns on the scale of fjords and channels. Continental Shelf Research 31, 272-281.

Peharda, M., Richardson, C. A., Mladineo, I., Sestanovic, S., Popovic, Z., Bolotin, J., Vrgoc, N., 2007. Age, growth and population structure of *Modiolus barbatus* from the Adriatic. Marine Biology 151 (2), 629-638.

Petersen, J.K., Bougrier, S., Smaal, A.C., Garen, P., Robert, S., Larsen, J.E.N., Brummelhuis, E., 2004. Intercalibration of mussel Mytilus edulis clearance rate measurements. Marine Ecology Progress Series 267, 187-194 DOI 10.3354/meps267187.

Pinhassi, J., Hagström, A., 2000. Seasonal succession in marine bacterioplankton. Aquatic Microbial Ecology 21, 245-256. doi: 10.3354/ame021245

Pizarro, G., Astoreca, R., Montecino, V., Paredes, M.A., Alarcón, G., Uribe, P., Guzmán, L., 2005. Patrones espaciales de la abundancia de la clorofila, su relación con la productividad primaria y la estructura de tamaños del fitoplancton en Julio y Noviembre de 2001 en la región de Aysén (43°-46°S). Revista Ciencia y Tecnología Marina 28(2), 27-42.

Prins, T. C., Smaal, A. D., Dame, R. F., 1998. A review of the feedbacks between bivalve grazing and ecosystem processes. Aquatic Ecology 31, 349-358

Quiñones, R. A., Fuentes, M., Montes, R. M., Soto, D., León-Muñoz, J., 2019. Environmental issues in Chilean salmon farming: a review. Reviews in Aquaculture 11, 375-402. doi: 10.1111/raq.12337

Quiroga, E., Ortíz, P., González-Saldías, R., Reid, B., Tapia, F.J., Pérez-Santos, I., Rebolledo, L., Mansilla, R., Pineda, C., Cari, I., Salinas, N., Montiel, A., Gerdes, D.,

2016. Seasonal benthic patterns in a glacial Patagonian fjord: The role of suspended sediment and terrestrial organic matter. Marine Ecology Progress Series 561, 31-50. doi: 10.3354/meps11903

Reid, G. K., Liutkus, M., Bennett, A., Robinson, S.M.C., MacDonald, B., Page, F., 2010. Absorption efficiency of blue mussels (*Mytilus edulis* and *M. trossulus*) feeding on Atlantic salmon (*Salmo salar*) feed and fecal particulates: Implications for integrated multi-trophic aquaculture. Aquaculture 299, 165-169

Rice, M. A., 1999. Control of eutrophication by bivalves: Filtration of particulates and removal of nitrogen through harvest of rapidly growing stocks. Journal of Shellfish Research 18 (1), 275.

Rice, M.A., Valliere, A., Gibson, M., Ganz, A., 2000. Ecological significance of the Providence River quahogs: Population filtration. Journal of Shellfish Research 19 (1), 580.

Riisgård, H.U., 1988. Efficiency of particle retention and filtra- tion rate in 6 species of northeast American bivalves. Marine Ecology Progress Series 45, 217-223

Riisgård, H.U, Larsen, P.S., 2000. A comment on experimental techniques for studying particle capture in filter-feeding bivalves. Limnology and Oceanography 45,1192-1195

Rosa, M., Ward, J. E., Shumway, S. E., 2018. Selective capture and ingestion of particles by suspension-feeding bivalve molluscs: A review. Journal of Shellfish Research 37 (4): 727-746 DOI: 10.2983/035.037.0405

Sarà, G., Zenone, A., Tomasello, A., 2009. Growth of *Mytilus galloprovincialis* (mollusca, bivalvia) close to fish farms: a case of integrated multi-trophic aquaculture within the Tyrrhenian Sea. Hydrobiologia 636, 129-136.

Schneider, W., Pérez-Santos, I., Ross, L., Bravo, L., Seguel, R., Hernández, F., 2014. On the hydrography of Puyuhuapi Channel (Chilean Patagonia). Progress in Oceanography 129, 8-18. doi10.1016/j.pocean.2014.03.007

Sebens, K., Sarà, G., Nishizaki, M., 2016. Energetics, particle capture, and growth dynamics of benthic suspension feeders. S. Rossi (ed.), Marine Animal Forest. DOI 10.1007/978-3-319-17001-5_17-1

Silva, N., 2008. Dissolved oxygen, pH, and nutrients in the austral Chilean channels and fjords. Progress in the oceanographic Knowledge of Chilean interior waters, from Puerto Montt to Cape Horn. N. Silva & S. Palma (eds.) Comité Oceanográfico Nacional – Pontificia Universidad Católica de Valparaíso, Valparaíso, pp. 37-43.

Silva, N., Rojas, N., Fedele, N., 2009. Water masses in the Humboldt Current System: Properties, distribution and the nitrate deficit as a chemical water mass tracer for Equatorial Subsurface Water off Chile. Deep-Sea Research II 56, 1004-1020.

Sievers, H., Silva, N., 2008. Water masses and circulation in austral Chilean channels and fjords. Progress in the Oceanographic Knowledge of Chilean Interior Waters, from Puerto Montt to Cape Horn, Comité Oceanográfico Nacional – Pontificia Universidad Católica de Valparaíso, Valparaíso, pp. 53-58.

Soto, D., Norambuena, F., 2004. Evaluation of salmon farming effects on marine systems in the inner seas of southern Chile: A large-scale mensurative experiments. Journal of Applied Ichthyology, 20, 493-501.

Stuart, V., Klumpp, D. W., 1984. Evidence for food-resource partitioning by kelp-bed filter feeders. Marine Ecology Progress Series 16, 27-37.

Sverdrup, H.U., 1953. On conditions for the vernal blooming of phytoplankton. ICES Journal of Marine Science 18, (3) 287-295.

Voudanta, E., Kormas, K. A., Monchy, S., Delegrange, A., Vincent, D., Genitsaris, S., Christaki, U., 2016. Mussel biofiltration effects on attached bacteria and unicellular eukaryotes in fish-rearing seawater. PeerJ 4:e1829; DOI 10.7717/peerj.1829

Wang X., Olsen L.M., Reitan K.I., Olsen Y., 2012. Discharge of nutrient wastes from salmon farms: environmental effects, and potential for integrated multi-trophic aquaculture. Aquaculture Environment Interactions 2, 267-283. doi: 10.3354/aei00044

Winter, J. E., 1978. A review on the knowledge of suspension-feeding in lamellibranchiate bivalves, with special reference to artificial aquaculture systems. Aquaculture 13, 1-33

Wright, R.T., Coffin, R.B., Ersing, C.P., Pearson, D., 1982. Field and laboratory measurements of bivalve filtration of natural marine bacterioplankton. Limnology and Oceanography 27, 91-98

Yoshikawa, T., Kanemata, K., Nakase, G., Eguchi, M., 2012. Microbial mineralization of organic matter in sinking particles, bottom sediments and seawater in a coastal fish culturing area. Aquaculture Research 43, 1741-1755

Yoshikawa, T., Eguchi, M., 2013. Planktonic processes contribute significantly to the organic carbon budget of a coastal fish-culturing area. Aquaculture Environment Interactions 4, 239-250. doi: 10.3354/aei00085

Yoshikawa, T., Kanemata, K., Nakase, G., Eguchi, M., 2017. Microbial decomposition process of organic matter in sinking particles, resuspendable particles, and bottom sediments at coastal fish farming area. Fisheries Science 83, 635-647 DOI 10.1007/s12562-017-1098-9

Zapata-Hernández, G., Sellanes, J., Mayr, C., Muñoz, P., 2014. Benthic food web in the

Comau fjord, Chile (42°S): preliminary assessment including a site with chemosynthetic activity. Progress in Oceanography 129, 149-158. http://dx.doi.org/10.1016/j.pocean.2014.03.005

II. OBJECTIVE AND SCIENTIFIC QUESTION OF THE THESIS

The main objectives of the thesis were to describe, study, and analyze the main pathways of production and utilization of autochthonous and allochthonus carbon by bacterial communities and their relative importance in sustaining benthic filter feeding communities.

For this purpose, this thesis was focused around the following questions:

1. What is the seasonal to interannual variability of the primary production and bacterial secondary production in the Puyuhuapi fjord? (Chapter 1: paper I and II and manuscript III presenting preliminary results)

This topic was evaluated through different multidisciplinary sampling campaigns that were carried out during different study periods (2008-2009, 2013-2015 and 2018) in the Puyuhuapi station. The results obtained allowed us to better understand which are the main factors that trigger the seasonal productivity cycle in fjords, and which are the key species (phytoplankton/bacteria) in terms of significance to annual productivity.

2. What is the relative importance of organic matter sources (allochthonous versus autochthonous) to the composition and activity of the bacterial community? (Chapter 2: manuscript IV presenting preliminary results)

This topic was evaluated via experimental studies (microcosm) designed to explore the response of bacterial community to different types of dissolved organic matter (DOM): autochthonous (derived from phytoplankton) and allochthonous (derived from pellet salmon food). The experiments were carried out seasonally in the Puyuhuapi study area during summer and winter periods between 2017-2019. The results obtained allowed us to identify which taxa are involved in the degradation of different DOM sources and what are the bacterial production rates according to the DOM pool (allochthonous versus autochthonous).

3. What is the relative importance of organic matter sources (allochthonous versus autochthonous) to the diet of benthic suspension feeder *Aulacomya atra*? (Chapter 3: manuscript V presenting preliminary results)

This topic was evaluated via stable isotopes measurements and via feeding experimental studies conducted in the Puyuhuapi study area during summer and winter periods between 2018 and 2019. The experiments were designed to explore the ingestion rates of *Aulacomya atra* fed with different types of organic matter: autochthonous (bacterial and microplanktonic community <150 µm) and allochthonous (pellet salmon food). Stable isotope measurements in *A*. *Atra* tissues reflected food assimilation in situ. The results obtained allowed us to examine the role of different food sources (autochthonous versus allochthonous) in the diet of this species and elucidate what are the major in situ carbon sources contributing to the nutrition of these organisms.

4. What is the role of the bacterial community and benthic suspension feeders in carbon cycling within the Puyuhuapi fjord? (Chapter 4: Synthesis)

This topic corresponds to the final part of this thesis and combines the results of previous chapters to build a synthesis on carbon flux within a fix Puyuhuapi fjord sampling station.

III. LIST OF PUBLICATIONS AND MANUSCRIPTS IN PREPARATION INCLUDED IN THIS THESIS

PAPER I: P., Montero, G., Daneri, F.J., Tapia, J.L., Iriarte, D.W., Crawford. (2017). Diatom blooms and primary production in a channel ecosystem of central Patagonia. Latin American Journal of Aquatic Research 45 (5): 999–1016.

PAPER II: P., Montero, I., Pérez-Santos, G., Daneri, M.H., Gutiérrez, G., Igor, R., Seguel, D., Purdie, D.W., Crawford. (2017). A winter dinoflagellate bloom drives high rates of primary production in a Patagonian fjord ecosystem. Estuarine, Coastal and Shelf Science 199 : 105–116.

PAPER III: G., Daneri, I., Pérez-Santos, **P., Montero,** B.G., Jacob, M.H., Gutiérrez, C., Medel, M., Castillo, O., Pizarro. Atmospheric-ocean forcing on phytoplankton productivity and carbon flow through the microbial food web in a Patagonia fjord system (44°S). Manuscript in preparation.

PAPER IV: P., Montero, M.H., Gutiérrez, G., Daneri, B.G., Jacob, J., Pavez. Influence of dissolved organic matter on bacterial production and community composition in fjords of Chilean Patagonia. Manuscript in preparation.

PAPER V : P., Montero, M., Coppari, F., Betti, G., Bavestrello, G., Daneri. Ingestion rates of benthic suspension feeder *Aulacomya atra* under different sources of organic matter (autochthonous and allochthonous). Manuscript in preparation.

IV. LIST OF OTHER PUBLICATIONS

During the period of my PhD work I have also contributed to the following publications:

1. B.G. Jacob, F. Tapia, R.A. Quiñones, R. Montes, M. Sobarzo, W. Schneider, G. Daneri, C.E. Morales, **P. Montero**, H.E. González (2018). Major changes in diatom abundance, productivity and net community metabolism in a windier and dryer coastal climate in the southern Humboldt Current. Progress in Oceanography 168: 196-209, doi:10.106/j.pocean.2018.10.001

2. J.L., Iriarte, Cuevas, L.A., Cornejo, F., Silva, N., González, H.E., Castro, L., **Montero, P**., Vargas, C.A., Daneri, G. (2018). Low spring primary production and microplankton carbon biomass in Subantarctic Patagonian channels and fjords (50-53°S). Arctic, Antarctic, and Alpine Research 50: 1, doi:10.1080/15230430.2018.1525186

3. Gutiérrez M.H., Narváez, D., Daneri, G., **Montero, P**., Pérez-Santos, I., Pantoja, S. (2018). Linking seasonal reduction of microbial diversity to increase in winter temperature of waters of a Chilean Patagonia fjord. Frontiers of Marine Science, doi:10.3389/fmars.2018.0027.

PAPER I

Diatom blooms and primary production in a channel ecosystem of central Patagonia

Lat. Am. J. Aquat. Res., 45(5): 999-1016, 2017
DOI: 10.3856/vol45-issue5-fulltext-16

Research Article

Diatom blooms and primary production in a channel ecosystem of central Patagonia

Paulina Montero[1,2], Giovanni Daneri[1,2], Fabián Tapia[2,3,4], Jose Luis Iriarte[2,5,6] & David Crawford[1]
[1]Centro de Investigación en Ecosistemas de la Patagonia (CIEP), Coyhaique, Chile
[2]COPAS Sur-Austral, Universidad de Concepción, Concepción, Chile
[3]Departamento de Oceanografia, Universidad de Concepción, Concepción, Chile
[4]INCAR, Universidad de Concepción, Concepción, Chile
[5]Instituto de Acuicultura, Universidad Austral de Chile, Puerto Montt, Chile
[6]Fondap-IDEAL, Universidad Austral de Chile, Valdivia, Chile
Corresponding author: Paulina Montero (pmontero@ciep.cl)

ABSTRACT. Here we report on the seasonal productivity cycle at a fixed station in the Puyuhuapi Channel (44ºS, 73ºW), Chilean Patagonia. The analysis of *in situ* water column data and longer-term records of satellite-derived surface ocean color (Chl-*a*) highlighted two contrasting seasons. A more productive period occurred between August and April, where depth-integrated gross primary production (GPP) estimates ranged from 0.1 to 2.9 g C m^{-2} d^{-1}, and a shorter, less-productive season lasted from May to July with GPP ranging from 0.03 to 0.3 g C m^{-2} d^{-1}. Diatoms of the genera *Pseudo-nitzschia*, *Skeletonema* and *Chaetoceros* dominated the phytoplankton, and showed a pronounced seasonality greatly influenced by prevailing environmental conditions. Warmer waters were associated with high concentrations of *Pseudo-nitzschia* spp., while high abundances of *Skeletonema* spp. and *Chaetoceros* spp. were associated with fresher silicate-rich waters. A marked *Skeletonema* spp. bloom characterized the onset of the productive season in August 2008, and with some exceptions, the highest levels of GPP (1.5 to 2.9 g C m^{-2} d^{-1}) were measured when *Skeletonema* dominated the phytoplankton community. Reduced production (low GPP) was observed during periods of increased discharge from the Cisnes River, whereas the "spring" diatom bloom (or late winter bloom in Puyuhuapi Channel) observed during August 2008 coincided with a ~50% drop in the freshwater discharge. We therefore suggest that periods of intensive freshwater Input, that increase the silicic acid concentrations in the upper layers, provide ideal growing conditions for diatoms as the freshwater flow subsequently recedes. Principal component analysis (PCA) suggests that a decrease in salinity, increase in silicic acid concentration, and growth of *Skeletonema* spp. and *Chaetoceros* spp., are probably key factors in the annual cycle of GPP in Puyuhuapi Channel.

Keywords: primary production, diatom blooms, channels ecosystem, Chilean fjords.

INTRODUCTION

Chilean Patagonia encompasses one of the most extensive fjord regions in the world (Iriarte *et al.*, 2014), with oceanographic conditions that can sustain unique ecosystems. Among the highly productive ecosystems found in the SE Pacific, the coastal upwelling system that spans the coast of central and northern Chile has been the focus of most research conducted over the past decades, although it is restricted to a relatively narrow coastal band (<50 km, Montecino *et al.*, 2006). Patagonian fjords, on the other hand, comprises *ca*. 240,000 km^2 of highly productive coastal waters (Iriarte *et al.*, 2014), and constitute eco-systems that have an enormous potential in terms of total productivity, transfer of food to higher trophic levels, and vertical export of carbon. Improving our understanding of primary productivity cycles and composition of phytoplankton communities in these waters is therefore of fundamental importance.

The productivity cycle within a number of Patagonian channels and fjords (41-51ºS) has been typically described in terms of two contrasting seasons: a productive season characterized by a marked spring diatom bloom followed by pulsed productivity events dominated by a sequence of different phytoplankton species, and then a non-productive season that predominantly features small phytoplankton cells (Iriarte

Corresponding editor: Sergio Palma

et al., 2007; Iriarte & González, 2008; Czypionka *et al.*, 2011; Montero *et al.*, 2011; Paredes & Montecinos, 2011). Despite considerable recent research, uncertainty remains regarding the factors that modulate the seasonal phase change within Chilean fjords system, from non-productive in late autumn-winter to highly productive in late winter-autumn. It is not clear whether similar factors control productivity cycles throughout of these channels and fjords, or whether the main environmental controls on these productivity cycles may vary across the region.

The onset of the productive season in Patagonia has been associated with mesoscale changes in the direction and intensity of meridional winds. Montero *et al.* (2011) reported that the onset of the productive season in the Reloncaví Fjord (41°S, 72°W) coincided with a late winter relaxation of prevailing poleward winds. This seasonal shift in predominant winds and improved light conditions has been shown to influence the productivity of fjord and channel ecosystems (Iriarte & González, 2008; Montero *et al.*, 2011). More locally, hydrodynamic patterns within a given fjord are strongly modulated by freshwater discharges, which can either intensify or weaken an estuarine type of circulation, and may modulate the occurrence and spatial extent of phytoplankton blooms (Goebel *et al.*, 2005; González *et al.*, 2013; Iriarte *et al.*, 2014; Jacob *et al.*, 2014). Freshwater inputs appear to stabilize the water column and increase the concentration of silicic acid in the upper layers, favouring the occurrence of diatom dominated phytoplankton blooms.

Diatoms are capable of fast growth and are well adapted to form large blooms (Wetz & Wheeler, 2007). They account for *ca*. 40% of the total oceanic primary production, making them a significant component of marine food webs (Sarthou *et al.*, 2005; Amin *et al.*, 2012), and key players in global biogeochemical cycles (Ferland *et al.*, 2011). Certain species are able to completely dominate a phytoplankton community (Legrand *et al.*, 2003). In Chilean fjords ecosystems, diatoms are known to represent a significant component of the overall phytoplankton biomass (Iriarte *et al.*, 2001; Cassis *et al.*, 2002; Alves-de-Souza *et al.*, 2008; Iriarte & González, 2008). In addition to efficiently transferring energy to higher trophic levels, diatoms make a significant contribution to the downward transfer of organic carbon (Iriarte *et al.*, 2007; González *et al.*, 2010; Montero *et al.*, 2011; Iriarte *et al.* 2013). Diatoms occur in highest abundance during the Patagonian fjord spring bloom, and are generally dominated by *Skeletonema* spp. and associated with high levels of primary production (Iriarte *et al.*, 2007; Montero *et al.*, 2011). Despite the significant contribution that diatoms make to overall fjord productivity, important questions remain unanswered: for example, which are the main factors that trigger diatom blooms in specific fjords and channels, and which are the key species in terms of significance to annual productivity.

In this study, we characterized the seasonal productivity cycle at a fixed station in the Puyuhuapi Channel (44ºS, 73ºW). The hydrography of the northern Puyuhuapi Channel is characterized by an estuarine type of circulation with a vertical two layer structure comprising a highly variable 5-10 m freshwater layer, and a more uniform and saltier subpycnocline layer (Schneider *et al.*, 2014 and references therein). The deeper saline water originates from Sub-Antarctic Surface Water characteristic of open ocean environments in these latitudes (Chaigneau & Pizarro, 2005). The freshwater upper layer is supplied by the Cisnes River, several smaller rivers, and rain runoff, and it is a permanent feature of the Puyuhuapi Channel, although the degree of mixing with deeper saline water is seasonally variable (Schneider *et al.*, 2014). Based on recent studies in other fjord ecosystems in the region, we hypothesized that the seasonal pattern of productivity in the Puyuhuapi area may be strongly influenced by freshwater input with a consequential series of blooms dominated by diatom species.

Gross primary production (GPP) and community respiration (CR) were measured in order to assess the trophic status of the water column in the study area on a seasonal basis. Finally, we analyzed the relationships between the main environmental variables (phytoplankton species composition, dissolved inorganic nutrients, temperature, salinity) and their potential association with seasonal changes in GPP of the study area.

MATERIALS AND METHODS

Study area and sampling strategy

The study area consisted of a fixed station in the Puyuhuapi Channel (44°42.6'S, 72°44.4'W), located at an average depth of 230 m and *ca.* 5 km NW of the Cisnes River mouth (Fig. 1). The channel runs in a N-NE direction and connects directly to the open sea via the Moraleda Channel at its mouth, and through the Jacaf Channel near the head (Schneider *et al.*, 2014; Fig. 1). The Puyuhuapi Channel receives freshwater discharge from the Ventisqueros (north and south), Pascua and Cisnes rivers, plus additional inputs from numerous creeks and rainfall (Calvete & Sobarzo, 2011). The freshwater input drives an estuarine type of circulation, with a thin layer of freshwater flowing from the continent, on top of a thicker layer of oceanic Sub-

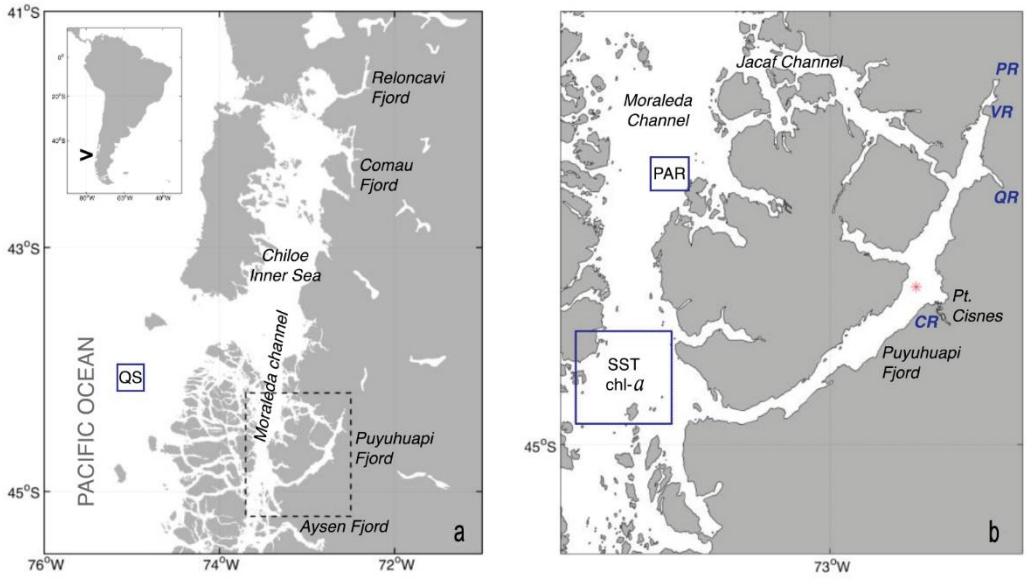

Figure 1. Location of the study area in Chilean Patagonia (A: dashed box enlarged in b) and position of the time series station in the Puyuhuapi Channel (B: asterisk). Solid squares in a and b indicate the points/areas for which satellite data on wind stress (QS), photosynthetically active radiations (PAR), Sea Surface Temperature (SST) and surface chlorophyll-*a* concentration (Chl-*a*) were obtained (see methods for details). Position of main rivers are indicated in (b) and correspond to the Cisnes (CR), Queulat (QR), Ventisquero (VR), and Pascua (PR) rivers.

Antarctic Waters (Silva *et al.*, 2009; Schneider *et al.*, 2014). Freshwater coming from the continent is loaded with silicic acid while Sub-Antarctic Waters (SAAW) is enriched with nitrate and orthophosphate (Silva, 2008). The Puyuhuapi Channel is an area of intensive salmon farming, and consequently receives large inputs of particulate and dissolved organic matter from both autochthonous (phytoplankton productivity) and allochthonnnous sources (freshwater input and aquaculture).

Sampling at the Puyuhuapi station was conducted approximately at monthly intervals between January and November 2008. Additionally, in summer (January 2008 and March 2009), autumn (April 2009), winter (May and July 2008) and spring (October 2008 and September 2009) intensive sampling campaigns (over periods of 3-7 consecutive days) were conducted.

Variability of atmospheric and sea-surface conditions

Satellite-derived data, dating from 2003 through late 2009, were used to characterize variability in atmospheric forcing and sea-surface conditions in an area close to the study site (Fig. 1). Data on wind stress were collected over a 25×25 km area from daily QuikSCAT level-3 images. This area represented a pixel centered on 44°7.5'S, 75°7.5'W, and located *ca*. 170 km NW of the channel's mouth. Good data were available from 96.6% of the 2471 records available for this pixel in 2003-2009. A time series of photosynthetically available radiation (PAR) for the same period was produced from 8-d composites of SeaWifs images (level 3), with a 9 km resolution. Data were acquired for a pixel centered at 44°30'S, 73°25'W, in the Moraleda Channel and *ca*. 50 km NW of the channel's mouth. Out of the 295 PAR images available for this pixel in 2003-2009, 98% contained good data. Finally, data on sea surface temperature (SST) and surface chlorophyll-*a* concentration (Chl-*a*) were acquired from 8 d composites of MODIS-Aqua images (level 3) with a 4 km spatial resolution. Weekly values of surface Chl-*a* were obtained by averaging data collected over a 5×7 pixel area (*i.e.*, 20×35 km) located near the mouth of the fjord, encompassing the latitudes 44°47.5'-44°57.7'S and longitudes 73°37.5'-73°22.5'W (see Fig. 1). Out of the 273 Chl-*a* and 314 SST images available for this area in 2003-2009, 78% and 94% contained good data. Any gaps within these four records of satellite-derived data were filled using linear interpolation.

Hydrography, nutrients and phytoplankton composition

Profiles of temperature, salinity and dissolved oxygen were gathered during each sampling day using a CTDO profiler (Ocean Seven 304, IDRONAUT, Italy). Water samples for analyses of inorganic nutrients and phyto-

plankton abundance were collected from three discrete depths (2, 10, and 20 m) using a 30-L Niskin bottle (General Oceanic, Inc.).

Water samples for nutrient analyses were filtered through GF/F filters and frozen at -20°C prior to spectrophotometric analysis in the laboratory. Concentrations of nitrate, orthophosphate, and silicic acid were determined according to methods given in Strickland & Parsons (1968). Samples for phyto-plankton cell counts were stored in 250 mL clear plastic bottles, preserved in a 1% Lugol iodine solution (alkaline). From each sample, a 10 mL sub-sample was placed in a sedimentation chamber and allowed to settle for 12 h (Utermöhl, 1958) prior to identification at 40 × and 100 × under an inverted microscope (Carl Zeiss, Axio Observer A.1). Estimates of phytoplankton (in the size range 2-200 μm) abundance at the three discrete depths were integrated down to 20 m, using a trapezoidal method.

Total and size-fractionated primary production and chlorophyll-*a* (Chl-*a*)

During each field campaign between January 2008 and September 2009, *in situ* experiments were conducted to measure gross primary production (GPP) and community respiration (CR). A total of 37 experiments were conducted and water incubations were performed on samples obtained from the same sampling depths indicated above (2, 10 and 20 m). GPP and CR rates were estimated from changes in dissolved oxygen concentrations observed during *in situ* incubation of light and dark bottles (Strickland, 1960). Water from the Niskin bottles was transferred into 125 mL (nominal volume) borosilicate bottles (gravimetrically calibrated) using a silicone tube. Five time-zero bottles, five light bottles, and five dark bottles were used for each incubation depth. Water samples were collected at dawn and were incubated during the whole light period (incubating time was 10.0 ± 1.3 h in the productive period (September-April) and 7.0 ± 0.7 h during the non-productive season (May-August). Time-zero bottles were fixed at the beginning of each experiment, whereas the light and dark incubation bottles were attached to a surface-tethered mooring system. The samples were incubated at the depth from which they were collected. Dissolved oxygen concentrations were determined according to the Winkler method (Strickland & Parsons, 1968), using an automatic Metrohom burette (Dosimat plus 865) and by visual end-point detection. Problems with the power supply in this isolated location prevented us from using a photometric end point detector. Daily GPP and CR rates were calculated as follows: GPP = (mean [O_2] light bottles - mean [O_2] dark bottles); CR = (mean [O_2] time zero bottles - mean [O_2] dark bottles) / (hours of incubation) ×24. GPP and CR values were converted from oxygen to carbon units using a conservative photosynthetic quotient (PQ) of 1.25 (Williams & Robertson, 1991) and a respiratory quotient (RQ) of 1. Discrete-depth estimates of GPP and CR rates were integrated down to 20 m using a trapezoidal method. The 20 m depth layer approximately corresponded to the 1% light depth measured during the productive season (21.7 ± 8.2; calculated using a Secchi disc as in Poole & Atkins, 1929). For total Chl-*a* determinations, three 100 mL water samples were filtered from each of the three sampling depths through MFS (Micro-filtration Systems) glass-fiber filters with 0.7 μm nominal pore size. Following filtration, samples were immediately frozen (-20ºC) until later analysis; pigments were extracted with 90% v/v acetone and then measured using a Turner Design TD-700 fluorometer according to standard procedures (Parsons *et al.*, 1984).

In order to provide additional information on the relative contribution of various size fractions to overall PP, primary production (PP) was estimated using the ^{14}C method (Steeman-Nielsen, 1952). Water samples were collected using Niskin bottles at 2, 10 and 20 m and placed in 100 mL polycarbonate bottles (two clear + one dark) to which were added 40 μCi labelled sodium bicarbonate ($NaH^{14}CO_3$). Bottles were placed in a natural light incubator for 4 h during the time of day with highest irradiance (approximately between 11 AM and 3 PM). Temperature was regulated in the incubator using a flow through of surface seawater. For the subsurface samples, light intensity was attenuated using a screen to approximately the level found at the depth where water was collected. Samples were manipulated under subdued light conditions during pre- and post-incubation periods. At the end of the incubations, samples were filtered for size fractionation as described below. Filters were then placed in 20 mL plastic scintillation vials and stored at -15ºC prior to analysis. Within one month, filters were dried in a fume-chamber for 48 h and the excess inorganic carbon was removed with HCl fumes for 24 h; 10 mL Ecolite liquid scintillation cocktail was added to vials which were then processed using a Beckman Liquid Scintillation Counter.

Size fractionation was performed on Chl-*a* and PP (post-incubation) samples using the following three size classes to separate the phytoplankton assemblage: microphytoplankton (>20 μm), nanophytoplankton (2-20 μm), and picophytoplankton (<2 μm). This size fractionation was performed on samples in three sequential steps: (1) for the nanophytoplankton fraction (2-20 μm), seawater (100 mL) was pre-filtered using 20 μm Nitex mesh and collected on a 2 μm Nuclepore

filter; (2) for the picoplankton fraction (0.2-2.0 µm), the filtrate from the 2 µm Nuclepore filter in step (1) was filtered again using a 0.7 µm MFS glass-fiber filter; (3) for the whole phytoplankton community, seawater (100 mL) was filtered through a 0.7 µm MFS glass-fiber filter. The microphytoplankton fraction was obtained by subtracting the estimated PP and Chl-*a* in steps (1) and (2) from the estimates in step (3). Depth-integrated values of PP and Chl-*a* were calculated down to 20 m, using trapezoidal integration. This size fractionation of Chl-*a* and PP was only conducted during the intensive sampling campaigns.

Statistical analyses

Cross-correlation analyses was conducted to test for associations between satellite-derived time series of meridional wind stress, surface PAR, SST, and surface Chl-*a* concentration. To assemble a set of data vectors that were amenable to these analyses, a weekly series of cumulative meridional wind stress was produced based on the initial and final dates of the composite Chl-*a* images. Climatologies of PAR, SST, and Chl-*a* series were used to calculate anomalies prior to the computation of lagged correlation coefficients. The significance levels for each of these analyses were computed according to the method outlined in Sciremammano (1979, see equations 7 and 16b). The 2 m sampling depth was used to represent upper mixed layer conditions because the pycnocline was located at approximately 6 m depth. The non-parametric Kruskal-Wallis test (H) was used to examine and test for significance of seasonal differences in GPP and CR. Clustering analysis was used to investigate temporal variation in phytoplankton community structure. A similarity matrix among samples was calculated using the Bray & Curtis method (1957), and a dendrogram constructed based on group average linkage. Given that several of our environmental measurements were non-independent (*e.g.*, salinity, temperature, inorganic nutrients, phytoplankton community, Chl-*a*), a principal component analysis (PCA) was conducted to combine these original variables into statistically independent environmental predictors for GPP. The data used in this analysis for temperature, salinity, and inorganic nutrients were depth-averages calculated over the upper 20 m, whereas phytoplankton community and Chl-*a* data corresponded to depth-integrated values calculated down to 20 m. A Spearman correlation analysis (r_s) was then conducted to assess the degree of association between these principal components and log-transformed GPP values.

RESULTS

Variability of atmospheric and sea-surface conditions

The 7-year time series of QuikSCAT data on meridional wind stress showed an alternation of periods with equatorward and poleward winds, each persisting for several days, with a scale of correlation of *ca*. 5 d, and no apparent annual pattern (Fig. 2a). This lack of a clear pattern of seasonal variability in wind forcing, and its high inter-annual variability, became more apparent in the climatology computed for wind stress (Fig. 2e). In contrast, surface PAR and SST time series showed a strong annual cycle (Figs. 2b-2c), which was also reflected by the low inter-annual variability (*i.e.* small error bars) shown in the climatology (Figs. 2f-2g).

Average daily PAR varied between *ca*. <10 E m^{-2} d^{-1} in winter and >40 E m^{-2} d^{-1} in summer, and average surface temperature between ca. 8 to 9°C in winter and >14°C in summer. Surface chlorophyll concentrations, on the other hand, showed high intra- and inter-annual variability with peaks of over 30 mg m^{-3} (Fig. 2d).

The climatology shows the existence of two distinct seasons: a low- chlorophyll (presumably less productive) period that spans the autumn and winter months (April-August) with concentrations averaging <5 mg m^{-3}, and a productive season in spring and summer (September-March) with average concentrations typically in the range 10 to 20 mg m^{-3}, typified by high seasonal variability (Fig. 2h). Phytoplankton biomass tended to increase rapidly in spring (September-October), decay in summer (December-January), and increase again in late summer (February-March, see Fig. 2h).

Surface PAR and SST were highly correlated at lag = 0 ($r = 0.64$, $P < 0.001$) and reached maximum correlation ($r = 0.77$, $P < 0.001$) at ~40 day lag, with increases in PAR preceding increases of SST. This high correlation combined with the lack of a clear annual signal in wind stress variability, suggest that the strong seasonality in SST near the Puyuhuapi Channel is mostly driven by changes in solar radiation. Weak but significant zero-lag correlations were found for surface Chl-*a* and cumulative meridional wind stress ($r = 0.35$, $P < 0.01$), PAR anomalies ($r = 0.30$, $P < 0.01$) and SST anomalies ($r = 0.23$, $P < 0.01$).

***In situ* hydrographic and nutrient measurements**

In general, the water column was characterized by a two-layer structure largely determined by vertical salinity changes (Fig. 3a), with the halocline usually being found above 10 m depth. Salinity profiles showed a surface layer (2 m) of low-salinity water (<20), particularly during productive periods (2008 and 2009) (Fig. 3a), while surface values >20 (21 to 25) were recorded during the non-productive period (2008). Below this layer and between 10 and 100 m depth, salinity fluctuated between 30 and 33 (Fig. 3a). Surface temperature decreased from >18°C in January 2008 to <7°C in August 2008 and from >15ºC in March 2009

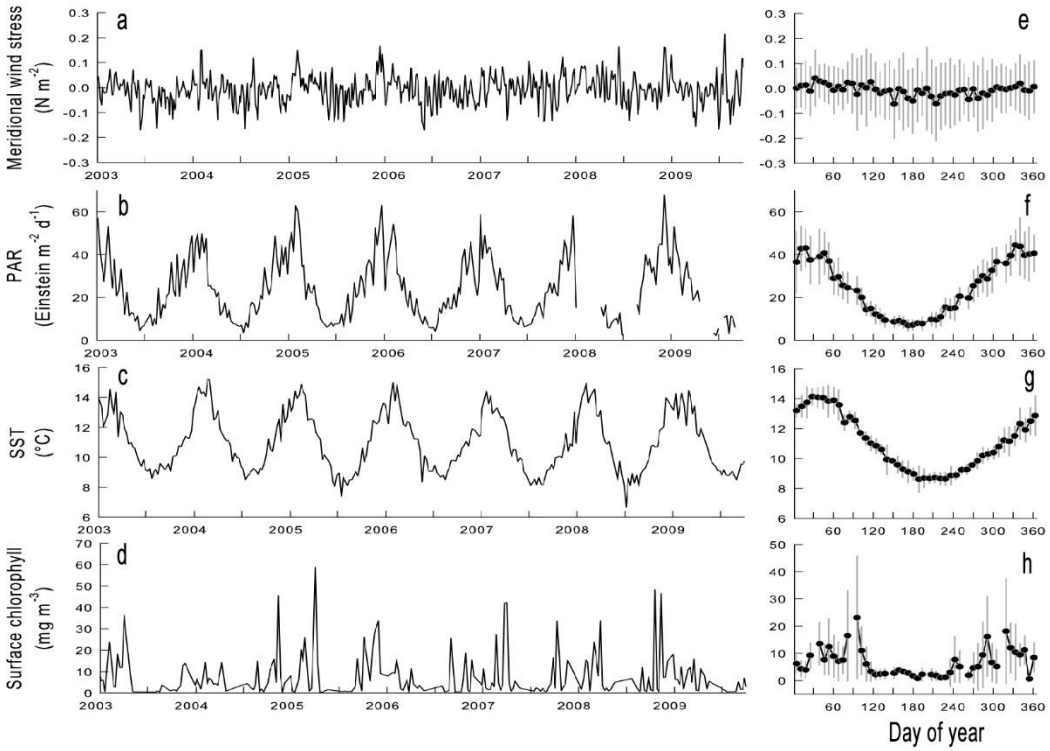

Figure 2. Satellite-derived time series (A-D) and climatologies (E-H) of meridional wind stress (A, E), surface PAR, *i.e.*, Photosynthetically Available Radiation (B, F), Sea Surface Temperature (C, G), and surface chlorophyll-*a* concentration (D, H). Wind stress data were obtained from daily QuikSCAT level-3 images with ~25 km spatial resolution, PAR data were produced from 8-d composites of SeaWifs images with 9 km resolution, whereas SST and Chl-*a* were extracted from 8-d composites of MODIS-Aqua images with 4 km resolution. See methods for more details. Symbols and error bars in E-H correspond to the mean ±1 SD.

to <9ºC in September 2009; these are similar ranges to those shown for the time series station (Figs. 2c, 2g) although maximum temperatures at the time series station were a little lower because of the greater influence of oceanic water. Thermal stratification decreased during May/June 2008 and September 2009, while winter cooling lead to a thermal inversion in July and August 2008 (Fig. 3b). Surface oxygen concentration increased from 3 to 4 mL O_2 L^{-1} during warm periods to 6 to 8 mL O_2 L^{-1} during cold periods. Maximum values (>8 mL O_2 L^{-1}) were recorded in October 2008 (Fig. 3c). Low dissolved oxygen concentrations (<3 mL O_2 L^{-1}) were observed during January and February 2008 below 20 and 30 m of depth, respectively. Then in April and September 2009 low oxygen values were also recorded below 50 m depth. For the rest of the study period, values were >3 mL O_2 L^{-1} into the depth layer.

Low surface concentrations of nitrate (<3 µM) were observed within the top 10 m during the productive periods in 2008 and 2009, while maximum concentrations of >10 µM were recorded in the non-productive months (Fig. 4a). Low orthophosphate concentrations (<1 µM) were observed within the top 10 m throughout most of the sampling, except in July 2008 and September 2009, where values ranged between 1 and 3.5 µM, with highest values occurring in September 2009 at 2 and 10 m. Orthophosphate concentrations were typically >1 µM at 30 m depth. Orthophosphate concentrations did not show marked seasonal differences (Fig. 4b). Silicic acid concentrations showed moderate surface concentrations (4 to 30 µM) during 2008 and very high surface values (100 to 132 µM) in 2009. Generally, concentrations were higher in surface waters than at 20 m depth (Fig. 4c). The increase in surface silicic acid coincided with the inputs of low-salinity water in the same period (shown in Fig. 3a).

Primary production and community respiration

The highest rates of GPP derived from O_2 incubations (0.3 to 47.9 mmol O_2 m^{-3} d^{-1}) were recorded at 2 m depth, whereas the lowest values (0.1 to 11.8 mmol O_2 m^{-3} d^{-1}) were observed at 20 m depth (Fig. 5a). CR rates showed the highest values at 20 m depth (0.3 to 27.9 mmol O_2 m^{-3} d^{-1}), with the lowest observed at 10 m

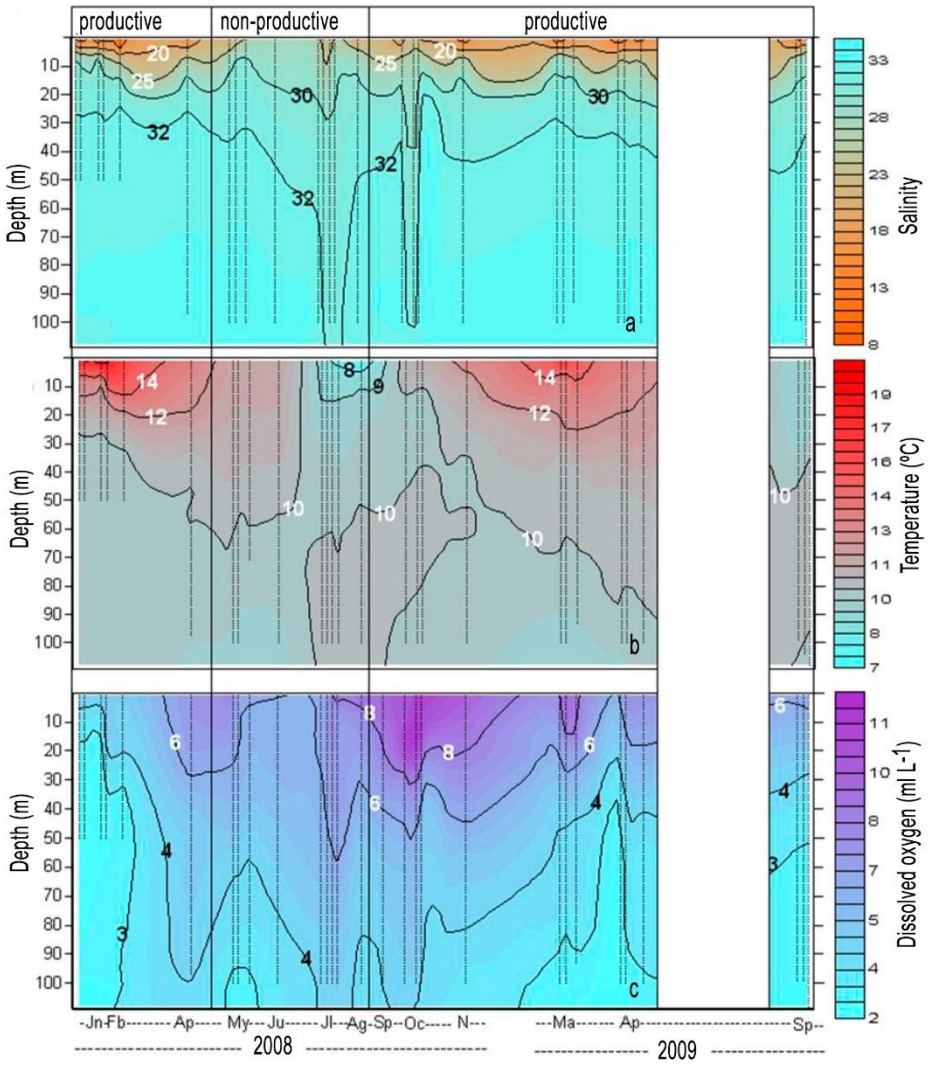

Figure 3. Temporal variability of hydrographic profiles at the Puyuhuapi Channel station: a) salinity, b) temperature (ºC), and c) dissolved oxygen (ml L^{-1}). Sampling times and depth range are indicated by dotted vertical lines.

depth (0.1 to 17.3 mmol O_2 m^{-3} d^{-1}). GPP/CR ratio, used as an index for the trophic status of the system, ranged from 0.01 to 17, with most experiments indicating a heterotrophic metabolism (GPP/CR < 1) (Fig. 5b).

Depth-integrated GPP showed significant differences between the productive and non-productive seasons ($H = 8$, $P < 0.05$, $n = 37$). Integrated GPP (down to 20 m) ranged from 0.03 to 2.9 g C m^{-2} d^{-1} over the annual cycle (Fig. 5c) with highest rates recorded during late winter and spring in August (2.9 g C m^{-2} d^{-1}) and November 2008 (2.4 g C m^{-2} d^{-1}), and low values (0.03 to 0.3 g C m^{-2} d^{-1}) observed from May to July 2008. Depth-integrated CR rates also showed significant seasonal differences ($H = 6$, $P < 0.05$, $n = 37$), with values ranging from 0.04 to 3.4 g C m^{-2} d^{-1} over an annual cycle (Fig. 5c). Maximum values were recorded in November 2008 (3.2 g C m^{-2} d^{-1}) and April 2009 (3.4 g C m^{-2} d^{-1}), while low rates (0.04 to 1 g C m^{-2} d^{-1}) were consistently observed in winter 2008.

The highest estimates of contribution of microphytoplankton (>20 µm) to total ^{14}C fixation (mean: 49%; range: 15 to 83%; n = 15) were recorded during the productive season, whereas picophytoplankton (<2 µm) showed maximum contributions (mean: 60%; range: 38 to 81%) during the non-productive season (Table 1). The nanophytoplankton size class (2-20 µm) did not show significant seasonal variations in contribution to total ^{14}C fixation. Depth-integrated GPP and PP values were positively correlated ($r_s = 0.68$, $P < 0.05$, $n = 23$; Fig. 6), although the slope of the regression indicates that ^{14}C derived PP tends to be higher than GPP.

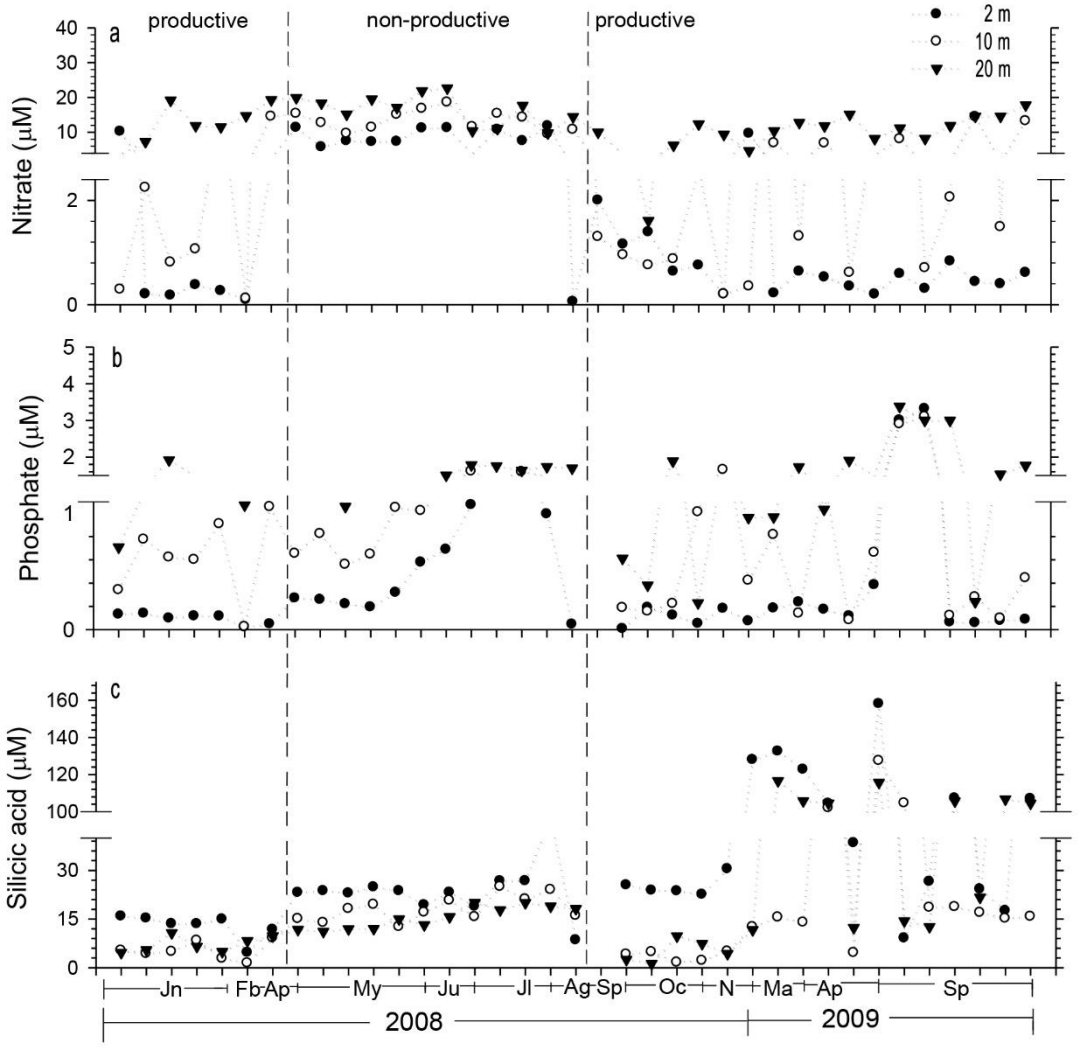

Figure 4. Temporal variability of dissolved inorganic nutrients at three depths at the Puyuhuapi station: a) nitrate, b) phosphate, and c) silicic acid. Sampling times and depths are indicated by dots.

Chlorophyll-*a* and phytoplankton community

The maximum depth-integrated phytoplankton biomass (166.2 mg Chl-*a* m^{-2}) was observed in late winter (August 2008), and coincided with the highest GPP measurements (2.9 g C m^{-2} d^{-1}); other than this maximum value, biomass ranged from 2.8 to 75.7 mg Chl-*a* m^{-2} in the productive season and 1.8 to 15.8 mg Chl-*a* m^{-2} in the non-productive season (Fig. 7).

Estimates of Chl-*a* partitioned into three size classes (<2 µm, 2-20 µm, >20 µm) revealed the dominance of picophytoplankton (<2 µm) during the non-productive season (May and July) throughout the entire water column. During the productive season, picophytoplankton was dominant only in January 2008 and September 2009 at 20 m depth (Table 1). Chlorophyll in the nanophytoplankton size class (between 2-20 µm) did not show significant variations over the annual cycle. Strong seasonal variability was observed for microphytoplankton (>20 µm), which showed a high relative contribution to total Chl-*a* during the productive season at 2 and 10 m depths; in contrast, low relative contributions were recorded during the non-productive season (Table 1).

Diatoms were the dominant group within the community, averaging 92% of microscope-examined phytoplankton abundance, followed by dinoflagellates (7%) and ciliates (1%).

Of the total recorded diatoms, five genera were the most abundant during the study period: *Skeletonema* (*S. costatum* and *S. pseudocostatum*), *Pseudo-nitzschia* (*Pseudo-nitzschia* spp. group *seriata* and *Pseudo-nitzschia* spp. group *delicatissima*), *Chaetoceros* (*Ch. decipiens*, *Ch. convolutus*, *Ch. didymus*, *Ch. radicans*, *Ch. curvisetus*, *Ch. debilis*, *Ch. similis*, *Ch. mitra* and

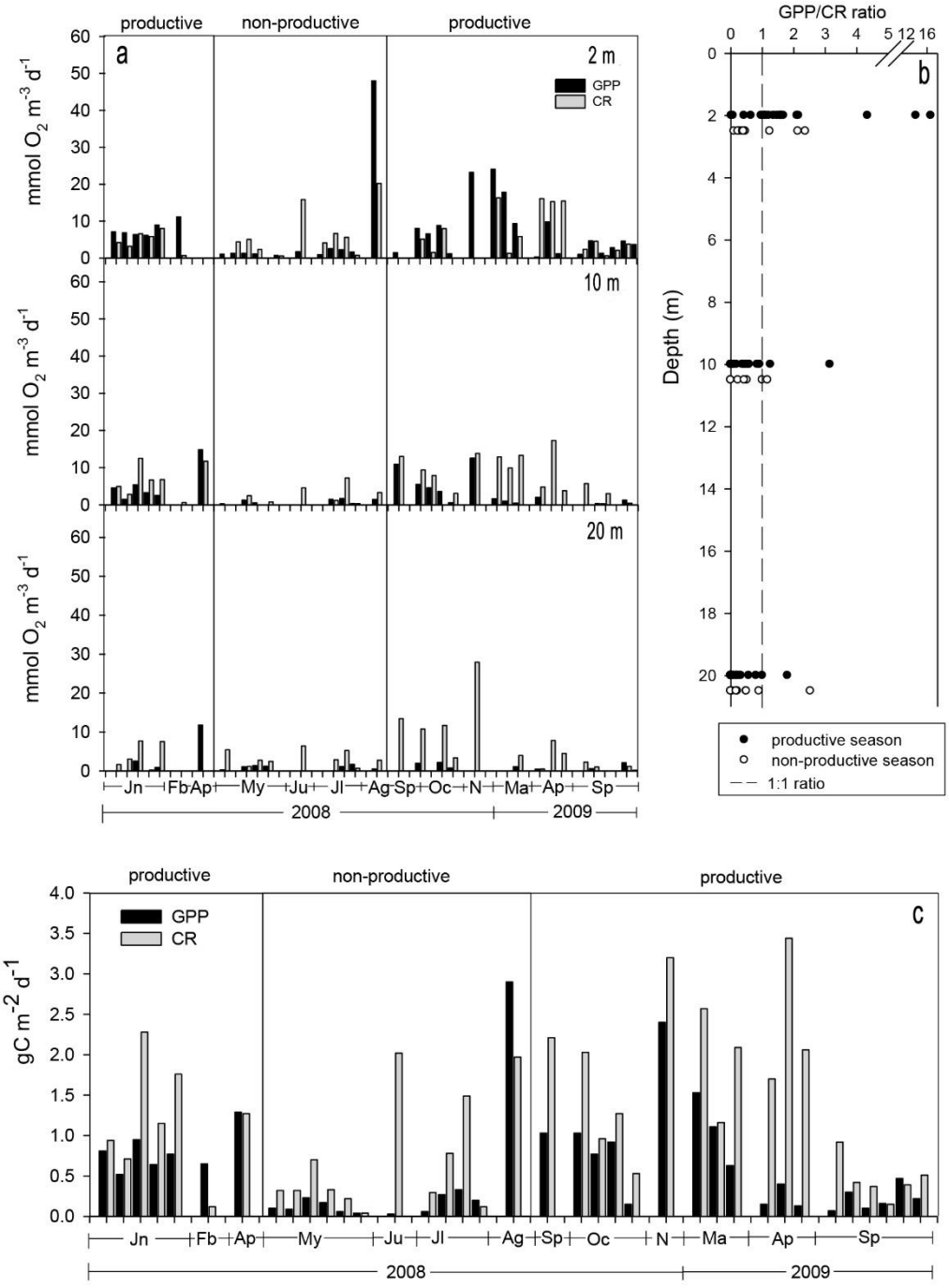

Figure 5. Vertical variability of gross primary production (GPP) and community respiration (CR) rates at the Puyuhuapi station. a) Seasonal changes in GPP and CR at three depths, b) vertical profile of GPP/CR ratios for all samples, and c) depth-integrated GPP and CR using dissolved oxygen changes converted to carbon units.

Chaetoceros sp.), *Thalassiosira* (*T. anguste-lineata*, *T. excentrica* and *Thalassiosira* sp.) and *Leptocylindrus* (*L. minimus* and *L. danicus*) (Fig. 8a).

Skeletonema spp., *Pseudo-nitzschia* spp. and *Chaetoceros* spp. were dominant and in more than one sampling contributed with values >50% of the total phytoplankton abundance, unlike *Thalassiosira* spp. and *Leptocylindrus* spp. that never reached or exceeded this percentage (Fig. 8a). The highest abundances of *Skeletonema* spp. (113×10^9 cells m^{-2}), *Pseudo-nitzschia* spp. (163×10^9 cells m^{-2}) and *Chaetoceros* spp. (63×10^9 cells m^{-2}) were recorded in August, February and October

Table 1. Contribution of microphytoplankton (>20 µm), nanophyoplankton (2-20 µm), and picophytoplankton (<2 µm) to total carbon (^{14}C) fixation rates. Total chlorophyll-*a* concentration at three depths during the intensive sampling, at the Puyuhuapi station.

Depth	Date	Contribution to total carbon fixation (%)			Contribution to total chlorophyll-*a* (%)		
		< 2 µm	2-20 µm	>20 µm	< 2 µm	2-20 µm	>20 µm
2 m	January 08	25	44	31	22	31	47
	May 08	38	29	33	39	32	29
	July 08	52	35	13	40	18	42
	October 08	11	20	69	26	13	61
	March 09	5	14	81	17	13	70
	April 09	8	11	81	44	9	47
	September 09	7	21	72	21	19	60
10 m	January 08	39	22	39	32	19	50
	May 08	65	27	8	45	31	24
	July 08	57	32	11	44	23	33
	October 08	11	16	73	19	17	64
	March 09	22	26	52	15	11	74
	April 09	7	10	83	39	22	39
	September 09	10	48	41	30	14	56
20 m	January 08	51	30	20	45	25	30
	May 08	79	11	10	50	38	12
	July 08	67	22	11	44	23	33
	October 08	41	36	23	25	11	64
	March 09	60	24	15	21	24	55
	April 09	40	22	38	41	48	11
	September 09	9	70	20	39	24	37

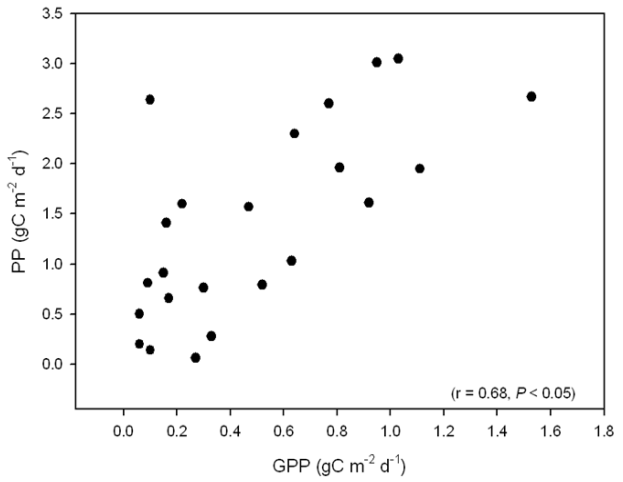

Figure 6. Correlation between gross primary production (GPP), using the oxygen technique, and primary production (PP) rates, estimated using ^{14}C technique at the Puyuhuapi station, during the intensive sampling campaigns.

2008, respectively, while low abundance values (5 to 25×10^9 cells m^{-2}) were observed in April (*Skeletonema* spp. and *Pseudo-nitzschia* spp.) and September 2009 (*Chaetoceros* spp.). *Thalassiosira* spp. were present throughout the study period, showing the highest (64×10^9 cells m^{-2}) and lowest ($<2\times10^9$ cells m^{-2}) abundances in January 2008 and September 2009, respectively. *Leptocylindrus* spp. were only recorded in September 2009 with abundances between 5 and 10×10^9 cells m^{-2} (Fig. 8a).

Diatoms that contributed <10% of the total phytoplankton abundance per sample such as *Actinoptychus vulgaris*, *Corethron hystrix*, *Coscinodiscus* sp., *Detonula pumila*, *Ditylum brightwellii*, *Eucampia zodiacus*, *Lauderia annulata*, *Guinardia delicatula*, *Melosira nummuloides*, *Rhizosolenia setigera*, *Rhizosolenia pungens*, *Stephanopyxis turris*, *Licmophora* sp., *Asterionella glacialis*, *Grammatophora marina*, *Thalasionema nitzschoides*, *Cylindrotheca closterium*, *Pleurosigma* sp. and *Nitzschia longissima* were grouped into the "other diatoms" group. This group showed its highest abundances (5 to 11×10^9 cells m^{-2}) in September 2009, however, it was in May 2008 when they dominated the phytoplankton community with abundances between 2 and 7×10^9 cells m^{-2}. The lowest abundances ($<1\times10^9$ cells m^{-2}) were observed in January and February 2008.

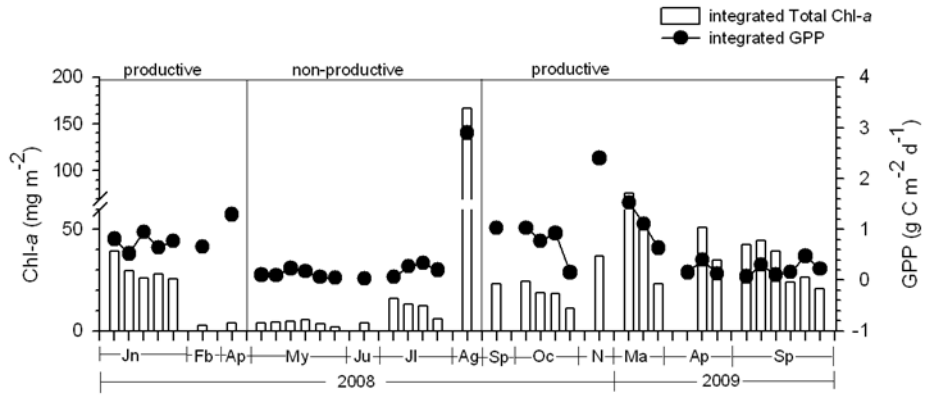

Figure 7. Temporal variability of depth-integrated (0-20 m) total chlorophyll-*a* and GPP at the Puyuhuapi station.

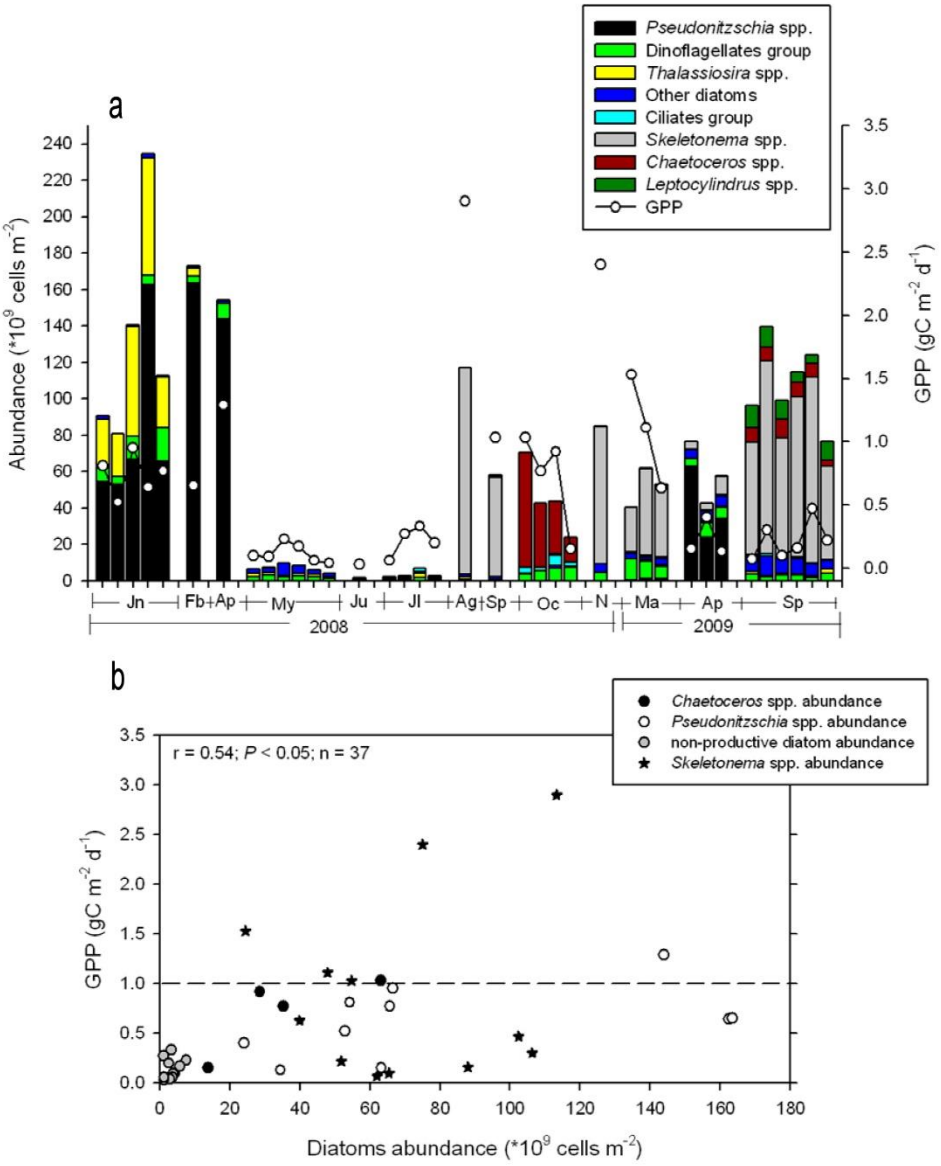

Figure 8. Phytoplankton abundance at the Puyuhuapi station. a) Seasonal variability and composition of phytoplankton community, and b) correlation between the dominant diatoms group and GPP values. R value and significance refers to correlation coefficient for all data points.

The dinoflagellate group was composed by *Dinophysis acuminata*, *D. acuta*, *D. rotundatum*, *Heterocapsa triquetra*, *Protoceratium reticulatum*, *Protoperidinium claudicans*, *Protoperidinium* spp., *Gymnodinium* spp., *Ceratium fusus*, *Ceratium lineatum*, *Ceratium* spp., *Prorocentrum micans* and *Alexandrium catenella*. They were present throughout the study period, except *A. catenella* that was only recorded in March 2009. The highest average abundances of this group were observed in January 2008 ($10 \pm 6\times10^9$ cells m^{-2}) and March 2009 ($9 \pm 2\times10^9$ cells m^{-2}) when sea surface temperature was >13ºC (shown in Fig. 3b). Low abundances were recorded during the non-productive season (0.3 to 3×10^9 cells m^{-2}).

The ciliate group had highest abundances of between 2 and 6×10^9 cells m^{-2} in October 2008 and minimum concentrations (0.2 to 1×10^9 cells m^{-2}) during the rest of study period.

Seasonal fluctuations in GPP correlated signify-cantly with the abundance of dominant diatoms (r_s = 0.54, n = 37, $P < 0.05$), suggesting that certain key species are mainly associated with high productivity events (Fig. 8b). In fact, the highest levels of GPP (>1.5 g C m^{-2} d^{-1}) were recorded when the phytoplankton community was dominated by *Skeletonema* spp. (Fig. 8b).

The highest phytoplankton abundances (23 to 235×10^9 cells m^{-2}) were generally associated with periods of higher productivity, whereas lowest abundances (2 to 10×10^9 cells m^{-2}) occurred during the non-productive season. However, a rapid increase in phytoplankton abundance (117×10^9 cell m^{-2}) was observed in August 2008 (late winter, non-productive period) suggesting an early onset of spring bloom (Fig. 8a).

The Bray-Curtis cluster analysis (based on the square root transformed phytoplankton abundance) detected four well-defined groups of samples and revealed a seasonal variability (Fig. 9) that coincided with the dominance of certain diatoms during an annual cycle (shown in Fig. 8a). Thus, *Pseudonitzschia* spp. was the dominant group recorded from January-April 2008 and April 2009 (productive season, cluster 1, Fig. 9), "other diatoms" group was from May-July 2008 (non-productive season, cluster 2), *Chaetoceros* spp. dominated the phytoplankton community in October 2008 (productive season, cluster 3) and *Skeletonema* spp. were dominant from August-November 2008, March 2009, and September 2009 (productive season, cluster 4) (Fig. 9).

The principal component analysis (PCA) showed a first (PC1) and second principal component (PC2) that explained 30% and 26.1% of total variance, respect-tively (Fig. 10a). PC1 was positively loaded with salinity and nitrate, while Chl-*a*, silicic acid, *Chaetoceros* spp. and *Skeletonema* spp. were found to be negatively loaded. The second PC was found to be related to a few variables; while salinity and phosphate were positively loaded to PC2, variables such as temperature and *Pseudo-nitzschia* spp. were found to be negatively loaded. The PCA analysis clearly separated three seasonal groups according to different environmental variables: a) a winter group related to salinity, nitrate and orthophosphate, b) a summer-autumn group related to temperature and abundance of *Pseudo-nitzschia* spp. (also dinoflagellates) and c) spring group associated with silicic acid and elevated Chl-*a*, and abundance of *Skeletonema* spp. and *Chaetoceros* spp. (Fig 10b). In this last group March 2009 (Ma09) is an exception because it corresponds to a summer month.

GPP was significantly correlated with PC1 (r_s = -0.6, n = 13, $P < 0.05$) but not with PC2 (r_s = -0.2, n = 13, $P > 0.05$) (Fig. 11).

DISCUSSION

The analysis of our *in situ* data and longer term records of satellite-derived surface Chl-*a* suggest that the productive season in the northern Puyuhuapi channel begins in late winter (August) and extends until autumn (April). The shorter non-productive season, on the other hand, spans the May-July period, *i.e.*, from late autumn to winter. The transition between these two periods appears to be rather abrupt, although the resolution of our *in situ* observations does not allow us to strongly substantiate this argument. However, similar shifts in other Patagonian fjords have been ascribed to fjord-scale hydrographic changes driven by a seasonal changes in mesoscale wind forcing and solar radiation (Iriarte & González, 2008; Montero *et al.*, 2011; Jacob *et al.*, 2014).

The non-productive season coincides with the seasonal solar radiation minimum, a stronger influence of saltier oceanic waters and a weakening of freshwater driven estuarine circulation, with consequent reduction in water column stratification. Saltier water is driven by predominant westerly winds from the Moraleda Channel into the Puyuhuapi Channel through the Jacaf Channel. In contrast, during the productive season (spring/summer, autumn), estuarine circulation tends to prevail and generates more pronounced water column stratification that is further promoted by increased solar radiation. The freshwater surface layer exits the Puyuhuapi Channel through the Jacaf Channel as water from the Cisnes River is pushed to the north and out towards the Moraleda channel. Overall, the hydrography

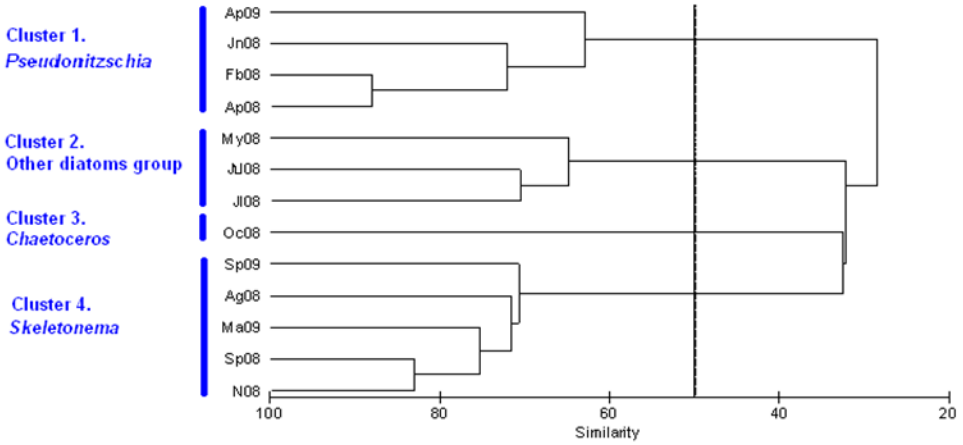

Figure 9. Similarity cluster analysis for samples of the phytoplankton community through the whole sampling campaign.

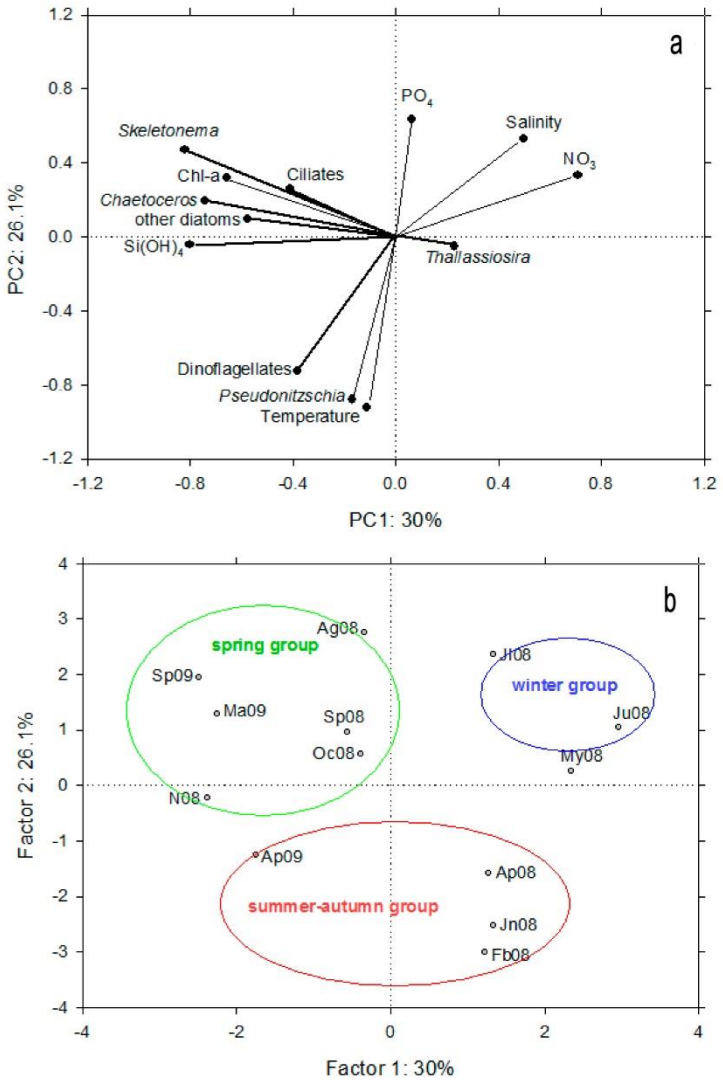

Figure 10. Principal component analysis (PCA). a) Ordination diagram of the physical and chemical (temperature, salinity, and inorganic nutrients correspond to depth-averages calculated over the upper 20 m) and biological variables (phytoplankton community and Chl-*a* data corresponded to depth-integrated values calculated down to 20 m), and b) ordination diagram of the sampling month.

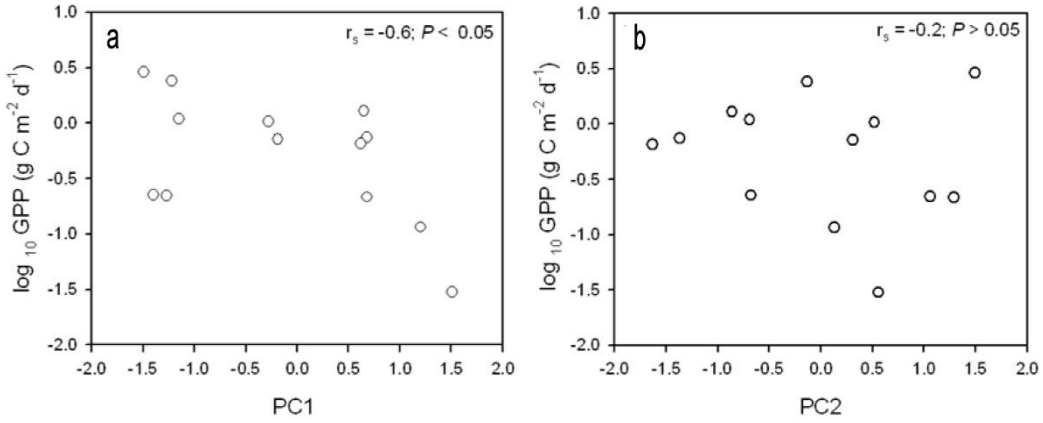

Figure 11. a) Significant correlation between gross primary production (log_{10} GPP) and the first principal component, b) non-significant correlation between gross primary production and the second principal component.

of the whole Puyuhuapi channel is strongly influenced by the Cisnes River, which is the main source of freshwater discharge into this basin (Calvete & Sobarzo, 2011; Schneider *et al.*, 2014).

In general, increased freshwater discharge into the channel coincides with increases in the concentrations of silicic acid (20 to 40 µM) and dissolved organic matter concentration, as well as an increase in underwater light attenuation. Periods of intensified freshwater input following a period of reduced flow seem to provide ideal growing conditions for phytoplankton in the Puyuhuapi Channel (G. Daneri, unpublished). However, the time lag in the phytoplankton's growth response can result in blooms appearing as the freshwater flow recedes. The spring diatom bloom (or late winter bloom in our case) recorded during August 2008 coincided with a ~50% drop in the discharge from the Cisnes River (from 379 $m^3 s^{-1}$ in July to 166 $m^3 s^{-1}$ in August 2008, Fig. 12). In contrast, we recorded reduced phytoplankton activity during periods of increased river freshwater discharge both during the 2008 non-productive period (>200 $m^3 s^{-1}$ between May and July, Fig. 12) and during the 2009 productive period (>200 $m^3 s^{-1}$ between March and September, Fig. 12). Increases in underwater light attenuation associated with increased freshwater input can also explain temporal and spatial variability in phytoplankton production in the fjord areas (Goebel *et al.*, 2005; Jacob *et al.*, 2014; Huovinen *et al.*, 2016).

The range of daily measurements of GPP obtained during the productive season at Puyuhuapi (0.03 to 2.9 g C $m^{-2} d^{-1}$) is in good agreement with high productivity estimates reported by previous studies conducted in other regions of coastal Patagonia, such as the inner sea of Chiloé (41.5º-43ºS; Iriarte *et al.*, 2007), the Reloncaví Fjord (41ºS; Montero *et al.*, 2011), the Aysén region (43º-46ºS; Pizarro *et al.*, 2005) and the Aysén Fjord (45ºS; Lafón *et al.*, submitted). Lowest GPP (0.03 to 0.3 g C $m^{-2} d^{-1}$) and Chl-*a* (2 to 16 mg m^{-2}) values were observed during the non-productive season (excluding August). The high variability of integrated GPP values observed during the productive season in Puyuhuapi reflects the pulsed nature and temporal heterogeneity of productivity cycles in the Patagonian fjord region generally. Productivity cycles in similar coastal environments can be modulated by a combination of biological and hydrodynamic controls, both top down (*e.g.*, grazing by predators; González *et al.*, 2011) and bottom-up processes associated to nutrient depletion and replenishment in the photic layer as a consequence of turbulent eddy formation (Farmer & Freeland, 1983), wind stress (Gibbs, 2001), and tidal currents (Cloern, 1982). The annual depth-integrated GPP estimated for the Puyuhuapi study site (329 g C $m^{-2} y^{-1}$) amounts to *ca*. 40% of the yearly GPP estimated for the exceptionally productive upwelling system off Concepción in central Chile (Daneri *et al.*, 2000; Montero *et al.*, 2007), and is of a similar order to estimates in other highly productive fjord ecosystems, such as the Howe sound (~500 g C $m^{-2} y^{-1}$) on the southern coast of British Columbia (Albright & McRae, 1987) and the Gullmar Fjord (~300 g C $m^{-2} y^{-1}$) on the Swedish Skagerrak coast (Lindahl *et al.*, 2009).

Despite these high primary production rates in the Puyuhuapi Channel, and a predominantly autotrophic metabolism in the surface layer (2 m), heterotrophic activity throughout the water column was also significant throughout the year, probably sustained by the input of allochthonous organic matter of terrestrial origin together with organic material derived from salmon cage farming; these sources would allow to use more organic carbon than that produced within the system (Montero *et al.*, 2011).

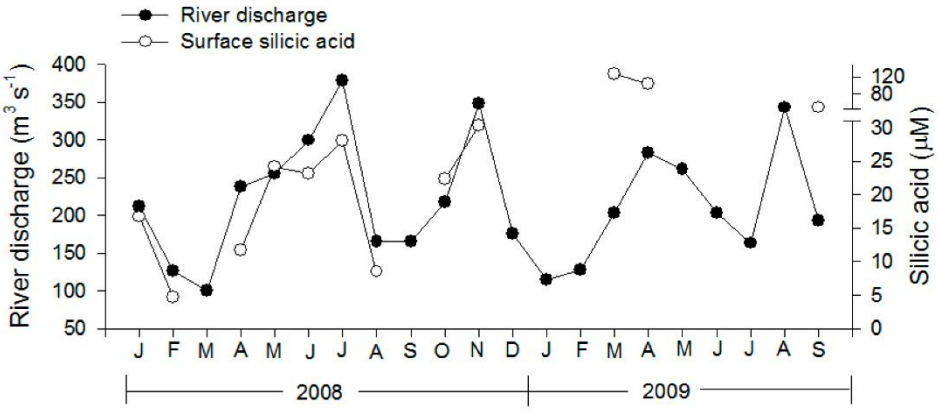

Figure 12. Cisnes River discharge and its association with the silicic acid measurements in surface water, at the Puyuhuapi station.

The phase change between productive and non-productive seasons in Puyuhuapi Channel was reflected in changes in relative abundance of the three-phytoplankton size fractions. Large phytoplankton (>20 µm; mainly diatoms) dominated total abundance and showed the highest contribution to total carbon fixation during the productive season. In contrast, the small picophytoplankton size fraction (<2 µm) was dominant during non-productive season when they made their maximum contributions to primary production rates. These results support the notion that diatoms tend to dominate in the productive season, while small photosynthetic cells become more important under harsher environmental conditions.

In our study, diatoms of the genera *Skeletonema, Chaetoceros* and *Pseudo-nitzschia* dominated and showed a marked seasonality that was reflected in the Bray-Curtis analysis. *Skeletonema* spp. generally dominated between the beginning of the productive season in late winter (August) and spring, while *Chaetoceros* spp. and *Pseudo-nitzschia* spp. dominated the spring and summer-autumn seasons, respectively. The PCA analysis suggested that this marked seasonality is driven by environmental conditions and suggested that warm waters were associated with high concentrations of *Pseudo-nitzschia* spp., whereas elevated abundances of *Skeletonema* spp. and *Chaetoceros* spp. were associated with silicate-rich waters. Our data are consistent with other studies in the southern fjord system of Patagonia, where the phytoplankton community shows recurring changes in dominance and diversity of a number of diatom species (Iriarte *et al.*, 2007; Alves-de-Souza *et al.*, 2008; Iriarte and González, 2008; Montero *et al.*, 2011), some of which have also been recorded in the sediments of the Puyuhuapi Channel (Rebolledo *et al.*, 2005).

The almost complete absence of coexisting species observed during the blooms of *Skeletonema* spp. in August, September and November 2008, and *Pseudo-nitzschia* spp. in February and April 2008 is indicative of a strong competitive ability of these genera. In a highly mixed and disturbed environment, enhanced competitive ability for resources is probably the main factor favouring the dominance of certain species. However it is interesting to note that field and laboratory experiments have shown that *Skeletonema* and *Pseudo-nitzschia* species can release allelophatic compounds (*e.g.*, Lundholm *et al.*, 2005*;* Yamasaki *et al.*, 2010; Xu *et al.*, 2015) that could also be a factor in promoting mono-specific blooms in the channel.

We observed an inverse association between diatoms and concentrations of nitrate and orthophosphate, reflecting the depletion of these nutrients from the water column by this dominant group. Despite the marked drawdown in concentrations during the productive season, nutrients tend not be depleted below the known half saturation constant of several diatoms, (*e.g.*, Eppley *et al.*, 1969); and this likely results from periodic entrainment processes that replenish these nutrients. The resulting continuous availability of nutrients is probably the major factor behind the exceptionally long productive season (from late winter to late autumn), observed for the Puyuhuapi Channel (this study) and Reloncaví Fjord (Montero *et al.*, 2011). The vertical separation in the sources of silicic acid from surface freshwater, and nitrate and phosphate from deeper oceanic water is an interesting feature of these fjord systems (Torres *et al.*, 2014). Because of this, nitrate and phosphate are replenished by entrainment of oceanic water, whereas the levels of silicic acid in Patagonian fjords are enhanced by river input which results in higher than normal ratios for $Si[OH]_4:NO_3$ (5) and $Si[OH]_4:PO_4$ (36). Thus, the observed dominance of diatoms in the phytoplankton

community of the study area was likely facilitated by a high concentration and relatively constant supply of silicic acid. The NO_3:PO_4 ratio (~9) also shows a deviation from Redfield, confirming the preferential assimilation of nitrogen in Chilean fjords (Iriarte *et al.*, 2007, 2013).

Maximum abundance of phytoplankton was observed when *Pseudo-nitzschia* spp. dominated (February to April 2008; 140 to 164×10^9 cells m^{-2}) but the highest GPP rates were associated with the presence of *Skeletonema* spp. during late winter (August; 113×10^9 cells m^{-2}) and spring (November; 75×10^9 cells m^{-2}). The high GPP, but lower abundance conditions associated with *Skeletonema* blooms may be the result of elevated photosynthetic rates shown by species of this genus (Han *et al.*, 1992; Liu *et al.*, 2005; Li *et al.*, 2009) and top-down controls (*e.g.*, grazing) being exerted on this species by zooplankton populations that peak in the area at the beginning of the productive season (González *et al.*, 2011).

GPP rates were significantly correlated with the first principal component, where high GPP values were more associated with negative (high silicic acid concentration, high Chl-*a*, and increase in abundance of *Skeletonema* and *Chaetoceros*) than positive values of PC1 (high nitrate concentration and high salinity). This suggests that the flow of freshwater (with high silicic acid concentration) into the channel could therefore be a key factor in regulating the onset of productive periods, and indeed in the overall annual productivity in Puyuhuapi Channel. Rebolledo *et al.* (2005) have noted a decrease in the contribution of freshwater diatoms to sediments of Puyuhuapi Channel since the 1970s, which they attributed to a decline in rainfall in the area associated with climate change. A variety of productivity proxies in sediments also suggest that periods of low rainfall have coincided with decreased overall productivity within the Puyuhuapi channel (Sepúlveda *et al.*, 2005). Over the whole system of Patagonian Fjords, the silicic acid to NO_3 deficit increases in a southerly direction, with the consequence of more frequent non-diatom blooms to the south (Torres *et al.*, 2014).

We therefore suggest that under a scenario of climate change characterized by reduced freshwater input into Patagonian Fjords such as Puyuhuapi Channel, the reduced supply of silicic acid may consequently alter the composition of phytoplankton community towards an increased proportion of dinoflagellates and/or other non-silicified species (Olsen *et al.*, 2014), and potentially change the biological productivity in the region. Low silicic acid concentrations could specifically also limit the presence of certain productive species in the water column such as *Skeletonema costatum*, which in addition to being associated with high levels of silicate in Patagonian fjords (Alves de Souza *et al.,* 2008; Labbé-Ibañez *et al.*, 2015), has been in this and other studies (Montero *et al.*, 2011) correlated significantly with high rates of primary production (GPP). Accordingly, the impact would not only be on community composition, but also on carbon export fluxes, and on the supply and transfer of food/organic matter to higher trophic levels in these unique coastal ecosystems.

ACKNOWLEDGEMENTS

This research was funded by FONDECYT 1070713 and (partially) COPAS Sur-Austral Program (CONICYT PFB-31) (G. Daneri and P. Montero). Funding for FT and JLI was provided by the COPAS Sur-Austral Program (CONICYT PFB-31).

REFERENCES

Albright, L.J. & S.K. McCrae. 1987. Annual bacterioplankton biomasses and productivities in a temperate west coast Canadian fjord. Appl. Environ. Microbiol., 53(6): 1277-1285.

Amin, S.A., M.S. Parker & E.V. Armbrust. 2012. Microbiol. Mol. Biol. R., 76(3): 667-684.

Alves-de-Souza, C., M.T. González & J.L. Iriarte. 2008. Functional groups in marine phytoplankton assemblages dominated by diatoms in fjords of southern Chile. J. Plankton Res., 30: 1233-1243.

Bray, J.R. & J.T. Curtis. 1957. An ordination of upland forest community of Southern Wisconsin. Ecol. Monogr., 27: 325-349.

Calvete, C. & M. Sobarzo. 2011. Quantification of the surface brackish water layer and frontal zones in southern Chilean fjords between Boca del Guafo (43º30'S) and Estero Elefantes (46º30'S). Cont. Shelf Res., 31(3-4): 162-171.

Cassis, D., P. Muñoz & S. Avaria. 2002. Variación temporal del fitoplancton entre 1993 y 1998 en una estación fija del Seno Aysén, Chile (45º26'S-73º00'W). Rev. Biol. Mar. Oceanogr., 37(1): 43-65.

Chaigneau, A. & O. Pizarro, 2005. Mean surface circulation and mesoscale turbulent flow characteristics in the eastern South Pacific from satellite tracked drifters. J. Geophys. Res., 110, C05014, doi: 10.1029/2004JC002628.

Cloern, J.E. 1982. Does the benthos control phytoplankton biomass in south San Francisco Bay? Mar Ecol. Prog. Ser., 9: 191-202.

Czypionka, T., C.A. Vargas, N. Silva, G. Daneri, H.E. González & J.L. Iriarte. 2011. Importance of mixotrophic nanoplankton in Aysén Fjord (Southern Chile) during austral winter. Cont. Shelf Res., 31(3-4): 216-224.

Daneri, G., V. Dellarossa, R. Quiñones, B. Jacob, P. Montero & O. Ulloa. 2000. Primary production and community respiration in the Humboldt Current System off Chile and associated oceanic areas. Mar. Ecol. Prog. Ser., 197: 41-49.

Eppley, R.W., J.N. Rogers & J.J. McCarthy. 1969. Half-saturation constants for uptake of nitrate and ammonium by marine phytoplankton. Limnol. Oceanogr., 14: 912-920.

Farmer, D.M. & H.J. Freeland. 1983. The physical oceanography of fjords. Prog. Oceanogr., 12: 147-220.

Ferland, J., M. Gosselin & M. Starr. 2011. Environmental control of summer primary production in the Hudson Bay system: the role of stratification. J. Mar. Syst., 88: 385-400.

Gibbs, M.T. 2001. Aspects of the structure and variability of the low-salinity-layer in Doubtful Sound, a New Zealand fjord. New Zeal. J. Mar Freshw. Res., 35: 59-72.

Goebel, N.L., S.R. Wing & P.W. Boyd. 2005. A mechanism for onset of diatom blooms in a fjord with persistent salinity stratification. Estuar. Coast. Shelf. Sci., 64: 546-560.

González, H.E., M.J. Calderon, L. Castro, A. Clement, L.A. Cuevas, G. Daneri, J.L. Iriarte, L. Lizárraga, R. Martínez, E. Menschel, N. Silva, C. Carrasco, C. Valenzuela, C.A. Vargas & C. Molinet. 2010. Primary Production and plankton dynamics in the Reloncaví Fjord and the Interior Sea of Chiloé, Northern Patagonia, Chile. Mar. Ecol. Prog. Ser., 402: 13-30.

González, H.E., L. Castro, G. Daneri, J.L. Iriarte, N. Silva, C.A. Vargas, R. Giesecke & N. Sánchez. 2011. Seasonal plankton variability in Chilean Patagonia fjords: carbon flow through the pelagic food web of Aysén Fjord and plankton dynamics in the Moraleda Channel basin. Cont. Shelf Res., 31: 225-243.

González, H.E., L.R. Castro, G. Daneri, J.L. Iriarte, N. Silva, F. Tapia, E. Teca & C.A. Vargas. 2013. Land-ocean gradient in haline stratification and its effects on plankton dynamics and trophic carbon fluxes in Chilean Patagonian fjords (47-50ºS). Prog. Oceanogr., 119: 32-47.

Huovinen, P., J. Ramírez & I. Gómez. 2016. Underwater optics in sub-Antarctic and Antarctic coastal ecosystems. PLoS ONE, 11(5): e0154887. doi:10. 1371/journal.pone.0154887.

Iriarte, J.L., A. Kusch, J. Osses & M. Ruiz. 2001. Phytoplankton biomass in the sub-Antarctic area of the Straits of Magellan (53ºS), Chile during spring-summer 1997/1998. Polar Biol., 24: 154-162.

Iriarte, J.L., H.E. González, K.K. Liu, C. Rivas & C. Valenzuela. 2007. Spatial and temporal variability of chlorophyll and primary productivity in surface waters of southern Chile (41.5-43ºS). Estuar. Coast. Shelf Sci., 74: 471-480.

Iriarte, J.L. & H.E. Gonzalez. 2008. Phytoplankton bloom ecology of the inner Sea of Chiloé, Southern Chile. Nova Hedwigia, Beiheft, 133: 67-79.

Iriarte, J.L., S. Pantoja, H.E. González, G. Silva, H. Paves, P. Labbé, L. Rebolledo, M. Van Ardelan & V. Häussermann. 2013. Assessing the micro-phyto-plankton response to nitrate in Comau Fjord (42ºS) in Patagonia (Chile), using a microcosms approach. Environ. Monit. Assess., 185: 5055-5070.

Iriarte, J.L., S. Pantoja & G. Daneri. 2014. Oceanographic processes in Chilean fjords of Patagonia: from small to large-scale studies. Prog. Oceanogr., 129: 1-7.

Jacob, B.G., F. Tapia, G. Daneri, J.L. Iriarte, P. Montero, M. Sobarzo & R.A. Quiñones. 2014. Springtime size-fractionated primary production across hydrographic and PAR-light gradients in Chilean Patagonia (41-50ºS). Progr. Oceanogr., 129: 75-84.

Lafón, A., P. Montero, G. Daneri, J.L. Iriarte, V. San Martín, M. Araya & C.A. Vargas. Allochthonous organic carbon sources and primary production in the Aysén Fjord, northern Patagonia. (submitted).

Legrand, C., K. Rengefors, G.O. Fistarol & E. Granéli. 2003. Allelopathy in phytoplankton - biochemical, ecological and evolutionary aspects. Phycologia, 42(4): 406-419.

Li, C., B. Zhu, H. Chen, Z. Liu, B. Cui, J. Wu, B. Li, H. Yu & M. Peng. 2009. The relationship between the *Skeletonema costatum* red tide and environmental factors in Hongsha Bay of Sanya, South China Sea. J. Coastal Res., 25(3): 651-658.

Lindahl, O., L. Andersson & A. Belgrano. 2009. Primary phytoplankton productivity in the Gullmar Fjord, Sweden: an evaluation of the 1985-2008 time series. Swed. Environ. Protec. Agency Rep., 6309, 35 pp.

Liu, D., J. Sun, J. Zou & J. Zhang. 2005. Phytoplankton succession during a red tide of *Skeletonema costatum* in Jiaozhou Bay of China. Mar. Pollut. Bull,. 50: 91-94.

Lundholm, N., P.J. Hansen & Y. Kotaki. 2005. Lack of allelopathic effects of the domoic acid-producing marine diatom *Pseudo-nitzschia multiseries*. Mar. Ecol. Prog. Ser., 288: 21-33.

Montecino, V., M.A. Paredes, P. Paolini & J. Rutllant. 2006. Revisiting chlorophyll data along the coast in north-central Chile, considering multiscale environmental variability. Rev. Chil. Hist. Nat., 79: 213-223.

Montero, P., G. Daneri, L.A. Cuevas, H.E. González, B. Jacob, L. Lizárraga & E. Menschel. 2007. Productivity cycles in the coastal upwelling area of Concepción: the importance of diatoms and bacterioplankton in the organic carbon flux. Prog. Oceanogr., 75(3): 518-530.

Montero, P., G. Daneri, H.E. González, J.L. Iriarte, F.J. Tapia, L. Lizárraga, N. Sanchez & O. Pizarro. 2011. Seasonal variability of primary production in a fjord ecosystem of the Chilean Patagonia: implications for the transfer of carbon within pelagic food webs. Cont. Shelf Res., 31: 202-215.

Olsen, L.M., K.L. Hernández, M. Van Anderlan, J.L. Iriarte, N. Sánchez, H.E. González, N. Tokle & Y. Olsen. 2014. Responses in the microbial food web to increased rates of nutrient supply in a southern Chilean fjord: possible implications of cage aquaculture. Aquacult. Environ. Interact., 6: 11-27.

Parsons, T.R., Y. Maita & C.M. Lalli. 1984. Counting, media and preservatives. In: T.R. Parsons, Y. Maita & C.M. Lalli (eds.). A manual of chemical and biological methods for seawater analysis. Pergamon Press, Oxford, 173 pp.

Paredes, M.A. & V. Montecino. 2011. Size diversity as an expression of phytoplankton community structure and the identification of its patterns on the scale off fjords and channels. Cont. Shelf Res., 31: 272-281.

Pizarro, G., R. Astoreca, V. Montecino, M.A. Paredes, G. Alarcón, P. Uribe & L. Guzmán. 2005. Patrones espaciales de la abundancia de la clorofila, su relación con la productividad primaria y la estructura de tamaños del fitoplancton en Julio y Noviembre de 2001 en la región de Aysén (43°-46°S). Rev. Cienc. Tecnol. Mar, 28(2): 27-42.

Poole, H.H. & W.R.G. Atkins. 1929. Photo-electric measurements of submarine illumination throughout the year. J. Mar. Biol. Assoc. UK, 16: 297-324.

Rebolledo, L., C.B. Lange, D. Figueroa, S. Pantoja, P. Muñoz & R. Castro. 2005. 20th century fluctuations in the abundance of siliceous microorganisms preserved in the sediments of the Puyuhuapi Channel (44°S), Chile. Rev. Chil. Hist. Nat., 78: 469-488.

Sarthou, G., K.R. Timmermans, S. Blain & P. Tréguer. 2005. Growth physiology and fate of diatoms in the ocean: a review. J. Sea Res., 53: 25-42.

Schneider, W., I. Pérez-Santos, L. Ross, L. Bravo, R. Seguel & F. Hernández. 2014. On the hydrography of Puyuhuapi Channel (Chilean Patagonia). Prog. Oceanogr., 129: 8-18.

Sciremammano, F. 1979. A suggestion for the presentation of correlations and their significance levels. J. Phys. Oceanogr., 9: 1273-1276.

Received: 30 December 2016; Accepted: 5 July 2017

Sepúlveda, J., S. Pantoja, K. Hughen C. Lange, F. Gonzalez, P. Muñoz, L. Rebolledo, R. Castro, S. Contreras, A. Ávila, P. Rossel, G. Lorca, M. Salamanca & N. Silva, 2005. Fluctuations in export productivity over the last century from sediments of a southern Chilean fjord (44ºS). Estuar. Coast. Shelf Sci., 65: 587-600.

Silva, N. 2008. Dissolved oxygen, pH, and nutrients in the austral Chilean channels and fjords. Progress in the oceanographic knowledge of Chilean interior waters, from Puerto Montt to Cape Horn. In: N. Silva & S. Palma (eds.). Comité Oceanográfico Nacional-Pontificia Universidad Católica de Valparaíso, Valparaíso, pp. 37-43.

Silva, N., N. Rojas & N. Fedele. 2009. Water masses in the Humboldt Current System: properties, distribution and the nitrate deficit as a chemical water mass tracer for Equatorial Subsurface Water off Chile. Deep-Sea Res. II, 56: 1004-1020.

Steeman-Nielsen, E. 1952. The use of radioactive carbon (C^{14}) for measuring organic production in the sea. J. Cons. Perm. Int. Explor. Mer, 18(2): 117-140.

Strickland, J.D.H. 1960. Measuring the production of marine phytoplankton. Bull. Fish Res. Bd. Can., 122: 1-172.

Strickland, J.D.H. & T.R. Parsons. 1968. A practical handbook of seawater analysis. Bull. Fish. Res. Bd. Can., 167 pp.

Torres, R., N. Silva, B. Reid & M. Frangopulos. 2014. Silicic acid enrichment of Subantarctic Surface Water from continental inputs along the Patagonian archipelago interior sea (41-56ºS). Prog. Oceanogr., 129: 50-61.

Utermöhl, H. 1958. Zur Vervollkommnung der quantitativen Phytoplankton-Methodik. Internationale Vereinigung für Theoretische und Angewandte Limnologie. Komitee für Limnologische Methoden, 9: 1-39.

Wetz, M.S. & P.A. Wheeler. 2007. Release of dissolved organic matter by coastal diatoms. Limnol. Oceanogr., 52(2): 798-807.

Williams, P.J.LeB. & J.E. Robertson. 1991. Overall planktonic oxygen and carbon dioxide metabolism: the problem of reconciling observations and calculations of photosynthetic quotients. J. Plankton Res., 13: 153-169.

Xu, N., Y.Z. Tang, S. Duan & C.J. Gobler. 2015. Ability of the marine diatoms *Pseudo-nitzschia multiseries* and *P. pungens* to inhibit the growth of co-occurring phytoplankton via allelopathy. Aquat. Microbiol. Ecol., 74: 29-41.

Yamazaki, Y., Y. Ohmichi, T. Shikata, M. Hirose, Y. Shimasaki, Y. Oshima & T. Honjo. 2010. Species-specific allelopathic effects of the diatom *Skeletonema costatum*. Thalassas, 27(1): 21-32.

PAPER II

A winter dinoflagellate bloom drives high rates of primary production in a Patagonian fjord ecosystem

Estuarine, Coastal and Shelf Science 199 (2017) 105–116

Contents lists available at ScienceDirect

Estuarine, Coastal and Shelf Science

journal homepage: www.elsevier.com/locate/ecss

A winter dinoflagellate bloom drives high rates of primary production in a Patagonian fjord ecosystem

P. Montero [a, b], I. Pérez-Santos [b, c, *], G. Daneri [a, b], M.H. Gutiérrez [b, d], G. Igor [a, b], R. Seguel [c], D. Purdie [e], D.W. Crawford [a]

[a] Centro de Investigación en Ecosistemas de la Patagonia (CIEP), Coyhaique, Chile
[b] COPAS Sur–Austral, Universidad de Concepción, Concepción, Chile
[c] Centro i~mar, Universidad de Los Lagos, Puerto Montt, Chile
[d] Departamento de Oceanografía, Universidad de Concepción, Concepción, Chile
[e] Ocean and Earth Science, National Oceanography Centre Southampton, University of Southampton, United Kingdom

ARTICLE INFO

Article history:
Received 31 December 2016
Received in revised form
7 September 2017
Accepted 26 September 2017
Available online 28 September 2017

Keywords:
Primary production
Mixing
Winter dinoflagellate blooms
Patagonian fjord

ABSTRACT

A dense winter bloom of the dinoflagellate *Heterocapsa triquetra* was observed at a fixed station (44°35.3′S; 72°43.6′W) in the Puyuhuapi Fjord in Chilean Patagonia during July 2015. *H. triquetra* dominated the phytoplankton community in the surface waters between 2 and 15 m ($13–58 \times 10^9$ cell m^{-2}), with abundances some 3 to 15 times higher than the total abundance of the diatom assemblage, which was dominated by *Skeletonema* spp. The high abundance of dinoflagellates was reflected in high rates of gross primary production (GPP; 0.6–1.6 g C m^{-2} d^{-1}) and chlorophyll-a concentration (Chl-a; 70–199.2 mg m^{-2}) that are comparable to levels reported in spring diatom blooms in similar Patagonian fjords. We identify the main forcing factors behind a pulse of organic matter production during the non-productive winter season, and test the hypothesis that low irradiance levels are a key factor limiting phytoplankton blooms and subsequent productivity during winter.

Principal Component Analysis (PCA) indicated that GPP rates were significantly correlated ($r = -0.8$, $p < 0.05$) with a decrease in salinity/temperature and the presence of the *Heterocapsa* bloom. The bloom occurred under low surface irradiance levels characteristic of austral winter and was accompanied by strong northern winds, associated with the passage of a low-pressure system, and a water column dominated by double diffusive layering. To our knowledge, this is the first report of a dense dinoflagellate bloom during deep austral winter in a Patagonian fjord, and our data challenge the paradigm of light limitation as a factor controlling phytoplankton blooms in this region in winter.

1. Introduction

In coastal waters around the world, dinoflagellate blooms have been typically associated with stratification of the water column during summer (Margalef, 1978; Legendre, 1990; Casas et al., 1999; Barton et al., 2013). However, in some estuaries of the northern hemisphere high abundances of these organisms have also been reported in winter, and can at times contribute significantly to annual phytoplankton carbon production (Sellner et al., 1991; Litaker et al., 2002a,b; Marshall et al., 2005). The dinoflagellates involved have clearly been able to thrive under some of the conditions encountered in winter such as relatively low temperature and irradiance (Litaker et al., 2002a,b), high nutrient availability, low grazing pressure and a stratified water column (Cohen, 1985; Litaker et al., 2002a,b; Millette et al., 2015).

The thecate dinoflagellate *Heterocapsa triquetra* is one of the most common winter bloom-forming species found in estuarine ecosystems (Baek et al., 2011), with low temperatures and strong atmospheric frontal systems in winter somehow creating a favorable niche for this species (Litaker et al., 2002a,b). Some species of *Heterocapsa* in cultures are able to grow at temperatures below 10 °C, and even below 0° C (Yamaguchi et al., 1997; Baek et al., 2011; Tas, 2015), and so may benefit from the seasonal drop in water temperature that might potentially reduce the presence of mesozooplankton grazers (Millette et al., 2015). In the northern

* Corresponding author. Centro i~mar, Universidad de Los Lagos, Puerto Montt, Chile.
E-mail address: ivan.perez@ulagos.cl (I. Pérez-Santos).

https://doi.org/10.1016/j.ecss.2017.09.027
0272-7714/

hemisphere, low-pressure systems are accompanied by regular rainfall and terrestrial runoff that supplies inorganic nutrients critical for initiation and development of these blooms (Litaker et al., 2002a). According to Mallin et al. (1991), Mallin (1994) and Baek et al. (2011), low salinity and high nitrate concentrations, resulting from heavy rains during winter, appear to be crucial for formation of blooms of *Heterocapsa triquetra*. Indeed, *H. triquetra* has a high rate of uptake and assimilation of nitrate (Mallin et al., 1991; Mallin, 1994), is tolerant of a wide range of salinities (10–40) (Lee et al., 2005), and might therefore be specifically favored by the environmental conditions encountered in winter.

In Patagonian fjords, winter conditions differ from the estuaries of the northern hemisphere, because increased freshwater input generally results in surface waters having high concentrations of silicic acid (Silva, 2008; Torres et al., 2014) but low concentrations of nitrate and phosphate (Silva, 2008; Silva and Vargas, 2014). Fertilization of surface fjord waters therefore requires increased supply of nitrate and phosphate from deeper waters through vertical mixing of the water column (Goebel et al., 2005), and this process may be strongly modulated by the passage of low-pressure systems during winter.

The general pattern of phytoplankton succession in the fjords of southern Chile is one of dominance by small flagellates (size range: 2–20 μm) during winter (Czypionka et al., 2011), a conspicuous diatom bloom in spring, followed by increased abundances of dinoflagellates in summer and early fall (Iriarte et al., 2005; Iriarte and González, 2008). This phytoplankton succession is consistent with the "Mandala" adopted by Margalef (1978) to conceptualize the role of nutrients and turbulence in phytoplankton growth strategies, where dinoflagellate blooms tend to develop in late summer under relatively nutrient-poor and low turbulence conditions. Blooms of *Heterocapsa triquetra* are not common in Patagonian fjords, and to date have been reported only during austral summer (Cassis et al., 2002). No other dinoflagellate has been previously reported to bloom during the deep Patagonian winter. Whereas spring blooms of diatoms such as *Skeletenoma*, are related to high levels of primary production (Iriarte et al., 2007b; Montero et al., 2011) and downward transfer of particulate organic carbon in Patagonian fjords (Iriarte et al., 2007b, 2013; González et al., 2010; Montero et al., 2011), dinoflagellate blooms appear to contribute poorly to export of organic matter and are more associated with recycling of carbon in near-surface waters (Iriarte et al., 2005, 2007a).

In Patagonian fjords and channels, irradiance is one of the principal factors regulating the annual cycle of primary productivity (Iriarte and González, 2008) which is typically divided into productive (late winter/early spring to late fall) and non-productive (winter) periods (Montero et al., 2011), and with most interest largely focused on the spring diatom bloom. Productivity during winter in Patagonia fjords has up to now been assumed to be limited by low temperatures and unfavorable light conditions, and therefore largely ignored, with the assumption that the winter period makes an insignificant contribution to total annual primary productivity, as generally found elsewhere (Sellner et al., 1991).

The mixing-stratification cycle is an important mechanism for controlling total phytoplankton production (Legendre and Rassoulzadegan, 1996) principally by regulating the light climate experienced by cells in the upper water column, as well as the supply of nutrients from deeper waters. In Patagonian fjords, water column mixing and destabilization can be driven by winds and the passage of low pressure systems, and therefore winter conditions could represent a favorable scenario for injection of nitrate and phosphate into surface waters, potentially stimulating phytoplankton production, as long as the irradiance levels are favorable.

A multidisciplinary sampling campaign was conducted in Puyuhuapi Fjord during July 2015 aiming to (1) identify the main forcing factors behind a pulse of organic matter production during the non-productive winter season, and (2) test the hypothesis that low irradiance levels are a key factor limiting phytoplankton blooms and subsequent productivity during winter.

2. Data and methodology

2.1. Study area

The study was conducted in the northern section of Puyuhuapi Fjord (Fig. 1A) at a fixed station where an oceanographic and meteorological buoy (44°35.3′ S; 72°43.6′ W) has been operational since 2012. The buoy has been moored at ~200-m depth and ca. 20 km NW of the mouth of the Cisnes River (Fig. 1B). Puyuhuapi Fjord runs in a N-NE direction and connects directly to the open sea via the Moraleda channel at its mouth, and through the Jacaf channel near the head (Schneider et al., 2014). The hydrography of the fjord is characterized by an estuarine type of circulation with a vertical two layer structure comprised of a highly variable 5–10 m deep freshwater layer overlying a more uniform, saltier subpycnocline layer (Schneider et al., 2014 and references therein). The deeper saline water originates from Sub-Antarctic Surface Water (SAAW) characteristic of open ocean environments in these latitudes (Chaigneau and Pizarro, 2005). The freshwater upper layer is mainly supplied by the Cisnes River and rain runoff (Schneider et al., 2014). The surface outflow of buoyant freshwater carries high concentrations of silicic acid derived from rivers, while SAAW waters are typically enriched with nitrate and orthophosphate (Silva, 2008). Surface salinity distribution in Puyuhuapi Fjord; with higher salinity in the north than in the south, suggests an intrusion of oceanic surface waters from the north via Jacaf Channel forced by westerly winds (Schneider et al., 2014).

We conducted a winter sampling campaign from 10 to 16 July 2015 at the Puyuhuapi Fjord station, where hydrographic profiles and water samples from different depths were collected every two days. In addition, between July 5 and July 17, 2015 data was continuously recorded by the buoy at the Puyuhuapi Fjord and at the nearby meteorological station.

2.2. Atmospheric and sea-surface data

The atmospheric data was recorded every 15 min with a meteorological station model HOBO U-30 (44° 35.46′ S/72° 44.21' W), located on land approximately 900 m distance from the buoy. In the water column, temperature, salinity, pH, dissolved oxygen and chlorophyll-a were recorded once per hour using a YSI model 6600 V2-4 multiparameter probe deployed at ~1 m depth below the buoy. Data were averaged for each day to eliminate the influence of semidiurnal tides and other high frequency forcings in the study area (Schneider et al., 2014). The discharge of the Cisnes River, with an hourly temporal resolution, was obtained from the Chilean Direction of Water (www.dga.cl).

2.3. Hydrography and micro-profiler measurements

Vertical profiles of temperature, salinity and fluorescence (WET Labs sensor) were recorded using a CTD SeaBird 25 at 8 Hz. Additionally, micro-profiler measurements were carried out with a Self Contained Autonomous Micro Profiler (SCAMP) in order to evaluate mixing processes and examine micro-layers of fluorescence. The SCAMP profiler recorded data at 100 Hz, or about 1 mm vertical resolution with a descending free fall speed of ~10 cm s^{-1} and is equipped with a fast conductivity (accuracy of ±5% of the full conductivity scale) and a fast temperature response sensor

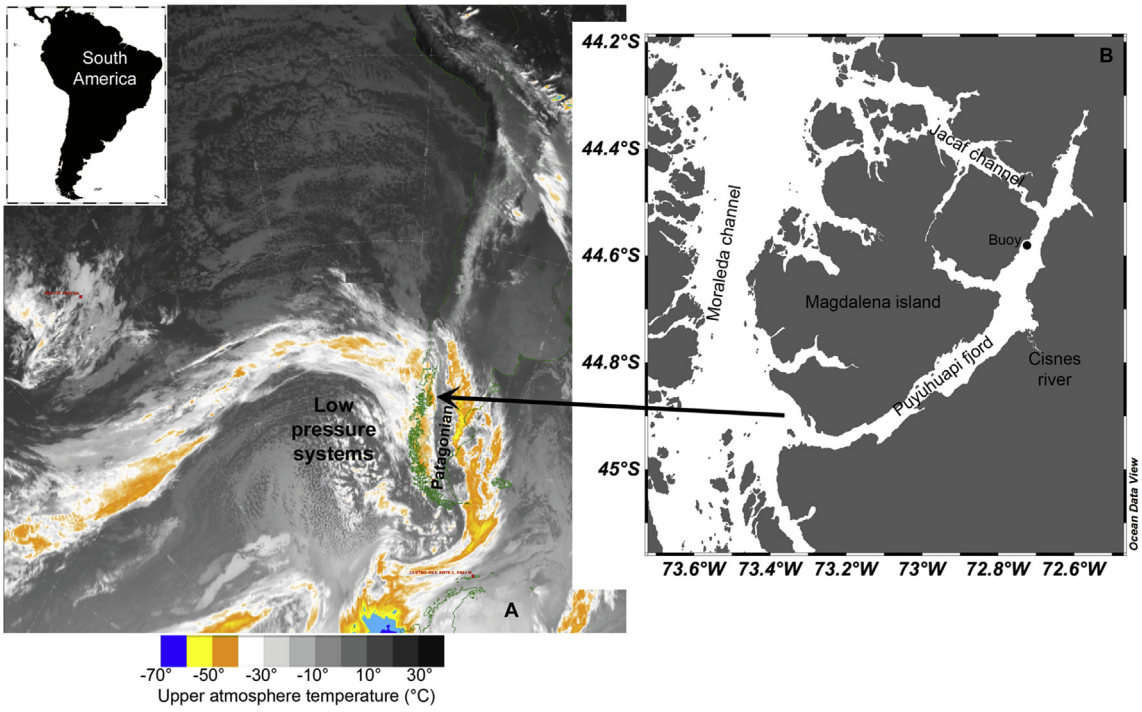

Fig. 1. (A) Infrared image of GOES-13 showing the influence of low pressure systems in Patagonian region. (B) Study area in Puyuhuapi Fjord.

(accuracy of 0.010 °C). The vertical gradients of temperature measurements were used to calculate dissipation rate of turbulent kinetic energy (ε) applying the Batchelor spectrum (Ruddick et al., 2000; Luketina and Imberger, 2001).

Using the dissipation rate of turbulent kinetic energy from the SCAMP profiler, the diapycnal eddy diffusivity (K_ρ) was calculated. The most commonly used formulation for estimation of K_ρ, was proposed by Osborn (1980):

$$K_\rho = \Gamma \frac{\varepsilon}{N^2}, \quad (1)$$

where Γ is the mixing efficiency, generally set to 0.2 (Thorpe, 2005), and N is the buoyancy frequency. Shih et al. (2005) noted that when the ratio $\varepsilon/\nu N^2$, with viscosity $\nu = 1.9 \times 10^{-6}$ m^2 s^{-1}, is larger than 100, the Osborn equation results in an overestimation. They propose a new parameterization for this case given by:

$$K_\rho = 2\nu\left(\frac{\varepsilon}{\nu N^2}\right)^{1/2}, \quad (2)$$

In this investigation we therefore applied equation (2) when $\varepsilon/\nu N^2 > 100$, equation (1) when $7 < \varepsilon/\nu N^2 < 100$, and considered null eddy diffusivity when $\varepsilon/\nu N^2 < 7$ (Cuypers et al., 2011).

The hydrographic data (profiles of temperature and salinity) was used to calculated the Turner angle (*Tu*, expressed in degrees of rotation) in order to determine the contributions of the double-diffusive layering (DL) process to the vertical mixing of the water column, and also to quantify the influence of temperature and salinity in the stratification of the water column (Ruddick, 1983). You (2002) proposed: when *Tu* is between −45° and −90° then DL is possible. When *Tu* is between −45° and 45° the water column is stable with respect to both temperature and salinity; and when *Tu* is between 45° and 90, salt fingering structures can be expected. According to this classification, DL can also be divided into strong (*Tu* between −90° and −75°), medium (*Tu* between −75° and −60°) and weak (*Tu* between −60° and −45°). Profiles of temperature and salinity were averaged every 1 m for SCAMP measurements to compute the *Tu* parameter.

2.4. Nutrients, chlorophyll-a and phytoplankton composition

Water samples for analyses of inorganic nutrients, chlorophyll-a (Chl-*a*) and phytoplankton abundance were collected each sampling day from 3 discrete depths (2, 5 and 15 m) using a 10-L Niskin bottle. Additional nutrient samples were collected from 50 to 100 m depths. Samples for nutrient analyses were filtered through GF/F filters and frozen at −20 °C prior to analysis in the laboratory. Concentrations of nitrate, orthophosphate, and silicic acid were determined spectrophotometrically according to methods given in Strickland and Parsons (1968).

For Chl-*a* determinations, samples were fractionated into the following three size classes of phytoplankton: microphytoplankton (>20 μm), nanophytoplankton (2–20 μm), and picophytoplankton (<2 μm). This fractionation procedure was performed in three sequential steps: (1) for the nanophytoplankton fraction (2–20 μm), 100 mL seawater was pre-filtered using 20-μm Nitex mesh and collected on a 2.0-μm Nuclepore filter; (2) for the picoplankton fraction (0.2–2.0 μm), the filtrate from the 2.0-μm Nuclepore filter in step (1) was filtered again onto a 0.7-μm MFS (Microfiltration Systems) glass-fiber filter; (3) for the whole phytoplankton community, 100 mL seawater was filtered through a 0.7-μm MFS glass-fiber filter. The microphytoplankton fraction was obtained by subtracting the estimated Chl-a in steps (1) and (2) from the estimates in step (3). Filters were immediately frozen (−20 °C) until later analysis; pigments were extracted with 90% v/v acetone and measured using a Turner Design TD-700 fluorometer according to standard procedures (Parsons et al., 1984). Depth-integrated values of Chl-a were calculated down to 15 m, using trapezoidal integration.

Samples for phytoplankton cell counts were stored in 250 ml

clear plastic bottles, and preserved in a 1% Lugol's iodine solution (alkaline). From each sample, a 10-mL sub-sample was placed in a sedimentation chamber and allowed to settle for 12 h (Utermöhl, 1958) prior to identification at 40× and 100× using an inverted microscope (Carl Zeiss, Axio Observer A.1). Fifty random fields were counted for each sample. Estimates of phytoplankton abundance at the three discrete depths were integrated down to 15 m, using a trapezoidal method.

2.5. Primary production

During each sampling day, *in situ* experiments were conducted to measure gross primary production (GPP). A total of 4 experiments were conducted during the study period and incubations were performed on water samples obtained from the same sampling depths indicated above (2, 5 and 15 m). GPP was estimated from changes in dissolved oxygen concentrations observed during *in situ* incubation of light and dark bottles (Strickland, 1960). Water from the Niskin bottle was transferred into 125 mL (nominal volume) borosilicate bottles (gravimetrically calibrated) using a silicone tube, whilst taking care to exclude air bubbles. Five time-zero bottles, five light bottles, and five dark bottles were used for each incubation depth. Time-zero bottles were fixed at the beginning of each experiment, whereas the light and dark bottles were incubated *in situ* attached to a surface-tethered mooring system. Water samples were collected at dawn and were incubated during the whole light period (incubating time was 7.0 ± 0.8 h). Dissolved oxygen concentrations were determined according to the Winkler method (Strickland and Parsons, 1968), using a Metrohom burette (Dosimat plus 865) and by automatic visual end-point detection (AULOX Measurement System). Daily GPP rates were calculated as follows: GPP = (mean [O_2] light bottles − mean [O_2] dark bottles). GPP values were converted from oxygen to carbon units using a conservative photosynthetic quotient (PQ) of 1.25 (Williams and Robertson, 1991). Discrete-depth estimates of GPP rates were integrated down to 15 m, using a trapezoidal method.

2.6. Statistical analyses

A principal component analysis (PCA) was performed to combine the variables chl-a, inorganic nutrients, temperature, salinity, dissolved oxygen concentration, photosynthetically active radiation (PAR) and abundance of phytoplankton species, into statistically independent environmental predictors for GPP values. The data used in this analysis corresponded to values obtained at each sampling depth during the study period. A Spearman correlation analysis (r_s) was then conducted to assess the degree of association between these principal components and log-transformed GPP values.

3. Results

3.1. Atmospheric and sea-surface conditions

Atmospheric conditions observed during the sampling period showed evidence of the passage of multiple low-pressure systems (LPS), characterized by north winds with intensities ranging from 5 to 20 m s^{-1} and low atmospheric pressure (Fig. 2A–B), and leaving an identifiable signal in the Cisnes River discharge (Fig. 2C). During the days of the study, surface water temperature and salinity (Fig. 2D and E) decreased during the passage of LPS (temperature 7–9 °C and salinity 10–15), whereas surface dissolved oxygen increased from 8 mL L^{-1} to 13 mL L^{-1} (Fig. 2F), possibly in response to the high surface values of chl-a (100 to >150 μg L^{-1}), (Fig. 2G). High surface pH values (8.5–9.2) were also recorded during periods where chl-a was high (Fig. 2H).

3.2. Hydrography and vertical mixing

The hydrography of Puyuhuapi Fjord was characterized by a vertical two-layer structure with a highly variable 0–10 m freshwater surface and a more uniform saltier lower layer (Fig. 3B). Brackish or saline estuarine waters (salinity < 31; Sievers and Silva, 2008) occupied the upper (0–20 m) layer of the water column while the deeper (20–40 m) layer showed a Modified Sub-Antarctic Water (MSAAW; Sievers and Silva, 2008), with salinities ~31 and temperatures around 11 °C. Temperature and salinity increased from surface to deeper waters during study period (Fig. 3A and B). The surface layer was colder than the deeper layer (Fig. 3A), thus resulting in a thermal inversion characteristic of winter months (Schneider et al., 2014).

A shallow pycnocline (~2 m) was observed during the days before and after (12th and 16th) the passage of the LPS on July 15, 2015, with a further step in density at 6.5 m (Fig. 3C). These density changes generated high buoyancy frequency within the pycnocline zone with values ranging from 0.01 to 0.02 s^{-2} (Fig. 3D). The shallower maximum of buoyancy frequency disappeared on July 15, and the slightly deeper maximum also decreased in intensity in response to the vertical homogenization of temperature and salinity (Fig. 3A and B), reflecting the water column mixing driven by the passage of the LPS. The water column was influenced by wind driven mixing down to approximately 30 m depth, but particularly above 7 m, with surface temperature and salinity increasing around 1.5 °C and 5, respectively on July 15 (Fig. 3A and B). The temperature gradient was high from the surface down to 17 m depth with a variation of between −2 and 2 °C m^{-1} (Fig. 3E).

The gradient of temperature and salinity with depth favored the occurrence of double-diffusive layering (DL) in 84% of the total data points with Turner angle values between −75° and −45° (Fig. 3F). The remaining 16% of the Turner angle data were between −45° and 45° (not shown on figure), corresponding to a stable water column with respect to temperature and salinity. In the diffusive layer, high values of dissipation rate of turbulent kinetic energy (ε) were obtained ranging from 10^{-5} to 10^{-4} W kg^{-1} (Fig. 3G). Before (black line) and after (red line) the influence of the LPS, the high values for ε were recorded between 4 and 21 m depth with maximum of $\varepsilon = 4.8 \times 10^{-4}$ W kg^{-1} and values decreased to the bottom ($\varepsilon = 10^{-9}$ - 10^{-5} W kg^{-1}). Hours after the passage of the LPS (blue line), the dissipation rate of turbulent kinetic energy showed two maxima, at 5 and 15 m depth with $\varepsilon = 5.1 \times 10^{-4}$ W kg^{-1}, and then ε diminished abruptly to $\varepsilon = 10^{-9}$ - 10^{-8} W kg^{-1} deeper in the water column. In response to the high ε (0–20 m), elevated values of diapycnal eddy diffusivity were obtained (3.5×10^{-3} m^2 s^{-1}) (Fig. 3H).

3.3. Nutrient measurements

Concentrations of nitrate <10 μM and low phosphate values (<0.2 μM) were observed within the top 5 m of water column. Below this layer and between 15 and 100 m depth, nitrate levels fluctuated between 9 and 21 μM and phosphate between 0.6 and 1.8 μM (Table 1). Silicic acid concentrations were higher (33–71 μM) within the top 5 m of water column than in deeper waters (19–60 μM) (Table 1), coinciding with the input of low-salinity water (Fig. 3B).

3.4. Phytoplankton community composition, chlorophyll-a and primary production

High depth-integrated total phytoplankton abundance

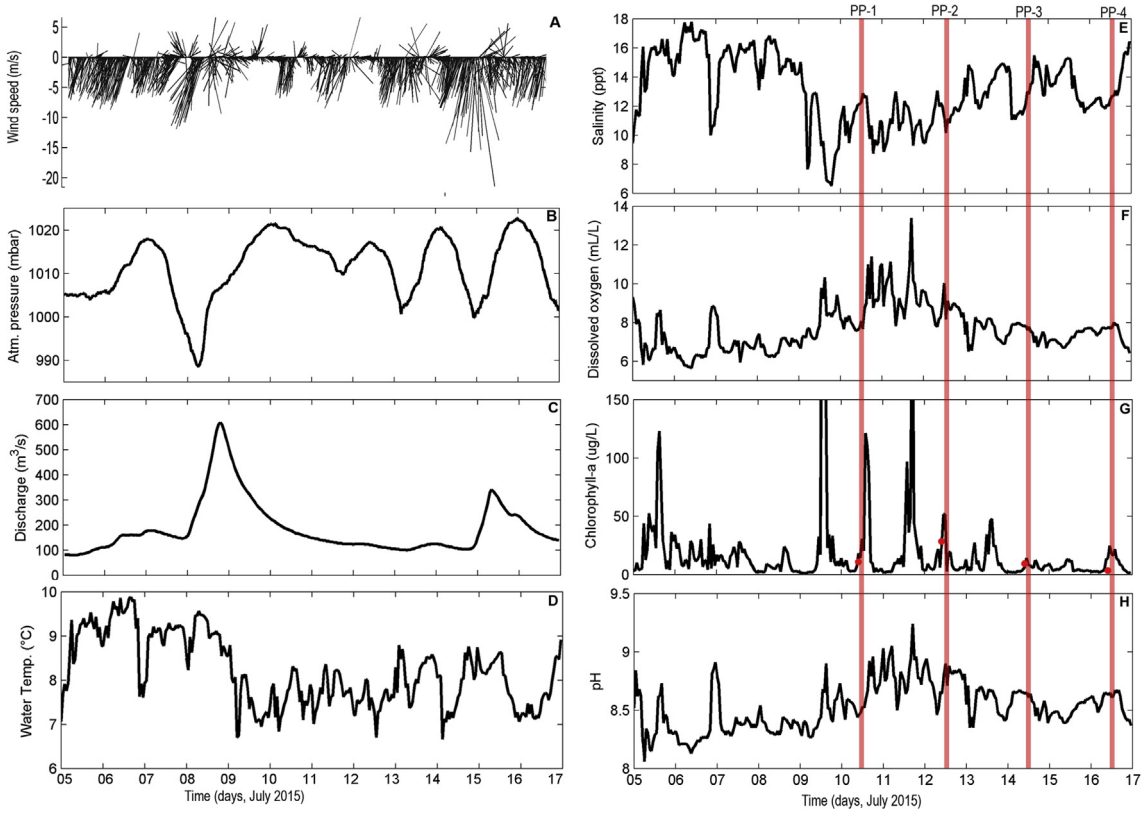

Fig. 2. (A–E) Wind speed (A) and air pressure (B) data in July 2015 taken from the meteorological station in Magdalena Island, located 900 m from the buoy position. (C) Cisnes River discharge. D-H represents temperature, salinity, dissolved oxygen, chlorophyll-a (fluorescence) and pH logged hourly in surface water at the Puyuhuapi buoy in July 2015.

(18–63 × 10^9 cell m^{-2}) and chl-a concentration (70–199.2 mg Chl-*a* m^{-2}) were observed during the study period, with a clear dominance (13–58 × 10^9 cell m^{-2}) by the dinoflagellate *Heterocapsa triquetra* and an almost complete absence of coexisting phytoplankton species (Fig. 4A). Diatoms were poorly represented in depth integrated totals in the water column, and consisted mainly of *Skeletonema* spp. (2–4 × 10^9 cell m^{-2}) (Fig. 4A). Higher abundances of phytoplankton (1–9 × 10^3 cell mL^{-1}) were observed in near-surface (2–5 m) than in subsurface (15 m) waters (<1 × 10^3 cell mL^{-1}) (Table 1). Consistently, in-situ measurements of chl-a ranged between 5.1 and 28.5 μg L^{-1} in surface water (2–5 m) and between 1.7 and 4.2 μg L^{-1} at 15 m depth (Table 1). Total Chl-*a* was dominated by the nanophytoplankton (2–20 μm) and microphytoplankton (>20 μm) fractions, with a very low proportion made up by the picophytoplankton (<2 μm) fraction (Fig. 4B).

GPP rates derived from O_2 incubations were higher (2.6–31.4 mmol O_2 m^{-3} d^{-1}) at 2 and 5 m than at 15 m (0.2–9.4 mmol O_2 m^{-3} d^{-1}) (Table 1), with values of depth-integrated GPP ranging from 0.6 to 1.6 g C m^{-2} d^{-1} over the study period (Fig. 4A).

Principal component analysis (PCA) showed first (PC-1) and second principal component (PC-2) explaining 64.9% and 13.9% of total variance, respectively (Fig. 5A). PC-1 was positively loaded with salinity, temperature, phosphate and nitrate, while Chl-a, silicic acid, dissolved oxygen and abundance of *Heterocapsa triquetra* were found to be negatively loaded. The PC-2 was shown to be related to a few variables, with abundance of *Skeletonema* spp. and silicic acid positively loaded and PAR negatively loaded (Fig. 5A).

The PCA analysis clearly showed an ordination of sampling sites according to depth, which involves the distribution of light (PAR) and the vertical separation in the sources of silicic acid from surface freshwater, and nitrate and phosphate from deeper oceanic water (Fig. 5A). In this ordination, and, as shown by fluorescence profile (Fig. 6), the highest concentration of phytoplankton was in surface waters (0–8 m above pycnocline). GPP was significantly correlated with PC-1 ($r_s = -0.8$, $n = 12$, $p < 0.05$) but not with PC-2 ($r_s = 0.07$, $n = 12$, $p > 0.05$) (Fig. 5B).

3.5. Vertical profiles of fluorescence

The data recorded by the fluorescence sensor on the CTD was used to describe changes in the relative position of the maximum of chl-a over the sampling period (Fig. 6). This data showed an absolute maximum of 104.3 mg m^{-3} chl-a at 1.5 m depth during July 12 at midday, but more generally, fluorescence maxima ranged from 20 to 50 mg m^{-3} chl-a and were concentrated in the upper few metres (Fig. 6). The PAR profiles presented demonstrate the low level of irradiance registered during this winter campaign, compared with other records from late spring 2013 and summer 2014 (Fig. 6) within the same study area.

The SCAMP microprofiler obtained high vertical resolution in profiles of fluorescence (units in voltage) that allowed the detection of a peculiar behavior of the dinoflagellate *Heterocapsa triquetra*, which was dominating the bloom. (1) During sunrise at 9:29 of July 12, a double maximum of fluorescence was recorded in the upper 5 m of the water column, at 1.5 m and 3 m (supplementary material, Fig. 1). Over time, the double maximum merged into one peak by 15:07. The double maximum structure was again detected at 8:00 during July 16 (supplementary material, Fig. 2) showing a similar behavior with time. (2) A deepening of the fluorescence maximum to 8 m depth was recorded in the afternoon at 16:06 on July 15,

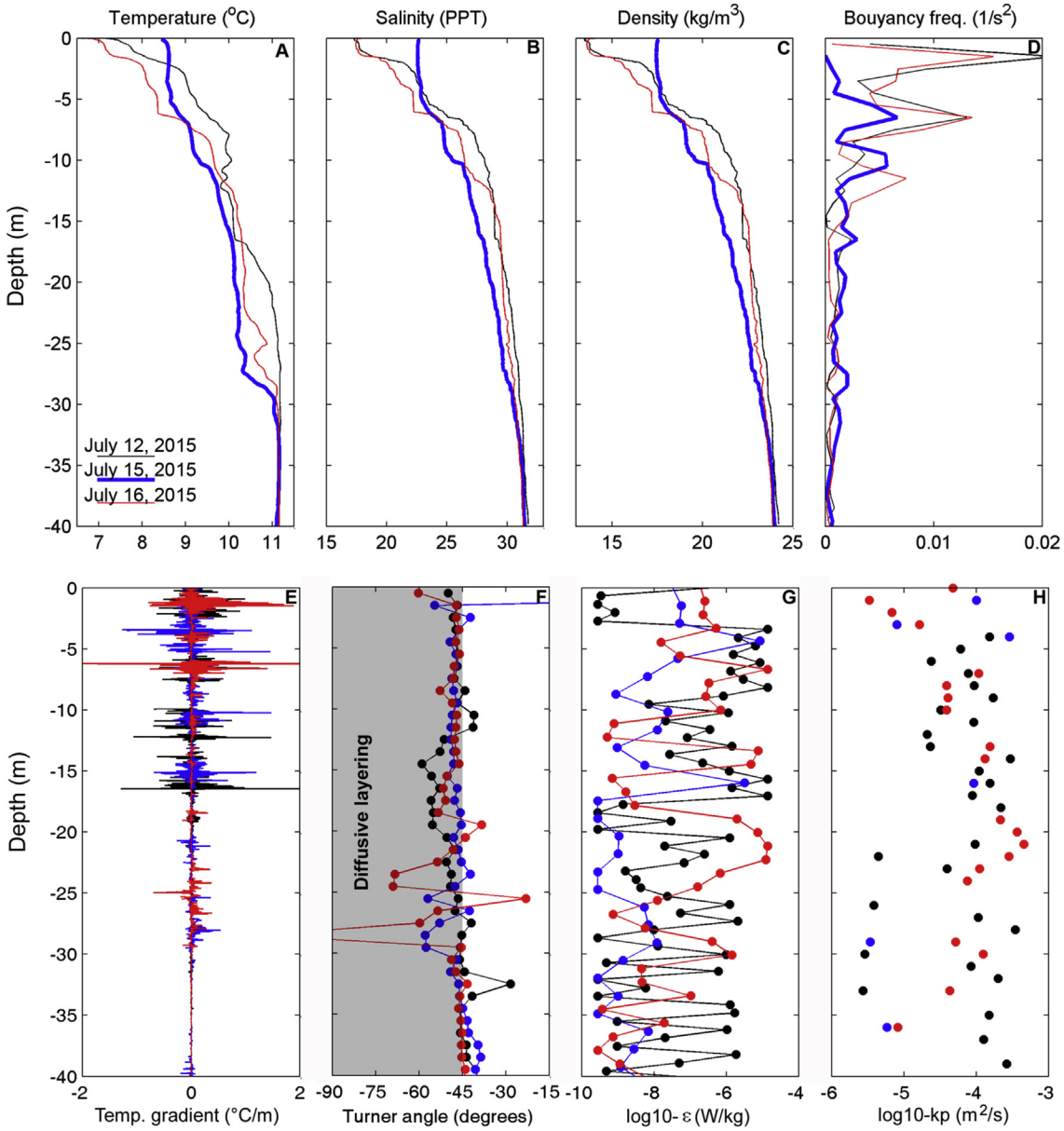

Fig. 3. High vertical resolution of physical properties from SCAM microprofiler showing the temperature (A), salinity (B), density (C), buoyancy frequency (D), temperature gradient (E), Turner angle (F), dissipation rate of turbulent kinetic energy (G) and the diapycnal eddy diffusivity (H) obtained before and after the passage of low pressure system.

hours after the passage of the low pressure system, and coinciding with the displacement of the pycnocline by vertical mixing (supplementary material, Fig. 1). In general the fluorescence peaks were observed over the position of the pycnocline. (3) A vertical migration pattern of the fluorescence peak was distinguished in all SCAMP profiles. At sunrise, the algae were concentrated between 2 and 5 m depth and started to ascend from 10:00 to 12:00. By noon, the maximum fluorescence peak reached very close to the surface and remained within the first 2 m, above the pycnocline (supplementary material, Fig. 2). The in-situ sampling confirmed that the phytoplankton assemblage was dominated by high abundance of *Heterocapsa triquetra* ($2–8 \times 10^3$ cell mL^{-1}) above the pycnocline (supplementary material, Figs. 1 and 2). The position of the maximum in cell abundance agreed with the fluorescence peak, particularly during the double maximum distribution, and this was supported by a consistently strong association between abundance of *Heterocapsa* and Chlorophyll-a in the PCA analysis.

4. Discussion

In the Patagonian fjords region of southern Chile (41-51°S) the phytoplankton community is typically dominated by large diatoms in spring and by nanoflagellates in winter (Iriarte et al., 2007b; Iriarte and González, 2008; Czypionka et al., 2011; Montero et al., 2011). To date, the seasonal cycle of phytoplankton productivity has been described in terms of two alternating periods: i) a productive season (typically extending from late August to May) characterized by the periodic occurrence of high rates of GPP ($1–3$ g C m^{-2} d^{-1}) and ii) a short non-productive season in deep winter (June and July) with much lower rates of GPP (<0.5 g C m^{-2} d^{-1}) (Pizarro et al., 2005; Iriarte et al., 2007b; Montero et al., 2011 and our own unpublished data). This decrease in photosynthetic

Table 1
Nutrient concentrations, Total Phytoplankton Abundance, Chlorophyll-a (chl-a), Gross Primary Production (GPP), Temperature (T), Salinity (S) and Irradiance (PAR) measured at different depths (Z) during the study period. The fluorescence data shown on July 10 corresponds to the profile taken on July 11.

Date	Station	Z	µM	µM	µM	10^3 cell mL^{-1}	mg L^{-1}	mg m^{-3}	mmol O_2 m^{-3} d^{-1}	°C	PPT	µE m^{-2} sec^{-1}
			NO_3	PO_4	$Si(OH)_4$	Abundance	Chl-a TOTAL	Fluorescence	GPP	T	S	PAR
10-Jul-15	BOYA	1	3.8	0.1	37.9	3.3	11.0	11.8	7.5	8.5	18	26.5
		5	10.0	0.1	32.7	1.2	6.7	2.2	2.6	9.7	25	7.7
		15	15.8	0.6	22.5	0.03	1.7	1.0	3.9	10.5	29	1.1
		50	15.6	1.1	19.3							
		100	11.1	0.9	29.5							
12-Jul-15	BOYA	2	1.1	0.2	49.8	8.6	28.5	73.7	31.4	7.9	17	2.9
		5	4.0	0.1	48.9	5.0	5.1	5.4	8.6	9.1	21	0.9
		15	8.5	0.6	36.5	0.2	1.7	1.1	0.2	10.1	28	0.1
		50	8.9	1.1	26.5							
		100	12.9	1.1	49.6							
14-Jul-15	BOYA	2	1.3	0.1	65.0	4.2	9.5	3.5	15.9	7.9	18	5.9
		5	3.1	0.2	55.8	4.7	14.6	16.8	11.8	8.8	22	1.0
		15	11.2	0.8	33.7	0.4	4.2	1.0	0.3	10.2	29	0.1
		50	13.4	1.8	18.8							
		100	20.4	1.4	27.6							
16-Jul-15	BOYA	2	2.9	0.2	70.6	3.8	3.5	5.3	6.7	8.0	19	6.8
		5	6.1	0.2	43.0	3.4	6.7	8.6	8.6	8.6	23	2.0
		15	14.1	0.9	31.5	0.7	2.9	1.2	9.4	10.2	29	02
		50	13.8	1.1	27.5							
		100	20.7	1.0	59.6							

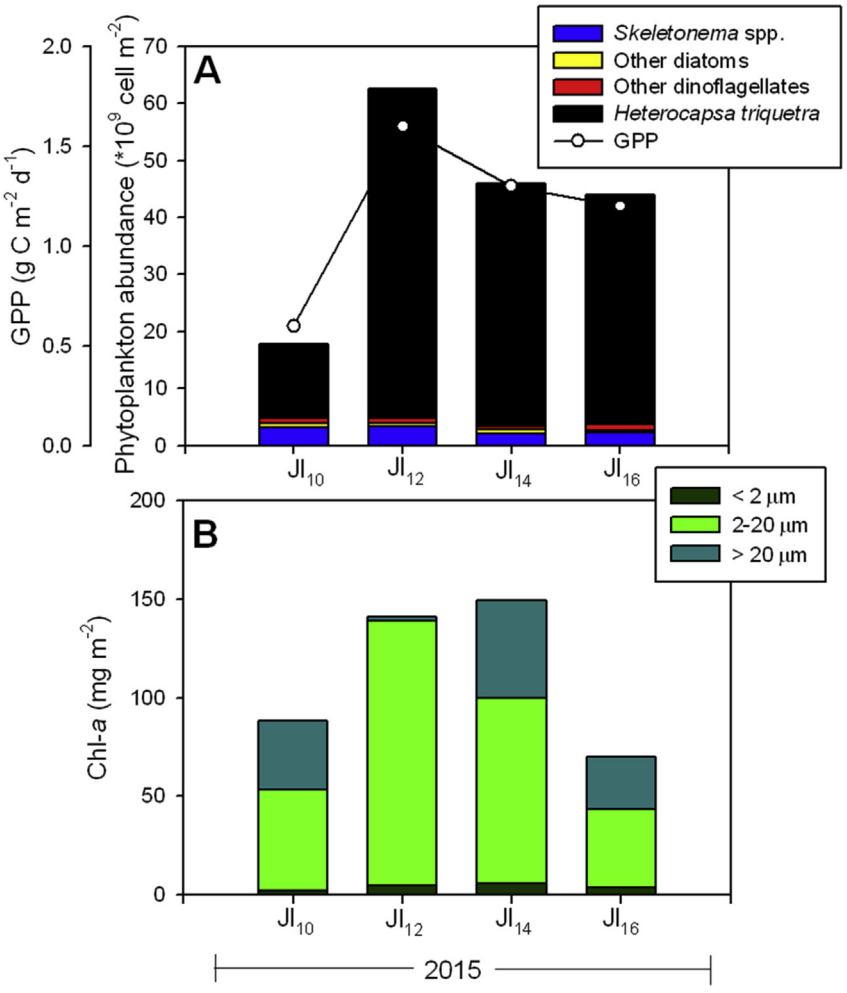

Fig. 4. (A) Total abundance of phytoplankton taxonomic groups combined with gross primary production GPP and (B) size-fractionated chlorophyll-a data.

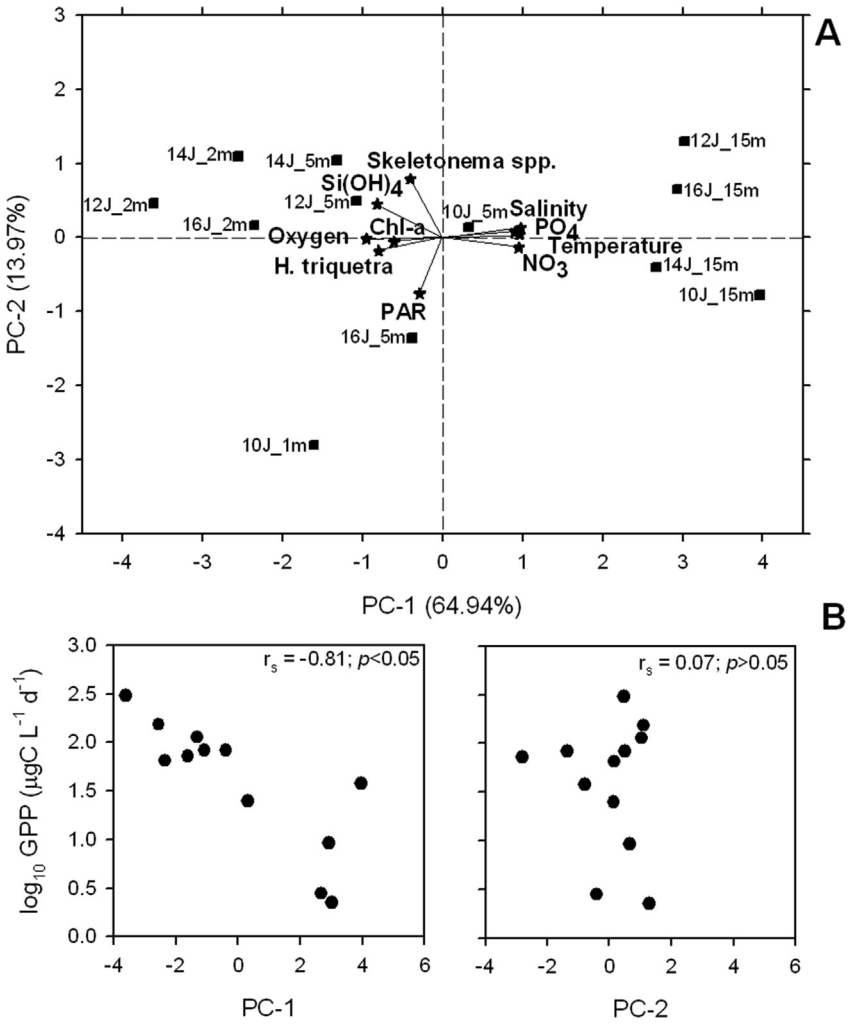

Fig. 5. (A) Principal component analysis (PCA) carried out between the dominant phytoplankton species and the physical and chemical parameters. (B) Correlations between principal components (1 and 2) and log-transformed GPP values.

activity during winter has been associated with the seasonal reduction in light intensity and day length that should inhibit blooming of highly productive diatom populations. Moreover, wind-mixing events in winter tend to distribute diatoms throughout a deeper mixed layer such that the average irradiance limits their photosynthesis and growth.

Here we report for the first time high levels of GPP (0.6–1.6 g C m^{-2} d^{-1}) associated with a dense bloom of the dinoflagellate *Heterocapsa triquetra* during the deep Patagonian winter. This finding contradicts the generally accepted paradigm that low light severely limits GPP rates during the winter in these Patagonian fjords (Iriarte et al., 2007b) and is not consistent with the classical "mandala" that describes a succession of phytoplankton groups culminating in blooms of dinoflagellates (Margalef, 1978).

Blooms of *Heterocapsa* species have also been reported during winter in the northern hemisphere, despite relatively short day lengths and atmospheric systems that bring cloudy conditions and hence significantly reduced incident irradiance (Litaker et al., 2002b). Our PCA analysis showed a weak relationship between *Heterocapsa* and irradiance, perhaps as a result of the ability of this species to tolerate and thrive at the low irradiance levels that characterize winter periods in Chilean fjords (Iriarte and González, 2008; Huovinen et al., 2016). Underwater irradiance was typically in the range of 1–50 µE m^{-2} s^{-1} in the upper 5–10 m, in contrast to much higher irradiance levels (10–500 µE m^{-2} s^{-1}) observed in spring-summer at the same location (Fig. 6). Once established, the abundance peak of the *Heterocapsa triquetra* bloom typically occurred at an irradiance of only 1–10 µE m^{-2} s^{-1} (Fig. 6), which is of the same order of magnitude as typical compensation irradiance levels for dinoflagellates (Richardson et al., 1983). Clearly these low irradiances partly result from self-shading, but the fact that high rates of GPP are maintained by *Heterocapsa triquetra* under such conditions is evidence for a remarkable photosynthetic efficiency at low light that must give this species a competitive edge under these winter conditions. pH values exceeding 8.5, and at times exceeding 9, were observed in association with the high levels of chlorophyll and dissolved oxygen associated with the bloom (Fig. 2) and provide further strong evidence for the high rates of primary productivity observed. This is supported by observations of pH in excess of 9 and a large drawdown in total dissolved inorganic carbon in monocultures of *Heterocapsa triquetra* (Hansen et al., 2007).

Under low light conditions, it has been suggested that mixotrophy by photosynthetic algae could confer an advantage over other phytoplankton species mainly due to the supplementary carbon source to balance low rates of photosynthesis (Legrand et al., 1998; Litaker et al., 2002a; Millette et al., 2017). Mixotrophy in several species of *Heterocapsa* could be a successful strategy for phagotrophic uptake of nitrogen and phosphorus when these

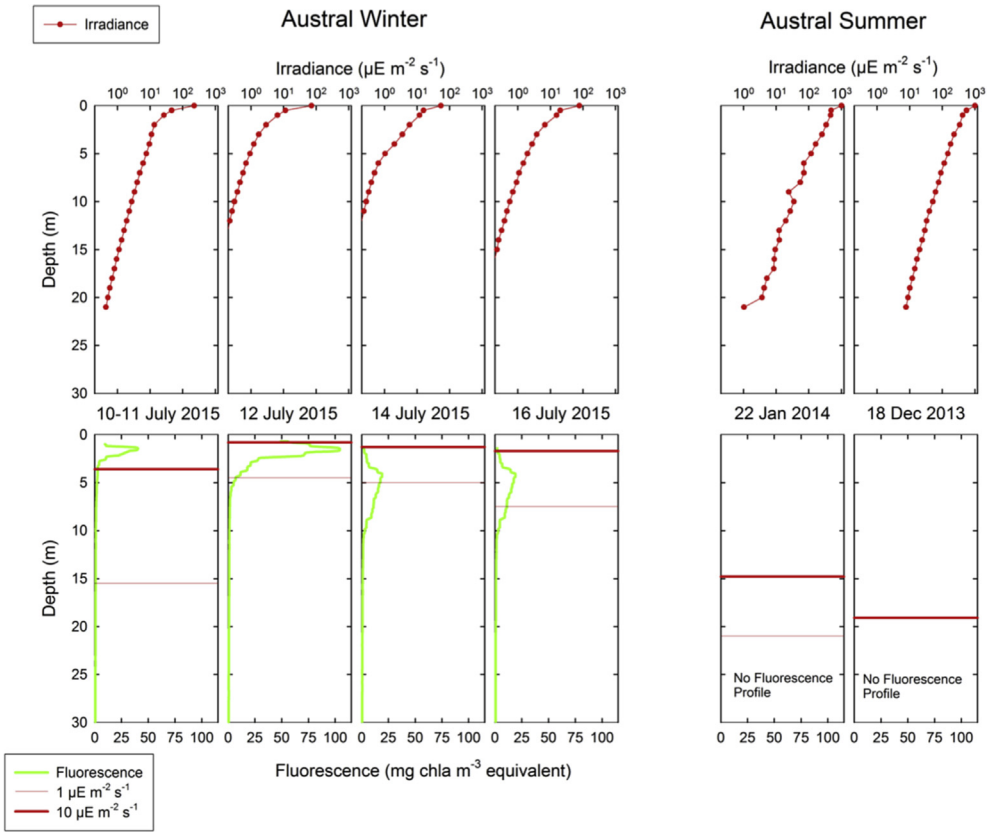

Fig. 6. Vertical profiles of fluorescence and underwater irradiance (photosynthetically active radiation, PAR) during July 2015. To the right are comparable profiles for austral summer 2014 and 2013 at the same location. In the lower panels, the depths of the occurrence of 1 and 10 μE m^{-2} s^{-1} levels are shown to approximate the compensation irradiance zone for dinoflagellates.

elements are limiting or when light limits photosynthesis (Legrand et al., 1998; Li et al., 1999; Millette et al., 2017). Despite the low irradiance levels recorded, our data suggest that GPP and pH were highest during July 12, co-incident with the peak in abundance of *H. triquetra* and in Chl-*a* concentrations (Fig. 4). However, a decrease in Chl-*a* during July 16, despite the high abundances observed (Fig. 4), suggests that self shading may have been limiting further growth, and therefore a mixotrophic mode of nutrition for the *Heterocapsa* bloom may have been conceivable at this stage of the bloom. Previous studies have indicated that the reduction in cellular Chl-a content in mixotrophic phytoplankton might be the consequence of an increase in growth rate due to feeding (Skovgaard, 1996a; Hansen et al., 2000; Skovgaard et al., 2000). We did not measure cellular Chl-a content of individual cells, but we did observe between July 14 and July 16 a decrease in total Chl-a from 149 to 70 mg m^{-2} associated with high *Heterocapsa* abundances of 43 and 40 × 10^9 cell m^{-2}, respectively (Fig. 4). It is therefore possible that *H. triquetra* may have supplemented phototrophy with mixotrophy during the study period. It is interesting that mixotrophy now features as an important functional trait in a recently revised version of Margalef's Mandala (Glibert, 2016).

Winter synoptic low-pressure systems (LPS) are associated with heavy rainfall and runoff that can supply inorganic nutrients critical for initiation and development of *Heterocapsa* blooms in the northern hemisphere (Litaker et al., 2002a). In the present study we also linked the bloom of *H. triquetra* to the passage of a synoptic low-pressure system that affected Puyuhuapi Fjord during our sampling campaign. Patagonian fjord ecosystems are generally surrounded by pristine woodland and low human population density, and therefore the increase in river runoff during LPS events does not generally deliver enhanced concentrations of inorganic nutrients to surface coastal waters, with the exception of silicic acid. The unique characteristics of Patagonian coastal waters mean that nitrate and phosphate concentrations are increased within surface waters (also marked by increases in surface T and S from deeper water) by mixing of the water column as a result of the passage of these LPS events.

The study area was subjected to the passage of several LPS events separated by intervals of two to four days. During these events, stronger northern winds (10–20 m s^{-1}) were recorded, and this contributed to mixing of the water column and the vertical displacement of the pycnocline. We suggest that these mixing and turbulence mechanisms supplied nutrients (nitrate and phosphate) from depth to surface waters, offering favorable conditions for growth of *H. triquetra* (summarized in Fig. 7). High-resolution vertical hydrographic profiles showed evidence for strong mixing in the upper 8 m of the water column that broke down stratification of surface waters (Fig. 3). The impact of LPS events was apparent down to a depth of ~30 m, where nitrate and phosphate were present at higher concentrations (>8 μmol L^{-1} nitrate, >0.6 μmol L^{-1} phosphate) and could be transported into surface waters through vertical mixing (Inall and Gillibrand, 2010; Silva and Vargas, 2014).

During the sampling period a thermal inversion layer covered the upper ~30 m of the water column, a feature of winter conditions caused by heat loss (Schneider et al., 2014), with salinity also increasing with depth owing to fresh water input into surface waters both from the Cisnes River discharge (Fig. 2C), and from rainfall. The presence of this cool-fresh water layer over warmer-salty waters contributed to the occurrence of double diffusive

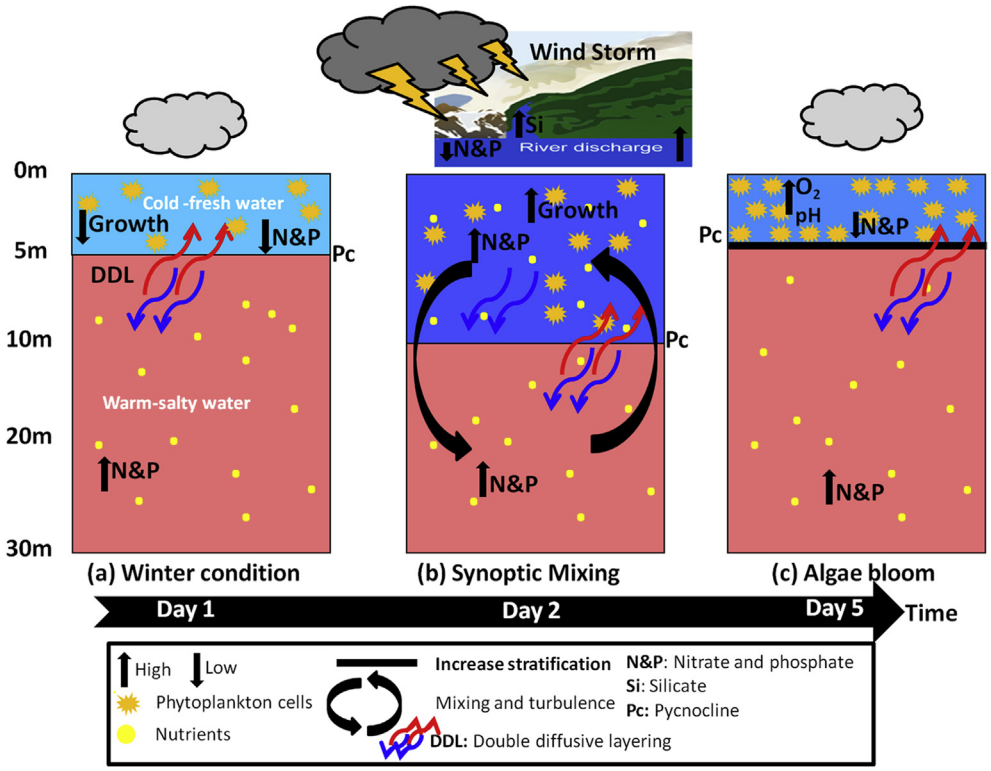

Fig. 7. Conceptual diagram showing the putative processes occurring during the development of the bloom.

layering (DL) events, which was supported by the presence of multiple thermohaline staircases (Fig. 3F). In Patagonian fjords, this DL is an important process (Pérez-Santos et al., 2013, 2014) that plays a significant role in vertical mixing of the water column and consequent injection of nutrients into surface waters. In addition, the dissipation rate of turbulent kinetic energy ($\varepsilon = 10^{-5}$–10^{-4} W kg^{-1}) and the diapycnal eddy diffusivity were high during the sampling period ($k\rho = 10^{-5}$–10^{-4} m^2 s^{-1}), highlighting the importance of turbulent mixing in supplying nutrients to surface waters.

Before the occurrence of bloom, the water column was characterized by relatively warmer and saltier surface water, with dissolved oxygen, chl-a and pH values typical of non-productive conditions. However, the passage of LPS (~990 mbar) on July 8 increased wind intensity and vertical mixing. This was followed by an increase in the Cisnes River discharge from 150 m^3 s^{-1} to 608 m^3 s^{-1} and a decrease in the surface water temperature and salinity, which stabilized the water column and created conditions favorable for both aggregation and growth of *H. triquetra* (Fig. 7). The low concentrations of nitrate and phosphate in surface water were augmented by vertical exchange with deeper water during the LPS event, and this injection of nutrients presumably satisfied the nutrient demand of the dinoflagellates (Fig. 7). PCA analysis showed an inverse association between abundance of *Heterocapsa* and concentrations of nitrate and phosphate, reflecting the depletion of these nutrients from surface water column by this dominant species.

The high-resolution vertical profiling of fluorescence confirmed a vertical migration pattern in which the population of *H. triquetra* ascended during the early hours of daylight, and then descended during the afternoon; we did not sample during dark hours. This migration behavior within the pycnocline persisted even during the influence of the strong LPS (although the abundance peak may have been deeper and more dispersed), and may have been related to nutrient uptake, selection of optimal light environment, or both. Clearly, without this vertical migration pattern, much of the population would have probably been subject to irradiance levels lower than the compensation irradiance and a bloom may not have developed.

Several authors have suggested that small flagellates, and particularly dinoflagellates, dominate phytoplanktonic communities when the water column is stratified (Eppley et al., 1978; Cohen, 1985). In our study, stratification resulted from a large influx of freshwater from the Cisnes River into the fjord, where surface salinities (1–5 m) were between 17 and 25 and temperatures between 8 and 10 °C. *Heterocapsa triquetra* has a wide tolerance to salinity (Mallin, 1994) and the ability to slowly adapt to low temperatures (Baek et al., 2011; Jephson et al., 2011). This physiological plasticity could therefore be directly involved with its capability to form blooms under harsh winter conditions.

Annual production in Puyuhuapi Fjord has been estimated at approximately 250 g C m^{-2} year^{-1}, with production in winter contributing only about 6% of this annual value (unpublished data). Blooms of *H. triquetra* as observed in a winter period previously described as non-productive, could therefore contribute significantly to annual productivity. GPP rates reported here were approximately three times higher than generally observed in Chilean fjords during winter, and are more comparable to rates reported during the productive season in Puyuhuapi Fjord (0.5–3 g C m^{-2} d^{-1}; unpublished data), in the Chiloé interior Sea (0.3–1 g C m^{-2} d^{-1}; Iriarte et al., 2007a,b) and in Reloncaví Fjord (0.9–2 g C m^{-2} d^{-1}; Montero et al., 2011).

Here we present the first report of a winter dinoflagellate bloom in the Patagonian fjords. These results improve our understanding of primary productivity cycles and composition of phytoplankton communities in Chilean fjords, and challenge the paradigm of winter as a low-productive period. We therefore reject the hypothesis that low irradiance levels limit the development of dense

phytoplankton blooms in winter in these fjords. Physiological plasticity and behavioural patterns may allow *Heterocapsa triquetra* to tolerate and thrive under conditions of low temperature, low salinity and low light characteristic of the deep Patagonian winter.

5. Conclusion

- A dinoflagellate bloom dominated by *Heterocapsa triquetra* was observed during austral winter and was associated with high rates of gross primary production.
- The vertical mixing produced by the double diffusive layering events and the impact of low-pressure systems on turbulent mixing favored the development of the *Heterocapsa triquetra* bloom through enhanced supply of nutrients.
- Vertical fluorescence profiles, considered as indicative of *Heterocapsa triquetra* abundance, showed a diurnal pattern of vertical migration above the pycnocline with a double layer distribution during the day. Accumulation of the population close to the surface may have facilitated development of the bloom, despite low irradiance.
- The phytoplankton bloom detected in austral winter challenges the paradigms of winter as a low-productive period and of low levels of irradiance as a key factor limiting phytoplankton blooms. This highlights the importance of synoptic events in the ecosystem productivity of Patagonian fjords.

Acknowledgements

This research was funded by FONDECYT 1131063 and COPAS Sur-Austral (CONICYT PFB-31/2017). Iván Pérez-Santos, is also funded by FONDECYT 11140161.

Appendix A. Supplementary data

Supplementary data related to this article can be found at https://doi.org/10.1016/j.ecss.2017.09.027.

References

Baek, S.H., Ki, J.S., Katano, T., You, K., Park, B.S., Shin, H.H., Shin, K., Kim, Y.O., Han, M., 2011. Dense winter bloom of the dinoflagellate *Heterocapsa triquetra* below the thick surface ice of brackish Lake Shihwa, Korea. Phycol. Res. 59, 273–285.

Barton, A.D., Finkel, Z.V., Ward, B.A., Johns, D.G., Follows, M.J., 2013. On the roles of cell size and trophic strategy in North Atlantic diatom and dinoflagellate communities. Limnol. Oceanogr. 58 (1), 254–266.

Casas, B., Varela, M., Bode, A., 1999. Seasonal succession of phytoplankton species on the coast of A Coruña (Galicia, northwest Spain). Bol. Inst. Esp. Oceanogr. 15 (1–4), 413–429.

Cassis, D., Muñoz, P., Avaria, S., 2002. Variación temporal del fitoplancton entre 1993 y 1998 en una estación fija del seno Aysén, Chile (45°26′S 73°00′W). Rev. Biol. Mar. Oceanogr. 37 (1), 43–65.

Chaigneau, A., Pizarro, O., 2005. Mean surface circulation and mesoscale turbulent flow characteristics in the eastern South Pacific from satellite tracked drifters. J Geophys. Res. Oceans 110, C05014. https://doi.org/10.1029/2004JC002628.

Cohen, R.R.H., 1985. Physical processes and the ecology of a winter dinoflagellate bloom of *Katodinium rotundatum*. Mar. Ecol. Prog. Ser. 26, 135–144.

Cuypers, Y., Bouruet-Aubertot, P., Marec, C., Fuda, J.L., 2011. Characterization of turbulence and validation of fine-scale parametrization in the Mediterranean Sea during BOUM experiment. Biogeosciences Discuss. 8, 8961–8998. https://doi.org/10.5194/bgd-8-8961-2011.

Czypionka, T., Vargas, C.A., Silva, N., Daneri, G., González, H.E., Iriarte, J.L., 2011. Importance of mixotrophic nanoplankton in Aysén Fjord Southern Chile during austral winter. Cont. Shelf Res. 31 (3–4), 216–224.

Eppley, R.W., Koeller, P., Wallace, G.T., 1978. Stirring influences the photoplankton species composition within enclosed columns of coastal seawater. J. Exp. Mar. Biol. Ecol. 32, 239.

Glibert, P.M., 2016. Margalef revisited: a new phytoplankton mandala incorporating twelve dimensions, including nutritional physiology. Harmful Algae 55, 25–30. https://doi.org/10.1016/j.hal.2016.01.008.

Goebel, N.L., Wing, S.R., Boyd, P.W., 2005. A mechanism for onset of diatom blooms in a fjord with persistent salinity stratification. Est. Coast. Shelf Sci. 64, 546–560.

González, H.E., Calderon, M.J., Castro, L., Clement, A., Cuevas, L.A., Daneri, G., Iriarte, J.L., Lizárraga, L., Martínez, R., Menschel, E., Silva, N., Carrasco, C., Valenzuela, C., Vargas, C.A., Molinet, C., 2010. Primary production and plankton dynamics in the Reloncaví fjord and the interior sea of Chiloé, northern Patagonia, Chile. Mar. Ecol. Prog. Ser. 402, 13–30.

Hansen, P.J., Lundholm, N., Rost, B., 2007. Growth limitation in marine red-tide dinoflagellates: effects of pH versus inorganic carbon availability. Mar. Ecol. Prog. Ser. 334, 63–71.

Hansen, P.J., Skovgaard, A., Glud, R.N., Stoecker, D.N., 2000. Physiology of the mixotrophic dinoflagellate *Fragilidium subglobosum*. II. Effects of time scale and prey concentration on photosynthetic performance. Mar. Ecol. Prog. Ser. 201, 137–146.

Huovinen, P., Ramírez, J., Gómez, I., 2016. Underwater optics in sub-antarctic and antarctic coastal ecosystems. PLoS ONE 11 (5), e0154887. https://doi.org/10.1371/journal.pone.0154887.

Inall, M.E., Gillibrand, P.A., 2010. The Physics of Mid-latitude Fjords: a Review, Geological Society, vol. 344. Special Publications, London, UK, pp. 17–33.

Iriarte, J.L., Quiñones, R.A., González, R.R., 2005. Relationship between biomass and enzymatic activity of a bloom-forming dinofalgellate (Dinophyceae) in southern Chile (41°S): a field approach. J. Plankton Res. 27 (2), 159–166.

Iriarte, J.L., Quiñones, R.A., González, R.R., Valenzuela, C.P., 2007a. Relación entre actividad enzimática y biomasa de ensambles fitoplanctónicos en el sistema pelágico. Invest. Mar. 35 (1), 71–84.

Iriarte, J.L., González, H.E., Liu, K.K., Rivas, C., Valenzuela, C.P., 2007b. Spatial and temporal variability of chlorophyll and primary productivity in surface waters of southern Chile. Estuarine. Coast. Shelf Sci. 74, 471–480.

Iriarte, J.L., González, H.E., 2008. Phytoplankton bloom ecology of the inner sea of Chiloé, southern Chile. Nova Hedwig. Beih. 133, 67–79.

Iriarte, J.L., Pantoja, S., González, H.E., Silva, G., Paves, H., Labbé, P., Rebolledo, L., Van Ardelan, M., Häussermann, V., 2013. Assessing the micro-phytoplankton response to nitrate in Comau Fjord (42°S) in Patagonia (Chile), using a microcosms approach. Environ. Monit. Assess. 185, 5055–5070. https://doi.org/10.1007/s10661-012-2925-1.

Jephson, T., Fagerberg, T., Carlsson, P., 2011. Dependency of dinoflagellate vertical migration on salinity stratification. Aquat. Microb. Ecol. 63, 255–264.

Lee, C.K., Lee, O.H., Lee, S.G., 2005. Impacts of temperature, salinity and irradiance on the growth of ten harmful algal bloom-forming microalgae isolated in Korean coastal water. Sea J. Korean Soc. Oceanogr. 10, 79–91 (In Korean).

Legendre, L., Rassoulzadegan, F., 1996. Food-web mediated export of biogenic carbon in oceans: hydrodynamic control. Mar. Ecol. Prog. Ser. 145, 179–193.

Legendre, L., 1990. The significance of microalgal blooms for fisheries and for the export of particulate organic carbon in oceans. J. Plankton. Res. 12 (4), 681–699.

Legrand, C., Granéli, E., Carlsson, P., 1998. Induced phagotrophy in the photosynthetic dinoflagellate *Heterocapsa triquetra*. Aquat. Microb. Ecol. 15, 65–75.

Li, A., Stoecker, D.N., Adolf, J.E., 1999. Feeding, pigmentation, photosynthesis and growth of the mixotrophic dinoflagellate Gyrodinium galatheanum. Aquat. Microb. Ecol. 19, 163–176.

Litaker, R.W., Tester, P.A., Duke, C.S., Kenney, B.E., Pinckney, J.L., Ramus, J., 2002a. Seasonal niche strategy of the bloom-forming dinoflagellate *Heterocapsa triquetra*. Mar. Ecol. Prog. Ser. 232, 45–62.

Litaker, R.W., Warner, V.E., Rhyne, C., Duke, C.S., Kenney, B.E., Ramus, J., Tester, P.A., 2002b. Effect of diel and interday variations in light on the cell division pattern and in situ growth rates of the bloom-forming dinoflagellate *Heterocapsa triquetra*. Mar. Ecol. Prog. Ser. 232, 63–74.

Luketina, D.A., Imberger, J., 2001. Determining turbulent kinetic energy dissipation from batchelor curve fitting. J. Atmos. Ocean. Technol. 18, 100–113. https://doi.org/10.1175/1520-0426.

Mallin, M.A., Paerl, H.W., Rudek, J., 1991. Seasonal phytoplankton composition, productivity and biomass in the Neuse River estuary, North Carolina. Estuar. Coast. Shelf Sci. 32, 609–623.

Mallin, M.A., 1994. Phytoplankton ecology of North Carolina estuaries. Estuaries 17 (3), 561–574.

Margalef, R., 1978. Life-forms of phytoplankton as survival alternatives in an unstable environment. Oceanol. Acta 1 (4), 493–509.

Marshall, H.G., Burchardi, L., Lacouture, R., 2005. A review of phytoplankton composition within Chesapeake bay and its tidal estuaries. J. Plankton. Res. 27 (11), 1083–1102.

Millette, N.C., Stoecker, D.K., Pierson, J.J., 2015. Top-down control by micro- and mesozooplankton on winter dinoflagellate blooms of *Heterocapsa rotundata*. Aquat. Microb. Ecol. 76, 15–25.

Millette, N.C., Pierson, J.J., Aceves, A., Stoecker, D.K., 2017. Mixotrophy in *Heterocapsa rotundata*: a mechanism for dominating the winter phytoplankton. Limnol. Oceanogr. 62, 836–845. https://doi.org/10.1002/lno.10470.

Montero, P., Daneri, G., González, H.E., Iriarte, J.L., Tapia, F.J., Lizárraga, L., Sanchez, N., Pizarro, O., 2011. Seasonal variability of primary production in a fjord ecosystem of the Chilean Patagonia: implications for the transfer of carbon within pelagic food webs. Cont. Shelf Res. 31, 202–215. https://doi.org/10.1016/j.csr.2010.09.003.

Osborn, T.R., 1980. Estimates of the local rate of vertical diffusion from dissipation measurements. J. Phys. Oceanogr. 10, 83–89.

Parsons, T.R., Maita, Y., Lalli, C.M., 1984. Counting, media and preservatives. Chapter 8. In: A Manual of Chemical and Biological Methods for Seawater Analysis. Pergamon Press, Toronto, p. 173.

Pérez-Santos, I., Vargas, J.G., Schneider, W., Parra, S., Ross, L., Valle-Levinson, A., 2013. Double diffusion from microstructure measurements in the Martínez and Baker channels, central Chilean Patagonia (47.85°S). Lat. Am. J. Aquat. Res. 41 (1)

https://doi.org/10.3856/vol41-issue1-fulltext-x.
Pérez-Santos, I., Garcés-Vargas, J., Schneider, W., Ross, L., Parra, S., Valle-Levinson, A., 2014. Double-diffusive layering and mixing in Patagonia fjords. Prog. Oceanogr. 129, 35–49.
Pizarro, G., Astoreca, R., Montecino, V., Paredes, M.A., Alarcón, G., Uribe, P., Guzmán, L., 2005. Patrones espaciales de la abundancia de la clorofila, su relación con la productividad primaria y la estructura de tamaños del fitoplancton en Julio y Noviembre de 2001 en la región de Aysén (43°-46°S). Rev. Cien. Tecn. Mar. 28 (2), 27–42.
Richardson, K., Beardall, J., Raven, J.A., 1983. Adaptation of unicellular algae to irradiance: an analysis of strategies. New Phytol. 93, 157–191.
Ruddick, B.R., 1983. A practical indicator of the stability of the water column to double-diffusive activity. Deep-Sea Res. 30, 1105–1107.
Ruddick, B., Anis, A., Thompson, K., 2000. Maximum likelihood spectral fitting: the batchelor spectrum. J. Atmos. Ocean. Technol. 17, 1541–1555. https://doi.org/10.1175/1520-0426.
Schneider, W., Pérez-Santos, I., Ross, L., Bravo, L., Seguel, R., Hernández, F., 2014. On the hydrography of Puyuhuapi channel (chilean Patagonia). Prog. Oceanogr. 129, 8–18. https://doi.org/10.1016/j.pocean.2014.03.007.
Sellner, K.G., Lacouture, R.V., Cibik, S.J., Brindley, A., Brownlee, S.G., 1991. Imporantance of a winter dinoflagellate-microflagellate bloom in the Patuxent river estuary. Estuar. Coast. shelf Sci. 32, 27–42.
Shih, L.H., Koseff, J.R., Ivey, G.N., Ferziger, J., 2005. Parameterization of turbulent fluxes and scales using homogeneous sheared stably stratified turbulence simulations. J. Fluid Mech. 525, 193–214.
Sievers, H., Silva, N., 2008. Water masses and circulation in austral Chilean channels and fjords. In: Progress in the Oceanographic Knowledge of Chilean Interior Waters, from Puerto Montt to Cape Horn. Comité Oceanográfico Nacional – Pontificia Universidad Católica de Valparaíso, Valparaíso, pp. 53–58.
Silva, N., 2008. Dissolved oxygen, pH, and nutrients in the austral Chilean channels and fjords. In: Silva, N., Palma, S. (Eds.), Progress in the Oceanographic Knowledge of Chilean Interior Waters, from Puerto Montt to Cape Horn. Comité Oceanográfico Nacional – Pontificia Universidad Católica de Valparaíso, Valparaíso, pp. 37–43.
Silva, N., Vargas, C., 2014. Hypoxia in chilean Patagonia fjords. Prog. Oceanogr. 129, 62–74.
Skovgaard, A., 1996a. Mixotrophy in *Fragilidium subglobosum* (Dinophyceae): growth and grazing responses as functions of light intensity. Mar. Ecol. Prog. Ser. 143, 247–253.
Skovgaard, A., Hansen, P.J., Stoecker, D.K., 2000. Fragilidium subglobosum. I. Effects of phagotrophy and irradiance on photosynthesis and carbon content. Mar. Ecol. Prog. Ser. 201, 129–136.
Strickland, J.D.H., Parsons, T.R., 1968. A practical handbook of seawater analysis. Bull. Fish. Res. Board Can. 167.
Strickland, J.D.H., 1960. Measuring the production of marine phytoplankton. Bull. Fish. Res. Board Can. 122, 1–172.
Tas, S., 2015. A prolonged red tide of *Heterocapsa triquetra* (Ehrenberg) F. Stein (Dinophyceae) and phytoplankton succession in a eutrophic estuary (Turkey). Medit. Mar. Sci. 16 (3), 621–627.
Torres, R., Silva, N., Reid, B., Frangopulos, M., 2014. Silicic acid enrichment of subantarctic surface water from continental inputs along the Patagonian archipelago interior sea (41–56°S). Prog. Oceanogr. 129, 50–61. https://doi.org/10.1016/j.pocean.2014.09.008.
Thorpe, S.A., 2005. The Turbulence Ocean. Cambridge Universty Press, CB2 2RU, UK, 426 pp.
Utermöhl, H., 1958. Zur Vervollkommnung der quantitativen Phytoplankton-Methodik. Internationale Vereinigung für Theoretische und Angewandte Limnologie. Kom. für Limnol. Methoden 9, 1–39.
Williams, P. J. LeB., Robertson, J.E., 1991. Overall planktonic oxygen and carbon dioxide metabolisms: the problem of reconciling observations and calculations of photosynthetic quotients. J. Plankton Res. 13 (153–169).
Yamaguchi, M., Itakura, S., Nagasaki, K., Matsuyama, Y., Uchida, T., Imai, I., 1997. Effects of temperature and salinity on the growth of the ride tide flagellates *Heterocapsa circularisquama* (Dinophyceae) and *Chatonella verruculosa* (Raphidophyceae). J. Plankton. Res. 19 (8), 1167–1174.
You, Y., 2002. A global ocean climatological atlas of the Turner angle: implications for double-diffusion and water-mass structure. Deep-Sea Res. I 49, 2075–2093.

MANUSCRIPT IN PREPARATION III

Atmospheric-ocean forcing on phytoplankton productivity and carbon flow through the microbial food web in a Patagonia fjord system (44°S)

Atmospheric-ocean forcing on phytoplankton productivity and carbon flow through the microbial food web in a Patagonia fjord system (44°S)

Giovanni Daneri, Iván Pérez-Santos, Paulina Montero, Bárbara Jacob, Marcelo Gutiérrez, Carolina Medel, Manuel Castillo, Oscar Pizarro.

1. INTRODUCTION

The southern tip of south America constitutes the southernmost extension of land north of the Antarctic peninsula and poses a unique land barrier to what otherwise would be a continuous circumpolar oceanic gyre of sub-Antarctic water characterized by high levels of inorganic nutrients (mainly nitrate and phosphate) and low chlorophyll levels. When approaching the southern tip of South America, this gyre, or west wind drift, bifurcates to the north as the highly productive Humboldt current, and to the south as the Cape Horn Current, which in oceanographic terms, has been largely understudied to date. The west wind drift pushes sub-Antarctic water into the intricate network of fjords and channels characterizing western Patagonia where its interaction with freshwater defines one of the largest estuarine systems on earth. The immense volume of freshwater derived from melting glaciers, rainfall and underground sources stabilizes the water column and is rich in silicic acid, iron and other trace elements. These chemical properties – when combined with the nitrate and phosphate provided by sub-Antarctic water – help to support high rates of primary productivity and community metabolism in Patagonian fjords that contribute significantly to biological productivity and carbon cycling both in the eastern South Pacific Ocean (González et al., 2010; 2011; 2013; Montero et al. 2011;Torres et al. 2011) and globally (Gattuso et al. 1998; Cloern et al. 2014; Smith et al. 2015).

In these fjords, local geographic features and major remote climatic and oceanographic forcing can act at different scales to impact upon water column structure and biological processes (Iriarte et al. 2014). Climatic conditions in Chilean Patagonia are characterized by sharp seasonal fluctuations in atmospheric forcing, such as changes in wind direction and stress, and precipitation (Pickard, 1971; Acha et al., 2004; Montero et al., 2011), with significant interannual variability in these conditions (Garreaud and Falvey,

2009; Garreaud et al., 2013; Narvaez et al, 2019). Despite such climatic and hydrographic heterogeneity within the Patagonian region (Pantoja et al, 2011; Iriarte et al, 2014), general patterns of spatial and temporal variability of primary productivity have in fact been identified (Aracena et al., 2011; Jacob et al., 2014, Montero et al, 2011, 2017a). The annual cycle of phytoplankton productivity (Iriarte and Gonzalez, 2008) has been typically characterized by a short low-productivity period during the winter, followed by an extended high productivity season that begins with a late winter bloom and extends to late fall (Iriarte et al., 2007; Montero et al., 2011). Seasonal shifts in the predominant winds drive mixing-stratification cycles, with consequences for water column irradiance that influences the annual cycle of productivity (Iriarte and González, 2008; Montero *et al*., 2011). Hydrodynamic patterns within a given fjord are also strongly modulated by freshwater discharges, which can either intensify or weaken an estuarine type circulation and the spatial extent of phytoplankton blooms (Goebel *et al*., 2005; González *et al*., 2013; Iriarte *et al*., 2014; Jacob *et al*., 2014). Freshwater discharge also provides the main source of silicic acid to the fjords, and this has recently been described as one of the key factors driving a late winter bloom, dominated by diatoms of the genera *Skeletonema* and *Chaetoceros* (Montero et al. 2017a).

Large-scale ocean-atmosphere dynamics have been identified such as the Pacific Decadal Oscillation (PDO), the El Niño and La Niña (ENSO) cycle, the Southern Annular Mode (SAM), and the Baroclinic Annular Mode (BAM). These dynamics combined with global climate trends, are significant influences on oceanographic conditions of the eastern South Pacific Ocean, and may impact the productive cycles of phytoplankton within fjords, potentially disrupting the trophic interactions and carbon transfer through the food web (Narvaez et al., 2019, León-Muñoz et al., 2018). For instance, analysis of long-term satellite data revealed a sharp break in the typical annual cycle of Chl-*a* concentration in the northern Inner Sea of Chiloé; this was forced by interannual changes in sea surface temperature anomaly and large-scale climate indices (Lara et al., 2016). This perturbation was followed by an abrupt decline in mussel larval abundance in 2010-2011, and a subsequent drop of 30% in mussel production, with clear social and economic consequences (Lara et al., 2016). In the summer of 2016, the dry conditions associated with a strong El Niño and positive phase of SAM weakened saline stratification of the water

column. This allowed the advection of saline and nutrient-rich waters into the euphotic zone, triggering an intense Harmful Algal Bloom (HAB) over a wide geographical area in coastal southern Chile with catastrophic consequences for human health, aquatic ecosystems and aquaculture economic activities (León-Muñoz et al., 2018).

The dominant frequencies of variability in large scale ocean-atmospheric forcing have been evaluated in the Patagonia region (Narváez et al., 2019). Among short scale climatic variability, an intraseasonal periodicity of 20-30 days associated with the BAM has been reported for the Southern hemisphere climate system (Thompson and Barnes, 2014; Ross et al., 2015; Narváez et al., 2019; Pérez-Santos et al., 2019). The BAM was associated with extreme low-pressure events (900 hPa) that resulted in deepening of the pycnocline in the Martinez Channel located in central Patagonia. This represents a good example of the potential hydrographic effects of BAM on fjord systems in the southern hemisphere (Ross et al., 2015). The hydrographic effects of the BAM may not be restricted to a single channel, and its influence could be synchronized within multiple fjords of Chilean Patagonia (Narváez et al., 2018), potentially, generating productivity pulses across the region (Narváez et al., 2018). Further climatic variability occurs on the synoptic scale, characterized by a cycle length of 16.5 d and by low and high atmospheric pressure systems (Pérez-Santos et al., 2019). Low atmospheric pressure systems (LAPS) have recently been shown to produce favorable conditions for elevated primary production, as was observed for a dense bloom of *Heterocapsa triquetra* during deep winter in a Puyuhuapi Fjord (Montero et al. 2017b). This dinoflagellate bloom occurred under low surface irradiance levels characteristic of austral winter, and coincided with strong northern winds and a water column dominated by a double diffusive layering (Montero et al. 2017a). Such observations contradict the generally accepted paradigm that low light severely limits productivity rates during winter (Iriarte et al., 2007), and introduces a novel scale of variability for biological productivity in Patagonia fjords that requires more focused research attention. The synoptic atmospheric forcing – as LAPS – has also been associated with cyclonic circulation reported as one of the physical processes impacting estuarine and fjord systems more generally (Litaker et al., 2002; Inall & Gillibrand, 2010). For instance, in the southeastern Bering Sea and Barents Sea, LAPS have been reported to induce vertical mixing and supply

of new nutrients into the euphotic layer (Sambrotto et al., 1986; Sakshaug et al, 1991; 1995; Sakshaug & Slagstad 1992).

These responses at the local-scale to macro-scale variability highlight the importance of larger-scale processes for hydrographic characteristics and phytoplankton productivity in localized Patagonian estuarine ecosystems. Additionally, over the entire Southern Hemisphere, the Southern Annular Mode (SAM) – or Antarctic Oscillation – is the leading mode of climate variability on timescales varying between intraseasonal and interannual (Thompson and Wallace, 2000). The SAM has shown a significant positive trend over the past 50 years largely attributed to stratospheric ozone depletion and increased greenhouse gases (Thompson et al., 2011). SAM has also been associated with anomalously dry conditions over southern South America due to the southward shift of the storm tracks (Gupta and England, 2006; Gillett et al., 2006 and references therein).

The potential impacts of positive and negative phases of SAM on the synoptic large-scale circulation (e.g. westerly winds) and local productivity has not been examined, despite the observation that the southern Patagonia (from 40°S to 56°S) the synoptic variability account 30% of the total variance over the various timescales (Pérez-Santos et al., 2019). Therefore an improved understanding is clearly required of how large-scale atmospheric processes determine various scales of variability of local phytoplankton productivity. Such information is key to characterizing biogeochemical cycles and estimating carbon sequestration capacity in order to improve planning and management decisions in those Patagonian fjords that are strongly impacted by anthropogenic activities such as aquaculture. In the present study, we assess the extent to which ocean-atmospheric forcing at synoptic (1-16 d), and seasonal (>90 d) temporal scale determines changes in phytoplankton composition and productivity at a single station in the Puyuhuapi Fjord. In addition, we evaluate the community net metabolism and carbon transfer from phytoplankton photosynthesis through the microbial community, in order to assess the role of prokaryotes in the cycling of organic matter. We hypothesize that the phytoplankton activity induced by ocean-atmospheric forcing at synoptic temporal scale makes a significant contribution to the annual productivity cycle in Patagonian fjord ecosystems.

2. MATERIALS AND METHODS

2.1 Study area and sampling strategy

The physical, chemical and biological measurements collected between 2008-2017, together with monthly records of measurements and instruments used in this study, are summarized in Table 1. Measurements from the meteorological/oceanographic buoy were collected in the northern section of the Puyuhuapi Fjord (44°33.3´S and 72°43.6´W), approximately 5 km NW of the Cisnes River mouth (Fig. 1). The buoy has been operative from September 2009 (www.cdom.cl), although the present study has considered the time series from 2010 to 2015 for wind speed and direction, sea surface temperature (SST), salinity, dissolved oxygen (DO) and solar radiation. Chl-a records (buoy) were collected from the buoy between 2012 and 2015 (Fig. 3). High resolution Acoustic Doppler Current Profiler (ADCP) measurements were carried out in the Jacaf Channel ca. 15 km NW of the buoy station (Fig. 1). River discharge data – with hourly temporal resolution – was obtained from the DGA station (Dirección General de Agua) located in the Cisnes River mouth during the period 2008-2015. Hydrographic, chemical and biological sampling at the Puyuhuapi station was conducted approximately at monthly intervals between January and November 2008; March and September 2009; June and December 2013; March and September 2014; July 2015; August 2016; March 2017. Additionally, intensive sampling campaigns (over periods of ~3-6 consecutive days) were also conducted.

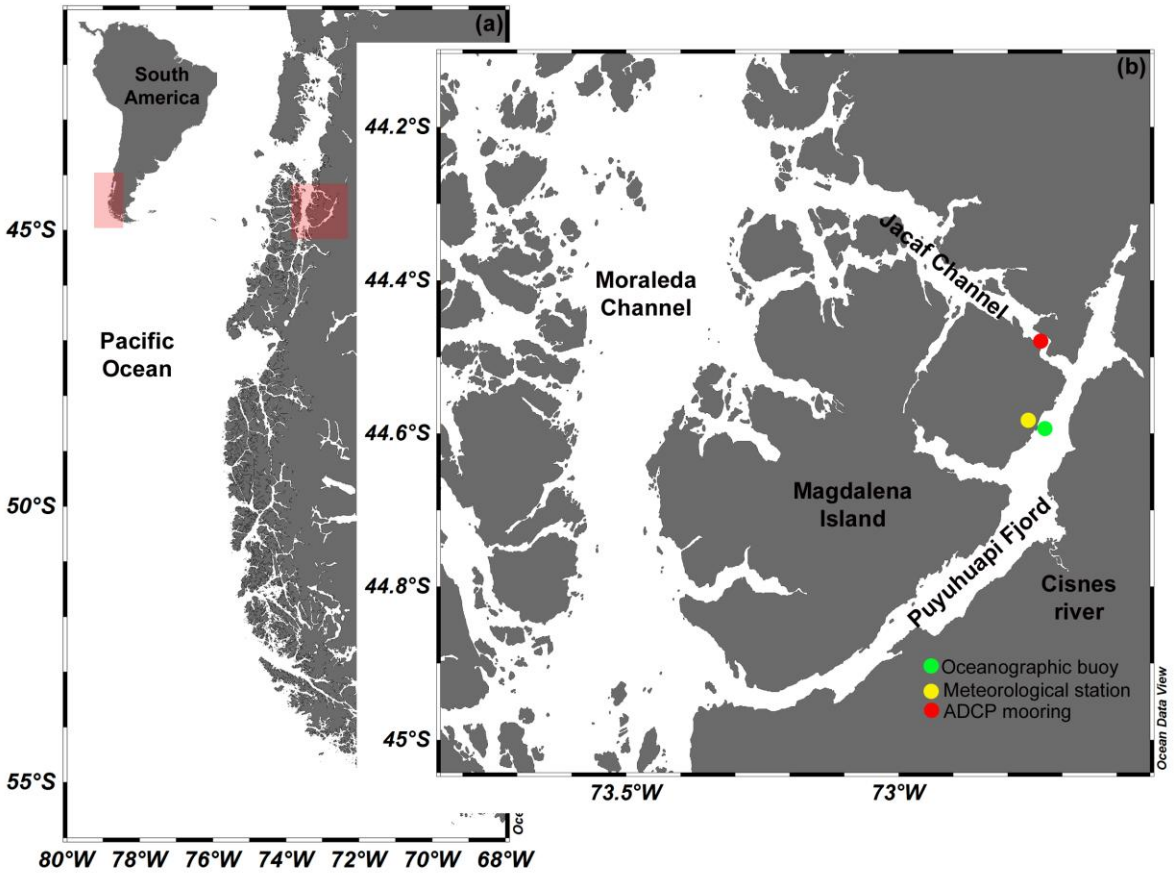

Figure 1. Map of the study area showing (a) the general region used for the regional satellite analysis of the surface wind regime and (b) the locations of the oceanographic and atmospheric stations in Puyuhuapi Fjord and Jacaf Channel.

Table 1. Summary of physical, chemical and biological measurements, collected between 2008 and 2017 in the study area, together with dates of monthly measurements.

Continuous measurements		**J**	**F**	**M**	**A**	**M**	**J**	**J**	**A**	**S**	**O**	**N**	**D**
Wind speed and direction, air temperature, atmospheric pressure. Puyuhuapi Fjord (MeteorologicalStation)	2010	-	-	-	-	-	-	-	-	-	-	-	-
	2011	-	-	-	x	x	x	x	x	x	x	x	x
	2012	x	x	x	x	x	x	x	x	x	x	x	x
	2013	x	x	x	x	x	x	x	-	x	-	-	-
	2014	-	-	-	x	x	x	x	x	-	x	x	x
	2015	x	x	x	x	x	x	x	x	x	x	x	x
	2016	x	x	x	x	x	-	x	x	x	x	x	x
	2017	x	x	x	-	-	-	-	-	-	-	-	-
Sea surface temperature and salinity Puyuhuapi Fjord (Buoy)	2010	-	-	-	-	-	-	x	x	X	x	x	x
	2011	x	x	x	x	x	x	x	x	x	x	x	x
	2012	x	x	x	x	x	x	x	x	x	x	x	x
	2013	x	x	-	-	-	x	x	x	x	-	-	x
	2014	x	x	-	x	x	x	x	x	x	x	-	x
	2015	x	x	x	x	x	x	x	x	x	x	x	x
	2016	x	x	x	x	-	x	x	x	x	x	x	x
	2017	x	x	x	-	-	-	-	-	-	-	-	-
Chlorophyll-*a* Puyuhuapi Fjord (Buoy)	2010	-	-	-	-	-	-	-	-	-	-	-	-
	2011	-	-	-	-	-	-	-	-	-	-	-	-
	2012	-	-	-	-	-	x	x	x	x	x	x	x
	2013	x	x	-	-	-	-	x	x	x	-	-	x
	2014	x	x	-	x	x	x	x	x	x	x	-	x
	2015	x	x	x	x	x	x	x	x	x	x	x	x
	2016	x	x	x	x	-	x	x	x	x	x	x	x
	2017	x	x	x	-	-	-	-	-	-	-	-	-
River Discharge Cisnes river	2010	x	x	-	x	x	x	x	x	x	x	x	x
	2011	x	x	x	x	x	x	x	x	x	x	x	x
	2012	x	x	x	x	x	-	x	x	x	x	x	x
	2013	x	x	x	x	-	x	x	x	x	x	x	x
	2014	x	x	x	x	x	x	x	x	-	-	-	-
	2015	-	-	x	x	x	x	x	x	x	x	-	-
ADCP Jacaf Channel	2010	-	-	-	-	-	-	-	-	-	-	-	-
	2011	-	-	-	-	-	-	-	-	-	-	-	-
	2012	-	-	-	-	-	-	-	-	-	-	-	-
	2013	-	-	-	-	-	-	-	-	-	-	-	-
	2014	-	-	-	-	-	-	-	x	x	x	x	x
	2015	x	x	x	x	x	-	-	-	-	-	-	-
	2016	-	-	-	-	-	-	-	-	-	-	-	-
	2017	-	-	-	-	-	-	-	-	-	-	-	-

Table 1. continuation.

Discrete measurements		J	F	M	A	M	J	J	A	S	O	N	D
	2008	-	-	-	x	x	x	x	x	x	x	x	x
Hydrography	2009	x	x	x	x	-	-	-	-	x	-	-	x
	2013	-	-	-	-	-	x	x	x	x	x	x	x
Puyuhuapi Fjord (Buoy)	2014	-	-	x	x	x	x	x	x	x	-	-	-
	2015	x	-	-	-	-	-	x	-	-	-	-	-
	2008	x	x	-	-	x	x	x	x	-	x	x	-
	2009	-	-	x	x	-	-	-	-	x	x	-	-
Inorganic nutrients	2013	-	-	-	-	-	x	x	x	x	x	x	x
	2014	x	-	x	x	x	x	x	x	x	-	-	-
Puyuhuapi Fjord (Buoy)	2015	-	-	-	-	-	-	x	-	-	-	-	-
	2016	-	-	-	-	-	-	-	x	-	-	-	-
	2017	-	-	x	-	-	-	-	-	-	-	-	-
	2008	x	-	-	x	x	x	x	x	x	x	x	-
	2009	-	-	x	x	-	-	-	-	x	x	-	-
Chlorophyll-a	2013	-	-	-	-	-	x	x	x	x	x	x	x
	2014	x	-	x	x	x	x	x	x	x	-	-	-
Puyuhuapi Fjord (Buoy)	2015	-	-	-	-	-	-	x	-	-	-	-	-
	2016	-	-	-	-	-	-	-	x	-	-	-	-
	2017	-	-	x	-	-	-	-	-	-	-	-	-
	2008	x	-	-	-	x	x	x	x	-	x	-	-
Dissolved organic carbon	2009	-	-	-	-	-	-	-	-	x	x	-	-
	2013	-	-	-	-	-	x	x	x	-	x	x	x
Puyuhuapi Fjord (Buoy)	2014	x	-	-	x	x	x	x	x	x	-	-	-
	2015	-	-	-	-	-	-	x	-	-	-	-	-
	2008	x	x	-	x	x	x	x	x	x	x	x	x
	2009	-	-	x	x	-	-	-	x	-	-	-	-
Phytoplankton composition	2013	-	-	-	-	-	x	x	x	x	x	x	x
	2014	x	-	x	x	x	x	x	x	x	-	-	-
Puyuhuapi Fjord (Buoy)	2015	-	-	-	-	-	-	-	-	-	-	-	-
	2016	-	-	-	-	-	-	-	x	-	-	-	-
	2017	-	-	x	-	-	-	-	-	-	-	-	-
	2008	x	-	-	x	x	-	x	-	-	x	-	-
	2009	-	-	-	-	-	-	-	-	-	x	-	-
Prokaryote secondary production	2013	-	-	-	-	-	-	-	-	-	-	-	-
	2014	-	-	x	x	x	x	x	x	x	-	-	-
Puyuhuapi Fjord (Buoy)	2015	-	-	-	-	-	-	x	-	-	-	-	-
	2016	-	-	-	-	-	-	-	x	-	-	-	-
	2017	-	-	x	-	-	-	-	-	-	-	-	-
Extracellular enzimatic activity	2013	-	-	-	-	-	-	-	x	-	-	-	-
Puyuhuapi Fjord (Buoy)	2014	-	-	x	-	-	-	x	-	-	-	x	-

2.2 Satellite surface wind data

The surface wind data was produced from Advanced Scatterometer (ASCAT) measurements (https://podaac.jpl.nasa.gov) taken during the period from 2010 to 2015. This data set is available with a daily temporal resolution, and with a regular spatial grid of 0.25° × 0.25°. The validation, details for the surface wind fields of this product, is presented in Bentamy and Croize-Fillon (2011). Daily surface wind data was used to calculate the long-term seasonal means presented in Fig. 2. In order to categorize the various time-distance scales of atmospheric systems, we have adopted the terms macro-, meso-, and micro-scale according to Orlanski (1975), Ray (1986) and Holton (1992).

2.3 Environmental data from buoy and meteorological station

The oceanographic buoy sited in the northern section of the Puyuhuapi Fjord – eequipped with atmospheric (wind speed and direction, air temperature and atmospheric pressure) and surface water sensors (temperature and conductivity) – provided data to facilitate understanding of fjord-atmospheric interactions. The meteorological data were collected at ~2.5 meters above sea level, with a temporal resolution of three minutes, and the data from the water column were recorded at hourly intervals at ~1-meter depth. Meteorological data from the oceanographic buoy was collected between April 2011 and July 2013. Another meteorological station was installed on the coast approximately 500 m from the buoy mooring, and provided additional atmospheric measurements for the region. This station recorded meteorological data every fifteen minutes (wind speed and direction, air temperature and atmospheric pressure) from April 2014 to December 2017. The data provided by the moored buoy and the meteorological station were combined to give hourly averages used to identify and characterize synoptic events of high Chl-*a* (>10 mg m^{-3}) forced by wind stress. Calculateion of wind stress assumed a constant air density of 1.2 kg m^{-3} and a dimensionless drag coefficient that is dependent on the wind strength (see Yelland and Taylor, 1996).

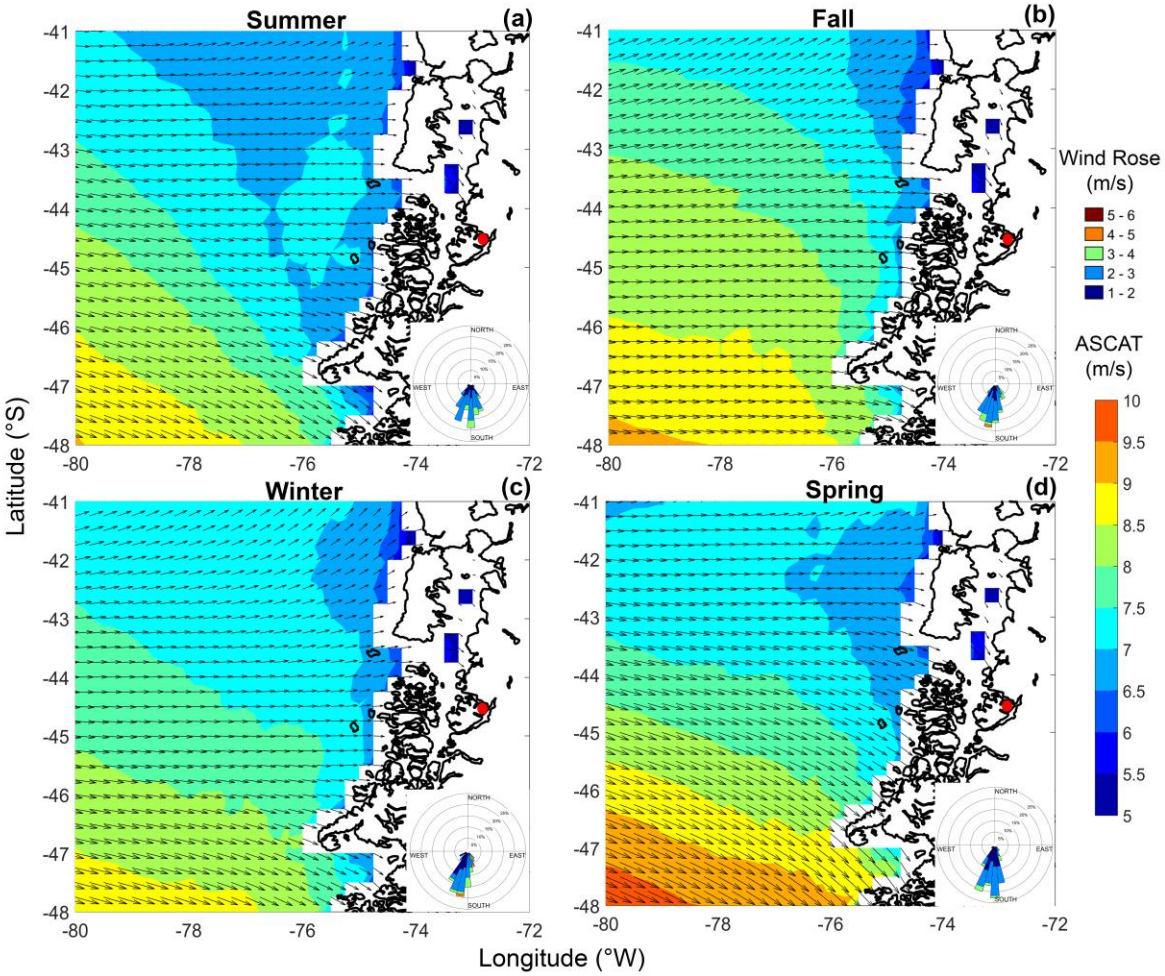

Figure 2. Long-term means of daily surface winds across the region, based on Seawinds sensors mounted on ASCAT scatterometers during the period 2010-2015, (a) Summer, (b) fall, (c) winter and (d) spring. The wind rose plots included in a-d represent the seasonal long-term means of daily surface wind speed and direction (2010-2015) from the oceanographic buoy installed in Puyuhuapi Fjord (red point).

2.4 Environmental data from buoy and meteorological station

The oceanographic buoy sited in the northern section of the Puyuhuapi Fjord – eequipped with atmospheric (wind speed and direction, air temperature and atmospheric pressure) and surface water sensors (temperature and conductivity) – provided data to facilitate understanding of fjord-atmospheric interactions. The meteorological data were

collected at ~2.5 meters above sea level, with a temporal resolution of three minutes, and the data from the water column were recorded at hourly intervals at ~1-meter depth. Meteorological data from the oceanographic buoy was collected between April 2011 and July 2013. Another meteorological station was installed on the coast approximately 500 m from the buoy mooring, and provided additional atmospheric measurements for the region. This station recorded meteorological data every fifteen minutes (wind speed and direction, air temperature and atmospheric pressure) from April 2014 to December 2017. The data provided by the moored buoy and the meteorological station were combined to give hourly averages used to identify and characterize synoptic events of high Chl-*a* (>10 mg m^{-3}) forced by wind stress. Calculateion of wind stress assumed a constant air density of 1.2 kg m^{-3} and a dimensionless drag coefficient that is dependent on the wind strength (see Yelland and Taylor, 1996).

2.5 Hydrographic and hydrodynamic data

Hydrographic profiles (temperature and salinity) were taken during the oceanographic campaigns carried out along the Puyuhuapi Fjord during the period 2008-2015 (Table 1). These profiles were recorded using a Seabird 25 CTD, sampling at 8 Hz with a descent rate of ~1 m s^{-1} and anominal vertical resolution of ~12 cm. Data were then averaged into 1 m bins, following Seabird recommendations. Salinity profiles were used to calculate the stratification parameter (n_s), defined by Haralambidou et al., (2010) as $n_s = \frac{S_{50m} - S_{surface}}{\frac{1}{2}(S_{50m} + S_{surface})}$, where $S_{surface}$ and S_{50m} were salinity measurements from the surface layer (1 meter depth) and from 50 meter depth. With n_s values >1, the water column is highly stratified, whit 0.1< ns >1, partial mixed condition dominated and whit n_s <0.1, the water column is fully mixed (see Fig. 4).

An upward-facing Acoustic Doppler Current Profiler (614.4 kHz Workhorse ADCP) equipped with pressure gauge was installed in a mooring system in the eastern part of Jacaf Channel from August 2014 to May 2015. Velocity measurements from the ADCP were collected every 10 minutes with a vertical bin resolution of 0.5 m down to ~30 meter depth.

2.6 Nutrients, chlorophyll-a, dissolved organic carbon and phytoplankton composition

Concentrations of dissolved nutrients, Chl-*a* and phytoplankton composition were measured over several oceanographic campaigns carried out in the Puyuhuapi Fjord during the period 2008-2017 (Table 1). Samples for analyses of these chemical and biological parameters were collected from 3 discrete depths (2, 10, and 20 m) in the water column using a 10-liter Niskin bottle. Water samples for nutrient analyses were filtered through GF/F filters and frozen at –20°C prior to spectrophotometric analysis in the laboratory. Concentrations of nitrate, orthophosphate, and silicic acid were determined according to methods given in Strickland and Parsons (1968). For total Chl-*a* determinations, 100 mL seawater samples were filtered through 0.7- μm MFS glass-fiber filters which were immediately frozen (–20 ºC) until later analysis; pigments were then extracted with 90% v/v acetone and measured using a Turner Design TD-700 fluorometer according to Parsons et al.(1984). Depth-integrated Chl-*a* was calculated to 20 m using trapezoidal integration. Samples for analysis of Dissolved Organic Carbon (DOC) were collected from each sampling depth, filtered through GF/F filters pre-combusted at 550°C for 4 hours and then frozen (–20 ºC) prior to analysis through a catalytic high combustion TOC-5000 Shimadzu. Prior to analysis, the water samples were acidified with 40 μL of phosphoric acid and decarbonated by purging with high purity CO_2 -free gas (Cuevas et al. 2004). Samples for phytoplankton cell counts were stored in 250 mL clear plastic bottles, preserved in a 1% Lugol's iodine solution (alkaline). From each sample, a 10 mL sub-sample was placed in a sedimentation chamber and allowed to settle for 12 h (Utermöhl, 1958) prior to identification at 40x and 100x under an inverted microscope (Carl Zeiss, Axio Observer A.1). Fifty random fields were counted for each sample. Estimates of phytoplankton abundance at the three discrete depths were integrated down to 20 m, using a trapezoidal method.

2.7 Primary production and community respiration

During each field campaign between January 2008 and March 2017 (Table 1), *in situ* experiments were conducted to measure gross primary production (GPP) and

community respiration (CR). A total of 62 experiments were conducted, with incubations performed on samples from the same sampling depths as indicated above (2, 10, and 20 m). GPP and CR rates were estimated from changes in dissolved oxygen concentrations measured during *in situ* incubation of light and dark bottles (Strickland, 1960). Water from the Niskin bottles was transferred using a silicone tube into 125 mL (nominal volume) borosilicate bottles that had previously been gravimetrically calibrated. Five time-zero bottles, five light bottles, and five dark bottles were used for each incubation depth. Time-zero bottles were fixed with solution A ($MnCl_2$ $4H_2O$) plus solution B (NaOH + NaI) at the beginning of each experiment, whereas the light and dark bottles were attached to a surface-tethered mooring system and incubated *in situ* at the depth of collection. Water samples were collected at dawn and were incubated during the whole light period (incubating time was 10 ± 1.3 hours in the spring-summer season and 7.0 ± 0.7 during autumn-winter season). Dissolved oxygen concentrations were determined according to the Winkler method (Strickland and Parsons, 1968), using a Metrohom burette (Dosimat plus 865) and by automatic visual end-point detection (AULOX Measurement System). GPP and CR values were converted from oxygen to carbon units using a conservative photosynthetic quotient (PQ) of 1.25 (Williams and Robertson, 1991) and a respiration quotient (RQ) of 1, respectively. Discrete-depth estimates of GPP and CR rates were integrated down to 20 m, using a trapezoidal method.

2.8 Prokaryote secondary production and extracellular enzymatic activity

A total of 35 prokaryote production (PP) experiments were performed during the period 2008-2017 (Table 1). Experiments were conducted using the same water samples taken for *in situ* GPP and CR incubations. Estimates of PP were based on the incorporation of Leucine into proteins, using the filter method (Simon and Azam, 1989) and the micro centrifuge method (Smith and Azam, 1992).

For PP experiments using the filter method (2008-2009), triplicate samples of 10 mL, together with a formalin-killed control were taken from each sampling depth and incubated with L-[^{14}C (U)]-leucine (300 mCi $mmol^{-1}$, 50nM final concentration) in the dark for 1 h. Incubations were terminated by adding cold analytical trichloroacetic acid (TCA)

50% w/v. After 10 min, the tube contents were filtered onto 0.22-µm pore size GSWP Millipore filters. The dried filters were transferred to borosilicate scintillation vials, where they were kept cool prior to radioisotopic analysis. The vials were treated with analytical ethyl acetate and 10 mL of liquid scintillate Ecolite added (+) (ICN). Samples were then counted for dpm using a Packard (Mod. 1600 TR) liquid scintillation counter.

For PP experiments using the microcentrifuge method (2014-2017 period), a blank and three samples (1.5 mL) were taken from each sampling depth and incubated with L-[3,4,5-^{3}H]-leucine (123.8 Ci mmol^{-1}, 40nM final concentration) in the dark for 1 h. After incubation, samples were extracted with 100% trichloroacetic acid (TCA), rinsed with 5% TCA and centrifuged at 13500 rpm twice for 15 minutes before removal of supernatant. To each sample was added 1 mL of liquid scintillation cocktail Ecoscint (National Diagnostic). Samples were counted for dpm using a Packard (Mod. 1600 TR) liquid scintillation counter.

Leucine incorporation rates were transformed into prokaryote carbon (i.e. bacteria and archaea) following the rationale of Simon and Azam (1989). PP was converted to prokaryote carbon utilization (i.e., Prokaryote Secondary Production, PSP) using a bacterial growth efficiency of 0.3 (del Giorgio and Cole., 1998). Throughout the text, PSP refers to gross prokaryote secondary production. Discrete-depth estimates of PSP were integrated down to 20 m using the trapezoidal method.

Extracellular enzymatic activity (2013-2014) was estimated based on dark incubations of duplicate 5 mL-aliquots of water with L-leucine-4-methylcoumarinyl-7-amide (MCA-Leu) at 100 µM final concentrations (Hoppe, 1983). Fluorescence was measured at time zero, and every ~30 minutes for 3h at 365 nm excitation and 455 nm emission. Calibration curves were constructed by measuring the fluorescence in seawater with the hydrolysis product MCA, at concentrations ranging between 0.03 and 0.5 µM. First order rate constants were calculated from the slope of the plot of ln (C_0/C_0-P) vs. time, where C_0 is the initial concentration of the substrate MCA-leu and P is the concentration of the product MCA at time t (Pantoja and Lee, 1994). Actual hydrolysis rates were calculated by multiplying rate constants by C_0. Discrete rates were depth-integrated throughout the water column, and carbon hydrolysis rates calculated using the conversion factor of 72 for MCA-leuMUF-cel (Hoppe, 1983).

2.9 Statistical analyses on physical, biological and chemical databases

In order to assess the dominant frequencies of variability in the time series of Chl-*a*, wind stress, salinity and SST, we conducted Morlet wavelet analysis following Torrence and Compo (1998). The time series collected by the buoy contained data gaps due to technical problems, and missing records of <7 days in the time series of Chl-a, salinity and SST were filled using linear interpolation. For data gaps >7 days, wavelets power spectra were calculated considering subsets containing >60 points of consecutive days following to Blauw et al. (2012). A non-parametric Mann-Whitney test was used to compare the oceanographic data obtained for the periods September-April with those from May-August.

Cluster analysis was used to investigate temporal variation in phytoplankton community structure. A similarity matrix among samples was calculated using the Bray & Curtis method (1957), and a dendrogram constructed based on complete average linkage. Given that several of our environmental measurements were non-independent (i.e. salinity, temperature, inorganic nutrients and abundance of phytoplankton species), a principal component analysis (PCA) was conducted to group the monthly samplings according to the joint variability of these variables. The data used in this analysis for salinity, temperature and inorganic nutrients were depth-averages calculated over the upper 20 m, whereas analysis of data for abundance of phytoplankton species were depth-integrated, calculated down to 20 m. Data were standardized prior to the computation of principal component.

3. RESULTS

3.1 Surface wind features and variability

The seasonal averages of surface winds during the period 2010-2015 demonstrated the dominance of westerlies winds throughout the year (Fig. 2), but between 41°S and 43°S, South-Westerly winds were observed during fall and winter (Fig. 2b and 2c). Wind was maximal during fall and spring (range 9-10 m s^{-1}) in the southern domain (Fig. 2b and 2d), but generally varied between 5-8 m s^{-1}. In the interior fjord, the combination of long-term data from the buoy and the meteorological station showed predominant winds from

the south and south westerly directions, with maximum wind speed during fall and winter (Fig. 2b and 2c).

3.2 Long-term monthly means of surface atmospheric, oceanographic and hydrological parameters

The long-term monthly means of water temperature, solar radiation, salinity and dissolved oxygen (DO) showed a predictable annual cycle (Fig. 3a-c and 3e), but in the case of river discharge and Chl-*a*, a semiannual maxima were observed (Fig. 3d and 3f). Increases and decreases in surface water temperatures during spring-summer and fall-winter coincided with maxima and minima in solar radiation intensity (Fig. 3a-b). Salinity decreased from September to December and remained lower in summer than in fall and winter due to increased river discharge, driven principally in summer by ice melting (Fig. 3c-d). The maximum DO occurred in September, with two maxima of Chl-*a* observed, one in May and other in October (Fig. 3e-f). As shown in Figure 2, the long-term monthly means of local surface wind from the oceanographic buoy together with the meteorological station showed the variability of zonal and meridional winds, and highlighted the dominance of southerly winds (Fig. 3g-h). More specifically, southerly winds increased in speed from late winter (September) to spring (Fig. 3h).

3.3 Relationship between mixing/stratification, salinity and inorganic nutrients

The degree of mixing and stratification of the water column was determined using the salinity data collected during both the hydrographic campaigns, and the oceanographic buoys installed in the northern part of Puyuhuapi Fjord (Fig. 4). The stratification parameter (n_s) highlighted the presence both of highly stratified water in the northern fjord, especially during spring and summer, and partially mixed conditions in the southern fjord region. During the winter season, lower values of n_s indicated partially mixed conditions throughout the fjord (Fig. 4a). The analyses showed that when surface salinity exceeded 29 psu, the water column was fully mixed, as shown by some profiles from winter 2011. The salinity time series provided by the buoy at ~1 m depth showed that salinity exceeded 29

several times a year mainly during fall and winter (Fig. 4b, red marks), sometimes exceeding 31 psu (Fig. 4c). The long-term monthly means of surface salinity over 29 psu demonstrated well-mixed conditions between April and August, with high variability observed in June (Fig. 4d). On the other hand, the highest nitrate/phosphate concentrations in the upper water column were observed during May and July associated with n_s values between 0.1 and 0.5, and the lowest concentrations observed during early spring and summer period associated with n_s values >0.5 and closer to 1, indicating more stratified conditions (See supplementary Fig. 1).

3.4 Atmospheric-ocean interactions

In order to explore the oceanographic processes that contribute to atmospheric-ocean interactions, the oceanographic buoy collected time series of surface winds, atmospheric pressure, Chl-*a* and dissolved oxygen (DO). Discharge of the Cisnes River, rainfall collected close to the town of Puerto Cisnes, and along and cross-channel velocities in the Jacaf channel, were also analyzed (Fig. 5). During our study, high southward winds were associated with measurements of low atmospheric pressure, evidencing the passage of several low atmospheric pressure systems (LAPS) through the region (Fig. 5a). These LAPS were also accompanied by increases in rainfall that contributed to the increased discharge of the Cisnes River (Fig. 5b). Concentrations of Chl-*a* and DO varied in a similar manner during LAPS events, suggesting production of oxygen by photosynthetic carbon fixation in the near surface waters monitored by the buoy (Fig. 5c). Currents in the fjord also responded to the stronger winds associated with LAPS. The cross-channel currents increased in intensity to ~30 cm s^{-1} in the upper ~10 m, while strong along-channel currents extended their influence down to 25 m, with a southward direction in response to the winds (Fig. 5d and 5e). This suggests that currents in the fjord switch from a predominantly northward direction, to southward during the passage of LAPS.

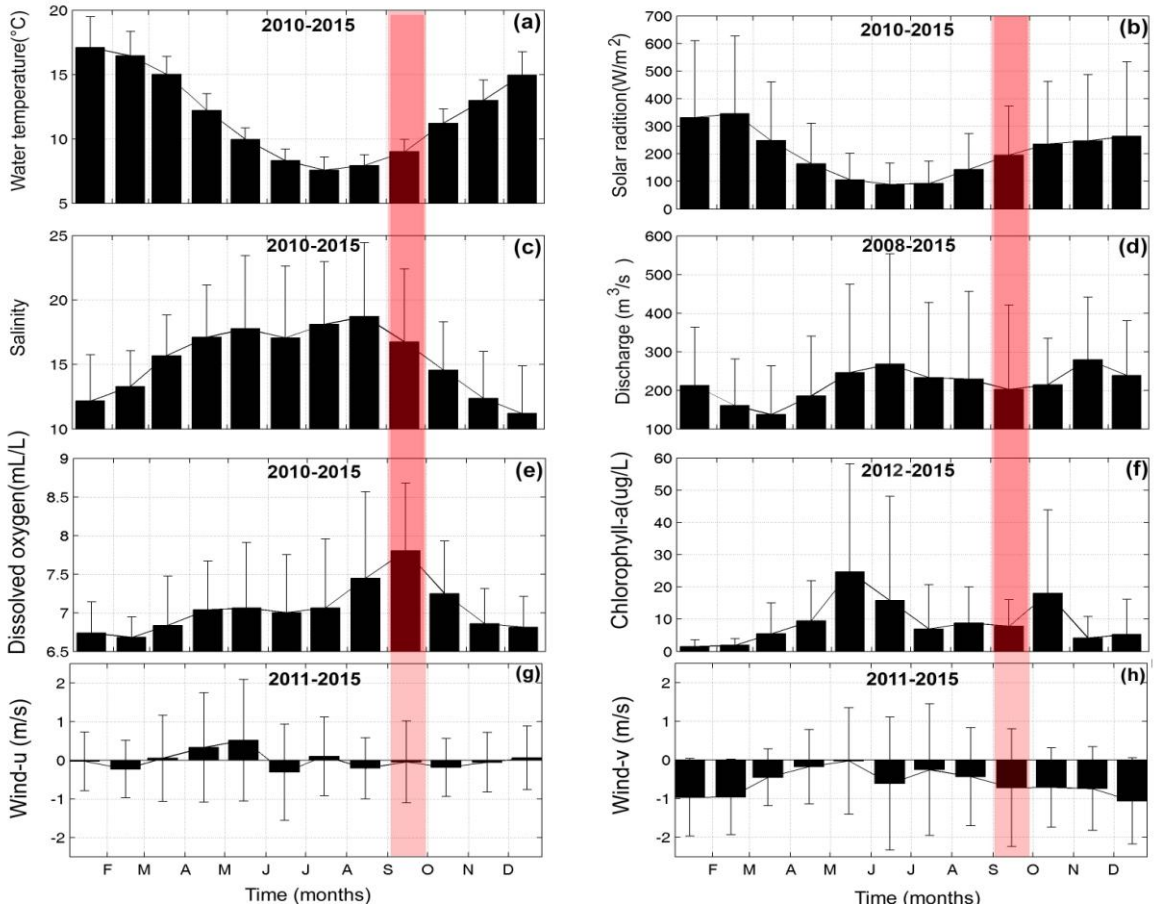

Figure 3. (a, b, c, e, and f) Measurements taken from the oceanographic buoy installed in Puyuhuapi Fjord. (d) Time series of discharge from Cisnes river at the DGA station located in the river mouth. The solar radiation time series (b) was constructed using data from the buoy (2010-2013) and the meteorological station (2014-2015). The red vertical shaded bar denoted the seasonal change from winter to spring. In (g) wind-u denotes the east–west component; + (-) winds blow from the east (west); (h) wind-v denotes the north–south component; + (-) winds blow from the north (south).

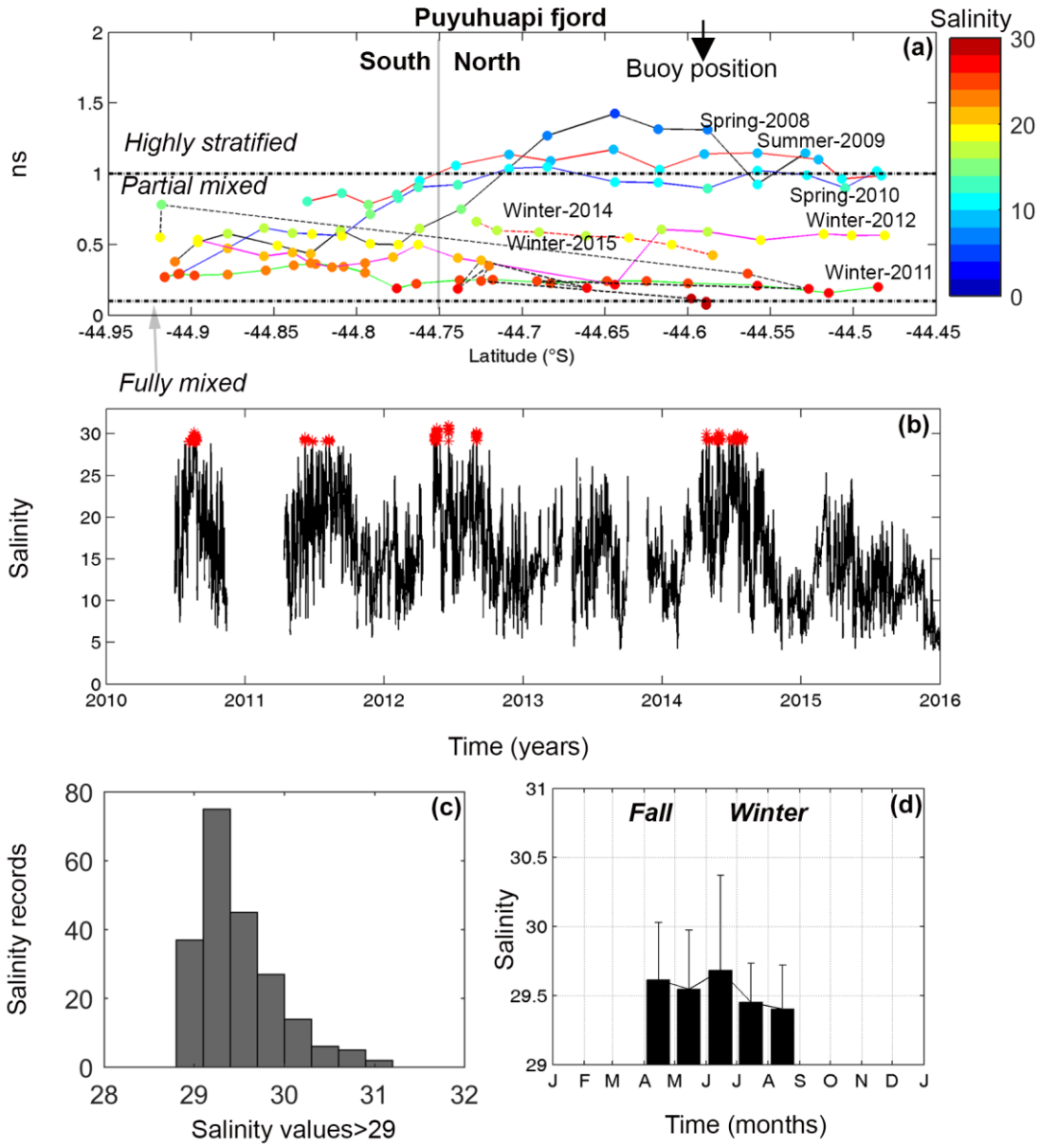

Figure 4. (a) Stability parameter (ns) calculated for oceanographic campaigns carried out along the Puyuhuapi Fjord. The color bar represents the salinity of the surface layer for each CTD station, and horizontal lines represent the ns parameter. (b) Time series of hourly surface salinity data obtained from the oceanographic buoy installed in Puyuhuapi Fjord. The red marks denote the salinity over 29 units. (c) The histogram of frequency of salinity records over 29 psu. (d) Long-term monthly mean and standard deviation of salinity values over 29 psu.

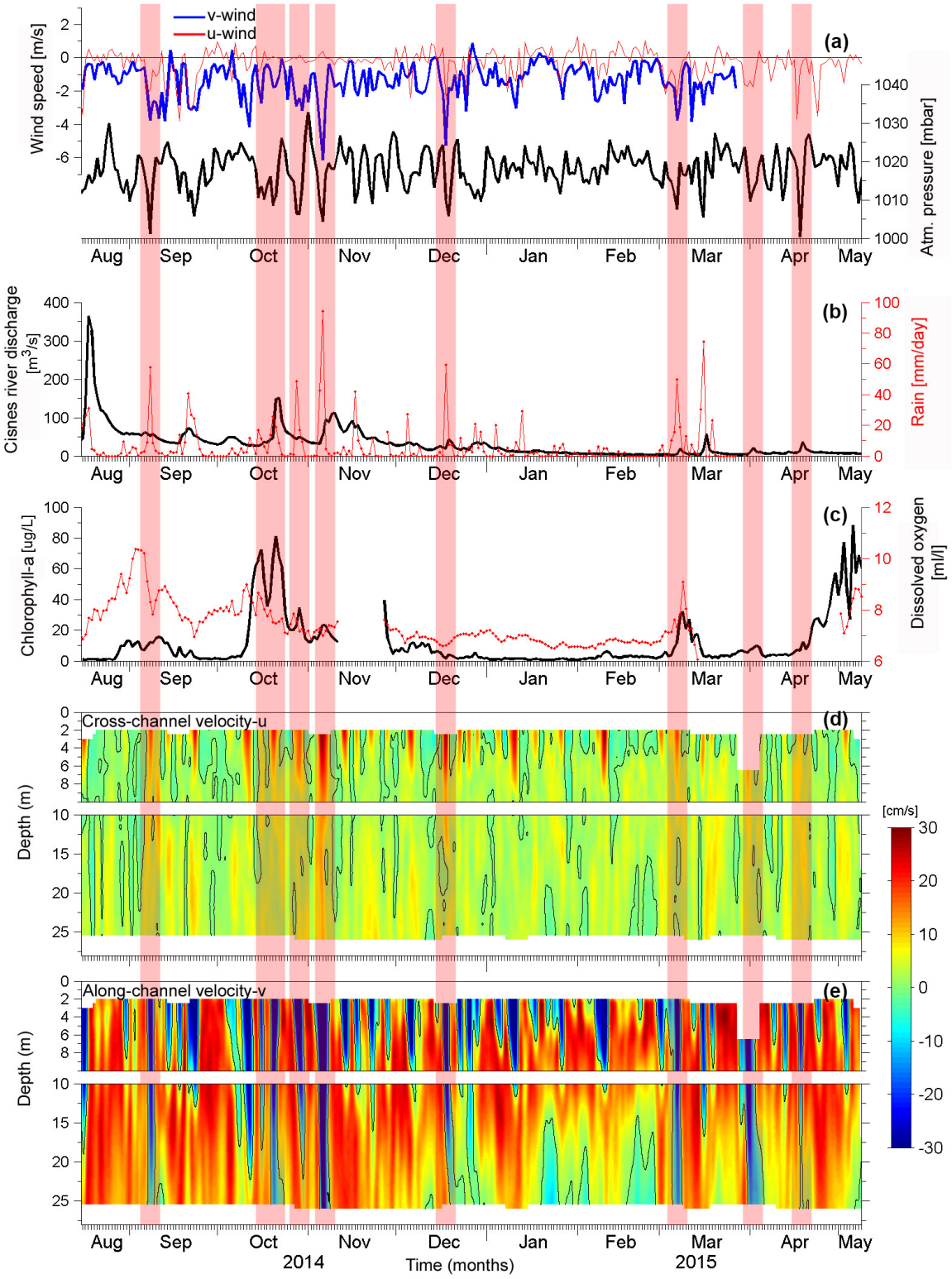

Figure 5. (a) Atmospheric data recorded by the meteorological station installed on Magdalena Island. (b) Cisnes River discharge and rainfall data from the DGA station located in the mouth of the Cisnes River. (c) Time series of chlorophyll-a and dissolved

oxygen from the oceanographic buoy installed in Puyuhuapi Fjord. (d and e) Cross and along channel current velocities over the upper 25 m, recorded by the ADCP moored in the eastern part of Jacaf Channel (see Fig. 1). All data were collected between August 2014 and May 2015. The red vertical shaded bars indicate examples of the response of oceanic variables to passage of low atmospheric pressure systems (LAPS) throughout the region.

3.5 Phytoplankton community

The mean abundance of phytoplankton showed a marked seasonality with the highest abundances (60-174 $\times 10^9$ cells m^{-2}) observed between September and April, and the lowest (4-11 $\times 10^9$ cells m^{-2}) between May and August (Fig. 6a). This represents a classic pattern that corresponds with the annual cycle of solar radiation and temperature (Fig. 3a, b). Nevertheless, within this cycle, relatively high abundances (27-76 $\times 10^9$ cells m^{-2}) were also recorded during a winter bloom and a late winter bloom of phytoplankton (Fig. 6a), which appeared to be associated with the passage of a low atmospheric pressure system (LAPS) and high silicic acid concentrations, respectively.

Seasonal fluctuations in phytoplankton abundance correlated significantly with GPP rates during an annual cycle ($r_s = 0.66$, $n = 12$, $p = 0.02$), although high phytoplankton abundances (>90 $\times 10^9$ cells m^{-2}) did not necessarily result in high GPP rates (>1 g C m^{-2} d^{-1}) (Fig. 6b). When data for the winter bloom and late winter bloom were added, high GPP values (1.1-2.6 g C m^{-2} d^{-1}) were associated with low abundances (15-76 $\times 10^9$ cells m^{-2}), although the correlation was not significant (Fig. 6c). This suggests that certain phytoplankton species are mainly associated with high productivity events at relatively low abundance. In our case, the highest levels of GPP were typically recorded when the phytoplankton community was dominated by *Heterocapsa triquetra* and *Skeletonema* spp. (Fig 7a, b).

In general, diatoms dominated the phytoplankton community between August and May, while dinoflagellates dominated between June and July (Fig. 7a, b). The Bray-Curtis cluster analysis detected four well-defined groups that represent the seasonal variability in phytoplankton composition (Fig. 8). This variability coincided with the two broad temperature regimes (Fig. 8), and with the dominance of certain key species during an

annual cycle (Fig. 7a,b). Thus, cluster 1 was associated with a warm regime and the dominance of the *Pseudo-nitzschia delicatissima* and *P. seriata* complex, whereas cluster 2 was associated with a warm regime and the high presence of *Rhizosolenia pungens* and *R.setigera*. Cluster 3 was associated with a mostly cold regime and the dominance of *Skeletonema* spp. and *Chaetoceros* spp,, and cluster 4 was associated with a cold regime and the dominance of *Heterocapsa triquetra* and *Gyrodinium* spp.

The principal component analysis (PCA) showed first (PC1) and second (PC2) principal components that explained 34.2% and 18.6% of total variance, respectively (Fig. 9). PC1 was positively loaded with salinity, NO_3^-, PO_4^{3-}, *Gymnodinium* spp., *Prorocentrum micans*, *Dictyocha speculum* and *Heterocapsa triquetra*, while temperature, the *Pseudo-nitzschia delicatissima*and *P. seriata* complexes, and *Rhizosolenia setigera* were found to be negatively loaded (Fig. 9). PC2 was positively loaded with Si, *Skeletonema* spp., *Chaetoceros* spp., *Leptocylindrus minimus*, *L.danicus*, *Alexandrium catenella* and *Gymnodinium* spp., while no variable was found to be negatively loaded. The PCA analysis clearly separated three groups according to different environmental variables and the presence of certain phytoplankton species: a) Dinoflagellates that were present mainly in the winter months and were associated with saltier waters, PO_4^{3-} and NO_3^-, b) Diatoms that were present mainly in spring and were associated with Silicic acid (Si) and, c) Diatoms that were present mainly in summer and were associated with higher temperatures in the water column.

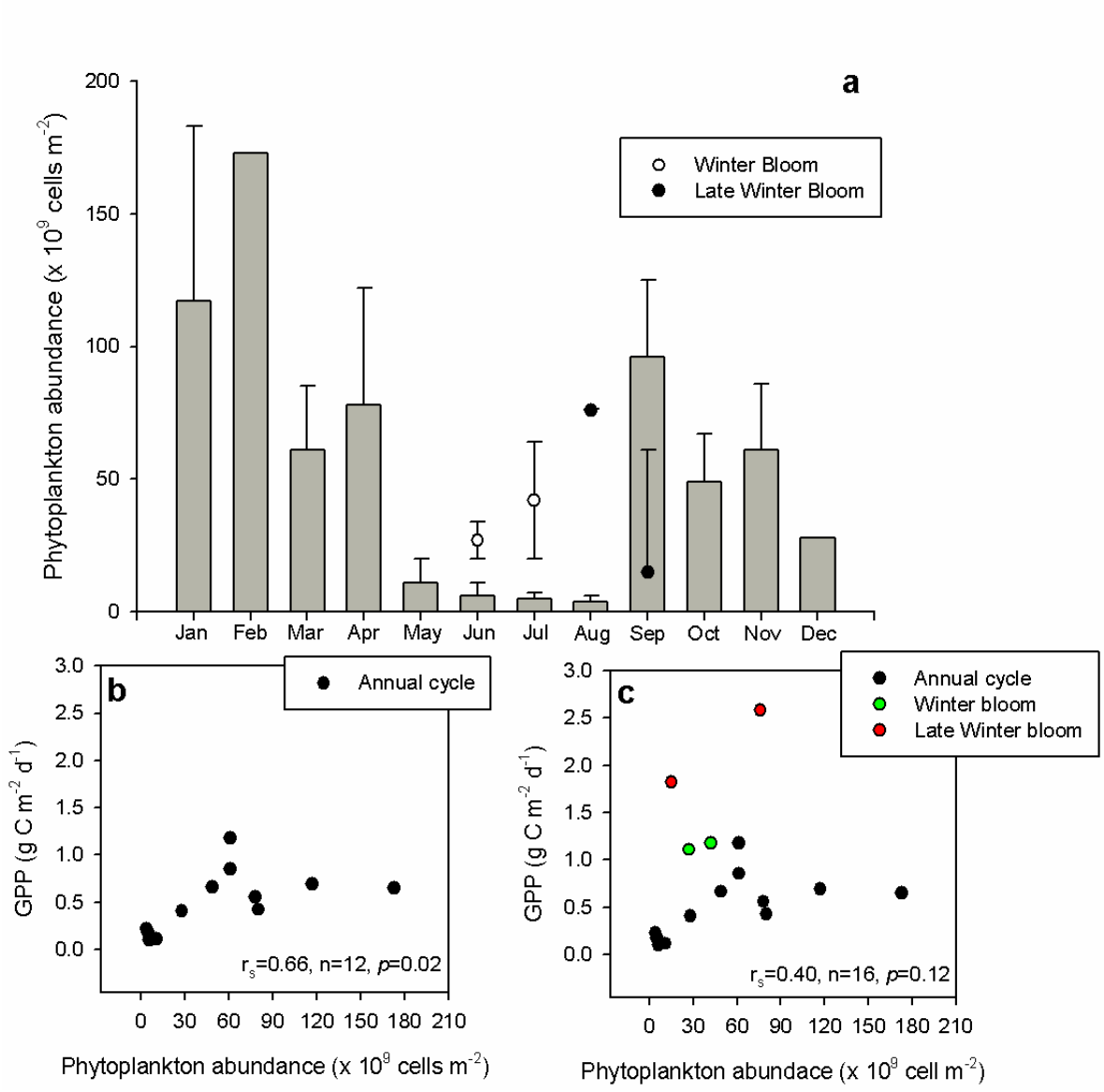

Figure 6. (a) Seasonal variability of phytoplankton abundance at the Puyuhuapi station. Grey vertical columns and error bars indicate mean (± error) for each month of the study period. White and black dots refer more specifically to the winter bloom, and late winter bloom. (b) Correlation between phytoplankton abundance and gross primary production (GPP) values during an annual cycle at the Puyuhuapi station. (c) Correlation between phytoplankton abundance and GPP over the annual cycle, but including the data for the winter bloom and late winter bloom at the Puyuhuapi station.

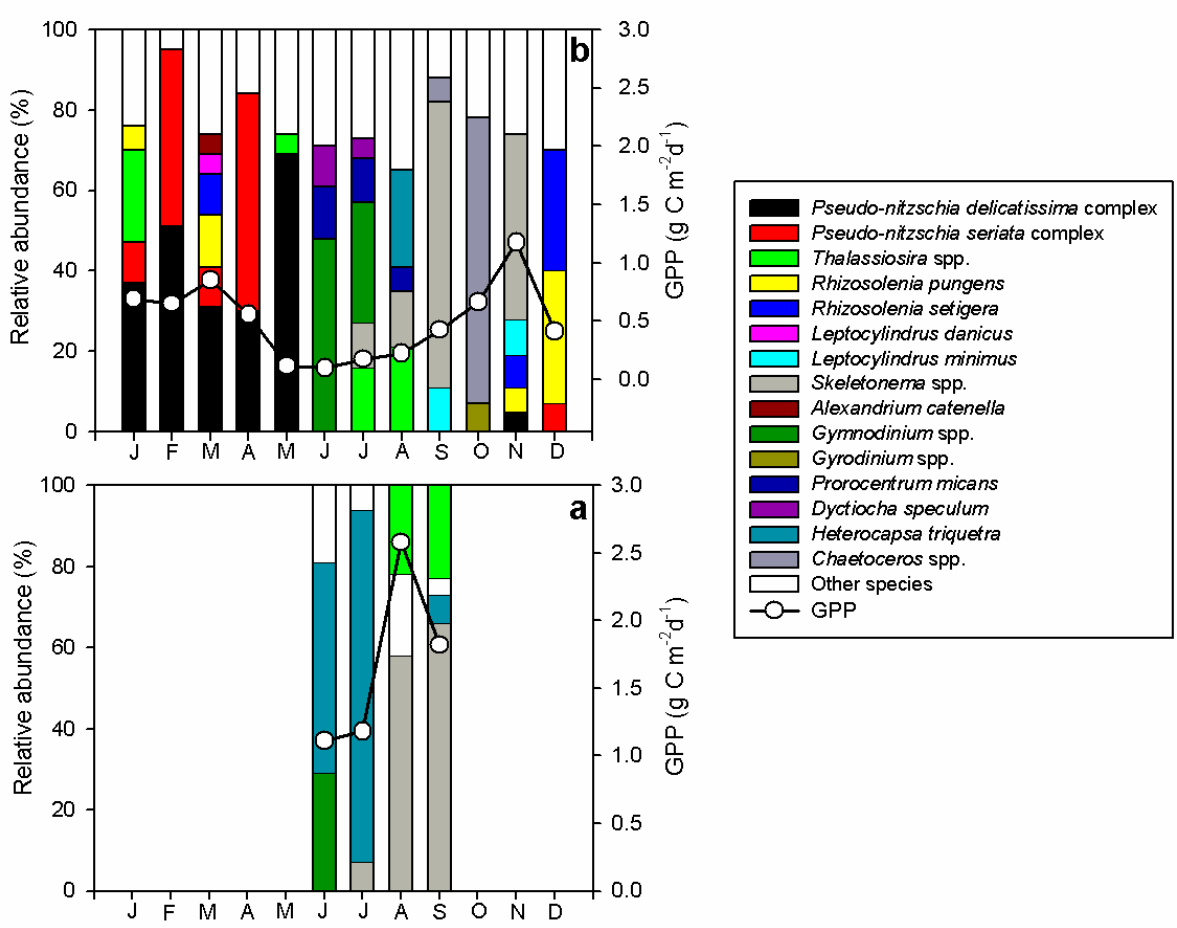

Figure 7. Relative abundance and composition of phytoplankton community associated with GPP values (a) during a winter bloom and a late winter bloom (LAWI) and (b) during an annual cycle.

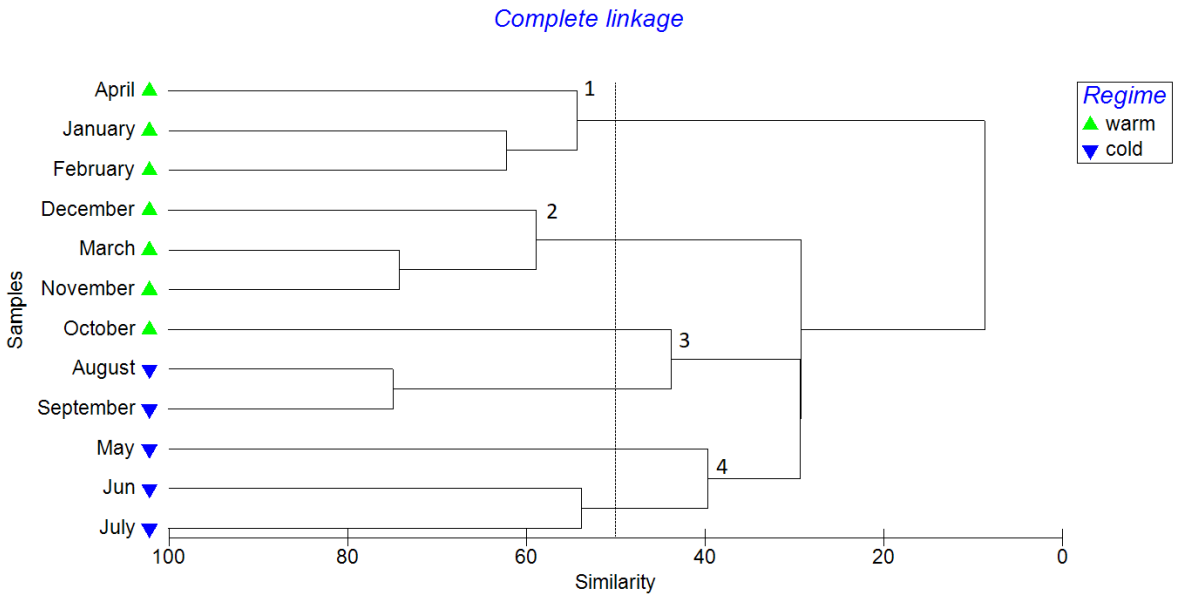

Figure 8. Similarity cluster analysis for samples of phytoplankton community composition during the study period.

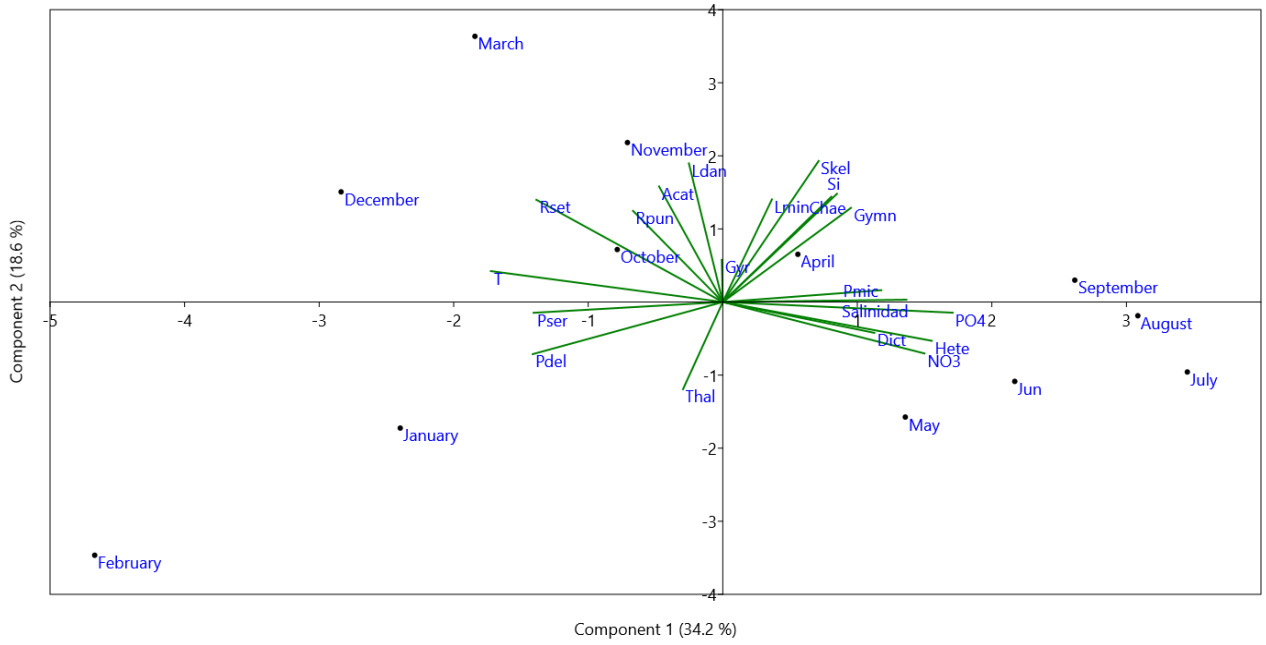

Figure 9. Principal component analysis (PCA). Seasonal ordination diagram of phytoplankton species shown in Figure 7, months and physical-chemical variables.

3.6 Community rates, biomass and inorganic nutrients

The annual cycle of biological variables was assessed in the study area (Fig. 10). Gross primary production (GPP) (Fig. 10a) and Chl-*a* concentration (Fig. 10f) exhibited marked seasonal cycles with significant differences between the September-April and May-August periods (Table 2). Depth integrated mean GPP and Chl-*a* concentrations were the highest between September and April (1.07 g C m^{-2} d^{-1}; range: 0.1-3.09 g C m^{-2} d^{-1} and 32 mg m^{-2}, range: 2.8-54.6 mg m^{-2}, respectively) and lowest between May and August (0.15g C m^{-2} d^{-1}, range: 0.1-0.22 g C m^{-2} d^{-1} and 11.3 mg m^{-2}, 9.9-12.6 mg m^{-2}, respectively). Nevertheless, superimposed on this annual cycle of monthly means, higher than average GPP rates (>2 g C m^{-2} d^{-1}) and Chl-*a* concentrations (>100 mg m^{-2}) occurred in August and September, and during June (>1.1 g C m^{-2} d^{-1}; 59.3 mg m^{-2}) and July (>1 g C m^{-2} d^{-1}; >70 mg m^{-2}) corresponding to the LAWI bloom and the winter bloom, respectively (Table 3). CR rates reached the highest values during August and September (LAWI bloom) and did not show a marked seasonal pattern (Fig. 10b; Table 2). In addition, CR rates were notably higher than GPP rates during much of the annual cycle, and consequently, the community net metabolism ratio (GPP/CR) suggested that heterotrophic processes dominated (GPP/CR < 1) (Fig. 10c). Depth-integrated prokaryote secondary production (PSP) showed a marked seasonal pattern with the highest values occurring between September and April (mean: 0.78 g C m^{-2} d^{-1}; range: 0.41-1.54 g C m^{-2} d^{-1}) and lowest between May and August (mean: 0.36 g C m^{-2} d^{-1}; range: 0.09-0.71g C m^{-2} d^{-1}), generally reflecting the variability shown by GPP and Chl-*a* biomass (Fig. 10d). The PSP/GPP ratio ranged between 52-427% in summer; 87-645% in autumn; 7.5-380% in winter and 59-428% in spring (Fig. 10e). Average PSP/GPP values generally exceeded 100% during the annual cycle, suggesting that microbial activity is probably subsidized by the input of allochtonous organic matter. Mean depth-integrated DOC concentrations did not show a seasonal pattern (Table 2), although the maximum did occur during September and October, corresponding to the most productive months (Fig. 10g). Maximum mean extracellular enzymatic activity (EEA occurred during August (98-176 µg C m^{-2} h^{-1}) and November (138 µg C m^{-2} h^{-1}), with minima in March (44.7 µg C m^{-2} h^{-1}) (Fig. 10h). High EEA values were also measured during July (86 µg C m^{-2} h^{-1}). However, the dataset for EEA was rather limited. Inorganic

nutrients showed a seasonal cycle (Table 2) with the highest/lowest mean concentrations during fall-early winter (NO_3^-= 13.7 µM; PO_4^{3-}=1.05µM) and spring-summer (NO_3^-= 6.25 µM; PO_4^{3-}= 0.94 µM), respectively. On the other hand, the variability (coefficient of variation; CV) was higher during spring-summer than during fall-early winter for nitrate (CV: 51%; CV: 29%) and phosphate (CV: 54%; CV: 41%), respectively. Concentrations of silicic acid did not show a marked seasonal pattern (Table 2).

Table 2. Mann-Whitney parameter (U) and p-value (statistical significance) were estimated using all data to assess the difference between the period September to April, and the period May to August. Data tested were depth-integrated (20 m depth) biological variables (GPP, CR, GPP/CR, PSP, PSP/GPP, Chl-a, DOC) and the averages (calculated to 20 m depth) of inorganic nutrients in the water column.

	GPP	CR	GPP/CR	PSP	PSP/GPP	Chl-*a*	DOC	NO_3	PO_4	Si
U	343	468	385	37	159	312	129	119	343	387
p	**0.02**	0.54	0.08	**0.00**	0.78	**0.04**	0.75	**0.00**	**0.03**	0.12

Table 3. Summary of discrete biological measurements (See Table 1) carried out in Puyuhuapi Fjord. Annual cycle represents measurements made during the years 2008–2017 (see methods and Table 1). Values presented below represent the mean (± stdev; n) for each period. Also shown are the data taken during the winter bloom, and the late winter (LAWI) bloom.

	Annual Cycle												**LAWI bloom**	**Winter bloom**
	Jan	**Feb**	**Mar**	**Apr**	**May**	**Jun**	**Jul**	**Aug**	**Sep**	**Oct**	**Nov**	**Dec**	**Ag–Sp**	**Jn–Jl**
GPP	0.69	0.65	0.85	0.55	0.11	0.1	0.17	0.22	0.46	0.66	1.17	0.41	2.75	1.16
SD; n	0.1; 6	–; 1	0.4; 5	0.4; 5	0.06; 7	0.09; 2	0.1; 6	0.1; 4	0.1; 10	0.3; 5	1; 3	–; 1	0.48; 5	0.4; 5
CR	1.5	0.12	1.86	2.02	0.47	1.47	1.31	0.91	1.11	1.16	2.13	0.18	4.31	1.88
SD; n	0.6; 6	–; 1	0.5; 5	0.8; 5	0.5; 7	0.7; 2	1.3; 6	0.7; 4	2.5; 10	0.5; 5	1.7; 3	–; 1	2.8; 5	0.8; 5
GPP/CR	0.53	5.41	0.48	0.35	0.39	0.09	0.42	0.32	0.75	0.54	1.68	2.27	0.86	0.7
SD; n	0.3; 6	–; 1	0.2; 5	0.4; 5	0.2; 7	0.1; 2	0.6; 6	0.1; 4	0.5; 10	0.2; 5	2.1; 3	–; 1	0.4; 5	0.6; 5
PSP	0.73	–	1.15	1.54	0.3	0.51	0.05	0.26	0.82	0.63	–	–	0.83	0.5
SD; n	0.3; 5		0.7; 2	–; 1	0.2; 7	–; 1	0.03; 4	0.3; 4	0.6; 2	0.1; 4			0.07; 3	0.1; 4
PSB:GPP	102	–	263	433	285	516	36	157	380	159	–	–	32.8	47.9
SD; n	45; 5		231; 2	–; 1	183; 7	–; 1	34; 4	114; 4	1.5; 2	179; 4			8.2; 3	23; 4
Chl-*a*	32.2	2.82	42	43	11.4	26.3	57.3	92	54.6	18.6	26.8	24.7	159	111.5
SD; n	7.7; 6	–; 1	21; 4	33; 4	20; 7	29; 3	66; 10	116; 5	52; 10	4; 5	14; 3	–; 1	80; 4	58; 5
DOC	1723	–	–	1725	1792	1377	1962	2331	2772	2124	1714	2129	3990	81
SD; n	156; 5			–; 1	112; 5	383; 2	366; 2	392, 3	1550; 8	879; 5	–; 1	–; 1	3261; 3	–; 1

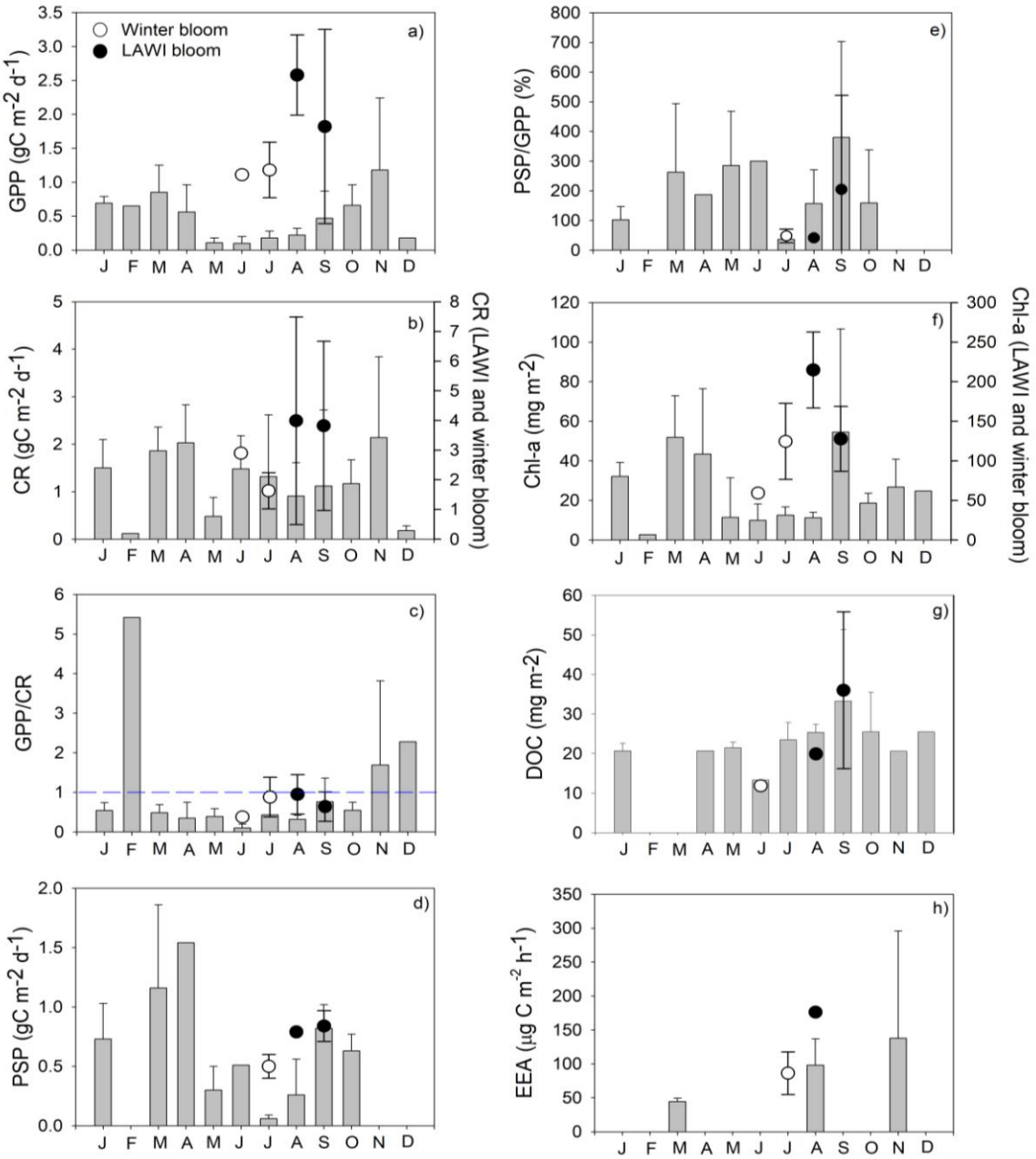

Figure 10. Vertical grey bars represent annual cycle of depth-integrated measurements (0–20m depth) in the Puyuhuapi Fjord. Superimposed on these data are the measurements taken during the winter bloom and during the late winter bloom (LAWI). (a) gross primary production (GPP), (b) community respiration (CR), (c) community net metabolism (GPP/CR), (d) prokaryote secondary production (PSP), (e) PSP/GPP), (f) Chlorophyll-a (Chl-a), (g) dissolved organic carbon (DOC), (h) extracellular enzymatic activity (EEA). Grey vertical bars indicate mean ± standard deviation for data obtained monthly between periods January and November 2008; March and September 2009; June and December 2013; March and September 2014; July 2015; August 2016; March 2017.

3.7 Prokaryote secondary production, gross primary production and community respiration relationship

To assess the relationships between depth-integrated physiological parameters we separated measurements according two contrasting periods: 1) the winter/spring period characterized by the highest freshwater inputs driven by precipitation and ice-melting; 2) summer/autumn period characterized by reduced influence of river discharge (Fig. 11). PSP estimates were significantly correlated with GPP rates during winter/spring ($r^2 = 0.5$; $p < 0.01$) and summer/autumn ($r^2 = 0.5$; $p = 0.002$), and the derived slopes for each fitted curve were significantly different (Fig. 11a). For example, for a given arbitrary GPP rate of 1.5 g C m^{-2} d^{-1}, the slopes against PSP were 0.2 in winter/spring and 0.85 in summer/autumn (See Supplementary material Fig. 2). Moreover, the CR rates were also significantly correlated with PSP during winter/spring ($r^2 = 0.6$; $p = 0.0002$) and summer/autumn ($r^2 = 0.41$; $p = 0.0067$) (Fig. 11b). The slope of fitted curve between CR and PSP for winter/spring measurements was one order of magnitude higher than that for the summer/autumn period. For example, for an arbitrary PSP rate of 0.8 g C m^{-2} d^{-1}, the slopes were 10.2 and 0.93 during winter/spring period and summer/autumn periods, respectively (See supplementary Fig 2).

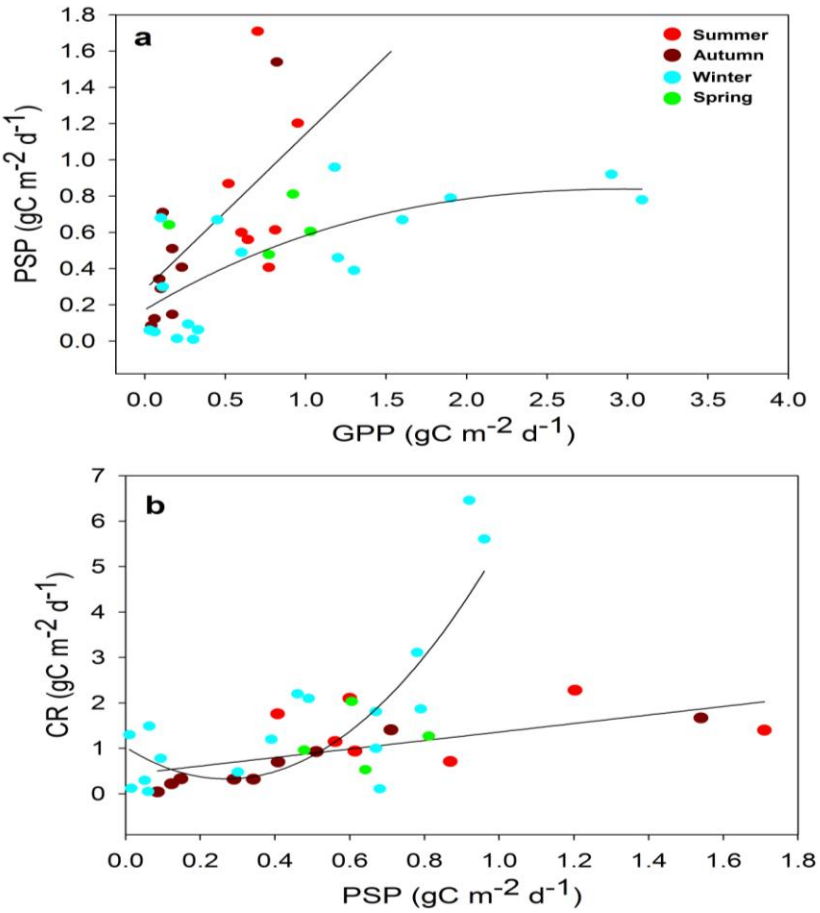

Figure 11. Relationship between depth-integrated (0- 20 m) physiological parameters: (a) Gross primary production (GPP) and prokaryote secondary production (PSP) and (b) prokaryote secondary production (PSP) and community respiration (CR). Data was obtained between January and November 2008; March and September 2009; June and December 2013; March and September 2014; July 2015; August 2016; March 2017. Additionally, intensive sampling campaigns were also included in this figure. Depth-integrated physiological parameters were separated according two contrasting periods: 1) the winter/spring (dots light blue/green) period characterized by the highest freshwater inputs driven by precipitation and ice-melting; 2) summer/autumn (dots red/brown) period characterized by a lower influence of river discharge. For GPP and PSP relationship a cubic function ($y=0.1732 + 0.5325*x - 0.1326* x^2 + 0.0097*x^3$) was adjusted with a coefficient of determination $R^2= 0.5$ and p-value= 0.01 (winter/spring); and a lineal function ($y= 0.2848 + 0.8586*x$) with $R^2= 0.5$ and p-value= 0.002 (summer/autumn). For CR and PSP relationship a quadratic polynomial function ($y=1.0266 - 5.1749*x + 9.5948*x^2$) was adjusted with a coefficient of determination $R^2= 0.6$ and p-value= 0.0002 (winter/spring); and a lineal function ($y= 0.4253 + 0.9364 * x$) with $R^2= 0.4$ and p-value= 0.0067 (summer/autumn).

3.8 Temporal variability of Chl-a, wind stress, salinity and SST

We performed a wavelet analysis on the time series (2013-2016) of Chl-*a*, wind stress, salinity and SST from the Puyuhuapi oceanographic buoy. This data analysis was focused on synoptic (2-16 d, intraseasonal (17-90 d) and seasonal (>90 d) time scales of variability. The Chl-*a* wavelet analysis revealed various dominant frequencies of variability, with significant periodicities of 1-16 days observed during autumn-winter 2015 (May-June), spring 2015 and 2016 (September-October) and summer 2016 (December-January-February) (Fig. 12a). Longer periodicities were also observed in the band of ~16-64 days during the later winter-spring period (September-October 2014), and ~32 days during May-Jun 2015. The wavelet power spectrum of daily wind stress showed dominance of the synoptic period (2-16 d) between May and September 2014, with lower persistency during 2016 (Fig. 12b). Variability in the band ~30-60 days were clearly observed during autumn–winter (May-June-July-August) in 2014 and 2015, but not during 2016. Significant variability on the scale of >100 days was observed during the spring and early summer in 2014 and 2016. The salinity wavelet analysis showed a dominance of 2-16 day periods during autumn-winter 2013, 2014, 2015 and 2016 (April to August) (Fig. 12c). SST wavelet analysis showed significant variability of 2-16 day periods, with fluctuations between 30 and 60 days spanning a longer time interval than synoptic periodicities during spring-summer 2014, 2015, 2016 and 2017 (September to March) (Fig. 12d).

3.9 Characterization of chlorophyll variability at the synoptic-scale

We identified 16 synoptic-scale events of high Chl-a concentration (>10 mg m^{-3}) from data collected by the buoy during the period 2013-2016 (Table 4). These events occurred during all seasons, but were more frequent during winter months. The duration of Chl-*a* pulses ranged between 3 and 16 days, and concentrations ranged from 12.2 mg m^{-3} to 32.1 mg m^{-3}. These pulses of Chl-*a* were forced by wind stress, principally at the synoptic-scale with magnitudes that ranged between 0.012-0.041 Nm^{-2} and that were also associated with high surface salinity (range: 12 to 27.5), suggesting increased mixing in the water

column. The response of maxima in Chl-a concentrations to wind stress events occurred with lags of 0, 1, 2, 3 and 4 days.

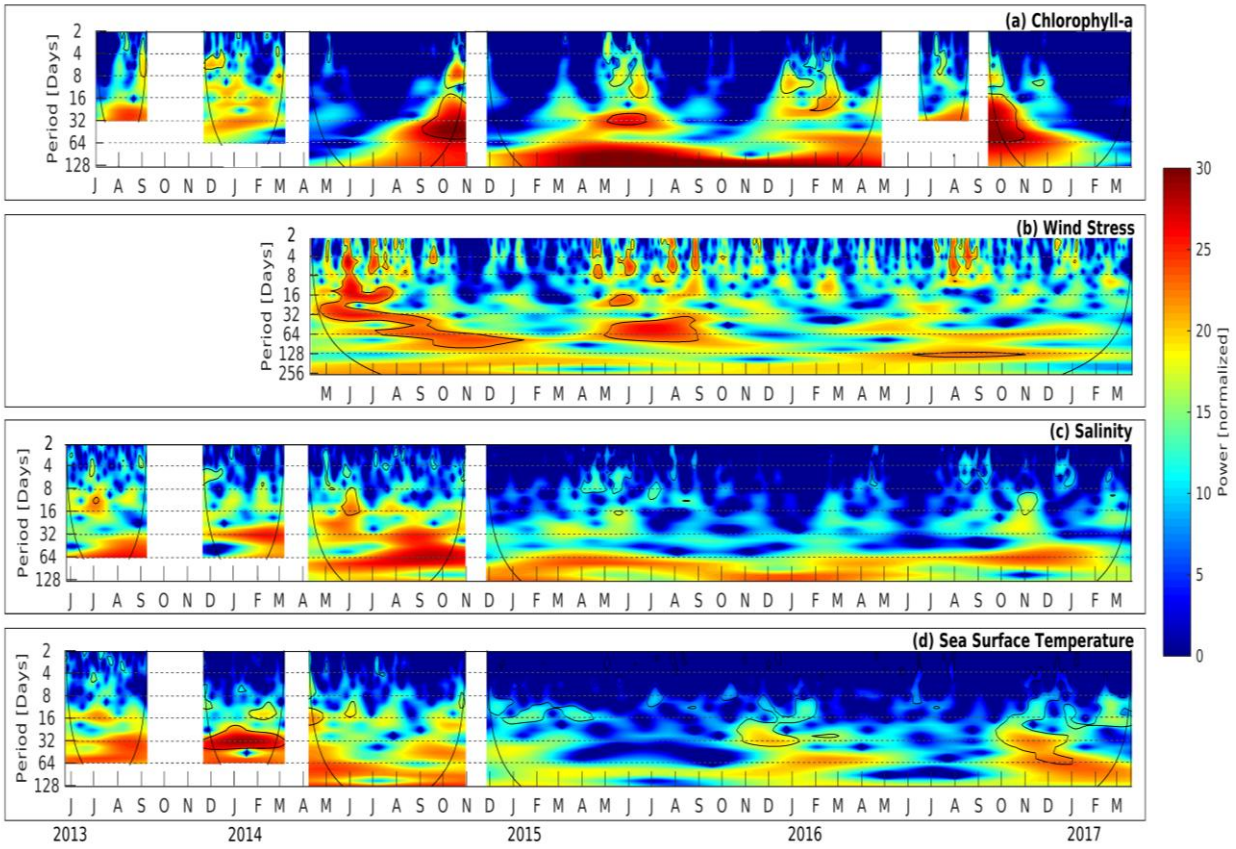

Figure 12. Wavelet analysis for the time series of chlorophyll-a (a), wind stress (b), salinity (c) and sea surface temperature (d). Color coding indicates the wavelet power (in units of normalized variance), ranging from low power (blue) to high power (red). Black lines represent the cone of influence below which the information is affected by edge effect. Power values inside black contours are significant at 95 %.

Table 4. Characterization of events of high Chl-a concentration (>10 mg m^{-3}, continuous measurements) occurring on the synoptic-scale during the period 2013-2016. These events were associated with wind stress and surface salinity in Puyuhuapi Fjord. Duration of Chl-a pulses and time-response between Chl-a pulse and maximum wind stress value are also given.

Season **Start and end date of chl-*a* pulse**	**Wind Stress [N m^{-2}]**	**Chl-*a* [mg m^{-3}]**	**Salinity [PSU]**	**Duration of Chl-*a* pulse [Days]**	**Time-response [Days] between Chl-*a* pulse and windstress**
SUMMER (JFM)					
05/03/2015-15/03/2015	0.018 - 0.024	3.1 - 32.1	13.4 - 22.5	10	2
30/03/2016- 06/04/2016	0.016 - 0.028	4.5 - 16.3	20.1 - 24.4	8	3
Mean	0.017 - 0.026	3.8 - 24.2	16.7 - 23.4		
AUTUMN (AMJ)					
25/04/2014- 01/05/2014	0.012 - 0.023	0.8 - 13.4	18.5 - 25.8	6	2
03/05/2014- 06/05/2014	0.017 - 0.034	3.5 - 19.2	18.2 - 27.5	3	2
21/06/2015- 28/06/2015	0.018 - 0.024	3.9 - 19.9	7.0 - 12.9	7	4
Mean	0.016 - 0.027	2.7 - 17.5	14.5 - 22.1		
WINTER (JAS)					
03/07/2015- 08-07-2015	0.012 - 0.026	7.2 - 23.3	8.4 - 12.8	5	0
07/07/2015- 14/07/2015	0.012 - 0.026	5.4 - 19.8	6.5 - 12.8	7	3
02/08/2013- 16/08/2013	n.d	2.5 - 20.2	15.5 - 23.4	14	n.d
07/09/2014- 16/09/2014	0.014 - 0.023	3.9 - 15.9	21.1 - 25.1	9	4
22/08/2015- 06/09/2015	0.013 - 0.041	6.8 - 20.3	7.2 - 17.3	16	2
14/09/2015- 19/09/2015	0.015 - 0.023	5.0 - 23.9	10.2 - 11.0	5	3
26/09/2015- 29/09/2015	0.015 - 0.026	4.8 - 12.2	11.7 - 16.12	3	0
Mean	0.014 - 0.028	5.1 - 19.3	11.5 - 16.9		
SPRING (OND)					
13/10/2015- 16/10/2015	0.017- 0.022	1.5 - 16.2	12.3 - 15.3	3	1
01/11/2016- 07/11/2016	0.018- 0.024	6.1 - 16.2	7.6 - 20.2	6	2
12/11/2016- 18/11/2016	0.017- 0.026	4.7 - 12.3	6.5 - 12.3	6	0
05/12/2014- 13/12/2014	0.015- 0.027	5.7 - 11.9	8.2 - 11.9	8	1
Mean	0.017 - 0.025	4.5 - 14.1	8.6 - 14.9		

4. SUPPLEMENTAL MATERIAL

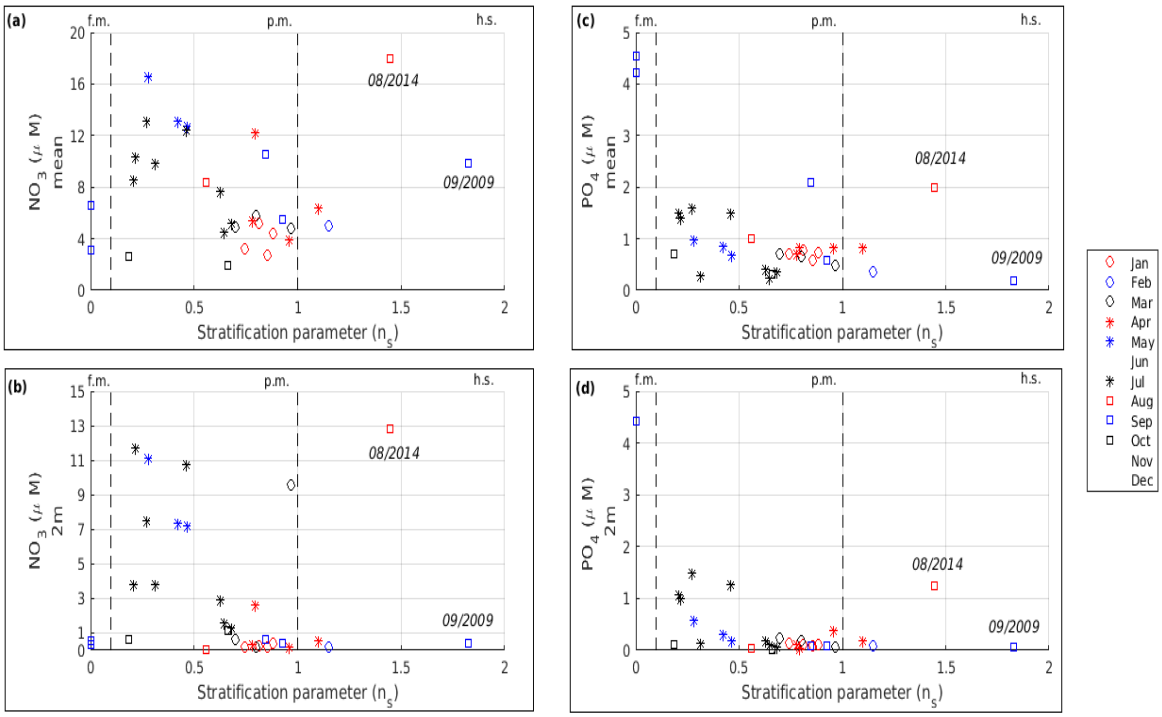

Supplementary material Figure 1. Relation between the stability parameter (ns) and inorganic nutrients (nitrate and phosphate) measured in Puyuhuapi during the period 2008-2015. Upper panels (a and c) show the mean surface concentrations (5-20 m), while lower panels (b and d) show the mean concentrations at 2 m depth. The values ns <0.1, 0.1< ns <1, ns >1 indicate a fully mixed (f. m.), partial mixed (p. m.) and highly stratified (h.s) water column, respectively. The outlier points in each panel represent LAWI bloom periods (i.e. dates 08/2014 and 09/2009) that showing high nutrient concentrations associated with a highly stratified water column.

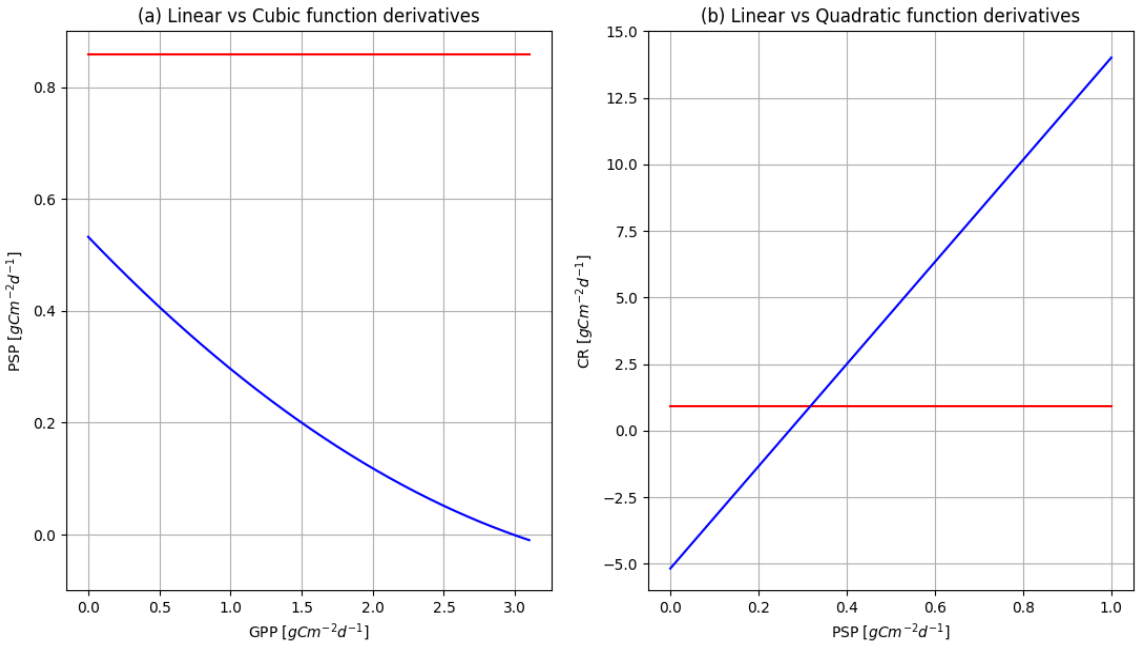

Supplementary material Figure 2. The slopes obtained from the adjustments of the relationships between (a) GPP and PSP and (b) PSP and CR, separated between the summer-autumn and winter-spring periods. The slopes are derived from linear and cubic (a) and linear and quadratic (b) model adjustments, respectively.

5. PRELIMINARY DISCUSSION

A better understanding of the factors that trigger phytoplankton productivity is essential for improved prediction of the occurrence of phytoplankton blooms and their impact on planktonic food webs in fjord environments. Availability of essential nutrients, light, and water column stability are key conditions promoting high levels of primary production. To date, however, we still lack a precise understanding of how these principal physical factors trigger the occurrence of phytoplankton blooms in Patagonian fjords.

The present study was undertaken in the northern part of the Puyuhuapi Fjord where the water column is characterised by a bi-layer system resulting from the interaction of oceanic subantarctic water, rich in nitrate and phosphate, and a surface input of freshwater (mainly from the Cisnes river) that is rich in silicic acid. Although silicic acid is not an essential nutrient for all types of phytoplankton, its requirement for diatom production makes it a key element in shaping the structure and functioning of marine pelagic food webs. The two-layer water column structure in Puyuhuapi Fjord represents a steady state condition under which new primary productivity can only be sustained by input of nutrients into the photic layer. In aquatic environments, nutrient supply to the photic layer can involve a variety of physical processes, such as winter overturn, wind mixing, upwelling, tidal mixing, and fjord seiche induced mixing. The highest values of annual primary productivity tend to be observed in marine ecosystems where pulsed productivity events – resulting from the periodical mixing – are followed by re-stratification of the water column. For example, this occurs in upwelling ecosystems such as the Humboldt Current System, where dense blooms respond to episodic occurrence of alongshore coastal upwelling favourable winds. Our study indicates that pulsed productivity events are also a feature of Puyuhuapi Fjord, where high annual productivity (0.5 kg C m^{-2} y^{-1}, our own unpublished data) is generated from periodic, physically mediated re-supply of nutrients to the photic layer throughout the year.

Strong seasonality and species succession also seem to be a characteristic of the phytoplankton communities present in the Puyuhuapi Fjord. Discrete monthly sampling in our study showed that diatoms dominated the phytoplankton community between August and May, with mixotrophic dinoflagellates dominating between June and July. Within these

broad groups, dominance by individual species of diatoms was correlated with changes in water column temperature. Diatom species such as *Pseudo-nitzschia delicatissima*, *P. seriata, Rhizosolenia pungens* and *R. setigera* were associated with warmer conditions, while *Skeletonema* spp. and *Chaetoceros* spp. were associated with colder conditions. These cold conditions were also associated with the dominance of two dinoflagellate taxa: *Heterocapsa triquetra* and *Gyrodinium* spp. Since species succession has the potential to affect the entire marine food web (Paulino et al., 2018), a better understanding is required of how phytoplankton community patterns are driven by physical forcing. However, the establishment of meaningful baseline information requires effective and regular long-term monitoring of the phytoplankton response to physical forcing in these fjord areas.

In general, the study indicated that mean phytoplankton abundance follows marked seasonality patterns associated with changes in solar radiation and temperature. Highest phytoplankton abundances were recorded during spring and summer (September to April) and lower numbers typically observed during the winter, a pattern similar to the seasonal trends in phytoplankton abundance and productivity reported for other Patagonian fjords (Montero et al ., 2011). These more general observations are also in agreement with the paradigm that divides fjord productivity patterns into two contrasting seasons: a short winter non-productive season, and an extended more productive season during the rest of the year (Iriarte et al., 2007; Iriarte and Gonzalez, 2008, Montero et al., 2011; 2017a). However, our novel data from the continuous measurement of Chl-a at the Puyuhapi buoy highlight the occurrence of enhanced Chl-a events throughout the year. This observation, coupled with the reported occurrence of two conspicuous phytoplankton blooms during winter (Montero et al., 2017a, b), indicate that year-round pulsed productivity events, rather than sharp seasonality, may make a more significant contribution than expected to the annual productivity of the Puyuhuapi Fjord area.

Wind appears to play a fundamental role in triggering these pulsed phytoplankton blooms. At the mesoscale, Puyuhuapi Fjord is under year-round influence of westerly winds, but in the interior of the fjord, winds are predominantly from the south and south westerly direction, with maximum wind speed during fall and winter. Intense wind events strongly influence surface circulation, and mix the water column (Perez et al., 2019), thus effectively injecting nutrients into the photic layer from below. Wind induced mixing

followed by water column re-stratification appears to represent one of the main factors controlling pulsed productivity events in Puyuhuapi Fjord.

Wavelet analysis performed on the Puyuhuapi buoy time series (2013-2016) revealed important synoptic (2-16d), intraseasonal (17-90 d) and seasonal (>90 d) time scales of variability in Chl-a, wind stress, salinity and SST. The wavelet power spectra showed significant periodicities of all these variables over the time scales examined. During the period 2013-2016, we identified 16 synoptic-scale events of high Chl-a forced by wind stress, principally at the synoptic scale. These events were also associated with elevated surface salinity, in turn associated with increased vertical mixing in the water column. A time lag of up to 4 days was apparent between wind stress and Chl-a increase concentration in the water column, and the duration of Chl-a pulses varied between 3 and 16 days. These events occurred during all seasons but were more frequent during winter months. These observations constitute a novel forcing mechanism (Montero et al., 2017a, b, and data from this paper) that appears to induce phytoplankton blooming even in the middle of winter in the Puyuhuapi Fjord.

In most coastal marine environments phytoplankton production shows a high degree of coupling with community respiration (CR). The ratio of GPP/CR is expected to be >1 in environments where the bulk of organic matter (OM) is derived from *in situ* produced OM (autochthonous). In contrast, GPP/CR ratios <1 are characteristic of environments subsidized by allochthonous OM. CR rates were notably higher than GPP rates during much of the annual cycle and consequently, the community net metabolism ratio (GPP/CR<1) suggested that heterotrophic processes dominated.

Fjord environments also receive large quantities of allochthonous organic matter (OM) of terrestrial origin. The amount of allochthonous OM is further augmented by the intense salmon farming activities within some Patagonian fjords. The potential for bacterial growth in Patagonian fjords is enhanced by input of this allochthonous OM. Bacterial utilization of a large fraction of allochthonous and autochthonous OM could play an important role in carbon cycling in Puyuhuapi Fjord.

An important fraction of CR respiration is typically contributed by bacterioplankton activity in marine environments. This can explain the significant correlation between CR

and Prokaryote Secondary Production (PSP) observed in our study. Our study also revealed that PSP and EEA showed a seasonal pattern similar to that observed for phytoplankton productivity. Highest values of PSP and EEA occurred between September and April, and lowest values between May and August.

6. REFERENCES

Acha, E.M., Mianzan, H.W., Guerrero, R.A., Favero, M., Bava, J., 2004. Marine fronts at the continental shelves of austral South America: Physical and ecological processes. Journal of Marine Systems 44(1-2), 83-105. doi.org/10.1016/j.jmarsys.2003.09.005

Abbate, M.C.L., Molinero, J.C., Guinder, V.A., Perillo, G.M., Freije, R.H., Sommer, U., Spetter, C.V., Marcovecchio, J.E., 2017. Time-varying environmental control of phytoplankton in a changing estuarine system. Science of the Total Environment 609, 1390-1400.

Aracena, C., Lange, C.B., Iriarte, J.L., Rebolledo, L., Pantoja, S., 2011. Latitudinal patterns of export production recorded in surface sediments of the Chilean Patagonian fjords (41º-55ºS) as a response to water column productivity. Continental Shelf Research 31, 340-355. doi.org/10.1016/j.csr.2010.08.008

Blauw AN., Benincà., E, Laane R.W.P.M., Greenwood N., Huisman J. 2012. Dancing with the Tides: Fluctuations of Coastal Phytoplankton Orchestrated by Different Oscillatory Modes of the Tidal Cycle. PLoS ONE 7 (11): e49319. doi:10.1371/journal.pone.0049319

Bentamy A., Croize-Fillon, D., 2012. Gridded surface wind fields from Metop/ASCAT measurements. International Journal of Remote Sensing 33(6), 1729-1754. doi.org/10.1080/01431161.2011.600348

Bray, J.R., Curtis, J.T,. 1957. An ordination of the upland forest community of Southern Wisconsin. Ecological Monographs 27(4), 325-349. doi.org/10.2307/1942268

Cloern, J.E., Foster, S.Q., Kleckner, A.E., 2014. Phytoplankton primary production in the world's estuarine-coastal ecosystems. Biogeosciences 11(9), 2477-2501.

Cuevas, L.A., Daneri, G., Jacob, B., Montero, P., 2004. Microbial abundance and activity in the seasonal upwelling area off Concepción (36°S), central Chile: a comparison of upwelling and non-upwelling conditions. Deep Sea Research Part II: Topical Studies in Oceanography 51(20-21), 2427-2440.

Del Giorgio, P.A., Cole, J.J., 1998. Bacterial growth efficiency in natural aquatic systems. Annual Review of Ecology and Systematics 29 (1), 503-541.

Garreaud, R.D., Falvey, M., 2009. The coastal winds off western subtropical South America in future climate scenarios. International Journal of Climatology 29(4), 543-554. http://doi.org/10.1002/joc.1716

Garreaud, R.D., Lopez, P., Minvielle, M., Rojas, M., 2013. Large-scale control on the Patagonian climate. Journal of Climate 26 (1), 215-230. http://doi.org/10.1175/JCLI-D-12-00001.1

Gattuso, J.P., Frankignoulle, M., Wollast, R., 1998. Carbon and carbonate metabolism in coastal aquatic ecosystems. Annual Review of Ecology and Systematics 29 (1), 405-434.

Gillett, N. P., Kell T. D., Jones P. D. 2006. Regional climate impacts of the Southern Annular Mode. Geophysical Reasearch Letters, 33, http://doi:10.1029/2006GL027721.

Goebel N.L., Wing S.R., Boyd P.W., 2005. A mechanism for onset of diatom blooms in a fjord with persistent salinity stratification. Estuarine, Coastal and Shelf Science 64 (2-3), 546-560.

González, H.E., Calderon, M.J., Castro, L., Clement, A., Cuevas, L.A., Daneri, G., Iriarte, J.L., Lizárraga, L., Martínez, R., Menschel, E., Silva, N., Carrasco, C., Valenzuela, C., Vargas, C.A., Molinet, C., 2010. Primary Production and plankton dynamics in

the Reloncaví Fjord and the Interior Sea of Chiloé, Northern Patagonia, Chile. Marine Ecology Progress Series 402, 13-30. doi.org/10.3354/meps08360

González, H.E., Castro, L., Daneri, G., Iriarte, J.L., Silva, N., Vargas, C.A., Giesecke, R., Sánchez. N., 2011. Seasonal plankton variability in Chilean Patagonia fjords: carbon flow through the pelagic food web of Aysén Fjord and plankton dynamics in the Moraleda Channel basin. Continental Shelf Research 31(3-4), 225-243. doi.org/10.1016/j.csr.2010.08.010

González, H.E., Castro, L.R., Daneri, G., Iriarte, J.L., Silva, N., Tapia, F., Teca, E., Vargas, C.A., 2013. Land–ocean gradient in haline stratification and its effects on plankton dynamics and trophic carbon fluxes in Chilean Patagonian fjords (47º-50ºS). Progress in Oceanography 119, 32-47doi.org/10.1016/j.pocean.2013.06.003

Gupta, A. S., and M. H. England., 2006. Coupled ocean-atmosphere-ice response to variations in the Southern Annular Mode, Journal of Climate 19, 4457- 4486.

Haralambidou, K., Sylaios, G., Tsihrintzis, V.A., 2010. Salt-wedge propagation in a Mediterranean micro-tidal river mouth. Estuarine, Coastal and Shelf Science 90 (4), 174-184.

Holton, J., 1992. An Introduction to Dynamic Meteorology. Academic Press, San Diego.

Hoppe, H.G., 1983. Significance of exoenzymatic activities in the ecology of brackish water: measurements by means of methylumbelliferyl-substrates. Marine Ecology Progress Series, 299-308.

Inall, M.E., Gillibrand, P.A., 2010. The physics of mid-latitude fjords: a review. Geological Society, London, Special Publications 344(1), 17-33. http://doi.org/10.1144/SP344.3

Iriarte, J.L., González, H.E., Liu, K.K., Rivas, C., Valenzuela, C., 2007. Spatial and temporal variability of chlorophyll and primary productivity in surface waters of southern Chile (41.5º-43°S). Estuarine, Coastal and Shelf Science 74, 471-480. https://doi.org/10.1016/j.ecss.2007.05.015

Iriarte, J.L., González, H.E., 2008. Phytoplankton bloom ecology of the Inner Sea of Chiloe, Southern Chile. Nova Hedwigia 133, 67-79.

Iriarte, J.L., Pantoja, S., Daneri, G., 2014. Oceanographic processes in Chilean fjords of Patagonia: from small to large-scale studies. Progress in Oceanography 129, 1-7. http://doi.org/10.1016/j.pocean.2014.10.004

Jacob, B.G., Tapia, F.J., Daneri, G., Iriarte, J.L., Montero, P., Sobarzo, M., Quiñones, R.A., 2014. Springtime size-fractionated primary production across hydrographic and PAR-light gradients in Chilean Patagonia (41º-50º S). Progress in Oceanography 129, 75-84. doi.org/10.1016/j.pocean.2014.08.003

Lara, C., Saldías, G.S., Tapia, F.J., Iriarte, J.L., Broitman, B.R., 2016. Interannual variability in temporal patterns of Chlorophyll–a and their potential influence on the supply of mussel larvae to inner waters in northern Patagonia (41–44 S). Journal of Marine Systems 155, 11-18. doi.org/10.1016/j.jmarsys.2015.10.010

León-Muñoz, J., Urbina, M.A., Garreaud, R., Iriarte, J.L., 2018. Hydroclimatic conditions trigger record harmful algal bloom in western Patagonia (summer 2016). Scientific Reports 8 (1), 1330.

Litaker R.W., Tester P.A., Duke C.S., Kenney B.E., Pinckney J.L., Ramus J., 2002. Seasonal niche strategy of the bloom-forming dinoflagellate *Heterocapsa triquetra*. Marine Ecology Progress Series 232, 45-62.

Lovenduski, N.S., Gruber, N., 2005. Impact of the Southern Annular Mode on Southern Ocean circulation and biology. Geophysical Research Letters 32 (11).

Molinet, C., 2010. Primary Production and plankton dynamics in the Reloncaví Fjord and the Interior Sea of Chiloé, Northern Patagonia, Chile. Marine Ecology Progress Series 402, 13-30.http://doi.org/10.3354/meps08360

Montero, P., Daneri, G., González, H.E., Iriarte, J.L., Tapia, F.J., Lizárraga, L., Sanchez, N., Pizarro, O., 2011. Seasonal variability of primary production in a fjord ecosystem of the Chilean Patagonia: Implications for the transfer of carbon within pelagic food webs. Continental Shelf Research 31, 202-215. doi.org/10.1016/j.csr.2010.09.003

Montero, P., Daneri, G., Tapia, F., Iriarte, J.L., Crawford, D., 2017a. Diatom blooms and primary production in a channel ecosystem of central Patagonia. Latin American Journal of Aquatic Research 45 (5), 999-1016.

Montero, P., Pérez-Santos, I., Daneri, G., Gutiérrez, M.H., Igor, G., Seguel, R., Purdie, D., Crawford, D.W., 2017b. A winter dinoflagellate bloom drives high rates of primary production in a Patagonian fjord ecosystem. Estuarine, Coastal and Shelf Science 199, 105-116. doi.org/10.1016/j.ecss.2017.09.027

Narváez, D.A., Vargas, C.A., Cuevas, L.A., García-Loyola, S.A., Lara, C., Segura, C., Tapia, J.F., Broitman, B.R., 2018. Dominant scales of subtidal variability in coastal hydrography of the Northern Chilean Patagonia. Journal of Marine Systems 193, 59-73.https://doi.org/10.1016/j.jmarsys.2018.12.008

Orlanski, I., 1975. A rational subdivision of scales for atmospheric processes. Bulletin of the American Meteorological Society 56, 527-530.

Pantoja, S., Lee, C., 1994. Cell-surface oxidation of amino acids in seawater. Limnology and Oceanography 39 (7), 1718-1726.

Pantoja, S., Iriarte, J.L., Daneri, G., 2011. Oceanography of the Chilean Patagonia. Continental Shelf Research 31(3-4), 149-153.

Parsons, T.R., Maita, Y., Lalli, C.M., 1984. Counting, media and preservatives. Chapter 8. In: A Manual of Chemical and Biological Methods for Seawater Analysis. Pergamon Press, Toronto, p. 173.

Pérez-Santos I., Seguel, R., Schenider, W., Linford, P., Donoso, D., Navarro, E., Amaya-Cárcamo, C., Pinilla, E., Daneri, G., 2019. Synoptic scale variability of surface winds and ocean response to atmospheric forcing in the eastern Austral Pacific Ocean. Ocean Science. doi.org/10.5194/os-2018-119

Pickard, G.L., 1971. Some physical oceanographic features of inlets of Chile. Journal of the Fisheries Board of Canada 28 (8), 1077-1106.

Ray, P.S., 1986. Mesoscale scale Meteorology and Forecasting. American Meteorological Society, Boston

Ross, L., Valle-Levinson, A., Pérez-Santos, I., Tapia, F. J., Schneider, W., 2015. Baroclinic annular variability of internal motions in a Patagonian fjord. Journal of Geophysical Research: Oceans 120 (8), 5668-5685. doi.org/10.5194/os-2018-119

Sakshaug, E., Slagstad, D., Holm-Hansen, O., 1991. Factors controlling the development of phytoplankton blooms in the Antarctic Ocean—a mathematical model. Marine Chemistry 35(1-4), 259-271. doi.org/10.1016/S0304-4203(09)90021-4

Sakshaug, E., Slagstad, D., 1992. Sea ice and wind: effects on primary productivity in the Barents Sea. Atmosphere-Ocean 30 (4), 579-591. doi.org/10.1080/07055900.1992.9649456

Sakshaug, E., Rey, F., Slagstad, D., 1995. Wind forcing of marine primary production in the northern atmospheric low-pressure belt. Ecology of Fjords and Coastal Waters. Elsevier, Amsterdam, 15-25.

Sambrotto, R.N., Niebauer, H.J., Goering, J.J., Iverson, R.L., 1986. Relationships among vertical mixing, nitrate uptake, and phytoplankton growth during the spring bloom in the southeast Bering Sea middle shelf. Continental Shelf Research 5 (1-2), 161-198.

Sathicq, M.B., Bauer, D.E., Gómez, N., 2015. Influence of El Niño Southern Oscillation phenomenon on coastal phytoplankton in a mixohaline ecosystem on the southeastern of South America: Río de la Plata estuary. Marine Pollution Bulletin 98 (1-2), 26-33.

Simon, M., Azam, F., 1989. Protein content and protein synthesis rates of planktonic marine bacteria. Marine Ecology Progress Series 51 (3), 201-213.

Smith, D.C., Azam, F., 1992. A simple, economical method for measuring bacterial protein synthesis rates in seawater using 3H-leucine. Marine Microbial Food Webs 6 (2), 107-114.

Smith, R.W., Bianchi, T.S., Allison, M., Savage, C., Galy, V., 2015. High rates of organic carbon burial in fjord sediments globally. Nature Geoscience 8 (6), 450.

Strickland, J.D.H., 1960. Measuring the production of marine phytoplankton. Fisheries Research Board of Canada Bulletin 122, 1-172.

Strickland, J.D.H., Parsons, T.R., 1968. A practical handbook of seawater analysis. Fisheries Research Board of Canada Bulletin, 167.

Thompson, D.W.J., Wallace, J. M., 2000, Annular modes in the extratropical circulation. Part I: Month-to-month variability. Journal of Climate 13 (5), 1000-1016.

Thompson, D.W.J., J. Wallace, M., Hegerl, G.C. 2000. Annular modes in the extratropical circulation. Part II: Trends. Journal of Climate, 13 (5), 10181036.

Thompson, D.W.J., Barnes, E.A., 2014. Periodic variability in the large-scale southern hemisphere atmospheric circulation. Science 343, 641-645.

Torrence, C., Compo, G., 1998. A practical guide to wavelet analysis. Bulletin of the American Meteorological Society 79, 61-78.

Torres, R., Pantoja, S., Harada, N., González, H.E., Daneri, G., Frangopulos, M., Rutllant, J.A., Duarte, C.M., Rúiz-Halpern, S., Mayol, E., Fukasawa, M., 2011. Air-sea CO_2 fluxes along the coast of Chile: From CO_2 outgassing in central northern upwelling waters to CO_2 uptake in southern Patagonian fjords. Journal of Geophysical Research 166, 1-17.

Utermöhl, H., 1958. Zur Vervollkommnung der quantitativen Phytoplankton-Methodik. Internationale Vereinigung für Theoretische und Angewandte Limnologie. Kom. für Limnol. Methoden 9, 1-39.

Williams, P.I., Robertson, J.E., 1991. Overall planktonic oxygen and carbon dioxide metabolisms: the problem of reconciling observations and calculations of photosynthetic quotients. Journal of Plankton Research 13, 153-169.

Yelland, M., Taylor, P.K., 1996. Wind Stress Measurements from the Open Ocean. Journal of Physical Oceanography 26(4), 541-558.

MANUSCRIPT IN PREPARATION IV

Influence of dissolved organic matter on bacterial production and community composition in fjords of Chilean Patagonia

Influence of dissolved organic matter on bacterial production and community composition in fjords of Chilean Patagonia

Paulina Montero, Marcelo Gutiérrez, Giovanni Daneri, Bárbara Jacob, Javiera Pavez, Amanda Paredes

1. INTRODUCTION

Chilean Patagonia (41°-56°S) encompasses one of the most extensive fjord regions in the world (Iriarte et al., 2014). These fjords are characterized by variable hydrobiological conditions associated with strong seasonal and latitudinal patterns in precipitation, freshwater discharge from rivers and glacier, and light availability (Aracena et al., 2011; Pantoja et al., 2011 and references therein). The region also supports high rates of biological productivity (Montero et al., 2011; 2017a, b) and contributes significantly to the carbon fluxes in coastal ecosystems (González et al., 2013, 2016). In fact the fjords act as a net sink of CO_2 (Torres et al., 2011) and as a site of significant burial of sedimentary organic carbon during the productive period (Sepúlveda et al., 2011; Smith et al., 2015). The continuing interaction between fresh waters and oceanic waters in Patagonia fjords (Schneider et al., 2014) allows the transport and exchange of large amounts of particulate and dissolved organic matter (POM and DOM) between terrestrial and open-ocean environments (Sievers and Silva, 2009; González et al., 2011), resulting in strong gradients of organic matter composition (González et al., 2019) and a variety of microorganisms (Gutiérrez et al., 2015).

In fjords, the DOM pool consists of a complex mixture of autochthonous and allochthonous components (Benner, 2002; Bianchi, 2007). The allochthonous supply is mainly associated with debris from terrestrial vegetation and soils (Bianchi, 2007) carried by freshwaters, whilst the autochthonous component is principally provided by in situ release from phytoplankton exudation, zooplankton grazing and excretion (Cole et al., 1982; Lignell, 1990; Nagata, 2000; Carpenter et al., 2005; Møller, 2005, 2007). In addition of these natural sources of organic matter, coastal environments also receive a supply of allochthonous organic substrates derived from anthropogenic activities. In the case of

Chilean fjords, an extensive salmon farming industry in the region is a significant source of allochthonous inorganic and organic material (Quiñones et al., 2019). While some studies have shown the potential effect of inorganic nutrient enrichment associated with salmon industry in Chilean fjords (e.g. Soto and Norambuena 2004; Iriarte et al., 2013), the effect of emergent organic substrate supply by fish excretion and defecation, and the unconsumed food (Wang et al., 2012, 2013a; Elizondo-Patrone et al., 2015; Kamjunque et al., 2017) remains a main challenge to be unravelled (Quiñones et al., 2019).

In aquatic ecosystems, DOM is a main substrate fuelling heterotrophic activity of microorganisms (Cole et al., 1982; Azam et al., 1983), with bacteria being considered one of its main consumers at the bottom of the pelagic food webs (Azam, 1998; del Giorgio and Cole, 1998; Turley et al., 2000; Cuevas et al., 2004; Montero et al., 2007, 2011; Attermeyer et al., 2014). Autochthonous DOM is consumed in preference to allochthonous substrates by the heterotrophic bacterial community (Kritzberg et al., 2004, 2005) because of its consistently higher nutritious quality and lability than compounds with a terrestrial origin (Sarmento and Gasol, 2012; Guillemette et al., 2013). Phytoplankton production is the principal source of autochthonous DOM that fuels heterotrophic activity of microorganisms (Azam and Malfatti, 2007; Buchan et al., 2014) and therefore phytoplankton blooms are an important driver behind dynamics of bacterial taxa that specialize in processing photosynthetically produced organic matter (Buchan et al., 2014). In the case of the DOM derived from salmon farming, this pool could also be an important source of organic substrates for the heterotrophic bacterial community (Yoshikawa et al., 2012; Yoshikawa and Eguchi, 2013; Nimptsch et al., 2015), mainly because of its high level of degradability (Nimptsch et al., 2015) and rich protein content (Yoshikawa et al., 2017).

The various phylogenetic groups of bacteria each consume specific molecules within the pool of DOM (Lucas et al., 2016). Thus, while some bacteria are able to readily break down labile compounds, other specialist bacteria can process higher molecular weight material (Gómez-Consarnau et al., 2012; Buchan et al., 2014; Landa et al., 2014; Logue et al., 2016; Camarena-Gómez et al., 2018). Therefore, DOM derived from different sources can provides a series of ecological niches that support the growth of highly diverse bacterial communities (Buchan et al., 2014; Blanchet et al., 2016; Hoikkala et al., 2016). However, due to the natural variability in the composition of microbial communities driven

by environmental factors (Pinhassi and Hagström, 2000), the responses of certain bacterial groups to specific DOM compounds may vary both spatially and seasonally (Bunse and Pinhassi, 2017). In Patagonian fjords, the diversity of the bacterial community in the water column can be modified by temperature, salinity, dissolved oxygen (Gutiérrez et al., 2018) and hydrological changes associated with meltwater discharge (Gutiérrez et al., 2015). In addition, the composition of phytoplankton can also influence the composition of prokaryotes in this region (Gutiérrez et al., 2018). Thus, the complex interplay between environmental variability and a variety of DOM source can impact the structure and function of pelagic microorganisms.

Recent studies suggest that late winter blooms, dominated by diatoms, sustain most of the annual productivity of Chilean Patagonia fjords (Montero et al., 2017a), and it is well know that salmon farming is the main aquaculture activity in the region (Buschman et al., 2006). In the present study we therefore addressed the question of how heterotrophic activity and community composition of bacterioplankton respond to the supply of allochthonous (derived from salmon food) compared with autochthonous (derived from phytoplankton) dissolved organic substrates. We focused our research on the effect of each DOM source on secondary production and degradative capability of prokaryotes and on their community structure, with particular emphasis on identification of key taxa involved in the degradation of autochthonous and allochthonous organic substrates. Experiments were conducted in contrasting seasons in order to evaluate both the influence of natural variability of microbial inoculums on responses to substrate addition, as well as the effect of salinity as a stressor for microorganisms inhabiting surface waters of the fjords. A more detailed knowledge of the ability of bacterial communities to process organic matter from these various sources is fundamental to improve our current understanding of carbon fluxes in Chilean fjords. Microbial diversity and activity are closely coupled to their physical and chemical environment and in turn to ecosystem function (Finlay, 1997; Campbell et al., 1998; Karl, 2007). In this context, changes in the quality and supply of dissolved materials in the water column – associated with climate change and/or anthropogenic activities – may have direct consequences for bacterial community structure and the trophic status of fjord ecosystems.

2. MATERIALS AND METHODS

2.1. Study area and sampling strategy

Within the general area of the Chilean Patagonia fjords (Fig. 1), two sampling sites were studied: 1) a fixed station located in the Puyuhuapi Fjord (Fig. 1a) and 2) three sampling stations located within the glacial fjord area of the Southern Patagonia Ice Field (Fig. 1b). Microcosm experiments were carried out to evaluate the response of the bacterial community to the addition of various DOM sources at the fixed station and the influence of salinity in the region under direct influence of the Patagonian Ice Fields. Sampling in the Puyuhuapi Fjord was conducted during five seasonal campaigns that encompassed two summers (March 2017, February 2019), one autumn (May 2018) and two winters (July 2018, July 2019) (Table 1). Sampling in the glacial fjord region was conducted during a research cruise (CIMAR 23 Fiordos) in spring (November 2017) (Table 1). In addition, during each sampling campaign (in both study areas), hydrographic conditions (temperature, salinity and dissolved oxygen), inorganic nutrients concentrations (NO_3, $Si(OH)_4$ and PO_4) and Chlorophyll-a were measured in the water column.

The Puyuhuapi Fjord extends for about 90 km between 44°19' S and 44°57' S in northern Chilean Patagonia and is connected with the coastal ocean by the Moraleda channel in the south, and the Jacaf channel in the north (Schneider et al., 2014). The Puyuhuapi Fjord is characterized by a two-layer estuarine type of circulation with fresher waters overlying more uniform saltier waters. Freshwater is mainly provided by the Cisnes River discharge, precipitations and terrestrial runoff (Schneider et al., 2014), while deeper saline water originates from Sub Antarctic Waters (SAAW) entering to the fjord. Surface freshwater is rich in silicic acid, while subsurface SAAW is typically enriched in nitrate and orthophosphate (Silva, 2008).

The Southern Patagonia Ice field is the largest temperate ice field in the Southern Hemisphere, extending for about 370 km between 48°15' S and 51°31' S at an average longitude of 73°30' W (Casassa et al., 2002). The ice field consists of 48 main basins and nearly 13000 km^2 of ice (Aniya et al., 1997). This area receives abundant precipitation and discharges considerable volumes of ice and meltwater to the fjords on the west side of

Patagonia (Casassa et al., 2002). Several of the glaciers in the region have shown high rates of frontal retreat and thinning during recent years (Rivera et al., 2012). This glacier melting also release high loads of suspended sediment into fjords, which attenuates light penetration through the water column (Jacob et al., 2014) and reduces the influence of silicic acid from continent (Torres et al., 2014). Changes in hydrographic properties as a result of meltwater input can therefore induce temporal and spatial changes in the structure of the microbial community (Gutiérrez et al., 2015).

2.2. Preparation of DOM supplements

The diatom *Skeletonema pseudocostatum* was selected as source of autochthonous DOM. *Skeletonema* group is one of the main constituents of the phytoplankton community in the Puyuhuapi Fjord and often responsible for late winter blooms (Montero et al., 2017a). Pure cultures of *S*. *pseudocostatum* (strain CSA-15) were obtained from COPAS Sur-Austral strain collection at the FICOLAB laboratory at the Department of Botany of the University of Concepción. The liquid culture of *S*. *pseudocostatum* was filtered through pre-combusted 0.7 μm glass fiber filters (Whatman GF/F) and the filtrate collected in a 1 litre pre-combusted glass bottle before being dispensed into the microcosms. This stock solution was kept refrigerated until the start of experiment.

Pellets of salmon food were used as representative source of allochthonous DOM. These pellets, obtained from the Salmon Technological Institute (INTESAL, Chile) were dissolved in distilled water and filtered through pre-combusted 0.7 μm glass fiber filters (Whatman GF/F). The filtrate was collected in a 1 litre pre-combusted glass bottle before being dispensed into the microcosms. The total mass of food pellets to be dissolved, were calculated to be the grams of carbon equivalent to that of the diatom culture for each sampling campaign. Carbon content of food pellets was measured using a LECO TruSpec® C/H/N analyzer. Biovolume of diatoms was estimated according Sun and Liu (2003) and total carbon content was estimated multiplying by 0.00000004 mg C the number of cells in the culture.

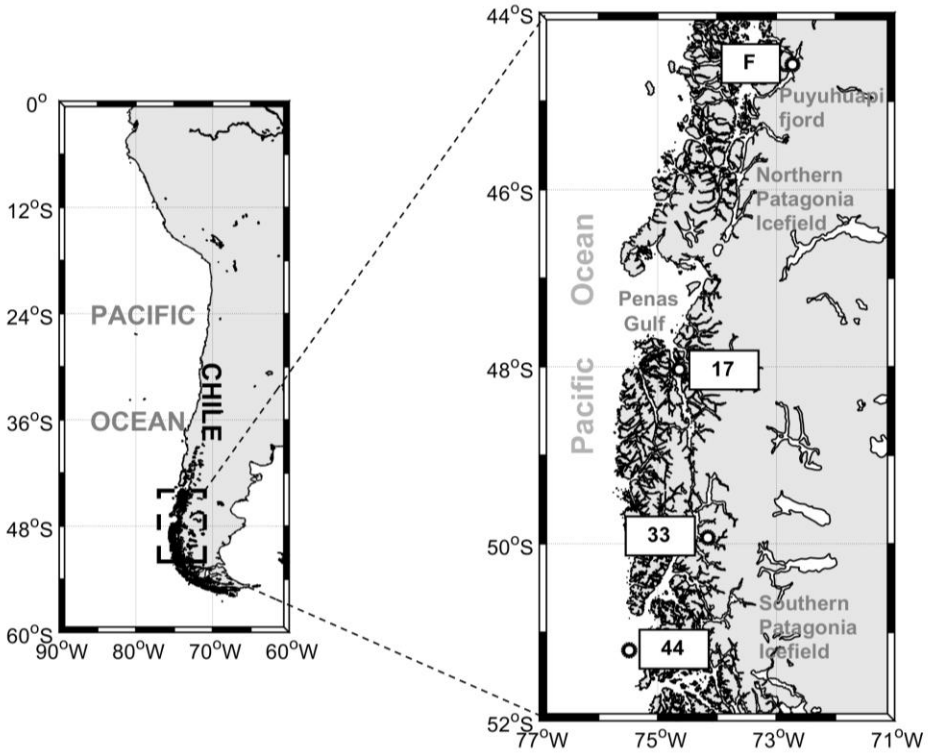

Figure 1. Map of the study area showing the locations of the sampling stations in the Puyuhuapi Fjord (F) and in the fjord area of the Southern Patagonian Ice Field (stations 17, 33 and 44).

2.3 Microcosm experiments in Puyuhuapi Fjord

Water samples were collected from depths of 2 and 20 meters at the Puyuhuapi fixed station (44°35' S; 72°43' W). Water samples obtained from each sampling depth were sieved through a 22-µm mesh to remove large zooplankton and phytoplankton. A peristaltic pump was then used to gently filter pre-sieved water through sterile membrane filters of 0.8-µm (Millipore) in order to separate the bacterial community from its potential predators, and then through a 0.2-µm filter to remove microorganism for use a negative controls (microcosm without bacterial community and without DOM addition supplements). Experimental treatments (microcosm with bacterial community and Diatoms-DOM addition, microcosm with bacterial community and Pellet-DOM addition) and positive

controls (microcosm with bacterial community without addition of DOM supplements) were prepared with water filtered through a 0.8-µm filter.

Eight 10-L foil plastic bags with light protection (Supel^{TM}-Inert) were used as "microcosms", which were filled with filtered water and supplied with DOM derived from diatoms and salmon food. At each sampling depth, two replicates for each treatment and control were prepared (Fig. 2a). All microcosms were incubated at in situ temperature, and were periodically sampled over four days (96 h) for microbial and chemical analyses.

2.4 Microcosm experiments in the fjord area of the Southern Patagonian Ice Field

Water samples were collected from 0 and 25 meters depth at three sampling stations during the research cruise CIMAR 23 Fiordos of the R/V Cabo de Hornos, in spring (November 2017). Stations were selected to showed different levels of influence of meltwaters, with station 33 (49°56' S; 74°9' W) having a higher glacial influence than station 17 (48°2' S; 74°38' W) and 44 (51°12' S; 75°29' W), which is under direct influence of oceanic waters (Fig. 1). Water samples for treatment and control were processed as indicated before. In order to assess the effect of salinity, treatment was filled with a 1:1 mixture of 0.8-µm filtered subsurface water and 0.2-µm filtered surface water (Mix treatment). The salinity delta in Mix treatment was 17.4, 8.8 and 2.2 at stations 17, 33 and 44, respectively. In addition, positive control was prepared with 0.8-µm filtered subsurface water. All microcosms were incubated on board at in situ temperature and were periodically sampled over three days (72 h) for microbial and chemical analyses (Fig. 2b).

2.5 Microbial analyses

Estimates of bacterial production (BP) were derived from incorporation of Leucine into proteins, using the centrifugation method (Smith and Azam, 1992). For these BP experiments a blank and three samples (1.5-mL) were taken from each microcosm and incubated with L-[3,4,5-^{3}H]-leucine (123.8 Ci mmol^{-1}, 40nM final concentration) in the dark for 1 h. After incubation, samples were extracted with 100% trichloroacetic acid (TCA), rinsed with 5% TCA and centrifuged at 13500 rpm twice for 15 minutes before

removal of supernatant. To each sample 1-mL of liquid scintillation cocktail (Ecoscint; National Diagnostic) was added. Samples were counted for dpm using a Packard (Mod. 1600 TR) liquid scintillation counter. Leucine incorporation rates were transformed into bacterial carbon (i.e. bacteria and archaea) following the rationale of Simon and Azam (1989). BP was converted to bacterial carbon utilization (i.e., Bacterial Secondary Production, BSP) using a bacterial growth efficiency of 0.36 (del Giorgio and Cole, 1998).

For extracellular enzymatic activity (EEA) experiments, 50-mL subsamples were removed from each microcosm at the defined sampling times. Duplicate 5 mL-aliquots of water were incubated in the dark with L-leucine-4-methylcoumarinyl-7-amide (MCA-Leu) at 100 μM final concentrations (Hoppe, 1983). Fluorescence was measured at time zero, and subsequently every ~30 minutes for 3h at 365 nm excitation and 455 nm emission. Calibration curves were constructed by measuring the fluorescence in water from each microcosm supplemented with the hydrolysis product MCA, at concentrations ranging between 0.03 and 0.5 μM. First order rate constants were calculated from the slope of the plot of ln (C_0/C_0-P) vs. time, where C_0 is the initial concentration of the substrate MCA-leu and P is the concentration of the product MCA at time t (Pantoja and Lee, 1994). Actual hydrolysis rates were calculated by multiplying rate constants by C_0.

Bacterial abundance (BA, including Bacteria and Archaea) was determined by flow cytometry. Duplicated (1350 μL) samples in cryovials were fixed using 150 μL of 1% glutaraldehyde, then gently mixed and left in the dark at room temperature for 10 min before quick-freezing in liquid nitrogen and storage at –80°C. In the laboratory, the samples were thawed at room temperature and stained with SYBR-Green I (4 μL) for 15 min in the dark and analysed on a flow cytometer (InFlux®) equipped with a 488 nm laser. Heterotrophic bacteria were detected using a 530 nm filter. To discriminate bacteria from other small fluorescent organisms, the intersection of SybrGreen vs forward scatter (FSC) and SybrGreen vs Chlorophyll was used.

Statistical differences in BSP, EEA and BA were tested by Mann-Whitney and Kruskal-Wallis analyses. These statistical analyses were performed using the PAST 3.25 software (Hammer et al., 2001) at an alpha level of 0.05.

For prokaryote diversity (PD), one to two liters of water subsamples from each treatment were filtered through 0.22 µm sterile membrane filters (Millipore) and stored at -20°C. DNA on filters was extracted using a PowerWater® DNA Isolation Kit and cleaned using a Power Clean® DNA Clean-up Kit (MOBIO Laboratories). Prokaryote 16S rRNA genes were amplified using primer set 515F (5'-GTGCCAGCMGCCGCGGTAA-3') and 806R (5'-GGACTACHVGGGTWTCTAAT-3'). Amplification and sequencing on an Illumina MiSeq platform were conducted in a commercial laboratory (Research and Testing Laboratory, Lubbock, TX, USA). The full MiqSeq data set is available at the National Center for Biotechnology Information Sequence Read Archive. Paired Illumina reads were processed using QIIME software package version 1.9.1 (Caporaso et al., 2010). Default QIIME parameters (*r=3, p=0.75, q=3, n=0*) were adopted for quality filtration as recommended by Bokulich et al (2013). Removal of potential chimeras was carried out using VSEARCH software version 1.10.2 (VSEARCH GitHub repository) and Uclust was used to cluster Operational Taxonomic Units (OTUs) at a 97% similarity threshold. Representative sequences from each OTU were classified by comparison with the Greengenes database (De Santis et al., 2006).

Analysis of beta and alpha diversity (Chao1) was carried out after removal of sequences identified as Chloroplast and after resampling with the rarefaction method using the minimum number of sequences per sample (5152). Similarity was estimated at the OTU level based on the Bray-Curtis distance matrix index and used as input to carry out Principal Coordinate Analysis (PCoA) ordination analysis in R version 3.1.2 using the package vegan (Oksanen et al., 2013). Statistical differences in the community composition between periods were tested by PERMANOVA analysis in R. OTU heatmaps were produced using filtered OTU table to identify the contribution of the main representative individual OTUs (representative OTUs defined as that containing more than 500 sequences) to the overall community composition of each sample. Rarefaction curves for each prokaryote community were generated from the means of 10 randomized data sets in Qiime. The Kruskal-Wallis non-parametric test was utilized to test differences in the abundance of individual OTUs between the initial and final incubation time and between periods.

The microbial variables in Puyuhuapi Fjord experiments were measured at time zero (T0), and after 12, 24, 48, 72 and 96 hours (T12, T24, T48, T72 and T96), except for negative controls, where variables were measured at T0, T48 and T96. In the fjord area of the Southern Patagonian Ice field, microbial variables were measured at T0, T24, T48 and T72 at each sampling stations.

2.6 Chemical analyses

Water samples (60-mL) for DOC analysis were collected from each microcosm. Samples were filtered through pre-combusted (450°C, 6 h) 25-mm GF/F filters (~0.7-µm) and frozen at –20 °C prior to analysis in the laboratory. DOC was determined using a catalytic high combustion TOC-5000 Shimadzu analyzer. Prior to analysis, the water samples were acidified with 40 µL of phosphoric acid and decarbonated by purging with high purity CO_2 free gas (Cuevas et al., 2004).

Water samples (500-mL) for analysis of nitrate (NO_3) and phosphate (PO_4) were collected from each microcosm, filtered through GF/F filters and then frozen at –20 °C prior to analysis in the laboratory. Concentrations of these inorganic nutrients were determined spectrophotometrically according to methods given in Strickland and Parsons (1968). DOC and inorganic nutrients were measured at the initial (T0) and final (T96) sampling times.

Statistical differences in DOC and inorganic nutrient concentrations (NO_3 and PO_4) were tested by Mann-Whitney and Kruskal-Wallis analyses. These statistical analyses were performed using the PAST 3.25 software (Hammer et al., 2001) at an alpha level of 0.05.

Table 1. Variables measured during microcosms experiments. BP (bacterial production), EEA (extracellular enzymatic activity), BA (bacterial abundance), PD (prokaryote diversity), DOC (dissolved organic carbon), Inorganic nutrients (nitrate NO_3 and phosphate PO_4).

Date	Station	Lat (S)	Long (W)	BP	EEA	BA	PD	DOC	Inorganic Nutrients
Puyuhuapi Fjord									
March 2017	Fixed	44° 35'	72° 43'	√	√		√		
May 2018	Fixed	44° 35'	72° 43'	√	√		√	√	
July 2018	Fixed	44° 35'	72° 43'	√	√	√	√	√	
February 2019	Fixed	44° 35'	72° 43'	√	√	√	√	√	√
July 2019	Fixed	44° 35'	72° 43'	√	√	√	√		√
Southern Ice Field									
November 2017	33	49° 56'	74° 9'	√	√		√	√	
	17	48° 2'	74° 38'	√	√		√	√	
	44	51° 12'	75° 29'	√	√		√	√	

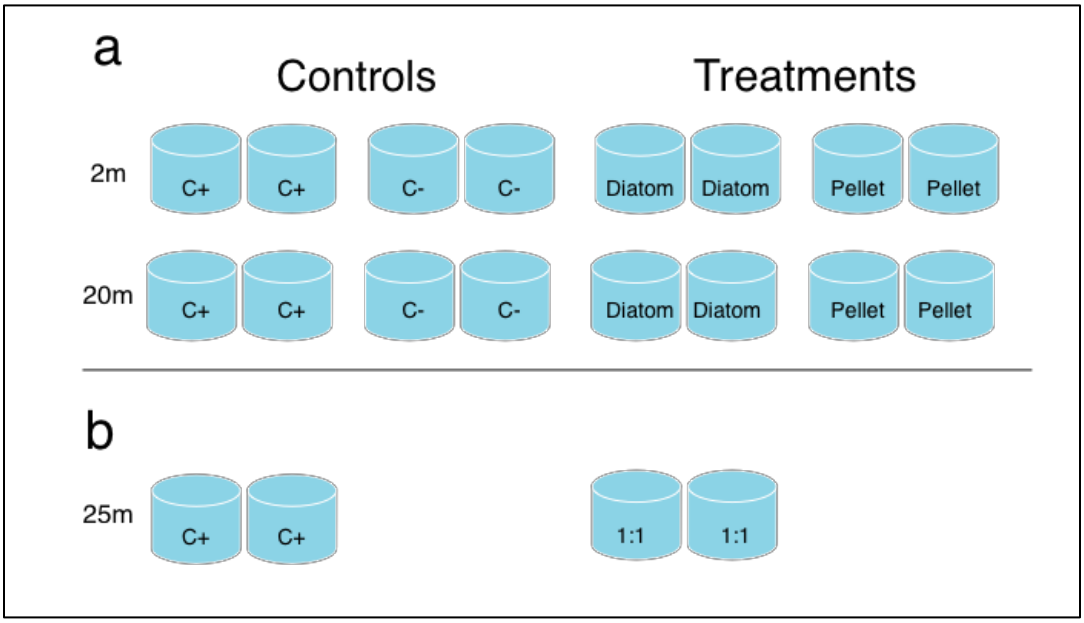

Figure 2. Experimental setup: a) the Puyuhuapi Fjord and b) the fjord area of the Southern Patagonian Ice Field.

3. RESULTS

3.1 Environmental variability between experimental periods

The water column of the fixed station in Puyuhuapi Fjord was characterized by a two-layer structure largely driven by vertical salinity changes (Fig. 3a). Profiles showed a surface layer (0-2 m) of low salinity with values between 16 and 21 PSU, except in May 2018 when values of 22 and 23 psu were recorded (Fig. 3a). Below this layer, and between 10 and 120 m depth, salinity varied between 30 and 33 PSU (Fig. 3a). Surface temperature decreased from15°C in summer (March 2017 and February 2019) to <9°C during winter months (May/July 2018 and July 2019). Winter cooling lead to a thermal inversion in July 2018 and July 2019 (Fig. 3a), while in May 2018 the temperature was homogenously distributed throughout the water column (Fig. 3a). High dissolved oxygen concentrations (>5 ml L^{-1}) were recorded in the surface layer (0-20 m) throughout the study period, while low dissolved oxygen concentrations (<3 ml L^{-1}) were observed below 80 m (Fig. 3a).

Low concentrations of Chlorophyll-a (<1 μg L^{-1}) were observed in the water column (0-20 m) mainly during February and July 2019 (Fig. 3b), while high concentrations (2-5 μg L^{-1}) were recorded within the upper 5 meters in March 2017, May and July 2018 (Fig. 3b). Chlorophyll-a concentrations of <2 μg L^{-1} were observed between 10 and 20 meters depths during all sampling campaigns (Fig. 3b).

Low concentrations of nitrate (<1 μM) were observed within the top 5 m of the water column in most sampling campaigns, except in July 2019, whereas concentrations between 11-21 μM were recorded between 10 and 20 m only during March 2017 and July 2019 (Fig. 3c). Phosphate concentrations (<0.5 μM) were observed within the top 5 m throughout the study period, except in July 2019 and high values (1.0-2.0 μM) were recorded mainly between 10 and 20 m depths in all sampling campaigns, except in February 2019 (Fig. 3c). Low silicic acid concentrations (<10 μM) were measured in the upper 20 m in all sampling campaigns except in July 2019, where higher concentrations were observed in surface waters (>30 μM) than in deeper waters (20 μM) (Fig. 3c).

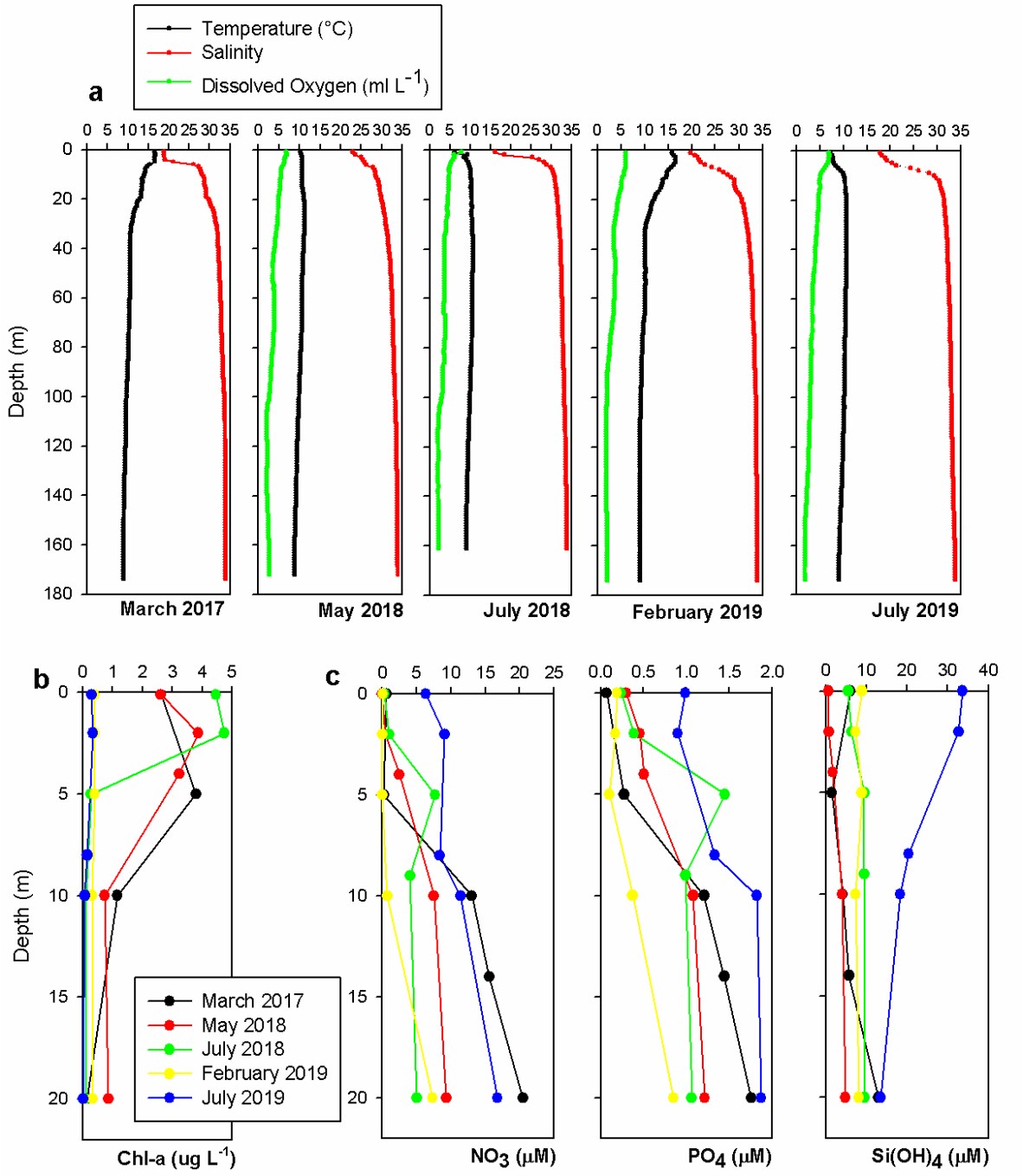

Figure 3. Vertical profiles of a) temperature, salinity, dissolved oxygen, and b) chlorophyll-a and inorganic nutrients (NO_3, $Si(OH)_4$ and PO_4) measured during each sampling campaign at the Puyuhuapi fixed station.

For the Southern Patagonia Ice field, surface salinity ranged from values <15 PSU at station 17 to >30 PSU at station 44 (Fig. 4a), and demonstrated the strong influence of meltwater at stations 17 and 33(located within the fjord area, Fig. 1) and oceanic water at station 44 (located next to the fjord area, Fig.1). The water column of stations 17 and 33 was characterized by a two-layer structure (Fig. 4a), whereas station 44 that showed a fully mixed water column (Fig. 4a). Salinity profiles from station 17 and 33 showed surface layers (0-5 m) of low-salinity water of 13-22 PSU and 22-25 PSU, respectively. Below this layer, and between 15 to 100 m depth, salinity fluctuated between 30-33 PSU at both sampling station (Fig. 4a). Salinity at station 44 varied from 31-33 PSU within the upper 30 m (Fig. 4a). A thermal inversion was observed in all sampling stations. At station 17 and 33 the surface temperature recorded within the top 3 m was 11°C while at station 44 the same temperature was recorded within the top 15 m (Fig. 4a). Temperature decreased with depth to 9°C at all sampling stations, reaching a minimum of 3°C at 22 m at station 33 (Fig. 4a). High dissolved oxygen concentrations (7-8 ml L^{-1}) were recorded in the surface layer (0-5 m) of all sampling stations (Fig. 4a), while low concentrations (5 mL L^{-1}) were observed below 60 m depth (Fig. 4a).

High concentrations (>8 μg L^{-1}) of Chlorophyll-a were recorded at the surface of station 44 (Fig. 4b), with lower concentrations of <1 μg L^{-1} present at stations 17 and 33 (Fig. 4b).

Inorganic nutrients were only measured at two stations (17 and 33), where low concentrations of nitrate (<4 μM) were observed in near-surface waters (0-10 m), with higher concentrations (6-10 μM) at 25 m (Fig. 4c). Similarly, at station 17 y 33, phosphate concentrations of <0.5 μM were recorded in surface waters (2 m), with higher values (0.7-0.9 μM) observed between 10 and 25 m (Fig. 4c). Silicic acid concentrations in the upper layer (0-25 m) ranged from <10 μM at station 33 to 6-14 μM at station 17 (Fig. 4c).

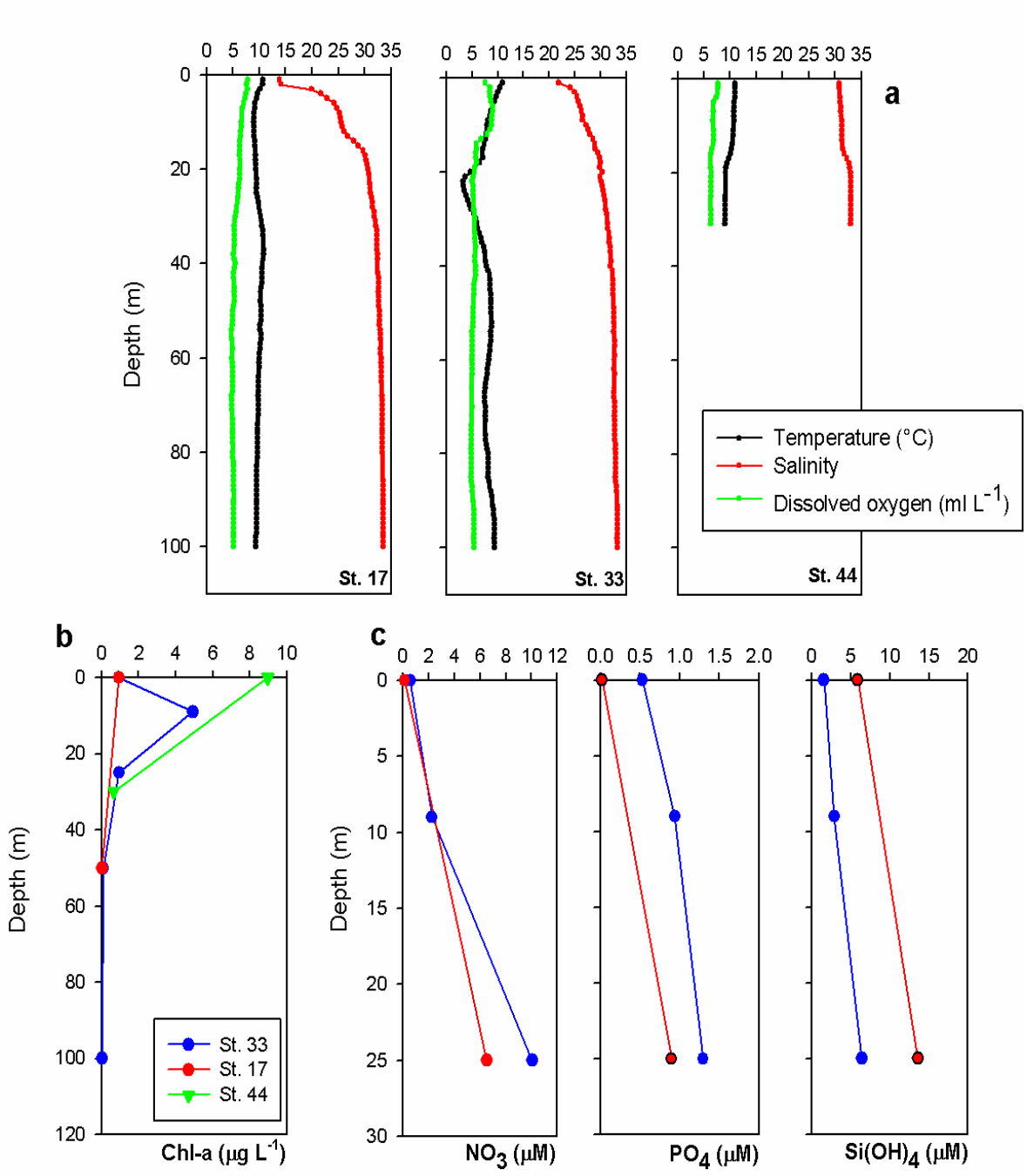

Figure 4. Vertical profiles of a) temperature, salinity, dissolved oxygen, and b) chlorophyll-a and inorganic nutrients (NO_3, $Si(OH)_4$ and PO_4) measured at several stations during the sampling campaign in the fjord area of the Southern Patagonian Ice Field.

3.2 Bacterial secondary production and extracellular enzymatic activity

3.2.1 Puyuhuapi Fjord

Discrete measurements of bacterial secondary production (BSP) (Fig. S1) and extracellular enzymatic activity (EEA) (Fig. S2) were used to calculate the integrated values during two periods of the experiment: Ti (0-1 days, 3 measurements: T0, T12 and T24) and Tf (2-4 days, 3 measurements: T48, T72, T96) (Fig. 5 and Fig. 6). Integrated BSP and EEA values in negative control were not calculated, because only three discrete measurements (T0, T48 and T96) were made during the experiment.

In almost all experiments, integrated BSP values obtained at Tf were significantly higher than those recorded at Ti (Mann-Whitney test, $p< 0.05$) (Fig. 5a, b). During each sampling campaign, and at both sampling depth, BSP recorded at Ti did not show significant differences between positive control (C+) and two treatments (Kruskal-Wallis test, $p> 0.05$) (Fig. 5a, b). In contrast, BSP at Tf were significantly different between positive control (C+) and treatments (Kruskal-Wallis test, $p< 0.05$) in surface water (July 2019) and in subsurface water (May 2018, July 2018, February 2019 and July 2019), mainly because BSP measured in the Pellet-DOM treatment (P) were higher than those recorded in the Diatom-DOM treatment (D) and in the positive control (C+) (Fig. 5a, b). In such cases, BSP in the Pellet-DOM treatment increased by a factor of 1.5 to 4.3 and by a factor of 2.1 to 3.1 compared to BSP measured in the positive control (C+) and Diatom-DOM treatment (D), respectively.

In surface waters, the highest BSP (419.2 ± 2.2 µg C L^{-1} d^{-1}) was recorded in the Pellet-DOM treatment (P) in March 2017, while the lowest (18.8 ± 0.8 µg C L^{-1} d^{-1}) was recorded in July 2018 in the positive control (C+) (Fig. 5a). In subsurface waters, the highest BSP (416.6 ± 5.7 µg C L^{-1} d^{-1}) was recorded in February 2019 in the Pellet-DOM treatment (P), while the lowest (10.7 ± 1.1 µg C L^{-1} d^{-1}) was recorded in July 2018 in the positive control (C+) (Fig. 5b). In general, maximum BSP measurements (>200 µg C L^{-1} d^{-1}) were always recorded in the Pellet-DOM treatment (P) at both sampling depth throughout the study period (Fig. 5a, b).

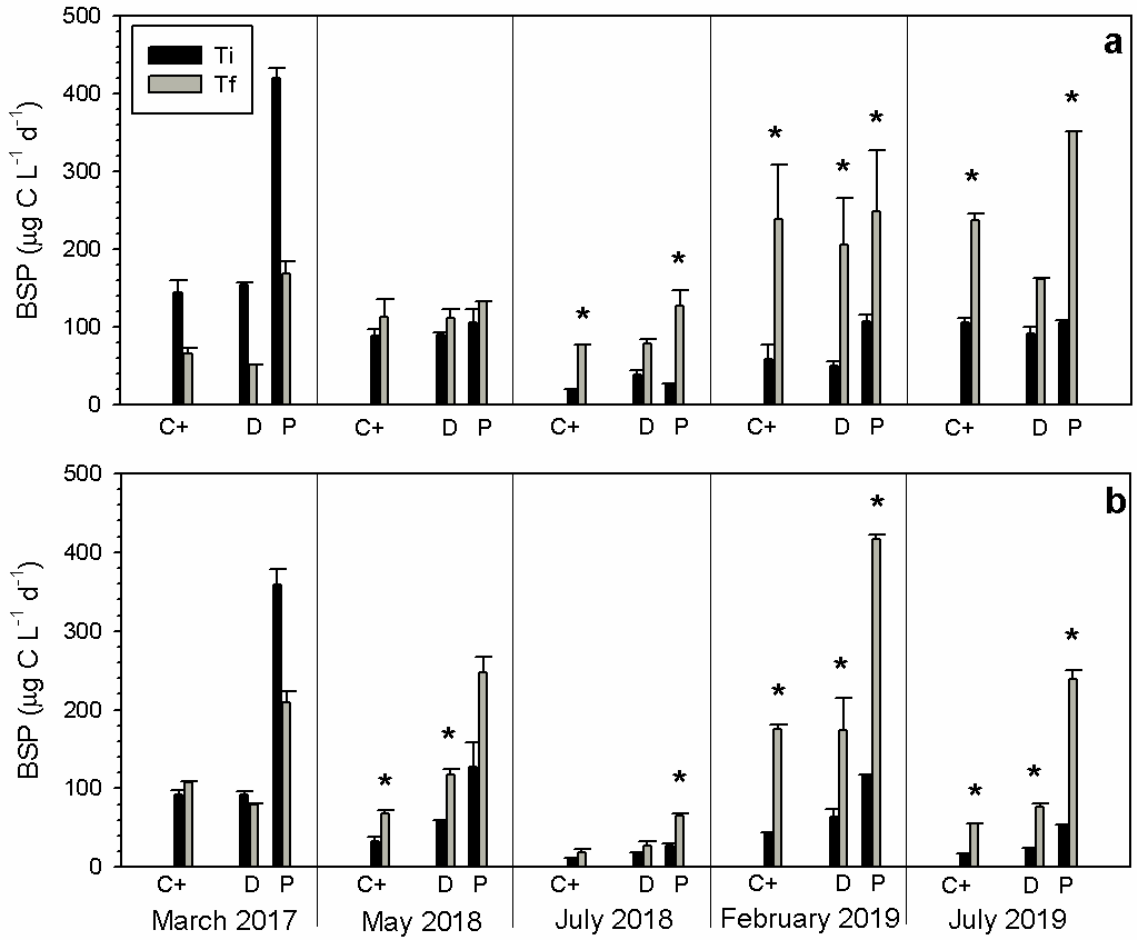

Figure 5. Integrated bacterial secondary production (BSP) recorded for surface (a) and subsurface waters (b) at Ti and Tf during the sampling campaigns in the Puyuhuapi fjord. * indicates significant differences between Ti and Tf. C+ (positive control), D (Diatom-DOM treatment), P (Pellet-DOM treatment).

In general, EEA measurements at Tf were significantly higher than those at Ti (Mann-Whitney test, $p< 0.05$) (Fig. 6a, b). During each sampling campaign, EEA recorded at Ti did not show significant differences between positive control (C+) and two treatments at both sampling depth (Kruskal-Wallis test, $p> 0.05$) (Fig. 6a, b). Instead, EEA values recorded at Tf showed significant differences (Kruskal-Wallis test, $p< 0.05$) in surface water (February 2019) and in subsurface water (May 2018 and February 2019), again due to the high values measured in the Pellet-DOM treatment (D) (Fig. 6a, b). EEA

measurements for the Pellet-DOM treatment (D) were 4.5-6.9 times greater than those measured in the positive control (C+), and 1.7-4.3 times greater than those in the Diatom-DOM treatment (D).

The highest EEA measurements were recorded in February 2019 in the Pellet-DOM treatment (D) in both surface (38.7 ± 2.3 µmol L^{-1} d^{-1}) and subsurface (42.4 ± 2.0 µmol L^{-1} d^{-1}) waters. The lowest measurements were recorded in July 2018 in the positive control (C+) in surface (1.4 ± 0.2 µmol L^{-1} d^{-1}) and subsurface (0.07 ± 0.01 µmol L^{-1} d^{-1}) waters (Fig. 6a, b).

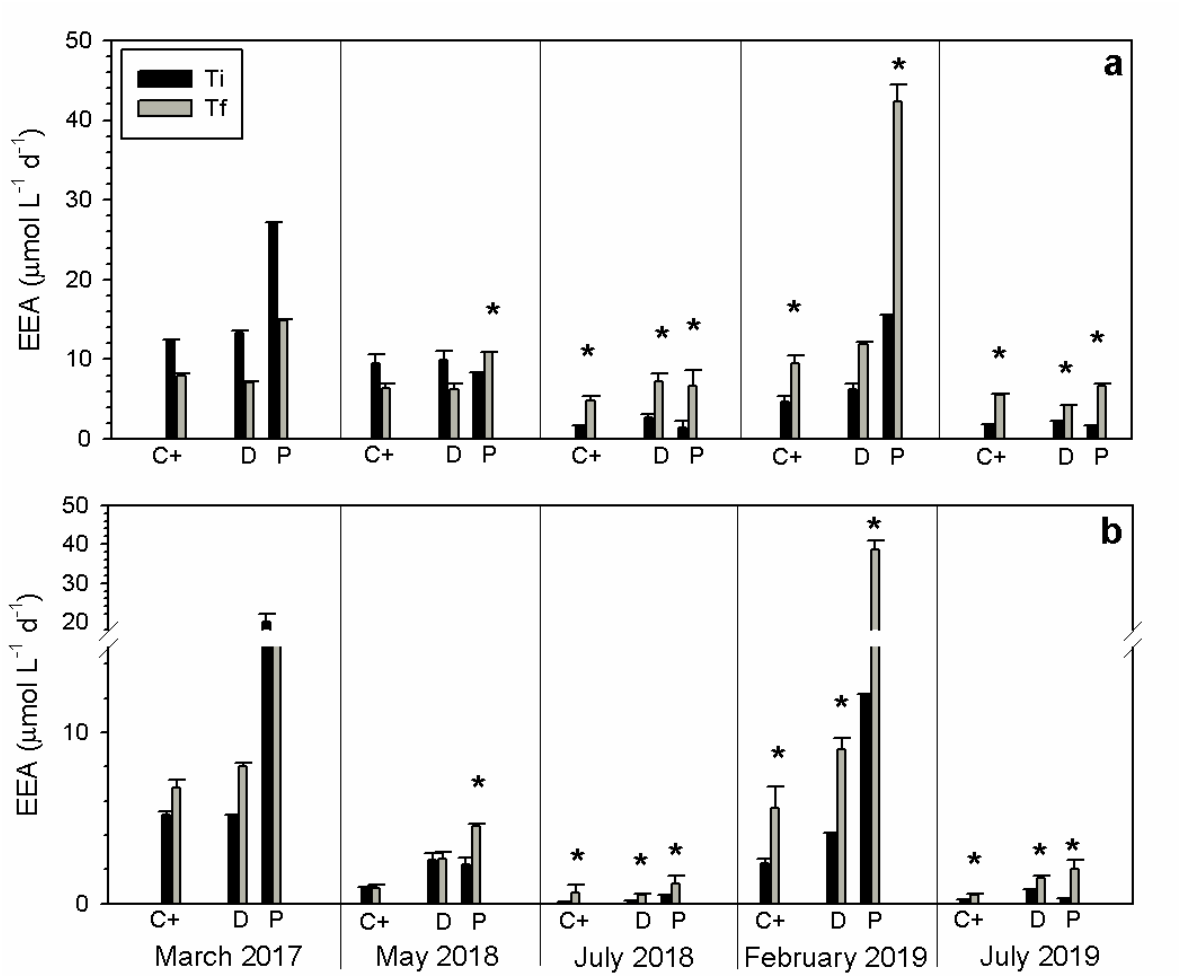

Figure 6. Integrated extracellular enzymatic activity (EEA) measured in surface (a) and subsurface waters (b) at Ti and Tf during the sampling campaigns in the Puyuhuapi Fjord. * indicates significant differences between Ti and Tf. C+ (positive control), D (Diatom-DOM treatment), P (Pellet-DOM treatment).

3.2.2 Fjord area of the Southern Patagonian Ice Field

Discrete measurements of BSP and EEA (Fig. S3), were used to calculate values integrated over two periods of the experiment: Ti (0-1 days, 2 measurements; T0 and T24) and Tf (2-3 days, 2 measurements, T48 and T72) (Fig. 7). For the 3 sampling stations, both BSP and EEA values measured in the positive control (C+) and the Mix treatment (M) (mix of filtered seawater, see methods) were significantly higher at Tf than at Ti (Mann-Whitney test $p< 0.05$) (Fig. 7a, b). Measurements of BSP and EEA at stations 17 and 33 showed no significant differences between control (C+) and Mix treatment (M), both at Ti and Tf (Mann-Whitney test, $p> 0.05$). In contrast, at station 44, BSP and EEA measurements at Tf showed significant differences between the positive control (C+) and the Mix treatment (M) (Mann-Whitney test, $p< 0.05$) (Fig. 7a, b).

The highest BSP value (101.6 ± 20 µg C L^{-1} d^{-1}) was recorded at station 44 (Fig. 7a), however no significant differences were observed between this measurement and those recorded at stations 17 and 33. The highest EEA value (3.2 ± 0.3 µmol L^{-1} d^{-1}) was also recorded at station 44 and was significantly higher than those measured at station 17 and 33 (Fig. 7b).

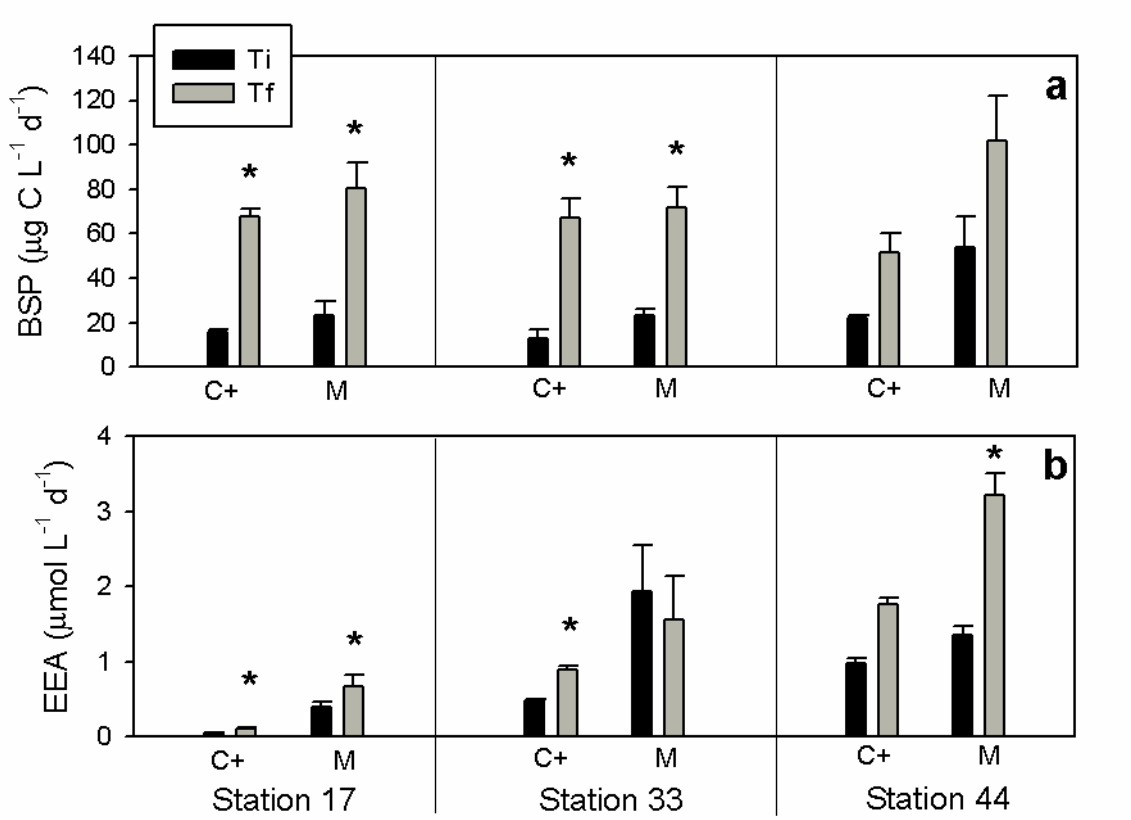

Figure 7. Integrated bacterial secondary production (BSP) (a) and extracellular enzymatic activity (EEA) (b) recorded at Ti and Tf in the sampling campaign of the Southern Patagonian Ice Field. * indicates significant differences between Ti and Tf. C+ (positive control), M (Mix treatment).

3.3 Bacterial abundance and community composition

3.3.1 Puyuhuapi Fjord

Bacterial abundance (BA) increased from T0 to T96 in all experiments (Fig. 8). Significant seasonal differences were observed in abundance from Pellet-DOM treatment (D) in surface, and from positive control (C+) and treatments (D and P) in subsurface waters (Kruskal-Wallis test, $p< 0.05$). The highest BA measurements (3000-7000 × 10^3 cell mL^{-1}) were recorded in surface and subsurface Pellet-DOM treatment (D) during February

2019 (Fig. 8c, d). The lowest abundances (<1000 × 10^3 cell mL^{-1}) were observed in subsurface waters during July 2018 and July 2019 in both the controls (C+ and C-) and the treatments (D and P) (Fig. 8b, f). In both surface and subsurface waters, no significant differences were observed in BA measurements between positive control (C+) and two treatments (D and P) (Kruskal-Wallis test, $p > 0.05$) during the winter (July 2018 and July 2019) experiments. In summer (February 2019), even though BA measurements in the Pellet-DOM treatment (P) were higher than those observed in the positive control (C+) and the Diatom-DOM treatment (D), no significant differences were observed both in surface and subsurface waters (Fig. 8c, d) (Kruskal-Wallis test, $p > 0.05$). BA measurements in both controls and in treatments were significantly higher in surface than in subsurface waters (Mann-Whitney test, $p < 0.05$) during July 2018 and July 2019 (Fig. 8a, b, d, f). In contrast, in February 2019, no significant differences were observed between BA in surface and subsurface waters (Mann-Whitney test, $p > 0.05$) (Fig. 8c, d).

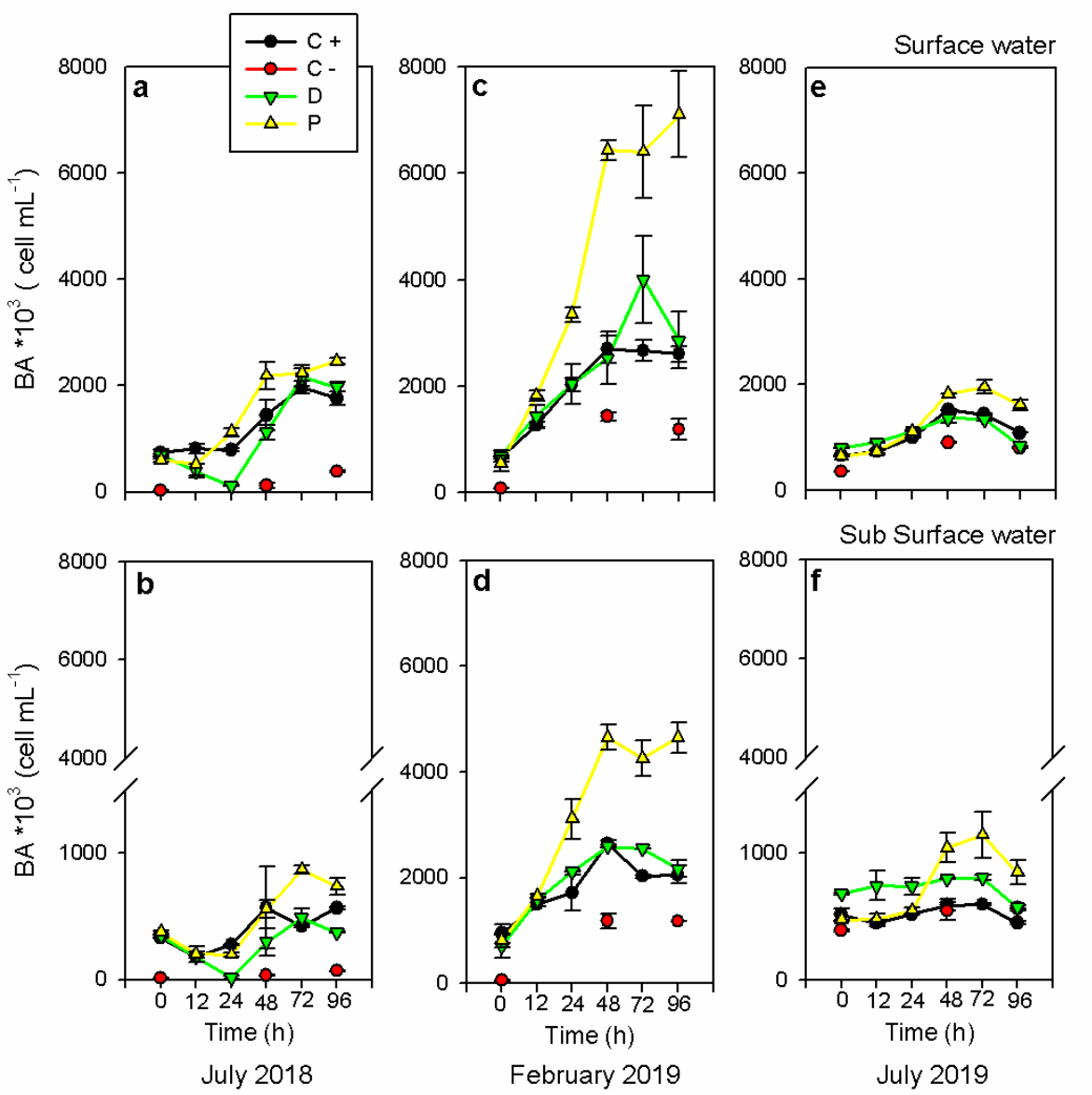

Figure 8. Bacterial abundance (BA) recorded with surface (a) and subsurface waters (b) during the experiments in the Puyuhuapi Fjord. Mean values ± SD of replicate microcosms are shown for each sampling time. C+ (positive control), C- (negative control), D (Diatom-DOM treatment), P (Pellet-DOM treatment).

3.3.2 Alpha and Beta diversity of bacterial community

Prokaryote diversity in the 0.22-0.8 μm size class was analysed. A total of 1,796,407 16S 16S rRNA gene sequences were compared, which correspond to more than 10,000 OTUs of Bacteria and 168 of Archaea after chimera and chloroplast removal. Rarefaction curves reached the curvilinear phase of sampling effort, where most had started to plateau. Alpha diversity measured as Chao1 ranged from 268 to 1402 in the complete dataset. At the initial time of incubations, the lowest measurements of Chao1 were observed in March 2017 in surface waters from Puyuhuapi Fjord (718 ± 186), with maximum values in subsurface waters of the fjord in May 2018 (1184 ± 93; Fig. 9A-C). In surface waters, major variations of Chao1 between t0 and tf were observed in the prokaryote community from July 2018, with richness decreasing in average more than 400 OTUs (Fig. 9A). In subsurface waters, a reduction in the diversity from t0 to tf was observed during all periods in Puyuhuapi Fjord (Fig. 9B), and was also observed in the region of glacial fjords of Southern Patagonian Icefield (Fig. 9C). Major changes in Chao1 were observed between T0 and Tf in May 2018 in Puyuhuapi and at Station 17 in the study area of glacial fjords (Fig. 9C). At tf in the surface waters of Puyuhuapi Fjord, species richness (Chao1) decreased in both treatments (Diatoms-DOM and Pellet-DOM) with respect to the positive control, during all three periods analyzed. A greater reduction of Chao1 (158-244 OTUs) was observed in the Pellet-DOM treatment (Fig. 9D). In subsurface waters, a similar pattern was observed in waters from March 2017, in contrast during May 2018 species richness increased ~150 OTUs in the Diatom-DOM treatment, and ~225 in the Pellet-DOM treatment compared with the positive control (Fig. 9E). In July 2018, a strong increase in diversity was observed in the Diatom-DOM treatment (294 OTUs, Fig. 9E). In the glacial fjord region, richness decreased in the mix treatment with respect to the control in the three stations assessed (Fig. 9F).

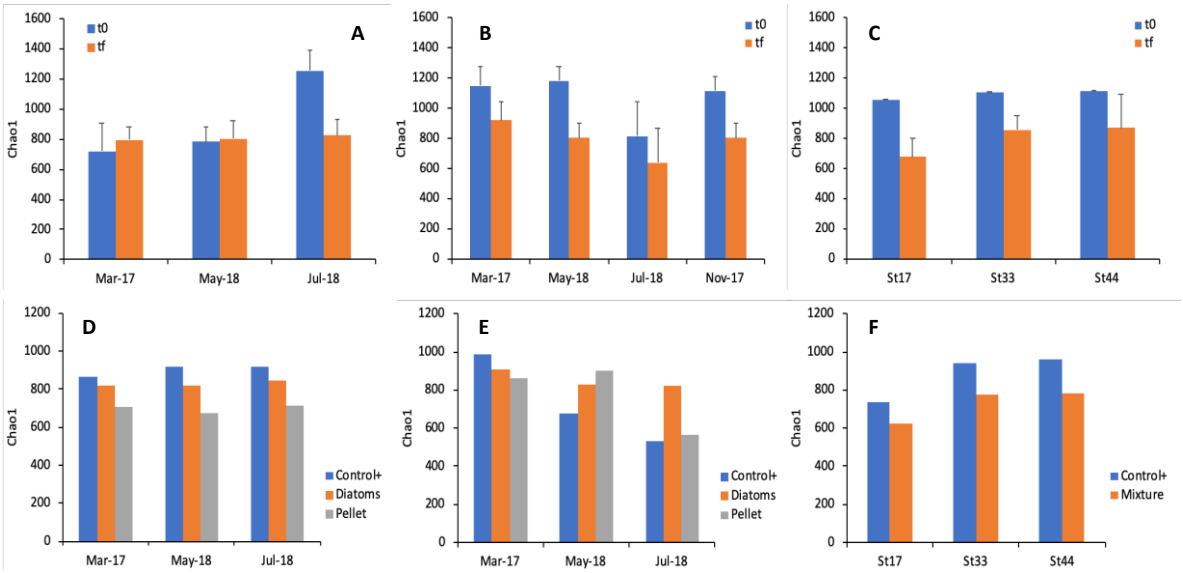

Figure 9. Average Chao1 diversity in controls and treatments in surface and subsurface waters at t0 and tf in the study periods at the fixed station at Puyuhuapi Fjord (A, B) and in the region of fjords of the Southern Patagonian Icefield (C). Chao 1 at tf is shown for control and two treatments in surface (D) and subsurface (E) waters in Puyuhuapi Fjord, and at three sampling stations in the glacial fjord region (F). t0 correspond to the measurement made at the beginning of the experiments. tf correspond to the measurement made at the last sampling time of the experiments: T96 in the Puyuhuapi Fjord and T72 in the glacial fjord region.

Principal coordinate analysis (PCoA) on control and treatments at t0, at the Puyuhuapi station, evidenced differences in beta-diversity both between periods, and between depths within a sampling period (Fig. 10A). For the region of glacial fjords, PCoA grouped prokaryote composition with that from waters of Puyuhuapi in July 2018, but showed singular communities for the different stations (Fig. 10A). At tf, PCoA evidenced decreased differences in beta-diversity between communities in May and July 2018 from Puyuhuapi Fjord, and the communities from the region of glacial fjords grouped within a single cluster (Fig. 10B). In addition, Pellet-DOM treatment in subsurface waters showed higher divergence in beta-diversity, particularly in March 2017 and July 2018 (Fig. 10B).

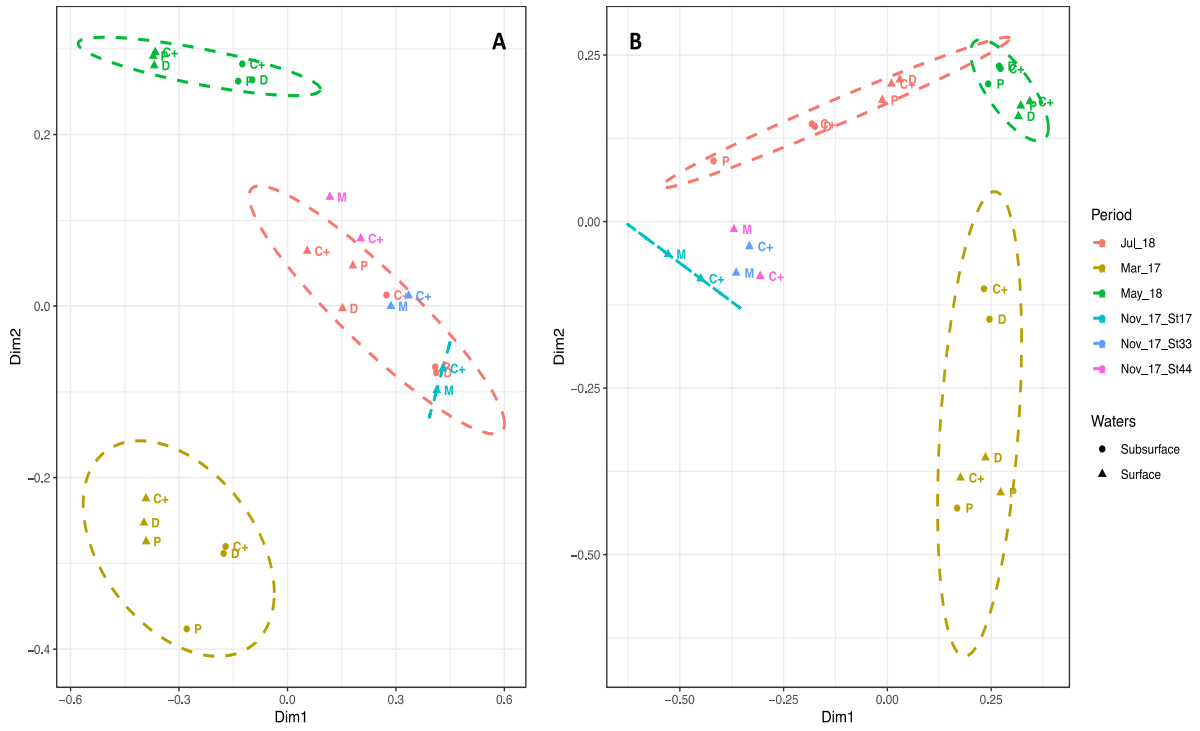

Figure 10. Principal Coordinate Analysis of various controls and treatments at t0 (A) and tf (B). t0 correspond to the measurement made at the beginning of the experiments. tf correspond to the measurement made at the last sampling time of the experiments: T96 in the Puyuhuapi Fjord and T72 in the glacial fjord region.

Representative prokaryote taxa were also identified at t0 for surface and subsurface waters in the Puyuhuapi Fjord and in the glacial fjord region (Fig. 11A-C). Members of the orders *Flavobacteriales* (>40% total OTUs) and *Rhodobacterales* (>20% - ca. 30%) predominated in surface waters of March 2017 and May 2018, whereas in July 2018 members of *Vibrionales* represented the highest fraction (~20%), followed by *Flavobacteriales*, *Rhodobacterales* and *Oceanospirillales* ranging between 10 and 15% (Fig. 11A). In subsurface waters (Fig. 11B), composition of representative taxa showed variability between periods in Puyuhuapi Fjord, with members of *Alteronomadales* (36%) and *Flavobacterales* (24%) being the most abundant taxa during March 2017; *Rhodobacterales* (30%) and *Flavobacterales* (19%) predominated in May 2018 and *Vibrionales* (31%), *Cenarcheales* (14%) and *Oceanospirillales* (13%) represented the

highest percentages in July 2018. In the glacial fjord region, the average composition of prokaryotes at t0 (Fig. 11B) was dominated by members of the order *Vibrionales* (24%) followed by *Ocenospirillales* (16%), *Alteromonadales* (15%) and *Flavobacterales* (11%). Changes in the relative abundance of representative taxa were also observed among stations with strong predominance of *Vibrionales* and *Oceanospirillales* at Station 17, while at Stations 33 and 44 members of *Altermonadales*, *Flavobacterales*, *Oceanospirillales* and *Rhodobacterales* made a higher overall contribution (Fig. 11C).

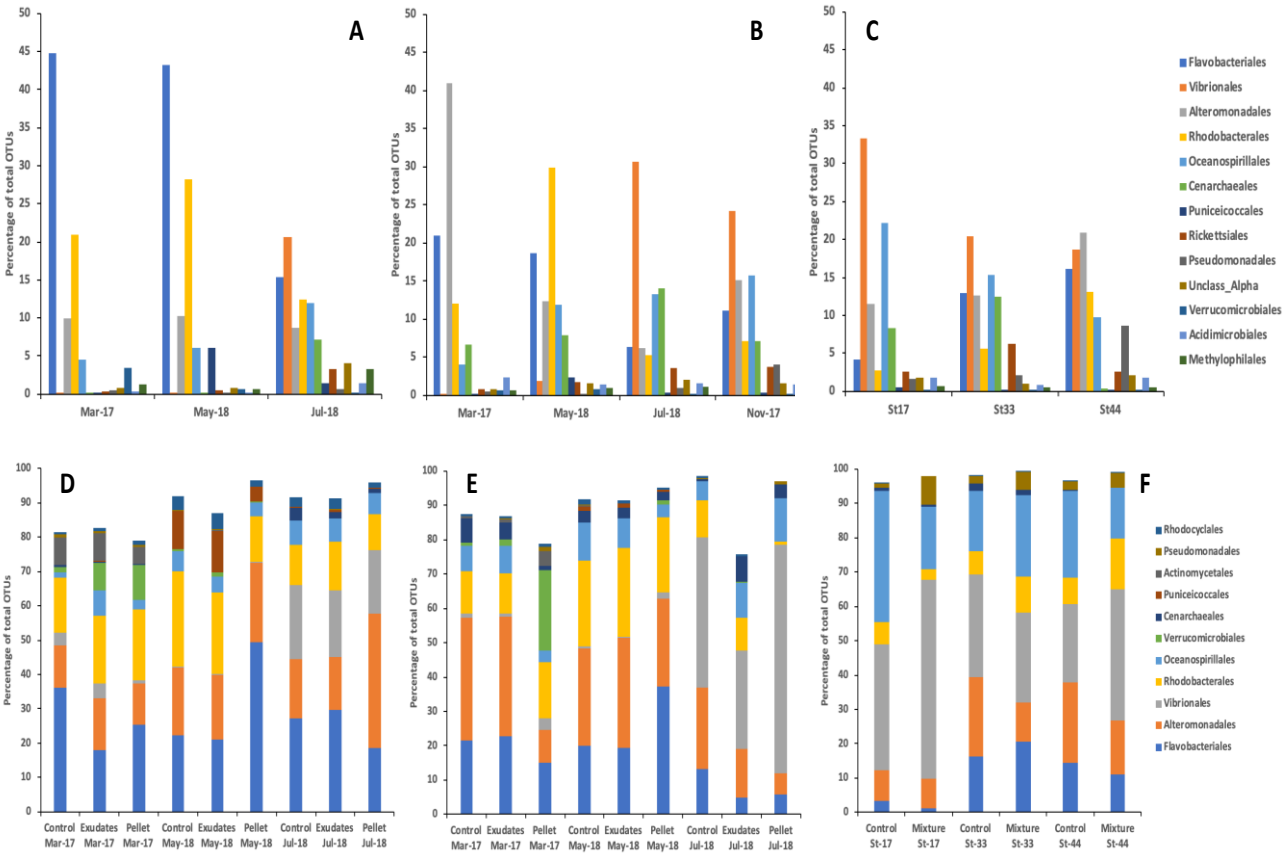

Figure 11. Representative taxa at the order level of prokaryotes at t0 (A-C) and tf (D-F) for different sampling periods in Puyhuapi Fjord and in the glacial fjord region. t0 correspond to the measurement made at the beginning of the experiments. tf correspond to the measurement made at the last sampling time of the experiments: T96 in the Puyuhuapi Fjord and T72 in the glacial fjord region.

In both controls and treatments at tf, the communities from surface waters of Puyuhuapi Fjord (Fig. 11D) were dominated by the orders *Flavobacteriales*, *Alteromonadales* and *Rhodobacterales,* which accounted for between 53 and 65% of the representative taxa during March 2017, and from 63 to 86% in May 2018. During July 2018, *Flavobacteriales*, *Alteromonadales* and *Vibrionales* accounted for between 65 and 76% (Fig. 11D). In subsurface waters (Fig. 11E), *Flavobacteriales*, *Alteromonadales* and *Rhodobacterales* represented 69% in the control and in the Diatom-DOM treatment in March 2017, and over 73% in control and treatments in May 2018. In March 2017, *Verrumicrobiales* dominated representative taxa with 24%, followed by *Rhodobacterales* (16%) and *Flavobacteriales* (15%) in food pellet treatment (Fig. 11E). In July 2018, *Flavobacteriales*, *Alteromonadales* and *Vibrionales* accounted for 80% taxa in the control. In the Diatom-DOM treatment *Alteromonadales*, *Vibrionales* and *Oceanospirillales* represented 53%, while *Vibrionales* predominated with 67% taxa in the Pellet-DOM treatment followed by *Oceanospirillales* with 13% (Fig. 11E). In the glacial fjord region (Fig. 11F), major differences were observed at station 17 where members of *Vibrionales* and *Oceanospirillales* showed notable changes between control and treatment at tf.

At the OTU level, average abundance of representative taxa showed various responses between t0 and tf, both for controls and treatments, and in both surface and subsurface waters (Fig. 12A, B). In surface waters, more than 50% of OTUs showed decreased abundance in the control and in the Pellet-DOM treatment, while in Diatom-DOM treatment 57% of representative OTUs increased their abundance between t0 and tf (Fig. 12A). Major changes were observed for members of *Flavobacterales*, *Alteromonadales* and *Rhodobacterales* (Fig. 12A). In subsurface waters, more than 50% of OTUs reduced their abundance in the control and the treatments, with a higher reduction (~57%) observed in the Pellet-DOM treatment (Fig. 12B). Among representative taxa, members of *Alteromonadales*, *Oceanospirillales*, *Flavobacterales*, *Vibrionales* and *Rhodobacterale*s showed major changes in subsurface waters (Fig. 12B). In surface waters of Puyuhuapi Fjord in March 2017 and May 2018, most of the OTUs at tf showed positive changes in their abundance in the treatments with respect to the control. In subsurface waters however, a reduction of more than 50% was observed in the Pellet-DOM treatment (Fig. 13A, B). During July 2018, major decreases in OTUs were observed in the Pellet-

DOM treatment for surface waters (Fig. 13C). In the glacial fjords, more than 50% of representative taxa showed decreases in abundance between t0 and tf (Fig. 13C). Moreover, at tf, differences were observed between stations in the abundance of OTUs in the mix treatment compared to the control (Fig. 13D).

Figure 12. Average changes in the abundance of representative OTUs in controls and the two treatments between t0 and tf. Data are shown for surface (A) and subsurface waters (B) of Puyuhuapi Fjord, and stations in the glacial fjord region (C). t0 correspond to the measurement made at the beginning of the experiments. tf correspond to the measurement made at the last sampling time of the experiments: T96 in the Puyuhuapi Fjord and T72 in the glacial fjord region.

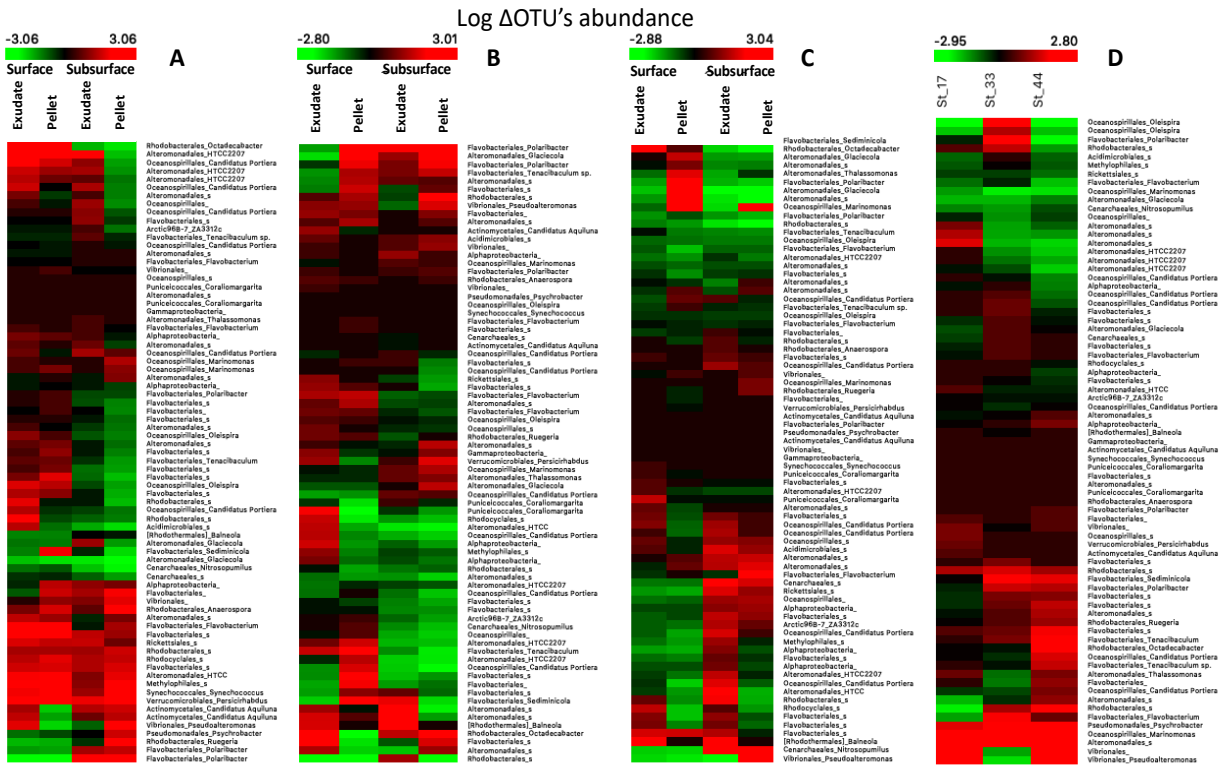

Figure 13. Changes in the abundance of representative OTUs at tf in treatments compared to the controls. Data are shown for surface and subsurface waters of Puyuhuapi fjord (A, B) and for the stations of the glacial fjord region (C). t0 correspond to the measurement made at the beginning of the experiments. tf correspond to the measurement made at the last sampling time of the experiments: T96 in the Puyuhuapi Fjord and T72 in the glacial fjord region.

3.3 Dissolved organic carbon and nutrients

3.3.1 Puyuhuapi Fjord

Dissolved organic carbon (DOC) concentrations measured in controls and treatments (surface and subsurface) decreased significantly from T0 to T96 (Mann-Whitney test, $p < 0.05$) in all sampling campaigns (Fig. 14). In July 2018 and February 2019, DOC measurements at both T0 and T96 showed no significant differences between controls and treatments for either of the sampling depths (Kruskal-Wallis test, $p > 0.05$) (Fig. 14). During May 2018, even though DOC measurements at T0 (in surface and subsurface waters) were higher in treatments (D and P) than in controls (C+ and C-), no significant differences were observed (Kruskal-Wallis test, $p > 0.05$) (Fig. 14a, b).

DOC consumption was estimated as the difference between the values measured at T0 and at T96. In May 2018, DOC consumption in surface waters was of 29 μM in the positive control (C+), 36 μM in the negative control (C-), 69 μM in the Diatom-DOC treatment (D) and 66 μM in the Pellet-DOM treatment (P). In subsurface waters DOC consumption was 9 μM in the positive control (C+), 23 μM in the negative control (C-), 90 μM in Diatom-DOM treatment (D) and 87 μM in the Pellet-DOM treatment (P). For both sampling depths, the consumption of DOC was higher in the two treatments than in the controls. In July 2018, DOC consumption in surface waters over 96 h was 43 μM in the positive control (C+), 39 μM in the negative control (C-), 77 μM in the Diatom-DOM treatment (D) and 69 μM in the Pellet-DOM treatment (P), again highlighting the higher consumption of DOC in treatments than in controls. In contrast, subsurface DOC consumption (26 μM in C+, 35 μM in C-, 34 μM in D and 36 μM in P) was quite similar between controls and treatments. In February 2019, DOC consumption again was similar in both surface (51 μM in C+, 37 μM in C-, 34 μM in D, and 49 μM in P) and subsurface waters (39 μM in C+, 38 μM in C-, 36 μM in D, and 46 μM in P).

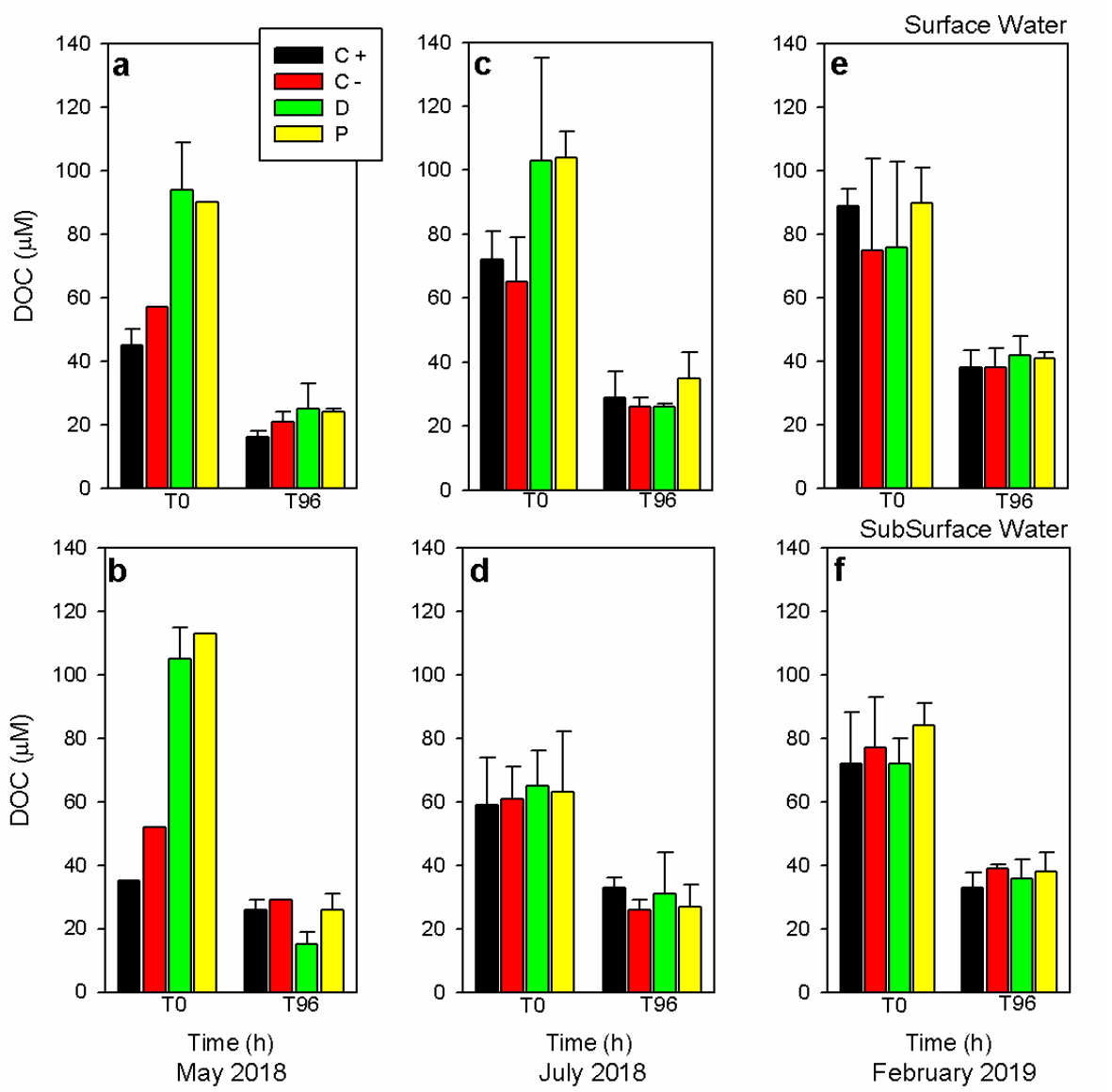

Figure 14. Dissolved organic Carbon (DOC) measured in surface and subsurface waters during the experiments in the Puyuhuapi Fjord. Mean values ± SD of replicate microcosms are shown for initial (T0) and final (T96) sampling times. C+ (positive control), C- (negative control), D (Diatom-DOM treatment), P (Pellet-DOM treatment).

Nitrate and phosphate concentrations both in controls (C+ and C-) and treatments (D and P) from surface and subsurface waters showed no significant differences between T0 and T96 (Mann-Whitney test, $p > 0.05$) during both sampling campaigns (Fig. 15). In general, nitrate and phosphate concentrations remained relatively constant from T0 to T96. During February 2019, phosphate concentrations at both depths were higher (0.8-2.2 µM) at T0 and T96 in the Pellet-DOM treatment (P) than those measured in Diatom-DOM treatment (D) (0-1.4 µM) and controls (C+ and C-) (0-1.3 µM). In July 2019, for both sampling depths over the 96 h, concentrations of nitrate (16.1-30.1 µM) and phosphate (2.9-4.3 µM) were higher in the Diatom-DOM treatment (D) than those measured in controls (0.7-1.9 µM phosphate, 5.7-14.7 µM nitrate) and the Pellet-DOM treatment (D) (0.9-1.9 µM phosphate, 6.1-14.6 µM) (Fig. 15). In February 2019, nitrate and phosphate concentrations in both controls (C+ and C-) and treatments (D and P) at T0 and T96 were lower in surface water than those measured in subsurface waters (Fig. 15). In contrast, during July 2019 nitrate and phosphate concentrations were similar between surface and subsurface waters (Fig. 15). Looking seasonally in the water column, nitrate and phosphate concentrations measurement in B4 station were higher in July 2019 than in February 2019 at both sampling depth (Fig. 3).

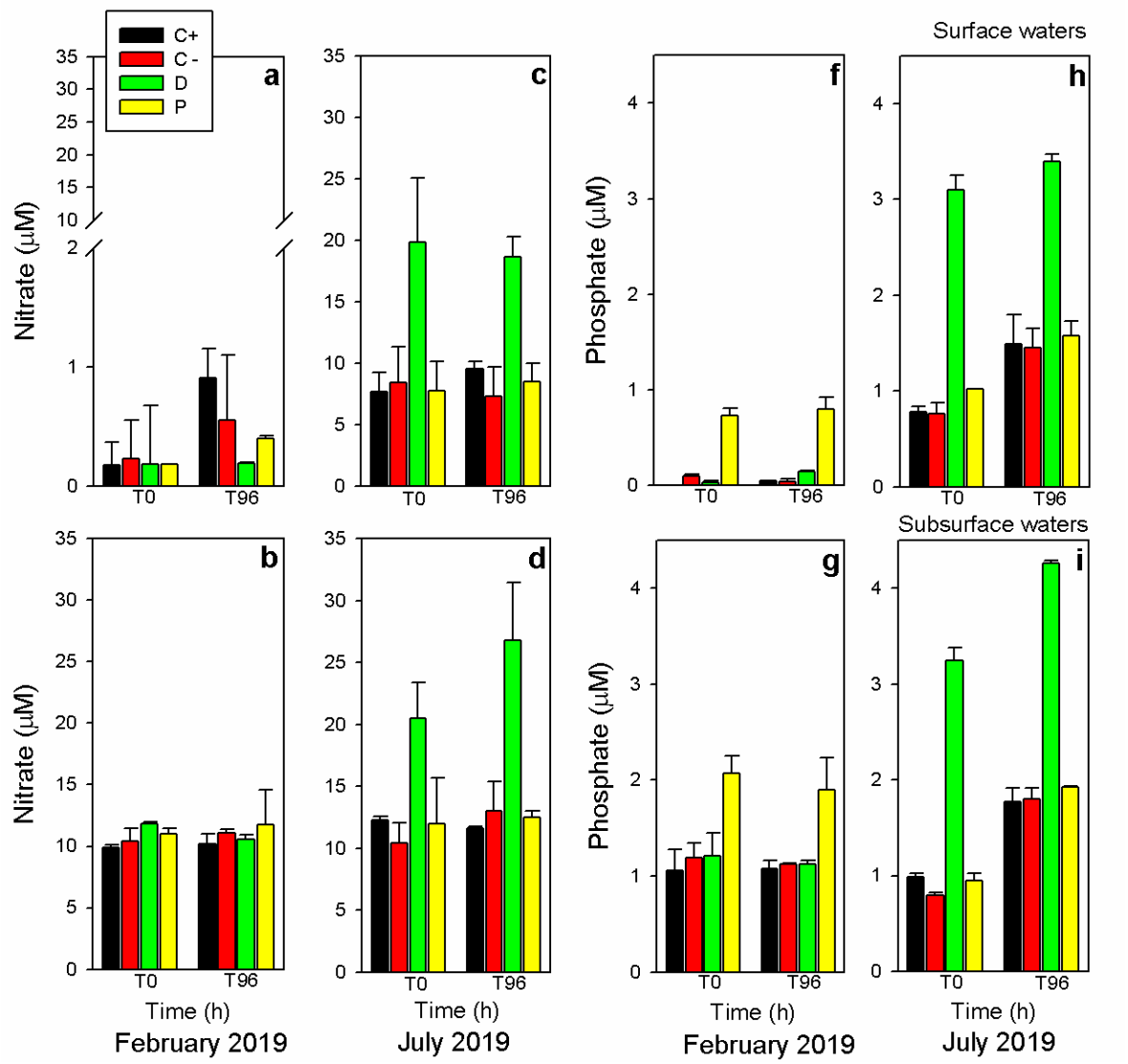

Figure 15. Concentrations of nitrate (a, b, c and d) and phosphate (f, g, h and j) measured in surface and subsurface waters during the experiments in the Puyuhuapi Fjord. Experiments were conducted in February and July 2019. Mean values ± SD of replicate microcosms are shown for initial (T0) and final (T96) sampling time. C+ (positive control), C- (negative control), D (Diatom-DOM treatment), P (Pellet-DOM treatment).

3.3.2 Fjord area of the Southern Patagonian Ice Field

Dissolved organic carbon (DOC) concentrations measured in all experiments decreased slightly from T0 to T72 (Fig. 11) with no significant differences (Mann-Whitney test, $p > 0.05$) (Fig. 16). The initial (T0) and final (T72) concentrations of DOC showed no significant differences between control (C+) and treatment (M) for all sampling stations (Mann-Whitney test, $p > 0.05$) (Fig. 11). Between T0 and T72, DOC consumption varied between 28, 29 and 78 μM in the positive control (C+) and between 35, 3 and 71 μM in the Mix treatment (M), at stations 17, 33 and 44, respectively (Fig. 16). The highest DOC consumption was recorded at station 44 in both control (C+) and Mix treatment (M) (Fig. 16)

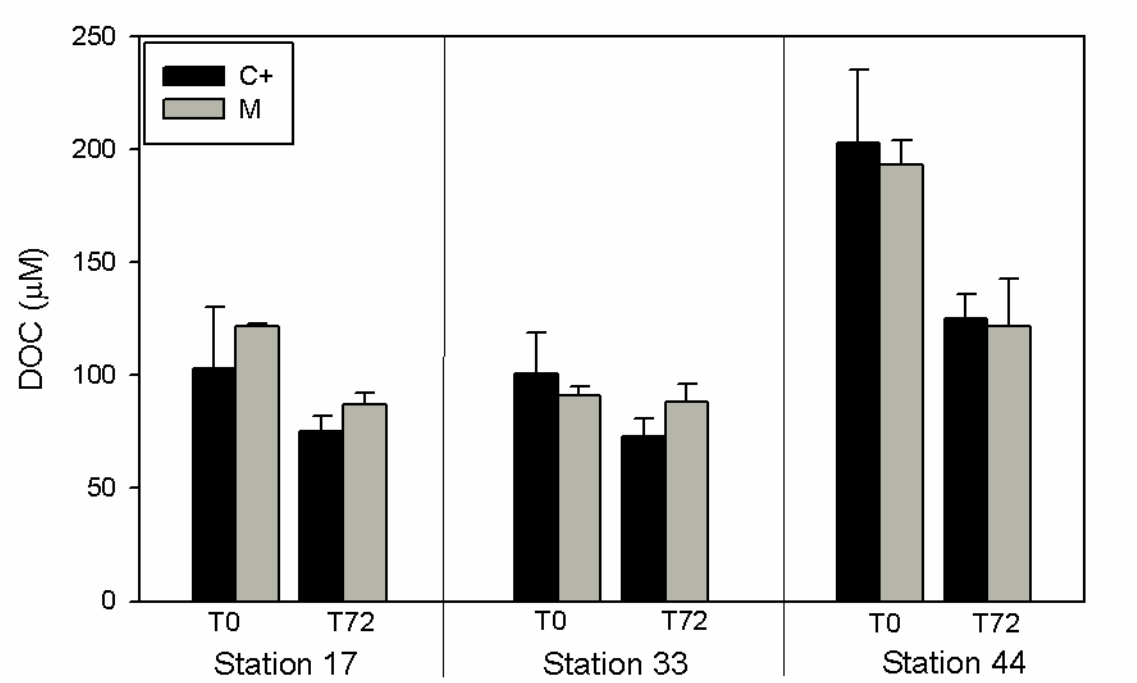

Figure 16. Dissolved organic Carbon (DOC) measured in Stations 17, 33 and 44 during the experiments conducted in the Southern Patagonian Ice Field. Mean values ± SD of replicate microcosms are shown for initial (T0) and final (T72) sampling time. C+ (positive control), M (Mix treatment).

4. PRELIMINARY CONCLUSIONS

Bacterial community was able to process both dissolved organic matter from salmon food pellets (allochthonous organic matter) and those derived from diatoms (autochthonous organic matter). However, bacterial production rates measured with allochthonous organic matter in Pellet-DOM treatments were higher than those measured with autochthonous material in the Diatom-DOM treatments and in the controls.

Major changes in the bacterial community composition were observed in allochthonous conditions (Pellet-DOM treatments) and when the salinity conditions were modified (Mix treatments). These changes were associated with a reduction of OTUs abundance and richness at the end of each experiment. This reduction suggests that a predominance of taxa, are able to process organic substrates supplied in treatments.

5. SUPPLEMENTAL FIGURES

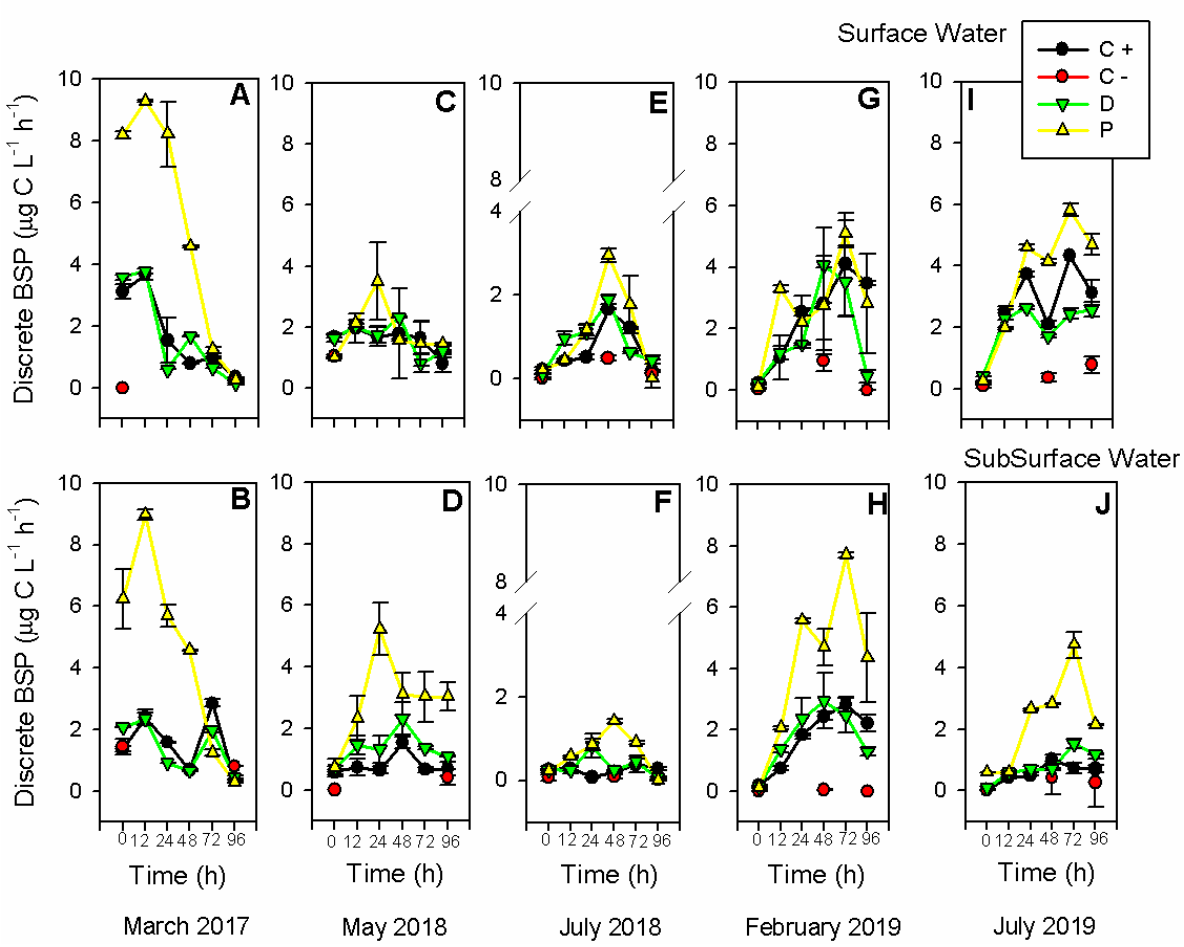

Figure S1. Discrete bacterial secondary production (BSP) measured in surface and in subsurface waters. Mean values ± SD of replicate microcosms are shown during the sampling time. C+ (positive control), C- (negative control), D (Diatom-DOM treatment), P (Pellet-DOM treatment).

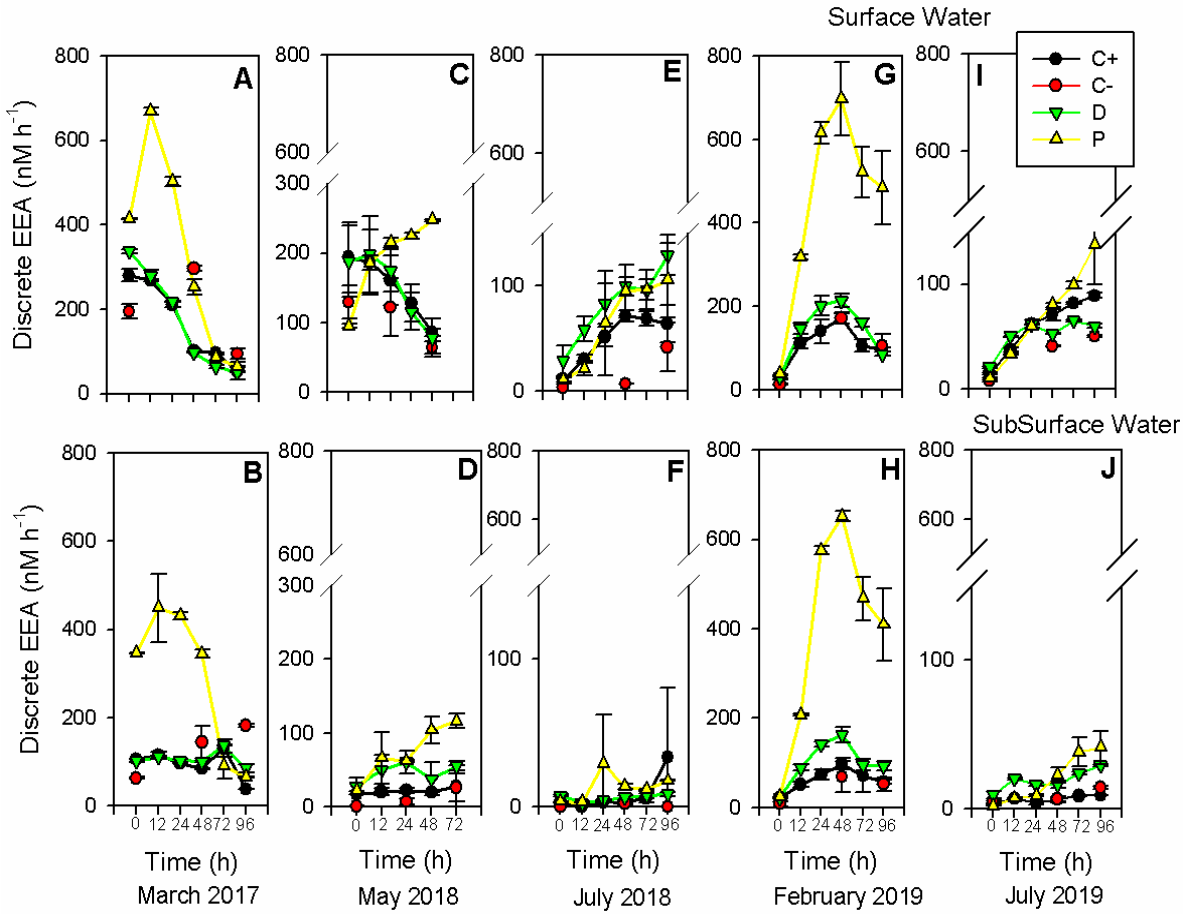

Figure S2. Discrete extracellular enzymatic activity (EEA) measured in surface and in subsurface waters. Mean values ± SD of replicate microcosms are shown during the sampling time. C+ (positive control), C- (negative control), D (Diatom-DOM treatment), P (Pellet-DOM treatment).

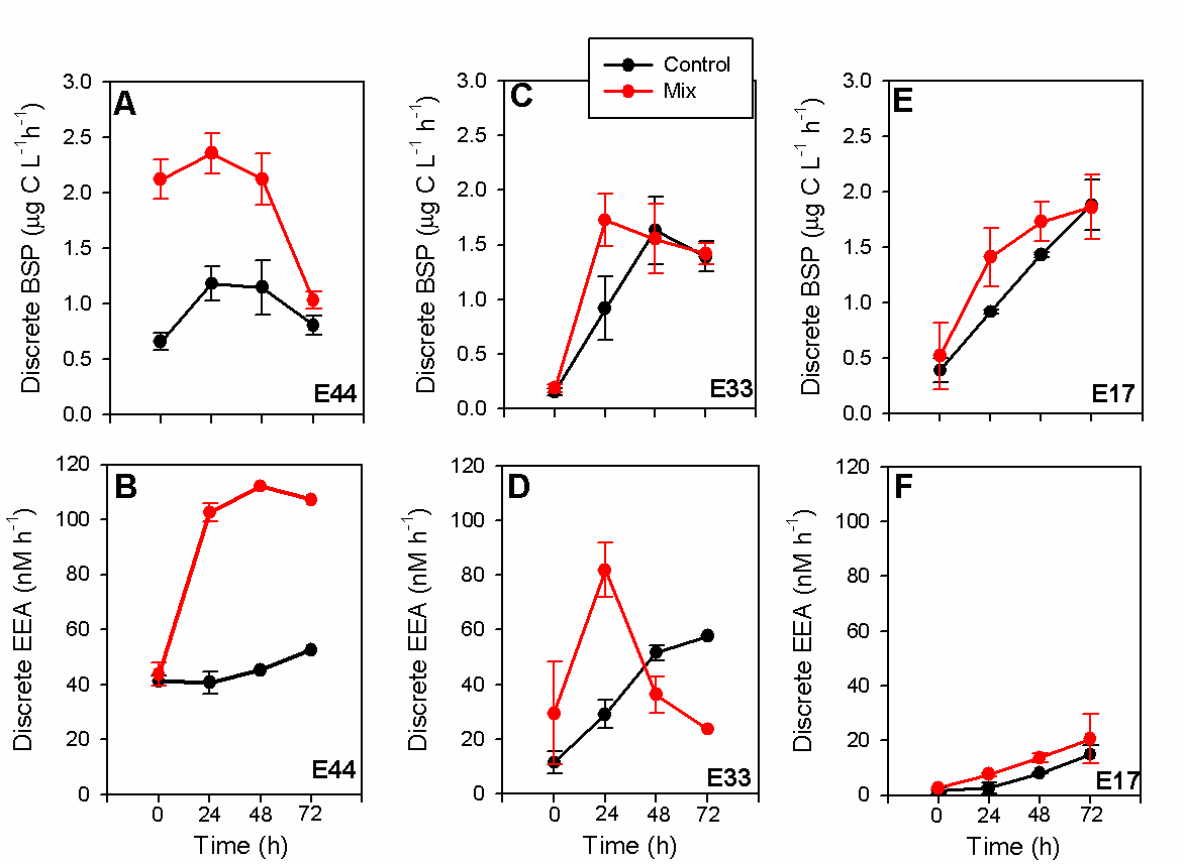

Figure S3. Discrete bacterial secondary production (BSP) and extracellular enzymatic activity (EEA) measured in the sampling campaign of the Southern Patagonian Ice Field. Mean values ± SD of replicate microcosms are shown during the sampling time in the control and in the Mix treatment.

6. REFERENCES

Aracena, C., Lange, C.B., Iriarte, J.L., Rebolledo, L., Pantoja, S., 2011. Latitudinal patterns of export production recorded in surface sediments of the Chilean Patagonian fjords (41–55°S) as a response to water column productivity. Continental Shelf Research 31, 340-355.

Attermeyer, K., Hornik, H., Kayler, Z. E., Bahr, A., Zwirnmann, E., Grossart, H. P., Premke, H., 2014. Enhanced bacterial decomposition with increasing addition of autochthonous to allochthonus carbon without any effect on bacterial community composition. Biogeosciences 11, 1479-1489. doi:10.5194/bg-11-1479-2014

Azam, F., Fenchel, T., Field, J.G., Gray J. S., Meyer-Reil, L. A., Thingstad, F., 1983. The ecological role of water-column microbes in the sea. Marine Ecology Progress Series 10, 257-263.

Azam, F., 1998. Microbial control of oceanic carbon flux: the plot thickens. Science 280, 694-696. doi: 10.1126/science.280.5364.694

Azam, F., Malfatti, F., 2007. Microbial structuring of marine ecosystems. Nature Reviews Microbiology 782-791 doi:10.1038/nrmicro1747

Benner, R., 2002. Chemical composition and reactivity. Biochemestry of marine dissolved organic matter. In D. A. Hansell, and C. A. Carlson (eds). pp 59-90.

Bianchi, T.S., 2007. Biogeochemistry of Estuaries. Oxford University Press. 706 pp

Blanchet, M., Pringault, O., Panagiotopoulos, C., Lefêvre, D., Charrière, B., Ghiglione, J.F. Fernandez, C., Aparicio, F.L., Marrasé, C., Catala, P., Oriol, P., Caparros, J., Joux, F., 2016. When riverine dissolved organic matter (DOM) meets labile DOM in

coastal waters: changes in bacterial community activity and composition. Aquatic Science. doi10.1007/s00027-016-0477-0

Bokulich, N. A., Subramanian, S., Faith, J. J., Gevers, D., Gordon, J. I., Knight, R., et al. (2013). Quality-filtering vastly improves diversity estimates from illumina amplicon sequencing. Nature Methods 10, 57-59. doi: 10.1038/nmeth.2276

Buchan, A., LeCleir, G.R., Gulvik, C.A., González, J.M., 2014. Master recyclers: features and functions of bacteria associated with phytoplankton blooms. Nature Reviews Microbiology. 12, 686-698. doi: 10.1038/nrmicro3326

Bunse, C., and Pinhassi, J. (2017). Marine bacterioplankton seasonal succession dynamics. Trends in Microbiology. 25, 494-505. doi: 10.1016/j.tim.2016.12.013

Buschman, A. H., Riquelme, V., Hernández-González, M. C., Varela, D., Jiménez, J. E., Henríquez, L. A., Vergara, P. A., Guíñez, R., Filún, L., 2006. A review of the impacts of salmonid farming on marine coastal ecosystems in the southeast Pacific. ICES Journal of Marine Science 63, 1338-1345. doi:10.1016/j.icesjms.2006.04.021

Camarena-Gómez, M. T., Lipsewers, T., Piiparinen, J., Eronen-Rasimus, E., Perez-Quemaliños, D., Hoikkala, L., Sobrino, C., Spilling, K., 2018. Shifts in phytoplankton community structure modify bacterial production, abundance and community composition. Aquatic Microbial Ecology 81, 149-170

Carpenter, S. R., Cole, J. J., Pace., M. L., Van de Bogert, M., Bade, D. L., Bastviken, D., Gille, C. M., Hodgson, J. R., Kitchell, J. F., Kritzberg, E. S., 2005. Ecosystem subsidies: terrestrial support of aquatic food webs from ^{13}C addition to contrasting lakes. Ecology 86 (10), 2737-2750

Caporaso, J. G., Kuczynski, J., Stombaugh, J., Bittinger, K., Bushman, F. D., Costello, E. K., et al. 2010. QIIME allows analysis of high- throughput community sequencing

data. Nature Methods 7, 335-336. doi: 10.1038/nmeth.f.303

Casassa, G., Rivera, A., Aniya, M., Naruse, R., 2002. Current Knowledge of the southern Patagonia Icefield. In: The Patagonian Icefields: A unique natural laboratory for environemental and climate change studies, edited by Gino Casassa et al., Kluwer academic/Plenum Publisher.

Cole, J. J., Likens, G. E., Strayer, D. L., 1982. Photosynthetically produced dissolved organic carbon: An important carbon source for planktonic bacterial. Limnology and Oceanography 27, 1080-1090.

Cuevas, L.A., Daneri, G., Jacob, B., Montero, P., 2004. Microbial abundance and activity in the seasonal upwelling area off Concepción (~36ºS), central Chile: a comparison of upwelling and non-upwelling conditions. Deep-Sea Research II 51, 2427-2440.

Del Giorgio, P. A., Cole, J. J., 1998. Bacterial growth efficiency in natural aquatic systems. Annual Review Ecology System 29, 503- 541.

DeSantis, T. Z., Hugenholtz, P., Larsen, N., Rojas, M. E., Brodie, L., Keller, K., et al., 2006. Greengenes, a chimera-checked 16S rRNA gene database and workbench compatible with ARB. Applied and Environmental Microbiology 72, 5069-5072. doi: 10.1128/AEM.03006-05

Elizondo-Patrone, C., Hernández, K., Yannicelli, B., Olsen L.M., Molina, V., 2015. The response of nitrifying microbial assemblages to ammonium (NH_4^+) enrichment from salmon farm activities in a northern Chilean Fjord. Estuarine, Coastal and Shelf Science 166, 131-142. doi.org/10.1016/j.ecss.2015.03.02.

Finlay, B. J., Maberly, S. C., and Cooper, J. I., 1997. Microbial diversity and ecosystem function. Oikos 80, 209-213. doi: 10.2307/3546587

Gómez-Consarnau, L., Lindh, M. V., Gasol, J. M., Pinhassi, J., 2012. Stricturing of bacterioplankton coomunities by specific dissolved organic carbon compounds. Environmental Microbiology 14 (9), 2361-2378. doi:10.1111/j.1462-2920.2012.02804.x

González, H.E., Castro, L.R., Daneri, G., Iriarte, J.L., Silva, N., Tapia, F., Teca, E., Vargas, C.A., 2013. Land-ocean gradient in haline stratification and its effects on plankton dynamics and trophic carbon fluxes in Chilean Patagonian fjords (47-50ºS). Progress in Oceanography 119, 32-47.

González, H.E., Graeve, M., Kattner, G., Silva, N., Castro, L., Iriarte, J.L., Osmán, L., Daneri, G., Vargas, C., 2016. Carbon flow through the pelagic food web in southern Chilean Patagonia: relevance of *Euphausia vallentini* as key species. Marine Ecology Progress Series 557, 91-110. doi.org/10.3354/meps11826.

González, H. E., Nimptsch, J., Giesecke, R., Silva, N., 2019. Organic matter distribution, composition and its possible fate in the Chilean North-Patagonian estuarine system. Science of the Total Environment 657, 1419-1431. doi.org/10.1016/j.scitotenv.2018.11.445

Guillemette. F., McCallister, S.L., del Giorgio, P.A., 2013. Differentiating the degradation dynamics of algal and terrestrial carbon within complex natural dissolved organic carbon in temperate lakes. Journal Geophysical Research: Biogeoscience 118, 963-973. doi:10.1002/jgrg.20077

Gutiérrez, M.H., Galand, P.E., Moffat, C., Pantoja, S., 2015. Melting glacier impacts community structure of Bacteria, Archaea and Fungi in a Chilean Patagonia fjord. Environmental Microbiology 17, 3882-3897.doi: 10.1111/1462-2920.12872

Gutiérrez, M.H., Narváez, D., Daneri, G., Montero, P., Pérez-Santos, I., Pantoja, S., 2018. Linking seasonal reduction of microbial diversity to increase in winter temperature

of waters of a Chilean Patagonia fjord. Frontiers in Marine Science 5:277. doi: 10.3389/fmars.2018.00277

Hoikkala, L., Tammert, H., Lignell, R., Eronen-Rasimus, E., Spilling, K., Kisand, V., 2016. Autochthonous dissolved organic matter drives bacterial community composition during a bloom of Filamentous Cyanobacteria. Frontiers in Marine Science 3:111. doi: 10.3389/fmars.2016.00111

Hoppe, H. G., 1983. Significance of exoenzymatic activities in the ecology of brackish water: measurements by means of methlylumbelliferyl-substrates. Marine Ecology Progress Series 11, 299-308

Iriarte, J.L., Pantoja, S., González, H.E., Silva, G., Paves, H., Labbé, P., Rebolledo, L., Van Ardelan, M., Häussermann, V., 2013. Assessing the micro-phytoplankton response to nitrate in Comau Fjord (42°S) in Patagonia (Chile), using a microcosms approach. Environmental Monitoring and Assessment doi.10.1007/s10661-012-2925-1.

Iriarte, J.L., Pantoja, S., Daneri, G., 2014. Oceanographic processes in Chilean fjords of Patagonia: from small to large-scale studies. Progress in Oceanography 129, 1-7.

Jacob, B.G., Tapia, F., Daneri, G., Iriarte, J.L., Montero, P., Sobarzo, M., Quiñones, R.A., 2014. Springtime size-fractionated primary production across hydrographic and PAR-light gradients in Chilean Patagonia (41-50ºS). Progress in Oceanography 129, 75-84. doi:10.1016/j.pocean.2014.08.003

Kamjunke, N., Nimptsch, J., Harir, M., Herzsprung, P., Schmitt-Kopplin, P., Neu, T.R., Graeber, D., Osorio, S., Valenzuela, J., Reyes, J.C., Woelfl, S., Hertkorn, N., 2017. Land-based salmon aquacultures change the quality and bacterial degradation of riverine dissolved organic matter. Scientific Reports **7**, 43739. doi: 10.1038/srep43739

Kritzberg, E.S., Cole, J.J., Pace, M.L., Granéli, W., Bade D., 2004. Autochthonous versus allochthonous carbon sources to bacteria: results from whole-lake ^{13}C addition experiments. Limnology and Oceanography 49, 588-596

Kritzberg, E.S., Cole, J.J., Pace, M.L., Granéli, W., 2005. Does autochthonous primary production drive variability in bacterial metabolism and growth efficiency in lakes dominated by terrestrial C inputs? Aquatic Microbial Ecology 38, 103-111.

Landa, M., Cottrel, M., Kirchman, D. L., Kaiser, K., Medeiros, P. M., Tremblay, L., Batailler, N., Caparros, J., Catala, P., Escoubeyrou, K., Oriol, L., Blain, S., Obernosterer, I., 2014. Phylogenetic and structural response of heterotrophic bacteria to dissolved organic matter of different chemical composition in a continuous culture study. Environmental Microbiology 16 (6), 1668-1681. doi:10.1111/1462-2920.12242

Lignell, R., 1990. Excretion of organic carbon by phytoplankton: its relation to algal biomass, primary productivity and bacterial secondary productivity in the Baltic Sea. Marine Ecology Progress Series 68, 85-99

Logue, J. B., Stedmon, C. A., Kellerman, A. M., Nielsen, N. J., Andersson, A. F., Laudon, H., Lindström, E. S., Kritzberg, E. S., 2016. Experimental insights into the importance of aquatic bacterial community composition to the degradation of dissolved organic matter. The ISME Journal 10, 533-545

Lucas, J., Koester, I., Wichels, A., Niggemann, J., Dittmar, T., Callies, U., Wiltshire, K.H., Gerdts, G., 2016. Short-term dynamics of North Sea bacterioplankton-dissolved organic matter coherence on molecular level. Frontiers in Microbiology 7:321. doi: 10.3389/fmicb.2016.00321

Moller, E. V., 2005. Sloppy feeding in marine copepods: prey-size-dependent production of dissolved organic carbon. Journal of plankton Research 27 (1), 27-35. doi:10.1093/plankt/fbh147

Moller, E. V., 2007. Production of dissolved organic carbon by sloppy feeding in the copepods *Acartia tonsa*, *Centropages typicus*, and *Temora longicornis*. Limnology and Oceanography 52 (1), 79-84

Montero, P., Daneri, G., González, H.E., Iriarte, J.L., F.J., Tapia, F.J. Lizárraga, L., Sanchez, N., Pizarro, O., 2011. Seasonal variability of primary production in a fjord ecosystem of the Chilean Patagonia: implications for the transfer of carbon within pelagic food webs. Continental Shelf Research 31, 202-215. doi:10.1016/j.csr.2010.09.003

Montero, P., Daneri, G., Tapia, F., Iriarte, J. L., Crawford, D., 2017a. Diatom blooms and primary production in a channel ecosystem of central Patagonia. Latin American Journal of Aquatic Research 45, 999-1016. doi: 10.3856/vol45-issue5-fulltext-16

Montero, P., Pérez-Santos, I., Daneri, G., Gutiérrez, M.H., Igor, G., Seguel, R., Purdie, D., Crawford, D.W., 2017b. A winter dinoflagellate bloom drives high rates of primary production in a Patagonian fjord ecosystem. Estuarine, Coastal and Shelf Science 199,105-116. doi: 10.1016/j.ecss.2017.09.027

Nagata, T., Fukuda, H., Fukuda, R., Koike, I., 2000. Bacterioplankton distribution and production in deep Pacific waters: Large-scale geographic variations and possible coupling with sinking particle fluxes. Limnology and Oceanography 45 (2), 426-435

Nimptsch, J., Woelfl, S., Osorio, S., Valenzuela, J., Ebersbach, P., von Tuempling, W., Palma, R., Encina, F., Figueroa, D., Kamjunke, N., Graeber, D., 2015. Tracing dissolved organic matter (DOM) from land-based aquaculture systems in North

Patagonia streams. Science of the Total Environment 537, 129-138. doi.org/10.1016/j.scitotenv.2015.07.160.

Pantoja, S., Lee, C., 1994. Cell-surface oxidation of amino acids in seawater. Limnology and Oceanography 39, 1718-1726.

Pantoja, S., Iriarte, J. L., Daneri, G., 2011. Oceanography of the Chilean Patagonia. Continental Shelf Research 31, 149-153.

Pinhassi, J., Hagström, A., 2000. Seasonal succession in marine bacterioplankton. Aquatic Microbial Ecology 21, 245-256. doi: 10.3354/ame021245

Quiñones, R. A., Fuentes, M., Montes, R. M., Soto, D., León-Muñoz, J., 2019. Environmental issues in Chilean salmon farming: a review. Reviews in Aquaculture 11, 375-402. doi: 10.1111/raq.12337

Rivera , A., Corripio, J., Bravo, C., Cisternas, S., 2012. Glaciar Jorge Montt (Chilean Patagonia) dynamics derived from photos obtained by fixed cameras and satellite feature tracking. Annals of Glaciology 53 (60) 147-155. doi: 10.3189/2012AoG60A152

Sarmento, H., Gasol, J. M., 2012. Use of phytoplankton-derived dissolved organic carbon by different types of bacterioplankton. Environmental Microbiology 14(9), 2348-2360. doi:10.1111/j.1462-2920.2012.02787.x

Schneider, W., Pérez-Santos, I., Ross, L., Bravo, L., Seguel, R., Hernández, F., 2014. On the hydrography of Puyuhuapi Channel (Chilean Patagonia). Progress in Oceanography 129, 8-18. doi10.1016/j.pocean.2014.03.007

Sepúlveda, J., Pantoja, S., and Hughen, K. A., 2011. Sources and distribution of organic matter in northern Patagonia fjords, Chile (~44-47° S): a multi- tracer approach for

carbon cycling assessment. Continental Shelf Resesearch 31, 315-329. doi: 10.1016/j.csr.2010.05.013

Silva, N., 2008. Dissolved oxygen, pH, and nutrients in the austral Chilean channels and fjords. Progress in the oceanographic Knowledge of Chilean interior waters, from Puerto Montt to Cape Horn. N. Silva & S. Palma (eds.) Comité Oceanográfico Nacional – Pontificia Universidad Católica de Valparaíso, Valparaíso, pp. 37-43.

Sievers, H., Silva, N., 2008. Water masses and circulation in austral Chilean channels and fjords. Progress in the Oceanographic Knowledge of Chilean Interior Waters, from Puerto Montt to Cape Horn, Comité Oceanográfico Nacional – Pontificia Universidad Católica de Valparaíso, Valparaíso, pp. 53-58.

Smith, D. C., Azam, F., 1992. A simple, economical method for measuring bacterial protein synthesis rates in seawater using ^{3}H-leucine. Marine microbial food webs 6 (2), 107-114.

Smith, R. W., Bianchi, T. S., Allison, M., Savage, C., and Galy, V., 2015. High rates of organic carbon burial in fjord sediments globally. Nature Geoscience 8, 450-454. doi: 10.1038/ngeo2421

Soto, D., Norambuena, F., 2004. Evaluation of salmon farming effects on marine systems in the inner seas of southern Chile: A large-scale mensurative experiments. Journal of Applied Ichthyology, 20, 493-501.

Strickland, J.D.H. & T.R. Parsons. 1968. A practical handbook of seawater analysis. Bulletin - Fisheries Research Board of Canada, 167 pp.

Torres, R., Pantoja, S., Harada, N., González, H. E., Daneri, G., Frangopulos, M., et al., 2011. Air-sea CO_2 fluxes along the coast of Chile: from CO_2 outgassing in central northern upwelling waters to CO_2 uptake in southern Patagonian fjords. Journal

Geophysical Research 116:C09006. doi: 10.1029/2010JC006344

Wang X., Olsen L.M., Reitan K.I., Olsen Y., 2012. Discharge of nutrient wastes from salmon farms: environmental effects, and potential for integrated multi-trophic aquaculture. Aquaculture Environment Interactions 2, 267-283. doi: 10.3354/aei00044

Yoshikawa, T., Kanemata, K., Nakase, G., Eguchi, M., 2012. Microbial mineralization of organic matter in sinking particles, bottom sediments and seawater in a coastal fish culturing area. Aquaculture Research 43, 1741-1755

Yoshikawa, T., Eguchi, M., 2013. Planktonic processes contribute significantly to the organic carbon budget of a coastal fish-culturing area. Aquaculture Environment Interactions 4, 239-250. doi: 10.3354/aei00085

Yoshikawa, T., Kanemata, K., Nakase, G., Eguchi, M., 2017. Microbial decomposition process of organic matter in sinking particles, resuspendable particles, and bottom sediments at coastal fish farming area. Fisheries Science 83, 635-647 DOI 10.1007/s12562-017-1098-9

Manuscript in preparation V

Ingestion rates of benthic suspension feeder *Aulacomya atra* under different sources of organic matter (autochthonous and allochthonous)

Ingestion rates of benthic suspension feeder *Aulacomya atra* under different sources of organic matter (autochthonous and allochthonous)

Paulina Montero, Martina Coppari, Federico Betti, Giorgio Bavestrello, Giovanni Daneri

1. INTRODUCTION

In aquatic ecosystems, animals that feed on suspended particles in the water are collectively known as filter feeders (Jørgensen, 1990). A large fraction of benthic suspension feeders specialize their food capture on phytoplankton, while others being area able to capture smaller particles such as bacteria or detrital material and small zooplankton (Sebens et al., 2016). Because these dwelling bottom organisms can process large amounts of suspended organic matter (OM) they are often major agents of benthic-pelagic coupling and nutrient cycling (Norkko et al., 2001).

Bivalves are dominant suspension feeders in benthic communities and exert key effects on coastal plankton by filtering large volumes of water (Prins et al., 1998). By consuming plankton, these animals divert resources from the water column to the sediments depressing pelagic production (Dolmer, 2000). The high consumption of phytoplankton biomass by mussels has been reported to alter pelagic food webs dynamics (Greene et al., 2011) and the "cleaning" potential of this animals has been proposed as a eutrophication control mechanism in coastal areas impacted by aquaculture (Rice, 1999; Rice et al., 2000). The filtration rate of a bivalve is a parameter of great ecological importance in aquatic ecosystems, which is critical to understanding the impact of these species on particles fluxes in coastal environments. Having determined the filtration rate and knowing the concentration of suspended particles in the water, it is possible to calculate the amount of food retained by the gills and ingested by the animal, as long as no pseudofaeces are produced (Winter, 1978).

Bivalves exhibit little or no movement and are dependent upon food sources available in the water column. The vertical flux of OM from phytoplankton (hereby referred as autochthonous OM) to benthic communities varies with fluctuations in surface primary production, which in Chilean fjord environments is driven by a complex

interaction of physical and atmospheric forcing (Montero et al., 2011; Montero et al., 2017a, b). Besides phytoplankton that is considered to be a major source of nutrition for these organisms (Vaughn and Hoellein, 2018), bacteria and detritus from terrestrial origin, have also been described as important sources of nutrition to bivalves during periods of low phytoplankton abundance (Langdon and Newell, 1990; Kreeger and Newell, 1996). Ribbed mussels such as *Aulacomya atra* are structurally adapted to retain small particles (Wright et al., 1982; Stuart and Klumpp, 1984) with a greater efficiency than most other species of bivalves, being therefore the bacterial community an appreciable contribution to the diet of this population (Langdon and Newell, 1990; Kreeger and Newell, 1996). Some authors have also indicated that filter-feeding bivalves have the capacity to assimilate organic material from salmon culture waste such as uneaten food pellets and fecal particles (Reid et al., 2010; MacDonald et al., 2012; Handa et al., 2012b).

In Chilean Patagonia fjords, salmon farming represents the main aquaculture activity (Buschman et al., 2006), mainly due to favourable physical/chemical water conditions for fish (Katz, 2006). This industry releases a large quantity of organic wastes that modify the load of particulate and dissolved material in the water column (Quiñones et al., 2019), and represent an important source of allochthonous OM input to the system (Iriarte et al., 2014). Salmon cage produce OM, together with OM of terrestrial origin and high amounts of autochthonous OM produced in situ by phytoplankton in fjords (Montero et al., 2011; Montero et al., 2017a, b) provide a potentially highly heterogeneous pool of food particles available to benthic consumers.

Puyuhuapi fjord (44°S; 72°W) hosts a large number of salmon farms and the mussel *Aulacomya atra* (Molina, 1782) is part of the benthic filter feeding community that grows within areas adjacent to salmon cages. *A. atra* forms large belts (up to 7 m wide) in the shallow infralittoral zone (5-10 m depth), within a thick layer of low-salinity, nutrient-enriched waters (Betti et al., 2017). This bivalve is distributed along the Pacific Ocean from El Callao, Peru to the Strait of Magellan in Chile, extending along the Atlantic Ocean from Southern Argentina to the South of Brazil being also present along the South African coast (Avendaño and Cantillánez, 2013). This widely distributed southern-hemisphere specie is of considerable social and economic importance for artisanal fishermen communities, both in South America and in South Africa (Carranza et al., 2009; Avendaño and Cantillánez,

2013; Caza et al., 2016). In several Chilean fjords *A. atra* also play a very important role as a key engineer specie helping to increase the benthic ecosystems biodiversity (Betti et al., 2017).

Considering the importance of filter feeding bivalves to pelagic-benthic coupling processes and benthic ecosystem resilience, it is fundamental to begin to understand the degree to which these organisms are processing both autochthonous and allochthonous OM in Chilean fjord ecosystems. Knowing the potential carbon assimilation and feeding dynamic of *A. atra* will contribute to a better understanding what is the contribution that filter feeding organisms make to carbon fluxes and on their potential as "ecosystem cleansing" organisms by reducing the salmon cage derived suspended OM load.

2. MATERIALS AND METHODS

2.1 Study area and *Aulacomya atra* sampling

The study area corresponds to the Puyuhuapi fjord (Fig. 1). This fjord runs in a N-NE direction and connects directly to the open sea via the Moraleda channel at its mouth, and through the Jacaf channel near the head (Schneider et al., 2014). The hydrography of this area is characterized by an estuarine type of circulation with a vertical two layer structure comprised of a highly variable 5-10 m deep freshwater layer overlying a more uniform, saltier sub-pycnocline layer (Schneider et al., 2014 and references therein). The deeper saline water originates from Sub-Antarctic Surface Water (SAAW) characteristic of open ocean environments in these latitudes (Chaigneau and Pizarro, 2005). The freshwater upper layer is mainly supplied by the Cisnes River and by rain runoff (Schneider et al., 2014). Higher surface salinity in the north than in the south, suggests an intrusion of oceanic surface waters into the north of Puyuhuapi via Jacaf Channel, forced by westerly winds (Schneider et al., 2014). The large contributions of particulate and dissolved organic matter, from both autochthonous (plankton community) and allochthonous sources (from freshwater input or salmon farming) present in the water column of Puyuhuapi fjord, lead to a complex pool of food available to benthic consumers.

Aulacomya atra sampling was conducted during summer (February) and winter (July) periods between 2018 and 2019 in the Puyuhuapi fjord (Table 1). During all sampling campaigns, samples of *A*. *atra* for feeding experiments were collected by scuba diving at depths ranging from 5 to 10 m from different sampling station (Fig. 1). After collection, mussels were transferred to the field laboratory located in Puerto Cisnes. After being cleaned of epiphytes and debris, they were maintained in a 200-litters seawater tank, with constant aeration and ambient temperature until the experiments were carried out (approximately 24h after collection). Additionally, samples of *A*. *atra* were collected for stable isotope analyses in the coastal area near each fjord sampling station (Fig. 1) in February 2018, July 2018 and February 2019

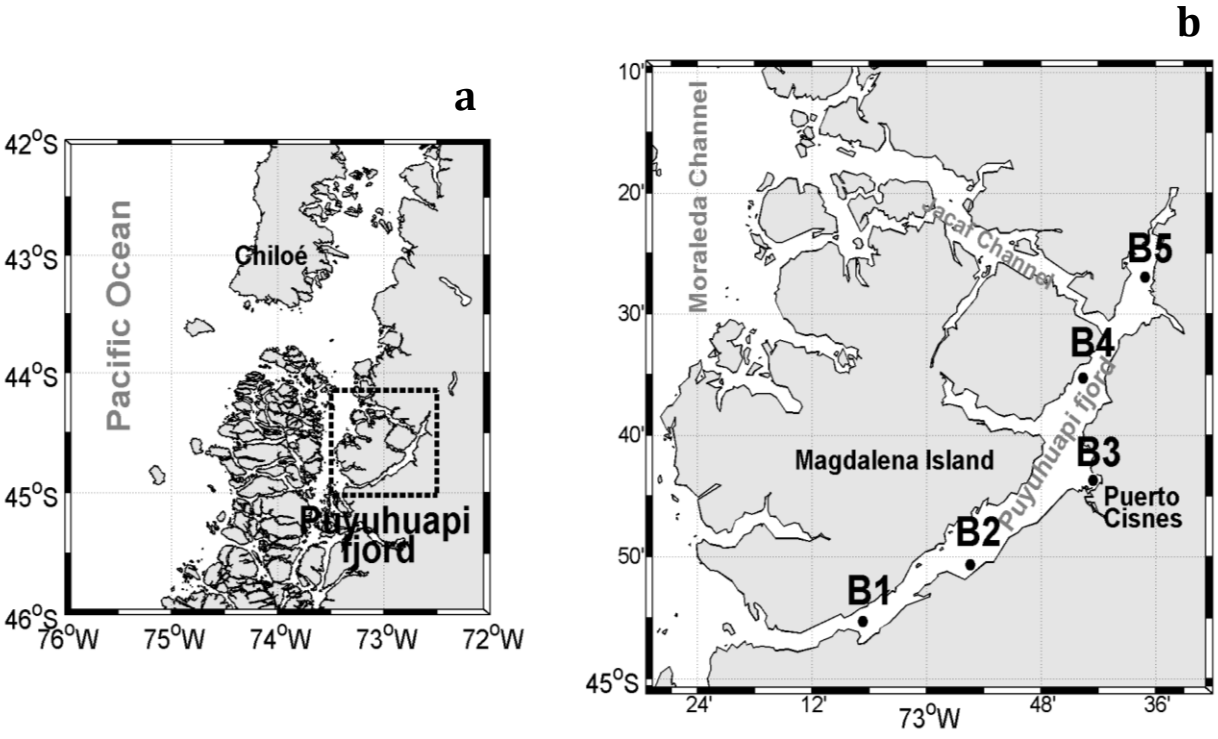

Fig. 1. Location of the study area in Chilean Patagonia (a, dashed box enlarged in b) and position of the sampling stations along the Puyuhuapi fjord.

Table 1. Date feeding experiments in Puyuhuapi fjord, indicating season and geographical position of sampling stations from which *Aulacomya atra* were collected.

Date	Experiment Code	Sampling Station	Latitude (S)	Longitude (W)	Season
21-feb-18	3	B5	44° 26.96'	72° 37.11'	summer
21-feb-18	4	B5	44° 26.96'	72° 37.11'	summer
22-feb-18	1	B5	44° 26.96'	72° 37.11'	summer
22-feb-18	2	B5	44° 26.96'	72° 37.11'	summer
21-feb-18	5	B5	44° 26.96'	72° 37.11'	summer
21-feb-18	6	B5	44° 26.96'	72° 37.11'	summer
25-feb-18	7	B2	44° 50.78'	72° 55.39'	summer
25-feb-18	8	B2	44° 50.78'	72° 55.39'	summer
25-feb-18	9	B2	44° 50.78'	72° 55.39'	summer
26-feb-18	10	B2	44° 50.78'	72° 55.39'	summer
26-feb-18	11	B2	44° 50.78'	72° 55.39'	summer
26-feb-18	12	B2	44° 50.78'	72° 55.39'	summer
16-jul-18	2	B3	44° 43.79'	72° 42.52'	winter
16-jul-18	4	B3	44° 43.79'	72° 42.52'	winter
17-jul-18	1	B3	44° 43.79'	72° 42.52'	winter
17-jul-18	3	B3	44° 43.79'	72° 42.52'	winter
22-feb-19	1	B5	44° 26.96'	72° 37.11'	summer
22-feb-19	2	B5	44° 26.96'	72° 37.11'	summer
23-feb-19	3	B3	44° 43.79'	72° 42.52'	summer
23-feb-19	4	B3	44° 43.79'	72° 42.52'	summer
23-feb-19	5	B3	44° 43.79'	72° 42.52'	summer
23-feb-19	6	B3	44° 43.79'	72° 42.52'	summer
25-feb-19	7	B2	44° 50.78'	72° 55.39'	summer
25-feb-19	8	B2	44° 50.78'	72° 55.39'	summer
25-feb-19	9	B2	44° 50.78'	72° 55.39'	summer
26-feb-19	10	B2	44° 50.78'	72° 55.39'	summer
08-jul-19	1	B3	44° 43.79'	72° 42.52'	winter
08-jul-19	2	B3	44° 43.79'	72° 42.52'	winter
09-jul-19	3	B3	44° 43.79'	72° 42.52'	winter
09-jul-19	4	B3	44° 43.79'	72° 42.52'	winter
09-jul-19	5	B3	44° 43.79'	72° 42.52'	winter
10-jul-19	6	B3	44° 43.79'	72° 42.52'	winter

2.2 Feeding experiments

The experiments were performed using plastic containers of 6 litters capacity, each supplied with an air pump (3L/min). An experimental container and a control container were used for each treatment. Three treatments with their controls were set up. The first two treatments consisted of two ambient seawater samples, while the third treatment contained seawater amended with OM derived from salmon food pellets.

The first treatment, hereby referred as Bacterial community treatment (BC_T), was prepared by filtering seawater by gravity onto 22-µm mesh to remove large zooplankton and microphytoplankton. Then, a peristaltic pump was used to gently filter this water through 0.8-µm sterile membrane filters (Millipore), in order to separate bacterioplankton from the rest of the planktonic community (including its potential predators). Experimental and control containers were filled with this water. The second treatment hereby referred as Planktonic community treatment (PC_T) was prepared by filtering seawater by gravity onto 150-µm mesh to remove large plankton species. Then, experiment and control containers were filled with this water. The third treatment consisted of 0.2-µm filtered seawater amended with salmon food pellet (PSF_T). This treatment was prepared by filtering seawater by gravity onto 22-µm mesh to remove large zooplankton and phytoplankton. Then, a peristaltic pump was used to gently filter this water through 0.2-µm sterile membrane filters (Millipore), in order to avoid the presence of any microorganism. Finally, one gram of pellet salmon food was grinded into fine particles using a mortar and added to the filtered water and experiment and control containers were filled with this water.

At the beginning of each experiment, one specimen of *Aulacomya* was placed in each experimental container, while the control container remained without individuals. The experiments begin as soon as *Aulacomya atra* valves opened. Triplicate water samples of 500 mL were taken from experimental and control containers at initial time (*t*1), and one hour later (*t*2). Samples from *t*1 and *t*2 were processed for particulate organic carbon (POC) analyses. Total POC was measured by filtering 500 mL water samples on pre-combusted GF/F glass fiber filters (4 h at 450°C). Filters were frozen at –20°C until analysis. Prior to analysis, the sample filters were thawed and acidified with HCL. After acidification, the

HCL was removed and the filters were dried at 50°C for 24 h. Filters were analysed at the Laboratory of Biogeochemestry and Applied Stable Isotopes (LABASI, PUC), Chile.

Grazing was calculated using the variation in the concentration of POC obtained in control and experimental containers. The rate of change in POC concentration (k) was calculated according to the Frost (1972) equation:

$$C_2 = C_1 e^{k(t2-t1)}$$

where C_1 and C_2 are POC concentrations (mg C mL^{-1}) in control container at initial ($t1$) and final time ($t2$), respectively. For each experimental container, the grazing coefficient (g) was calculated from Frost (1972) equation:

$$C_2' = C_1' e^{(k-g)(t2-t1)}$$

where C_1' and C_2' are POC concentrations (mg C mL^{-1}) in experimental container at initial ($t1$) and final time ($t2$), respectively, and k is the rate of change in particle concentration in control container.

The clearance rate, CR (volume swept clear per individual per time) was calculated as follows:

$$CR = V\left(\frac{g}{n}\right)$$

where V is the volume of the container (L), n is the number of *A. atra* in the experimental container and g is the grazing coefficient (h^{-1}). Clearance rate were standardized to a 1g (dry flesh weight) (Cranford et al., 2011). Finally, the ingestion rate, I (particles ingested per individual per time) was calculated as the product of CR (L $individual^{-1}$ h^{-1}) and the concentration of POC (mg L^{-1}) using the following formula:

$$I = CR \times C$$

where C is the particle concentration (POC) in the experimental container, calculated as:

$$C = \frac{C_2' - C_1'}{(t2 - t1)(k - g)}$$

The significance of grazing on each food type (treatments) was tested by comparing the rate of change in particle concentration of POC in control and experimental containers with a 2-tailed Wilcoxon test.

After each experiment, shell lengths and wet and dry (24 h at 60°C) flesh weights were determined for each individual used. To determine ash-free dry weight (AFDW), dry tissue of each individual was combusted at 500°C for 5 h.

A total of 32 experiments were conducted in the study area (Table 1); 11 of them did not show grazing (Table 2, negative values), and therefore the data was not included in the results. Finally, the results correspond to 21 experiments: 7 conducted under PC_T (autochthonous source), 9 under BC_T (autochthonous source) and 5 under PSF_T (allochthonous source).

2.3 Stable Isotopes

Samples of *A. atra* were processed for stable isotope analyses during February 2018, July 2018 and February 2019. The organisms were collected by scuba diving at depths ranging from 5 to 10 m in the coastal area near each fjord sampling station (Fig. 1). After collection mussels were transferred to the field laboratory located in Puerto Cisnes. The organisms were maintained in a filtered seawater (0.2 µm) plastic container during 24h and then they were rinsed with distilled water and frozen at –20°C. Frozen samples were thawed and dissected. *Aulacomya* tissues were frozen, lyophilized, and grinded prior to analysis. In addition, in order to estimate the stable isotope signal in suspended particulate organic matter (SPOM), samples were collected from three depths (2, 10 and 20 m) for almost an annual cycle (March 2018 to February 2019). Water samples (5 L) were filtered under gentle vacuum through GF/F filters (pre combusted for 4 h at 450°C) and refrigerated until analysis. Additionally, the isotopic signal from pellet salmon food used in the feeding

experiments also was measured. Tissues and filters were analysed at the Laboratory of Biogeochemestry and Applied Stable Isotopes (LABASI, PUC, Chile) with an Isotope Ratio Mass Spectrometer (Thermo Fisher Scientific, Delta V Advantage IRMS) coupled with and Elemental Analyzer (Flash, EA 2000). Data are expressed in the standard ∂ unit notation:

$$\partial^{13}C \text{ or } \partial^{15}N = \left(\left(\frac{R\ sample}{R\ standard}\right) - 1\right) \times 1000\ ‰$$

where R represents the $^{13}C/^{12}C$ or $^{15}N/^{14}N$ ratio for $\partial\ ^{13}C$ and $\partial\ ^{15}N$, respectively.

The potential *in situ* food source of *A*. *atra* was related which those sources that are depleted by 1‰ in $\partial\ ^{13}C$ and by 3-4‰ in $\partial\ ^{15}N$ compared to the tissues of *Aulacomya* (Minagawa and Wada, 1984; Rau et al., 1990; Post, 2002).

3. RESULTS

3.1 Feeding on different sources of organic matter

Differences in POC concentration between control and experimental containers were used to measure grazing by the *Aulacomya atra* (Table 2). The rate of change of POC from different sources of organic matter (treatments) (Fig. 2) showed significant differences between control and experimental containers under all treatments (Wilcoxon test, $p < 0.05$), indicating that *A*. *atra* is able to capture both plankton derived from autochthonous OM (BC_T, PC_T) and salmon food pellets derived from allochthonous OM (PSF_T).

No significant differences were observed in CR (Kruskal-Wallis test, $p > 0.05$) for the different food sources that were captured by *A*. *atra* (Fig. 3a). The relationship between dry flesh weight and clearance rate in *A*. *atra*; observed mainly during the 2019 summer campaign, indicated that as the weight of organisms increases, higher clearance rates are observed (Fig. 3b). Because specimens of similar size (109 ± 8 mm) were used in the experiments, the effect of body size on clearance rate was not examined. The weight-standardized clearance rate (CRs) showed the same patron than CR, although the values

observed were lower (Fig. 4, Table 2). Seasonally, CR and CRs were significantly higher in summer than in winter (Kolmogorov-Smirnov test, $p < 0.05$).

The highest ingestion rate values ranged from 0.25 to 20.9 mg C individual^{-1} h^{-1} and were observed in the PSF_T treatment (Fig. 5, Table 2). In contrast, ingestion rates recorded under autochthonous feeding conditions were significantly lower (Kruskal-Wallis test, $p < 0.05$), showing values between 0.01 and 0.31 mg C individual^{-1} h^{-1} in PC_T and between 0.03 and 1.31 mg C individual^{-1} h^{-1} in BC_T (Fig. 5, Table 2). Ingestion rates (mg C individual^{-1} h^{-1}) and food concentration were positively correlated (Fig. 5, $r^2 = 0.81$, $p < 0.05$) and saturation was not observed.

Table 2. Variables measured during feeding experiments. **Kc**: rate of change in particle concentration in control container, **Kg**: rate of change in particle concentration in experimental container, **g**: grazing coefficient, **C rate**: Clearance rate standardized by individual, **C rate(s)**: Clearance rate standardized by weight, **I rate**: Ingestion rate standardized by individual and **D.Weight**: dry weight.

Experiment						L ind^{-1} h^{-1}	mg C ind^{-1} h^{-1}	gr	mm	L g^{-1} h^{-1}
Code	Date	Kc	Kg	g	Treatment	C rate	I rate	D.Weight	Length	C rate (s)
1	22-feb-18	-0.44	-0.06	**-0.38**	PC_T			6	132	
7	25-feb-18	0.06	0.16	**-0.11**	PC_T			7	120	
1	22-feb-19	0.49	1.17	**-0.68**	PC_T			7	115	
2	22-feb-19	0.003	0.82	**-0.82**	PC_T			5	100	
4	16-jul-18	-0.12	0.05	**-0.17**	PC_T			6	112	
2	22-feb-18	0.34	0.33	0.01	PC_T	0.08	0.04	8	126	0.01
8	25-feb-18	0.06	-0.06	0.11	PC_T	0.68	0.17	2	106	0.30
2	16-jul-18	-0.34	-0.39	0.06	PC_T	0.34	0.12	6	111	0.05
9	25-feb-19	0.10	-0.12	0.22	PC_T	1.30	0.31	8	106	0.14
4	09-jul-19	-0.03	-0.21	0.18	PC_T	1.06	0.19	6	98	0.16
5	09-jul-19	-0.03	-0.04	0.01	PC_T	0.08	0.01	4	97	0.02
6	10-jul-19	-0.05	-0.10	0.05	PC_T	0.30	0.04	6	101	0.05
3	21-feb-18	0.18	0.25	**-0.07**	BC_T			13	128	
9	25-feb-18	0.10	0.19	**-0.10**	BC_T			6	119	
10	26-feb-18	0.07	0.16	**-0.08**	BC_T			11	115	
4	21-feb-18	0.23	0.20	0.03	BC_T	0.16	0.03	7	137	0.02
1	17-jul-18	0.17	0.00	0.17	BC_T	1.03	0.28	7	109	0.12
5	23-feb-19	1.06	0.07	1.00	BC_T	5.98	1.31	12	118	0.42
6	23-feb-19	1.33	1.15	0.19	BC_T	1.11	0.10	3	112	0.34
7	25-feb-19	0.67	0.27	0.40	BC_T	2.39	0.41	4	95	0.59
8	25-feb-19	0.60	0.29	0.31	BC_T	1.88	0.33	4	110	0.40
1	08-jul-19	0.02	-0.10	0.13	BC_T	0.76	0.10	5	92	0.12
2	08-jul-19	-0.14	-0.17	0.04	BC_T	0.24	0.03	6	110	0.03
3	09-jul-19	0.02	-0.11	0.12	BC_T	0.73	0.10	4	111	0.19
6	21-feb-18	-0.54	0.40	**-0.94**	PSF_T			6	125	
12	26-feb-18	-0.68	0.29	**-0.97**	PSF_T			5	103	
4	23-feb-19	-0.83	-0.47	**-0.37**	PSF_T			7	101	
5	21-feb-18	0.29	0.27	0.02	PSF_T	0.13	0.25	6	111	0.02
11	26-feb-18	0.18	-0.06	0.23	PSF_T	1.40	2.19	4	109	0.36
3	17-jul-18	1.69	0.85	0.85	PSF_T	5.07	11.38	7	124	0.65
3	23-feb-19	1.23	0.59	0.64	PSF_T	3.82	20.89	7	106	0.48
10	26-feb-19	0.32	-0.01	0.33	PSF_T	1.98	10.41	5	105	0.36

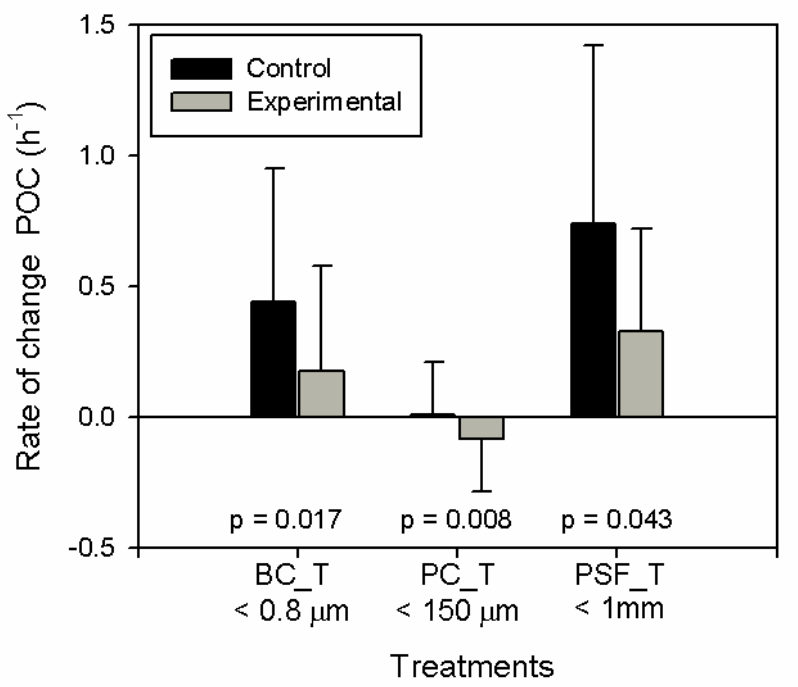

Figure 2. Rate of change in POC concentrations (average ± SD) from feeding experiments in control and experimental containers under three different treatments: bacterial community treatment (BC_T), planktonic community treatment (PC_T) and salmon food pellet treatment (PSF_T). The mean value in both control and experimental containers correspond to all experiments carried out under the same treatment with a positive grazing coefficient (Table 2).

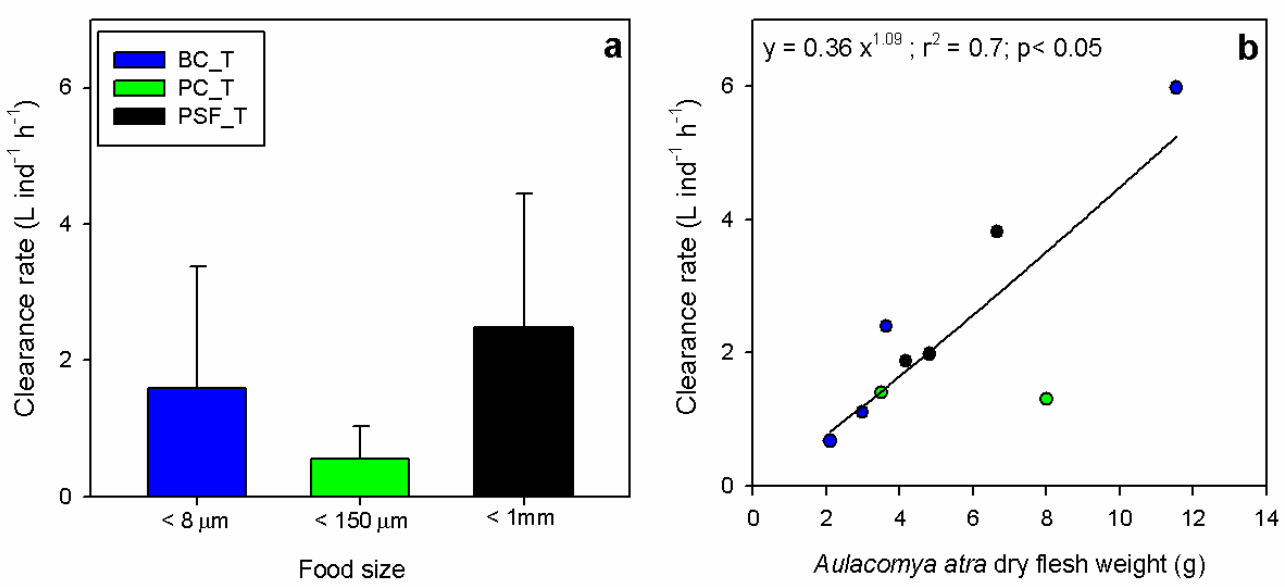

Figure 3. (a) *Aulacomya atra* clearance rate (average ± SD) from feeding experiments under three different treatments: bacterial community treatment (BC_T), planktonic community treatment (PC_T) and salmon food pellet treatment (PSF_T). (b) Clearance rate as a function of dry flesh weight in *A. atra*, during summer campaign in 2019.

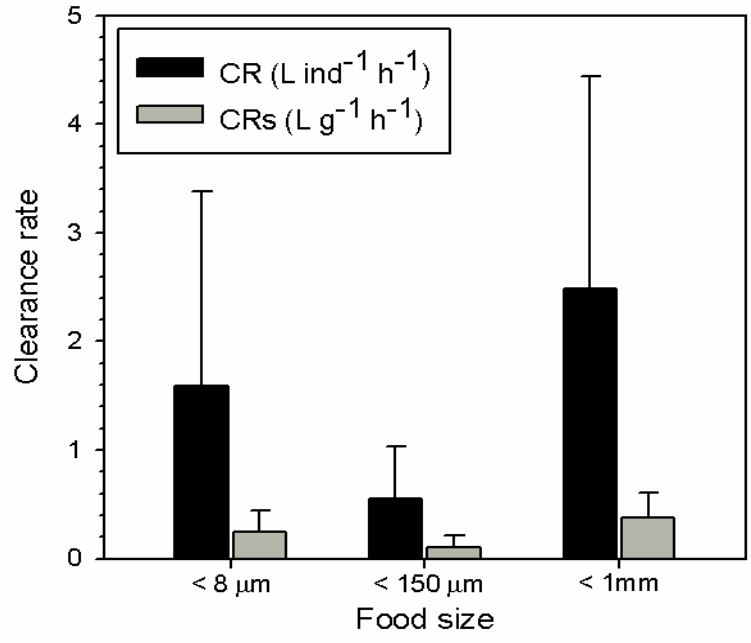

Figure 4. Comparison between *Aulacomya atra* clearance rates (average ± SD) from feeding experiments under three different treatments: bacterial community treatment (BC_T), planktonic community treatment (PC_T) and salmon food pellet treatment (PSF_T).

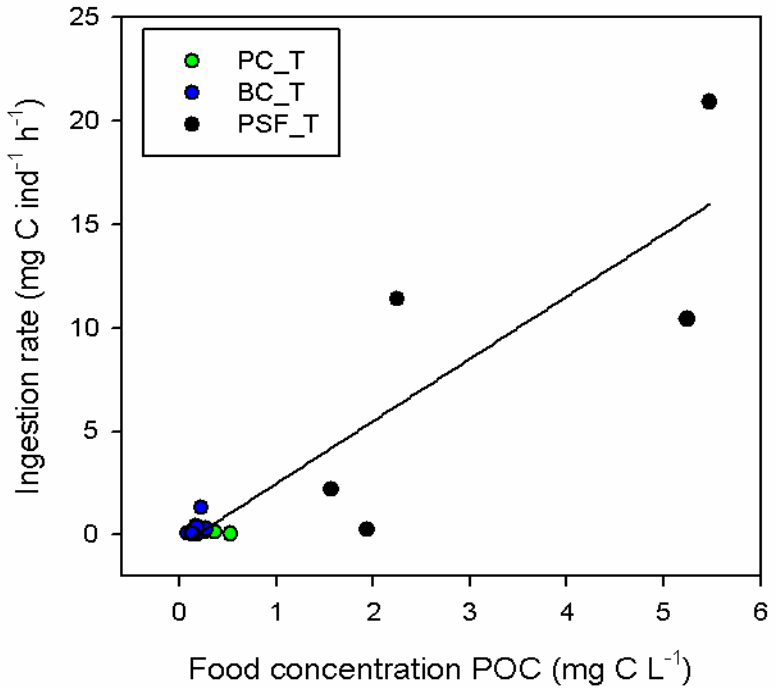

Figure 5. Relation between food concentrations of POC offered in each type of treatment – bacterial community treatment (BC_T), planktonic community treatment (PC_T), salmon food pellet treatment (PSF_T) – and ingestion rate of *Aulacomya atra* during feeding experiments.

3.2 Stable isotopes

∂^{13}C and ∂^{15}N values (mean ± SD) for SPOM and *Aulacomya atra* tissues are summarized in Table 3. The ∂^{13}C values of *Aulacomya atra* were significantly different (Kruskal-Wallis test, $p< 0.05$) between February 2018 (-18.4 ± 0.8‰), July 2018 (-18.6 ± 0.7‰) and February 2019 (-20.9 ± 0.9‰) (Table 3). ∂^{15}N values, however, were similar across study period (February 2018: 8.9 ± 0.8‰; July 2018: 8.7 ± 0.2‰; February 2019: 9.6 ± 0.7‰) and showed no significant differences (Kruskal-Wallis test, $p> 0.05$) (Table 3). The ∂^{13}C values of SPOM measured from March 2018 to July 2018 (-24.4 ± 1.7‰) and from August 2018 to February 2019 (-25.2 ± 0.4‰) were significantly most depleted (Kruskal-Wallis test, $p> 0.05$) than those measured in *A. atra* tissues in July 2018 (-18.6 ± 0.7‰) and February 2019 (-20.9 ± 0.9‰) (Table 3). Likewise, the ∂^{15}N values of SPOM

measured from March 2018 to July 2018 (6.9 ± 0.6‰) and from August 2018 to February 2019 (5.5 ± 0.6‰) were significantly lower (Kruskal-Wallis test, $p > 0.05$) than those measured in *A*. *atra* tissues in July 2018 (8.7 ± 0.2‰) and February 2019 (9.6 ± 0.7‰) (Table 3).

In general, a well-defined spatial gradient in the carbon and nitrogen signal from tissues of *A*. *atra* was not observed into the fjord from B1 to B5 stations (Fig. 1). However, significant differences between sampling stations were observed in July 2018 for the carbon signal and in February 2018/2019 for the nitrogen signal (Kruskal-Wallis test, $p < 0.05$) (Fig. 6). During July 2018, $\partial^{13}C$ values of *A*. *atra* were more enriched at stations B1 (-18.1 ± 0.2‰) and B5 (-17.8 ± 0.4‰) than in the rest of sampling stations, while in February 2018 and February 2019, stations B2 (9.6 ± 0.6‰) and B1 (10.5 ± 0.2‰) recorded the highest $\partial^{15}N$ values of *A*. *atra*, respectively (Table 3).

The carbon signal from *Aulacomya atra* tissues throughout study period indicated that this specie preferentially exploits food resources with a marked signal of marine organic matter (from -17.7 to -21.7‰) (Fig. 6a). Marine signal correspond to those of phytoplankton derived from particulate organic matter (POM) present in the water column ($\partial^{13}C$ between -18 and -22‰; Goericke and Fry, 1994). However, when we add to the graph the average isotopic composition of the pellet salmon food used in our feeding experiments ($\partial^{13}C$ -21.9 ± 2.4‰, $\partial^{15}N$ 8.0 ± 2.3‰) as well as those reported $\partial^{13}C$ and $\partial^{15}N$ values for pellet salmon food from other studies ($\partial^{13}C$ -22.7 ± 1.1‰, $\partial^{15}N$ 8.3 ± 2.1‰ from Sarà et al., 2004 and $\partial^{13}C$ -22.9 ± 0.2‰, $\partial^{15}N$ 4.9 ± 0.1‰ from Sanz-Lazaro and Sanchez-Jerez) (Fig. 6b), is not so clear to estimate the contribution of this allochthonous material in the food preference of *Aulacomya*, mainly due the values from pellet overlaps the range of the marine signal end-member. Only the ^{15}N enrichment in *A*. *atra* tissues of 3-4‰ between this specie and food source could indicate phytoplankton consumption (Rau et al., 1990) (Fig. 6a).

In the study area, marine carbon signal and possibly those from pellet salmon food were mainly recorded in the SPOM samples measured at 2 m depth between March and July 2018 in stations B4 and B3 (Fig. 6). In the rest of study period (August-February 2019) and in general between 10 and 20 meters deep, $\partial^{13}C$ values were more influenced by terrestrial organic matter ($\partial^{13}C$ between -30 and -25‰ ; Lafon et al., 2014) (Fig. 6).

Table 3. $\partial^{13}C$ and $\partial^{15}N$ values (mean ± SD) measured in *Aulacomya atra* tissues and in samples of suspended particulate organic matter (SPOM) in Puyuhuapi Fjord during the study period.

Date	Sampling Station	Taxon	$\delta^{13}C$	SD	n	$\delta^{15}N$	SD	n
February 2018	B1	*A. atra*	-17.93	0.92	3	9.00	0.25	3
February 2018	B2	*A. atra*	-17.70	0.99	3	9.61	0.63	3
February 2018	B4	*A. atra*	-19.57	0.66	3	7.86	0.29	3
February 2018	B5	*A. atra*	-18.48	0.73	3	9.18	0.32	3
March-July 2018	B4	SPOM 2m	-22.78	4.01	4	6.35	1.81	4
March-July 2018	B4	SPOM 10m	-23.53	1.12	4	6.44	1.43	4
March-July 2018	B4	SPOM 20m	-26.20	2.77	4	7.92	2.43	4
March-July 2018	B3	SPOM 2m	-23.18	4.88	4	6.95	2.29	4
March-July 2018	B3	SPOM 20m	-26.11	2.14	4	7.09	1.08	4
July 2018	B1	*A. atra*	-18.06	0.16	3	8.94	0.34	3
July 2018	B2	*A. atra*	-19.44	0.63	3	8.47	0.49	3
July 2018	B3	*A. atra*	-18.53	0.18	3	8.93	0.51	3
July 2018	B4	*A. atra*	-18.99	0.28	3	8.64	0.43	3
July 2018	B5	*A. atra*	-17.81	0.40	3	8.72	0.56	3
August 2018-February 2019	B4	SPOM 2m	-24.68	1.01	7	5.44	1.56	7
August 2018-February 2019	B4	SPOM 10m	-25.34	2.22	7	4.98	2.15	7
August 2018-February 2019	B4	SPOM 20m	-25.51	2.41	7	6.18	3.42	7
February 2019	B1	*A. atra*	-19.50	0.28	3	10.46	0.22	3
February 2019	B2	*A. atra*	-21.14	0.86	3	9.82	0.60	3
February 2019	B3	*A. atra*	-21.69	0.11	3	9.25	0.24	3
February 2019	B4	*A. atra*	-21.29	0.54	3	8.60	0.34	3
February 2019	B5	*A. atra*	-21.31	0.13	3	9.63	0.14	3

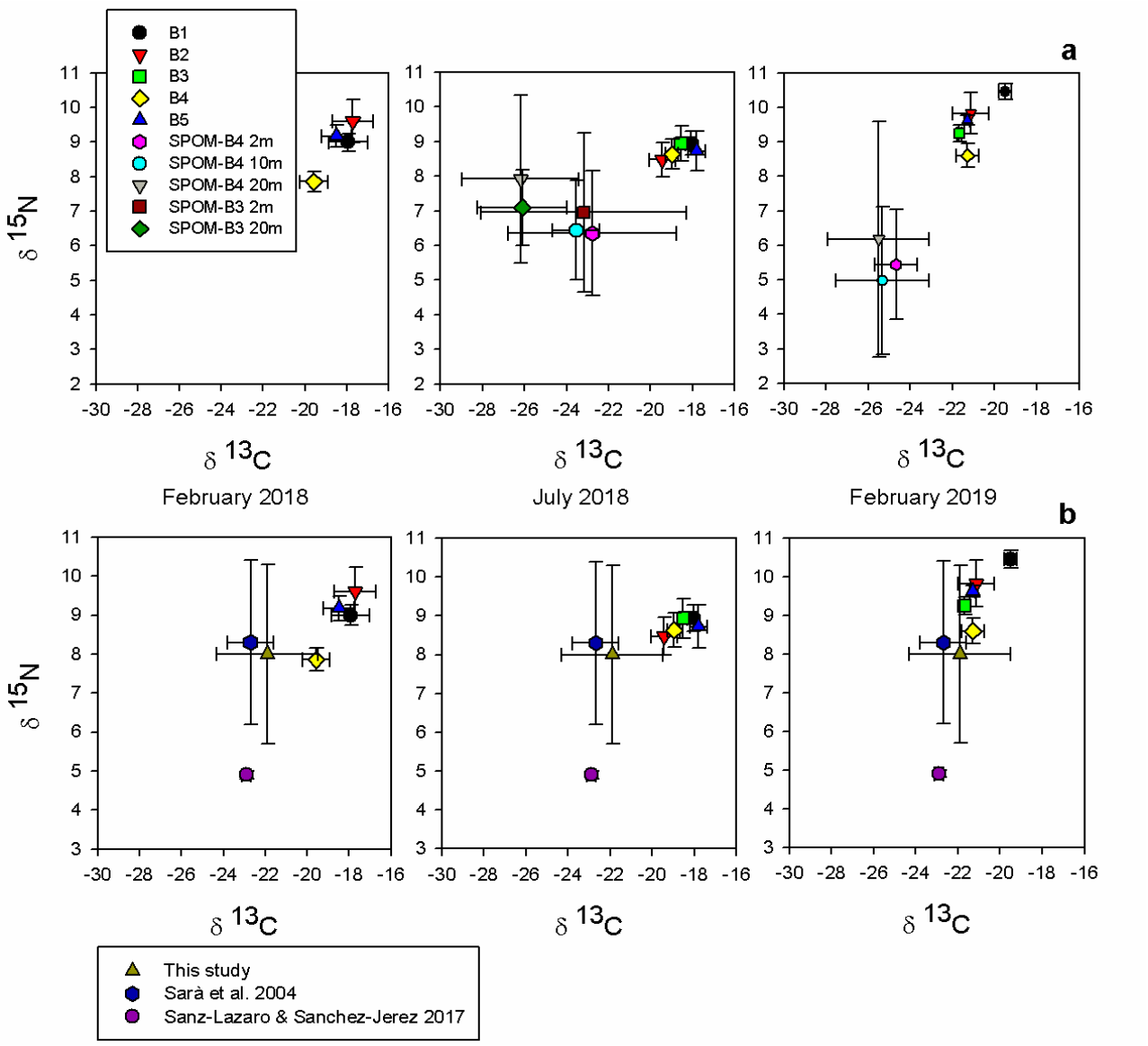

Figure 6. (a) $\partial^{13}C$ and $\partial^{15}N$ biplot showing stable isotopic composition in *Aulacomya atra* tissues and in samples of suspended particulate organic matter (SPOM). Samples of *Aulacomya atra* were obtained from different sampling stations across the Puyuhuapi fjord (from B1 to B5). Samples of SPOM were obtained from different sampling depths in stations B4 and B3. (b) $\partial^{13}C$ and $\partial^{15}N$ biplot showing stable isotopic composition in *Aulacomya atra* tissues and in pellet salmon food from this study and others.

4. PRELIMINARY CONCLUSIONS

Aulacomya atra is able to capture both autochthonous OM (bacteria and planktonic community) and allochthonous OM (salmon food pellets).

The highest ingestion rates (clearance rate x food concentration) were observed under allochthonous treatment. In contrast, ingestion rates recorded under autochthonous feeding conditions (bacteria and plankton community) were significantly lower. This could be associated to higher concentration of food particles in the salmon pellet food treatment, since the clearance rates were not significantly different between treatments.

The mean clearance rate of the bacteria treatment was higher than the planktonic community treatment (although the difference was not statistically significant). This seems to confirm the ability of *Aulacomya atra* to efficiently retain small size particles (< 0.8 um). Thus allowing them to incorporate bacteria as part of their diet.

The isotopic carbon signal in *Aulacomya atra* tissues throughout study period indicated that this specie preferentially exploits food resources with a marked marine OM signal (phytoplankton autochthonous OM). However the possible assimilation of allochthonous OM from salmon farming by this specie cannot be ruled out because the range of the isotopic signal of salmon food pellets overlaps the range of the marine signal found in the tissues of *Aulacomya atra*.

5. REFERRENCES

Avendaño, M., Cantillánez, M., 2014. Reproductive cycle of Aulacomya ater [Bivalvia: Mytilidae (Molina 1782)] in Punta Arenas Cove (Antofagasta Region, Chile). Aquaculture International. DOI 10.1007/s10499-013-9743-5

Betti, F., Bavestrello, G., Bo, M., Enrichetti, F., Loi, A., Wabderlingh, A., Pérez-Santos, I., Daneri, G., 2017. Benthic biodiversity and ecological gradients in the Seno Magdalena (Puyuhuapi Fjord, Chile). Estuarine, Coastal and Shelf 198, 269-278. dx.doi.org/10.1016/j.ecss.2017.09.018

Buschman, A. H., Riquelme, V., Hernández-González, M. C., Varela, D., Jiménez, J. E., Henríquez, L. A., Vergara, P. A., Guíñez, R., Filún, L., 2006. A review of the impacts of salmonid farming on marine coastal ecosystems in the southeast Pacific. ICES Journal of marine Science 63, 1338-1345. doi:10.1016/j.icesjms.2006.04.021

Carranza, A., Defeo, O., Beck, M., Castilla, J., 2009. Linking fisheries management and conservation in bioengineering species: the case of South American mussels (Mytilidae). Review in Fish Biology and Fisheries 19 (3), 349-366

Caza, F., Cledon, M., St-Pierre, Y., 2016. Biomonitoring climate change and pollution in marine ecosystems. A review on *Aulacomya ater*. Journal of Marine Biology. dx.doi.org/10.1155/2016/7183813

Chaigneau, A., Pizarro, O., 2005. Mean surface circulation and mesoscale turbulent flow characteristics in the eastern South Pacific from satellite tracked drifters. Journal Geophysical Research 110, C05014. doi:10.1029/2004JC002628 2005.

Cranford, P. J., Ward, J. E., Shumway, S. E., 2011. Bivalve filter feeding: variability and limits of the aquaculture biofilter. Chapter 4 Shellfish Aquaculture and the environment, First edition. Edited by Sandra E. Shumway 81-124

Dolmer P. 2000. Feeding activity of mussels *Mytilus edulis* related to near-bed currents and phytoplankton biomass. Journal of Sea Research 44:221–231 DOI 10.1016/S1385-1101(00)00052-6

Frost, B. W., 1972. Effects of size and concentration of food particles on the feeding behaviour of the marine planktonic copepod *Calanus pacificus*. Limnology and Oceanography 17 (6), 805-815

Goericke, R., Fry, B., 1994. Variations of marine plankton $\delta^{13}C$ with latitude, temperature, and dissolved CO_2 in the world ocean. Global Biogeochemical Cycles 8 (1), 85-90

Greene, V. E., Sullivan, L. J., Thompson, J. K., Kimmerer, W. J., 2011. Grazing impact of the invasive clam Corbula amurensis on the microplankton assemblage of the northern San Francisco Estuary. Marine Ecology Progress Series 431, 183-193. doi: 10.3354/meps09099

Handa, A., Ranheim, A., Olsen, A.J., Altin, D., Reitan, K. I., Olsen, Y., Reinertsen, H., 2012. Incorporation of salmon fish feed and feces components in mussel (*Mytilus edulis*): Implications for integrated multi-trophic aquaculture in cool-temperate North Atlantic waters. Aquaculture 370/371, 40-53. dx.doi.org/10.1016/j.aquaculture.2012.09.030

Iriarte, J.L., Pantoja, S., Daneri, G., 2014. Oceanographic processes in Chilean fjords of Patagonia: from small to large-scale studies. Progress in Oceanography 129, 1-7

Jørgensen, C.B., 1990. Bivalve filter feeding: hydrodynamics, bioenergetics, physiology and ecology. Olsen & Olsen. Fredensborg, Denemar.

Katz, J., 2006. Salmon farming in Chile. In: Chandra, V. (Ed.), Technology, Adaptation, and Exports: How Some Developing Countries Got it Right. World Bank Publications, Washington DC, pp. 193e344.

Kreeger, D. A., Newell, R. I. E., 1996. Ingestion and assimilation of carbon from cellulotyc bacteria and heterotrophic flagellates by the mussels *Geukensia demisa* and *Mytilus edulis* (Bivalvia, Mollusca). Aquatic Microbial Ecology 11, 205-214

Lafon, A., Silva, N., Vargas, C. A., 2014. Contribution of allochthonous organic carbon across the Serrano River basin and the adjacent fjord system in Southern Chilean Patagonia: Insights from the combined use of stable isotope and fatty acid biomarkers. Progress in Oceanography 129 part A, 98-113. dx.doi.org/10.1016/j.pocean.2014.03.004

Langdon, C. J., Newell, R. I., 1990. Utilization of detritus and bacteria as food sources by two bivalve suspension-feeders, the oyster *Crassotrea virginica* and the mussel *Geukensia demisa*. Marine Ecology Progress Series 58, 299-310

MacDonald, B. A., Robinson, S. M. C., Barrington, K. A., 2011. Feeding activity of mussels (Mytilus edulis) held in the field at an integrated multi-trophic aquaculture (IMTA) site (Salmo salar) and exposed to fish food in the laboratory. Aquaculture 314, 244-251. doi:10.1016/j.aquaculture.2011.01.045

Minagawa, M., Wada, E., 1984. Stepwise enrichment of 15N along food chains: further evidence and the relation between ∂^{15}N and animal age. Geochemica et Cosmochimica Acta 48, 1135-1140

Montero, P., Daneri, G., González, H.E., Iriarte, J.L., F.J., Tapia, F.J. Lizárraga, L., Sanchez, N., Pizarro, O., 2011. Seasonal variability of primary production in a fjord ecosystem of the Chilean Patagonia: implications for the transfer of carbon within pelagic food webs. Continental Shelf Research 31, 202-215. doi:10.1016/j.csr.2010.09.003

Montero, P., Daneri, G., Tapia, F., Iriarte, J. L., Crawford, D., 2017a. Diatom blooms and primary production in a channel ecosystem of central Patagonia. Latin America Journal of Aquatic Research. 45, 999-1016. doi: 10.3856/vol45-issue5-fulltext-16

Montero, P., Pérez-Santos, I., Daneri, G., Gutiérrez, M.H., Igor, G., Seguel, R., Purdie, D., Crawford, D.W., 2017b. A winter dinoflagellate bloom drives high rates of primary production in a Patagonian fjord ecosystem. Estuarine, Coastal and Shelf Science 199,105-116. doi: 10.1016/j.ecss.2017.09.027

Norkko, A., Hewitt, J. E., Thrush, S. F., 2001. Benthic-pelagic coupling and suspension-feeding bivalves: linking site-specific sediment flux and biodeposition to benthic community structure. Limnology and Oceanography 56 (8), 2067-20172

Post, D. M., 2002. Using stable isotopes to estimate trophic position: models, method, and assumptions. Ecology 83 (2), 703-718

Prins, T. C., Smaal, A. D., Dame, R. F., 1998. A review of the feedbacks between bivalve grazing and ecosystem processes. Aquatic Ecology 31, 349-358

Quiñones, R. A., Fuentes, M., Montes, R. M., Soto, D., León-Muñoz, J., 2019. Environmental issues in Chilean salmon farming: a review. Reviews in Aquaculture 11, 375-402. doi: 10.1111/raq.12337

Rau, G. H., Teyssie, J. L., Rassoulzadegan, F., Fowler, S. W., 1990. $^{13}C/^{12}C$ and $^{15}N/^{14}N$ variations among size-fractionated marine particles: Implications for their origin and trophic relationships. Marine Ecology Progress Series 59, 33-38.

Reid, G. K., Liutkus, M., Bennett, A., Robinson, S.M.C., MacDonald, B., Page, F., 2010. Absorption efficiency of blue mussels (*Mytilus edulis* and *M. trossulus*) feeding on Atlantic salmon (*Salmo salar*) feed and fecal particulates: Implications for integrated multi-trophic aquaculture. Aquaculture 299, 165-169

Rice, M. A., 1999. Control of eutrophication by bivalves: Filtration of particulates and removal of nitrogen through harvest of rapidly growing stocks. Journal of Shellfish Reserach 18 (1), 275.

Rice, M.A., Valliere, A., Gibson, M., Ganz, A., 2000. Ecological significance of the Providence River quahogs: Population filtration. Journal of Shellfish Reserach 19 (1), 580.

Sanz-Lazaro, C., Sanchez-Jerez, P., 2017. Mussels do not directly assimilate fish farm wastes: shifting the rationales of integrated multi´trophic aquaculture to a broader scale. Journal of Environmental Management 201, 82-88. dx.doi.org/10.1016/j.jenvman.2017.06.029

Sarà, G., Scilipoti, D., Mazzola, A., Modica, A., 2004. Effects of fish farming waste to sedimentary and particulate organic matter in a southern Mediterranean area (Gulf of Castellammare, Sicily): a multiple stable isotope study ($d^{13}C$ and $d^{15}N$). Aquaculture 234, 199e213.

Schneider, W., Pérez-Santos, I., Ross, L., Bravo, L., Seguel, R., Hernández, F., 2014. On the hydrography of Puyuhuapi Channel (Chilean Patagonia). Progress in Oceanography 129, 8-18. doi10.1016/j.pocean.2014.03.007

Sebens, K., Sarà, G., Nishizaki, M., 2016. Energetics, particle capture, and growth dynamics of benthic suspension feeders. S. Rossi (ed.), Marine Animal Forest. DOI 10.1007/978-3-319-17001-5_17-1

Stuart, V., Klumpp, D. W., 1984. Evidence for food-resource partitioning by kelp-bed filter feeders. Marine Ecology Progress Series 16, 27-37.

Vaughn, C.C., Hoellin, T. J., 2018. Bivalve impacts in freshwater and marine ecosystems. Annual Review of Ecology, Evolution and Systematics 49, 183-208.

DOI.org/10.1146/annurev-ecolsys-110617-062703

Winter, J. E., 1978. A review on the knowledge of suspension-feeding in lamellibranchiate bivalves, with special reference to artificial aquaculture systems. Aquaculture 13, 1-33

Wright, R.T., Coffin, R.B., Ersing, C.P., Pearson, D., 1982. Field and laboratory measurements of bivalve filtration of natural marine bacterioplankton. Limnology and Oceanography 27, 91-98

SYNTHESIS

What is the role of the bacterial community and benthic suspension feeders in carbon cycling within the Puyuhuapi fjord?

What is the role of the bacterial community and benthic suspension feeders in carbon cycling within the Puyuhuapi fjord?

This research describes the main pathways of production and utilization of autochthonous and allochthonous carbon by bacterial communities and their relative importance in sustaining benthic filter feeder bivalves.

Phytoplankton blooms dominated by diatoms and dinoflagellates were primarily responsible for the high rates of organic matter (OM) production measured in the Puyuhuapi Fjord. In general, *Skeletonema* spp. (diatom) and *Heterocapsa triquetra* (dinoflagellate) were dominant in low salinity waters, highlighting the importance of freshwater to create favourable conditions for aggregation and growth of phytoplankton. Freshwater input tends to stabilize the water column and increase the silicic acid concentration in upper layers. Although silicic acid is not an essential nutrient for all types of phytoplankton, its requirement for diatom production makes it a key element in shaping the structure and functioning of marine pelagic food webs.

The annual cycle of primary production in the Puyuhuapi fjord did not show a marked seasonal pattern. High rates of OM production were recorded both in spring and in winter. In addition, data from the continuous measurement of Chl-a at the Puyuhapi buoy highlight the occurrence of enhanced Chl-a concentrations throughout the year, indicating that year-round pulsed productivity events, rather than sharp seasonality, may make a more significant contribution than expected to the annual productivity of the Puyuhuapi Fjord area. These results suggest that the annual cycle of primary production in this fjord may be changing and showing every time a less predictable phytoplankton succession model.

Community respiration rates (CR) were notably higher than primary production rates (GPP) during much of the annual cycle, indicating that the system use more organic carbon than what is produced locally (autochthonous organic matter). The significant correlation between bacterial production with GPP and CR rates, coupled to the high percentage utilization of GPP by bacterial community (over 100%), confirm that both autochthonous and allochthonous OM are being used and represent important substrates for bacterial growth in the Puyuhuapi Fjord. According to our experiments, bacterial community was able to process both dissolved organic matter from salmon food pellets

(allochthonous organic matter) and those derived from diatoms (autochthonous organic matter). However, bacterial production rates measured in the salmon food pellet treatments were higher than those measured in the diatom treatments, probably because salmon food has a high level of degradability which allows it to be quickly processed (Nimptsch et al., 2015).

Our findings, clearly demonstrated that a predominant bacterial taxa were able to process the allochthonous OM derived from salmon food. Therefore, bacterial utilization of this allochthonous load in the water column could be key to reduce the potential impact of organic waste generated by fish farm. In this context, bacterial community play an important role in fjords ecosystems, where they offer a permanent path for the transfer of energy and carbon and potentially reducing aquaculture perturbations.

The high load of OM from autochthonous and allochthonous source in the Puyuhuapi Fjord leads to a complex pool of food available to benthic consumers.

Our results showed that *Aulacomya atra* – dominant specie within the benthic filter feeding community that grows within areas adjacent to salmon cages – preferentially exploits food resources with a marked marine isotopic carbon signal (phytoplankton) in the Puyuhuapi Fjord. However, the possible assimilation of allochthonous OM from salmon farming by this species cannot be ruled out because the range of the isotopic signal of salmon food pellets overlaps the range of the marine signal found in the tissues of *Aulacomya atra*. In addition, the results from our feeding experiments conducted in the laboratory indicate that this specie is able to capture both autochthonous OM (bacteria and planktonic community) and allochthonous OM (salmon food pellets). The ability of *Aulacomya atra* to efficiently retain small size particles (< 0.8 um), allows them to incorporate bacteria as an important part of their diet. Thus, allochthonous OM (from terrestrial origin or from salmon farming) could enter the benthic food web as material assimilated through bacteria. This possible trophic link between bacteria and filter species such as *Aulacomya atra* shows the important role of these two communities in the pelagic-benthic coupling in the Puyuhuapi Fjord and their potential as "ecosystem cleansing" organisms by reducing the salmon cage derived suspended OM load.